

The University of Adelaide

Repurposing of Robenidine and Characterization of Novel Analogues for Treatment of Infectious Diseases

Rebecca Jane Abraham
12-1-2017

Table of Contents

List of Figures	6
List of Tables	7
Abstract	8
Declaration by Author.....	10
Acknowledgements.....	11
List of Abbreviations used in the thesis	15
Chapter 1: Literature Review	20
1.1 Introduction	21
1.2 Antimicrobial discovery	21
1.3 Robenidine as a potential antibacterial agent	22
1.3.1 Safety and toxicity of robenidine.....	22
1.3.2 Spectrum of activity of robenidine	22
1.3.3 Mechanism of action of robenidine	23
1.3.4 The repurposing of robenidine	27
1.4 Bacterial infections.....	27
1.4.1 Bacterial resistance mechanisms	28
1.4.2 Antimicrobials that affect bacterial membranes	29
1.4.2.1 Antimicrobial peptides	30
1.4.2.2 Cationic antimicrobial peptides	30
1.4.2.3 Lipopeptides	31
1.4.2.4 Glycopeptides	31
1.4.2.5 Advantages and disadvantages of using antimicrobial peptides	31
1.4.2.6 Other classes of bacterial cell membrane inhibitors	32
1.4.2.7 Porphyrins.....	32
1.4.2.8 Quinoline-like molecules.....	32
1.4.2.9 Riminophenazines	32
1.5 Protistan infections.....	33
1.5.1 Kinetoplasts – <i>Trypanosoma brucei</i> and <i>Leishmania donovani</i>	33
1.5.2 Current drugs in the treatment of leishmaniasis and trypanosomiasis	35
1.5.3 Diplomonads - <i>Giardia duodenalis</i>	37
1.5.4 Current drug therapies available for the treatment of <i>Giardia</i>	39
1.5.5 Potential anti-giardial candidates identified in assays to date	43

1.5.6 Approach to anti-giardial screening.....	45
1.5.7 Current <i>in vitro</i> screening of potential anti-giardials.....	46
1.5.8 Current <i>in vivo</i> screening of anti-giardial compounds.....	48
1.5.9 Suggested experimental screening flow for anti-giardial discovery.....	50
1.6 Aims and outline of thesis.....	54
Chapter 2: Robenidine Analogues as Gram-positive Antibacterial Agents.....	55
2.1 Statement of Authorship.....	56
2.2 Abstract.....	59
2.3 Introduction.....	60
2.4 Results and Discussion.....	61
<i>^a<15% compound loss in 60 min. ^bBelow sensitivity limit of 7 µL/min/mg protein based on 0.4 mg/L microsomal protein concentration. ^cBelow sensitivity limit based on 0.4 mg/mL microsomal protein concentration. ^dThe microsome-predicted hepatic extraction ratios (E_H), obtained based on relative rates of test compound degradation in vitro, were used to classify compounds as low (<0.3), intermediate (0.3-0.7), high (0.7-0.95), or very high (>0.95) extraction compounds.</i>	73
2.5 Conclusions.....	73
2.6 Experimental.....	74
2.6.1 Chemistry - General Methods.....	74
2.6.2 Microbiology.....	75
Chapter 3: Potential of Novel Robenidine Analogues as Antibacterial Agents Targeting Gram-Negative Pathogens.....	78
3.1 Statement of Authorship.....	79
3.2 Abstract.....	80
3.3 Article.....	80
Chapter 4: Anti-trypanosomatid Activity of Novel Robenidine Analogue.....	89
4.1 Statement of Authorship.....	90
4.2 Abstract.....	91
4.3 Introduction.....	92
4.4 Materials and methods.....	95
4.4.1 Antimicrobial agents.....	95
4.4.2 <i>Leishmania donovani</i> screening.....	95
4.4.3 <i>Trypanosoma brucei</i> screening.....	95
4.4.4 Cell toxicity assays.....	96

4.5 Results	96
4.6 Discussion	99
Chapter 5: Antigiardial Activity and Mechanism of Action of Robenidine and a Library of Related Novel Aminoguanidines	102
5.1 Statement of Authorship.....	103
5.2 Abstract	104
5.3 Introduction	105
5.4 Materials and methods	106
5.4.1 Chemicals	106
5.4.2 Cell culture	106
5.4.3 <i>In vitro</i> drug efficacy assays	106
5.4.4 Recovery assay	107
5.4.5 Antibacterial activity	108
5.4.6 Mechanism of Action Studies.....	108
5.4.7 Cytotoxicity	109
5.4.8 <i>In-vivo</i> Toxicity of Select Analogues	109
5.4.9 Statistical analysis.....	110
5.5 Results and discussion.....	110
5.5.1 Antigiardial activity	110
5.5.2 Recovery assay	128
5.5.3 Mechanism of action	130
5.5.4 <i>In vivo</i> toxicity of select analogues.....	137
5.6 Conclusion.....	137
Chapter 6: Development of Animal Models of Giardiasis	138
Chapter 6.1: Cross-Species Transmission of <i>Giardia duodenalis</i> in Livestock	139
6.1.1 Statement of Authorship.....	141
6.1.2 Abstract:	142
6.1.3 Article:.....	142
6.2 <i>Giardia duodenalis</i> Mouse Model for the Development of Novel Antigiardial Agents .	148
6.2.1 Statement of Authorship.....	149
6.2.2 Abstract:	151
6.2.3 Article.....	151
Chapter 7: General Discussion and Conclusions	156

7.1 Introduction	157
7.2 General aims and chapter summaries	157
7.3 Major findings, implications and future work arising from this thesis	159
1. Antibacterial activity of robenidine and several analogues	159
2. Antitrypanosomal activity of robenidine and select analogues.....	160
3. Antileishmanial activity of robenidine and select analogues	160
4. The anti-giardial potential of novel analogues of robenidine.....	161
5. Establishment of an animal model of giardiasis.....	162
6. Cross-species transmission of <i>Giardia duodenalis</i>	162
7.4 Implications of the findings of this thesis	163
7.5 Future work arising from this thesis.....	163
7.6 Conclusions	164
Appendices.....	165
Appendix 1: Materials and Methods for chemical synthesis of compounds described in Chapter 2	166
Appendix 2: Analysis of Appropriate Broth for Bacterial Assays with Robenidine Analogues.....	185
Appendix 3: Development of Spheroplasts and Regeneration Efficiency Experiments....	189
References.....	196

List of Figures

Figure 1.1 Inhibition of macromolecular synthesis by robenidine	24
Figure 1.2 The effect of robenidine on ATP release from <i>S. aureus</i> ATCC 29213	25
Figure 1.3: Structure of CGP 40215A	26
Figure 1.4 Lifecycle of <i>Leishmania</i>	34
Figure 1.5 Lifecycle of <i>Trypanosoma</i> sp	35
Figure 1.6 Drug structures of currently and historically used anti-giardials	40
Figure 1.6 Structures of experimental drugs for treatment of giardiasis	44
Figure 1.7 Efficacy models for anti-giardial drug discovery	53
Figure 2.1 Graphical abstract	59
Figure 2.2 Chemical structure of robenidine	60
Figure 2.3 Time-kill assay	72
Figure 3.1 The activity of robenidine against <i>E. coli</i> spheroplasts	83
Figure 3.2 Morphological effect of robenidine on <i>E. coli</i> spheroplasts after 24-hour exposure	84
Figure 4.1 Antitrypanosomatid activity of robenidine and 19 structural analogues	98
Figure 5.1 Inhibition of adherence of <i>Giardia duodenalis</i> by robenidine (812) and two structural analogues, 062 and 099	116
Figure 5.2: Recovery assay of <i>Giardia duodenalis</i> exposed to robenidine and selected robenidine analogues.	129
Figure 5.3 Transmission electron microscopy of <i>Giardia duodenalis</i> trophozoites.....	131
Figure 5.4 Scanning electron microscopy of <i>Giardia duodenalis</i>	132
Figure 5.5 Scanning electron microscopy of <i>Giardia duodenalis</i> exposed to robenidine (812)	134
Figure 5.6 Scanning electron microscopy images of <i>Giardia duodenalis</i> exposed to 135	135
Figure 5.7 Scanning electron microscopy of <i>Giardia duodenalis</i> after exposure to 139	136
Figure A3.1 Ideal temperature to incubate <i>E. coli</i> spheroplasts.	195

List of Tables

Table 2.1 The inhibition of MRSA, VRE, <i>E. coli</i> and <i>P. aeruginosa</i> growth by 1,3-aminoguanidine Schiff base analogues possessing mono-substituted aromatic rings (1 – 31).	63
Table 2.2 The inhibition of MRSA, VRE, <i>E. coli</i> and <i>P. aeruginosa</i> growth by 1,3-diaminoguanidine Schiff base analogues possessing di-, tri- and poly-substituted aromatic rings (32 - 57).	65
Table 2.3 Inhibition of MRSA and VRE by 1,3-diaminoguanidine Schiff bases bearing extended linkers, non-aromatic and isosteric phenyl ring replacements (58 – 67).	67
Table 2.4 Inhibition of MRSA and VRE by 1,3-diaminoguanidine Schiff base analogues (68 – 80) bearing imine substitution	69
Table 2.5 MIC and MBC concentrations for 1, 27, 69 and ampicillin against 20 clinically isolated MRSA and 4 ATCC MSSA bacterial strains.	70
Table 2.6 MIC for 1, 27 69 and clofazimine against <i>E. coli</i> ATCC 25922 and <i>P. aeruginosa</i> ATCC 27853.	71
Table 2.7 physiochemical and Metabolism	73
Table 3.1 Selection of analogues chosen to be tested for antibacterial activity against both Gram-positive and Gram-negative bacteria	85
Table 3.2 Selection of robenidine analogues screened for antibacterial activity	87
Table 4.1 Chemical identity of the novel chemical entities tested for inhibitory activity against <i>Leishmania donovani</i> and <i>Trypanosoma brucei</i>	94
Table 4.2 The selectivity of active analogues for trypanosomatid parasites over mammalian cells	99
Table 5.1 Antigiardial activity of 1,3-Diaminoguanidine Schiff Base analogues with mono-substituted aromatic rings.	110
Table 5.2 Antigiardial activity of 1,3-Diaminoguanidine Schiff base analogues with di-, tri- and polysubstituted aromatic rings	117
Table 5.3 Antigiardial activity of 1,3-Diaminoguanidine Schiff base analogues with imine substitutions	119
Table 5.4 Antigiardial activity of 1,3-Diaminoguanidine Schiff Base analogues with extended linkers and nonaromatic and isosteric phenyl ring replacements	120
Table 5.5 Antigiardial activity of 1,3-Diaminoguanidine Schiff Base analogues with non-symmetrical substitution of the guanidine linker	122
Table 5.6 Antigiardial activity of substituted phenylmethylidene guanidines.	123
Table 5.7 Antigiardial activity of 1,4-bis pyrimidine analogues with mono-, di-, tri- and poly-substituted aromatic rings, imine substitution.	124
Table 5.8 Antigiardial activity of 1,4-bis pyrimidine analogues with extended linkers and nonaromatic and isosteric phenyl ring replacements	126
Table 5.9 Antigiardial activity of robenidine analogues with a triazine core	127
Table A3.1 The induction of spheroplast transformation in various species of bacteria	193
Table A3.2 The regeneration of <i>E. coli</i> spheroplasts on various solid media.	194

Abstract

Infectious diseases are one of the leading causes of morbidity and mortality worldwide. Diseases caused by single-celled organisms, such as bacteria and protista, cause billions of infections per year. One of the leading weapons in the fight against infectious diseases are antimicrobials. However, the efficacy of antimicrobials is decreasing as the development of antimicrobial resistance increases. At the same time as increasing levels of resistance are observed there is a lack of new antimicrobial agents entering the market and many big pharmaceutical companies have suspended antimicrobial drug discovery programs as financial return is small. Due to the lack of novel treatments for infectious diseases and increasing treatment failures it is essential that new chemical entities are explored to fill this gap.

In this thesis a novel library of compounds based on the structure of robenidine, an approved antimicrobial used to prevent coccidiosis in chickens and rabbits, was investigated as potential antimicrobial agents. Initial experiments focussed on the antibacterial activity of the library against representative pathogenic bacteria. Activity was assessed according to CLSI guidelines. The spectrum of activity of the majority of analogues investigated was limited to Gram-positive bacteria, with promising MICs as low as 1.3 μM . However, through the use of outer-membrane permeabilising agents and spheroplast induction, it was discovered that the target site of robenidine and some of the related analogues was also present in Gram-negative organisms. This led to the development of a small subset of analogues which demonstrated intrinsic activity against the Gram-negative pathogens *Escherichia coli* and *Pseudomonas aeruginosa* with MICs as low as 52 μM . Furthermore, kill kinetic studies revealed that robenidine and related analogues had a bactericidal mechanism of action.

The next series of experiments focussed on the characterisation of the antiparasitic activity of the library against the protists *Trypanosoma brucei*, *Leishmania donovani* and *Giardia duodenalis*. Several of the analogues demonstrated activity against these parasites with some promising results against *Leishmania donovani* including a small number of analogues with selectivity indices (SI) for the parasite above 20 (an SI of >10 is considered selective). In addition, activity against *G. duodenalis* was also promising ($\text{IC}_{50} < 1 \mu\text{M}$). In total 121 analogues were tested against *G. duodenalis* with 13 being selective for *Giardia* with no antibacterial activity and limited, if any, toxicity towards mammalian cells. MICs for the most

promising analogues were $\leq 2.8 \mu\text{M}$. Electron microscopy studies to elucidate the mechanism or site of action of this class of antimicrobials against *G. duodenalis* demonstrated that the two most promising compounds both caused rapid disintegration of the cell membrane and the development of cyst-like structures, while one analogue also appeared to interfere with cell division.

Finally, in order to test *in vivo* efficacy an animal model was effectively established in neonatal mice.

In conclusion this thesis demonstrated for the first time the potential for this library of compounds to become therapeutic agents for a range of infectious diseases. In particular, the selective activity of several analogues for *Giardia* over other microorganisms and mammalian cells was demonstrated for the first time, highlighting the potential for this library of analogues. In addition, insight into the unique mechanism of action of a select group of compounds against *G. duodenalis* was demonstrated.

Declaration by Author

I certify that this work contains no material which has been accepted for the award of any other degree or diploma in my name, in any university or other tertiary institution and, to the best of my knowledge and belief, contains no material previously published or written by another person, except where due reference has been made in the text. In addition, I certify that no part of this work will, in the future, be used in a submission in my name, for any other degree or diploma in any university or other tertiary institution without the prior approval of the University of Adelaide and where applicable, any partner institution responsible for the joint-award of this degree. I give consent to this copy of my thesis when deposited in the University Library, being made available for loan and photocopying, subject to the provisions of the Copyright Act 1968. I acknowledge that copyright of published works contained within this thesis resides with the copyright holder(s) of those works. I also give permission for the digital version of my thesis to be made available on the web, via the University's digital research repository, the Library Search and also through web search engines, unless permission has been granted by the University to restrict access for a period of time.

I acknowledge the support I have received for my research through the provision of an Australian Government Research Training Program Scholarship.

Rebecca Abraham

Acknowledgements

First, I would like to thank my supervisors, Dr. Ryan O’Handley and Prof. Darren Trott, for taking a chance with me and providing the opportunity for me to complete a PhD. I will always be grateful for the support, encouragement and friendship they provided throughout my PhD.

I would specifically like to thank Ryan for allowing me to develop and follow my own interests throughout my PhD, helping me to grow as an independent researcher. I would like to thank him for his encouragement to attend conferences and training courses throughout my candidature and for introducing me to many other researchers in my area.

I specifically thank Darren for his unwavering passion for science and the enthusiasm he injected into my project as well as his attention to detail.

I would like to thank Dr. Stephen Page for his invaluable involvement in this project and his continual optimism for all areas of the study.

I would also like to thank Neoculi Pty. Ltd. for providing financial support for this project as required.

I would like to thank Dr. Armando Jardim and Dr. Norma Batista who hosted me at the Institute of Parasitology at McGill University. I would also like to thank Prof. Tim Geary who put me in contact with Armando and facilitated the trip.

I would like to make a special thanks to the Australian Society of Parasitology for providing financial assistance to travel to McGill University and visit the Jardim Lab, as well as providing financial assistance to attend the society’s Annual General Meeting in 2014 and 2016. I would also like to thank the society and its members who organized and participated in the 2016 Concepts in Parasitology course which I attended.

I would like to thank all the people who provided me with assistance and friendship at both the University of Adelaide and Murdoch University, especially Dr. Mark O’Dea who was essential in establishing the giardiasis mouse model at Murdoch University. Also the staff at the Centre for Microscopy at both Adelaide University and the University of Western Australia.

Finally, I would like to thank my family for their support throughout my candidature.

I especially like to thank my husband Sam Abraham. Sam provided continuous encouragement from the beginning and his experience was invaluable.

I am always indebted to my parent’s in-law, Pastor Abraham Thomas and Achamma (Molly) Abraham who stayed with us for several months after the birth of both my children, without their help, it would have been a struggle to finish my PhD.

I also thank my mum and dad and grandparents for encouraging me to achieve the things I set my mind to.

I dedicate this thesis to my mother, Cheryl Lesley Joss (1959-2006).

“And we know that in all things God works for the good of those who love him, who have been called according to his purpose.”

Romans 8:28, NIV

Peer reviewed papers arising from this thesis:

Abraham, R.J., O'Dea, M., Rusdi, B., Page, S.W., O'Handley, R., Abraham, S., 2018. *Giardia duodenalis* mouse model for the development of novel anti-giardial agents. *Journal of microbiological methods* 145, 7-9.

Abraham, R.J., Stevens, A.J., Young, K.A., Russell, C., Qvist, A., Khazandi, M., Wong, H.S., Abraham, S., Ogunniyi, A.D., Page, S.W., O'Handley, R., McCluskey, A., Trott, D.J., 2016a. Robenidine Analogues as Gram-Positive Antibacterial Agents. *J Med Chem* 59, 2126-2138.

Other papers published during candidature (not included in this thesis):

Abraham, S., O'Dea, M., Trott, D.J., **Abraham, R.J.**, Hughes, D., Pang, S., McKew, G., Cheong, E.Y.L., Merlino, J., Saputra, S., Malik, R., Gottlieb, T., 2016b. Isolation and plasmid characterization of carbapenemase (IMP-4) producing *Salmonella enterica* Typhimurium from cats. *Scientific Reports* 6, 35527.

Saputra, S., Jordan, D., Mitchell, T., Wong, H.S., **Abraham, R.J.**, Kidsley, A., Turnidge, J., Trott, D.J., Abraham, S., 2017. Antimicrobial resistance in clinical *Escherichia coli* isolated from companion animals in Australia. *Veterinary Microbiology* 211, 43-50.

Worthing, K.A., Abraham, S., Pang, S., Coombs, G.W., Saputra, S., Jordan, D., Wong, H.S., **Abraham, R.J.**, Trott, D.J., Norris, J.M., 2017, ahead of print. Molecular characterisation of methicillin-resistant *Staphylococcus aureus* isolated from Australian animals and veterinarians. *Microbial Drug Resistance*.

Worthing, K.A., Coombs, G.W., Pang, S., Abraham, S., Saputra, S., Trott, D.J., Jordan, D., Wong, H.S., **Abraham, R.J.**, Norris, J.M., 2016. Isolation of *mecC* MRSA in Australia. *J Antimicrob Chemoth* 71, 2348-2349.

First author conference proceedings arising from this thesis:

Abraham RJ, Trott D, Page SW, O'Handley R. (2014) *In vitro* activity of a new anti-giardial compound using a modified adherence assay. Australian Society of Parasitology, Annual Scientific Meeting, Canberra.

Abraham RJ, Trott D, Page SW, O'Handley R. (2014) *In vitro* activity of a new antimicrobial compound. Australian Society of Medical Research, South Australia Branch Meeting, Adelaide.

Abraham RJ, Wong HS, Khazandi M, Abraham S, Page SW, O'Handley R, Trott D. (2015) Evaluating the efficacy of three potential antibacterial agents *in vitro*; NCL812, NCL062 and NCL099. Australian Society of Antimicrobials, Annual Scientific Meeting, Brisbane.

Abraham RJ, Bautiste-Lopez NL, Stevens AJ, McCluskey A, Trott D, Jardim A, Page S, O’Handley R. (2015) *In vitro* activity and therapeutic potential of 20 novel aminoguanidines against *Trypanosoma brucei* and *Leishmania donovani*. Australian Society of Parasitology, Annual Scientific Meeting, New Zealand

Abraham RJ, Abraham S, Zahedi A, Ryan U, Page SW, Trott D, O’Handley R. (2016) Cross-species transmission of *Giardia duodenalis*. Australian Society of Parasitology, Annual Scientific Meeting, Brisbane

Patents arising from this thesis:

Page S, Stevens A, McCluskey A, Keenan M, **Abraham R.** (2016) methods for treating protozoal infections, WO 2016033635 A1.

List of Abbreviations used in the thesis

μL	microlitre
μM	micromolar
$^{13}\text{C-NMR}$	carbon NMR
$^1\text{H-NMR}$	proton NMR
ad lib	as much and as often as desired
AdoMet	S-adenosylmethionine
ADP	adenosine diphosphate
ATCC	american tissue culture collection
ATP	adenosine triphosphate
ATPase	adenosine triphosphatase
Bp	base pairs
br s	broad sinlet
$^{\circ}\text{C}$	celcius
CAMBH	cation-adjusted Mueller-Hinton broth
CAMPs	cationic antimicrobial peptides
CA-MRSA	community acquired methicillin-resistant <i>Staphylococcus aureus</i>
CFU	colony forming units
CL_{int}	intrinsic clearence rates
CLSI	Clinical Laboratory Standards Institute
Cm	centimetres
CMCA	Centre for Microscopy, Characterisation and Analysis
CNS	central nervous system
D	doublet

d.p.i.	days post inoculation
DAPI	4',6-diamidino-2-phenylindole
dd	doublet of doublets
ddd	doublet of doublets of doublets
DEPTQ	polarization transfer quaternary
DME-L+	Dulbecco's Modified Eagle's Medium
DMEM	Dulbecco's Modified Eagle's Medium
DMSO	dimethyl sulfoxide
DMSO- <i>d</i> ₆	deuterated dimethyl sulfoxide
DNA	deoxyribonucleic acid
dt	doublet of triplets
EC ₅₀	half maximal effective concentration
EDTA	ethylenediaminetetraacetic acid
E _H	hepatic extraction
EtOH	ethanol
FCS	foetal calf serum
FDA	food and drug administration
g	grams
X g	g-force
g/mol	grams/mole
<i>gdh</i>	glutamate dehydrogenase gene
gHMBC	gradient heteronuclear multiple bond correlation
gHSQC	gradient heteronuclear single quantum correlation
GI ₅₀	concentration to achieve 50 % Growth inhibition
GIT	gastrointestinal tract

HA-MRSA	hospital acquired methicillin-resistant <i>Staphylococcus aureus</i>
HAT	human African trypanosomiasis
HCl	hydrochloric acid
HPLC	high performance liquid chromatography
hrs	hours
HTS	high throughput screening
Hz	hertz
IC ₅₀	half maximal inhibitory concentration
<i>J</i>	coupling constant
kg	kilogram
LB	Luria Bertanini
LBB	Luria Bertanini broth
LD ₅₀	the amount of a material which causes death in 50% of a group of test animals
m	multiplet
M	molar
M.P.	melting point
MBC	minimum bactericidal concentration
MBC ₅₀	minimum bactericidal concentration required to kill 50% of isolates
MBC ₉₀	minimum bactericidal concentration required to kill 90% of isolates
MBEC	minimum biofilm eliminating concentration
MDR	Multi-drug resistant
MEM	minimum essential media
mg	milligram
MHz	megahertz

MIC	minimum inhibitory concentration
MIC ₅₀	minimum inhibitory concentration required to kill 50% of isolates
MIC ₉₀	minimum inhibitory concentration required to kill 90% of isolates
ml	millilitre
mM	millimolar
MRSA	methicillin-resistant <i>Staphylococcus aureus</i>
MSSA	methicillin-sensitive <i>Staphylococcus aureus</i>
MTT	3-(4,5-dimethylthiazol-2-yl)-2,5-diphenyltetrazolium bromide
mw	molecular weight
Mz	metronidazole
NADH	nicotinamide adenine dinucleotide
NCL	Neoculi
nm	nanometres
NMR	nuclear magnetic resonance
NOAEL	no observable adverse effect level
OD	optical density
p.o.	orally
PBS	phosphate buffered saline
PCR	polymerase chain reaction
PFOR	pyruvate:ferredoxin oxidoreductase
PKPD	pharmacokinetic/pharmacodynamic
PMBN	polymyxin B nonapeptide
ppm	parts per million
q	quartet
quin	quintet

RNA	ribonucleic acid
rpm	rotations per minute
RPMI1640	Roswell Park Memorial Institute medium 1640
s	singlet
SAR	structure activity relationship
SD	standard deviation
SDM-79	procyclic form culture media
SE	standard error of the mean
SEM	scanning Electron Microscopy
SI	selectivity Index
SNPs	single nucleotide polymorphisms
sRNAs	small RNAs
t	triplet
td	triplet of doublets
TEM	transmission electron microscopy
<i>tpi</i>	triose phosphate isomerase
TYI-S-33	tripticase, yeast extract, iron-serum medium
U/ml	units per millilitre
µg	microgram
UK	United Kingdom
vol	volume
VRE	vancomycin-resistant <i>Enterococci</i>
WHO	World Health Organisation
XTT	(2,3-Bis-(2-Methoxy-4-Nitro-5-Sulfophenyl)-2 <i>H</i> -Tetrazolium-5-Carboxanilide)
δ	chemical shift

Chapter 1: Literature Review

1.1 Introduction

Before the introduction of antimicrobial agents, infectious diseases were the leading cause of death worldwide. In pre-antimicrobial America 30% of deaths were caused by pneumonia, tuberculosis or diarrhoeal disease. Infant mortality was high (10%) and life expectancy was low (47 years)(Cohen, 2000). With the discovery and clinical introduction of antibiotics starting in the 1930s and extending into the 1970s, mortality from bacterial infectious disease decreased rapidly while life expectancy increased dramatically. Similarly, after the introduction of antimicrobials in the UK, death in childhood due to *Streptococcus pyogenes* decreased by 50% (Cohen, 2000). This led to antimicrobials receiving the title of ‘miracle drugs’ and optimism for the treatment of infectious agents with antimicrobial compounds was high and it was believed that most bacterial infectious diseases would be brought under control or completely eradicated (Cohen, 2000; Fauci, 2005). This optimism lasted into the early 1970s as numerous new antimicrobial compounds were released onto the market (Spellberg, 2008). Currently, however, infectious diseases are the second highest cause of death worldwide (Fauci, 2005). Adding to this dilemma is the alarming increase of antimicrobial resistance seen in many pathogens worldwide while the number of antimicrobial drugs being developed is decreasing (French, 2010; Norrby et al., 2005; Spellberg et al., 2004; Ventola, 2015)

1.2 Antimicrobial discovery

There are two main pathways for the discovery of new antimicrobial agents; the traditional ‘top-down’ or activity centred approach and the ‘bottom-up’ or target centred approach (Debouck and Goodfellow, 1999; Tejman-Yarden and Eckmann, 2011). The activity centred approach has delivered all the currently used antimicrobial agents for bacterial species and enteric pathogenic protista. The target centred approach is a more recent strategy to discover new drugs as technology has improved significantly since the discovery of the first antimicrobials, potentially allowing the design of compounds that will exploit specific drug targets. However, this approach has proven disappointing as it is difficult to predict the *in vivo* efficacy of potential newly synthesised compounds (Mills, 2003; Tejman-Yarden and Eckmann, 2011).

A third approach to drug development becoming more frequently utilised focusses on the ‘repurposing’ of an already registered, approved or known drug for alternative indications. This method has received recent attention as the cost and time to development of potential drugs can be reduced significantly. Repurposing may be an important tool to plug the gap in combating infectious diseases while novel compounds are investigated for drug potential (Oprea et al., 2011).

1.3 Robenidine as a potential antibacterial agent

Neoculi Pty. Ltd. is a small pharmaceutical company which has identified robenidine, a widely used anticoccidial in the poultry industry, as a potential treatment for bacterial infections and other protista. Preliminary research instigated by the company has identified potent *in vitro* activity of robenidine against Gram-positive bacteria including methicillin-resistant *Staphylococcus aureus* (MRSA) and vancomycin-resistant *Enterococcus* spp. (VRE), prompting the development of a large library of structural analogues of robenidine.

Robenidine is a non-chiral, synthetic, chlorophenylbenzylidene derivative with a guanidine core which has been used as an anticoccidial agent in the poultry industry since 1972 and is also used in the commercial rabbit industry (Kantor et al., 1970). It is used in the poultry industry to control coccidial infections caused by *Eimeria tenella*, *E. necatrix*, *E. acervulina*, *E. brunetti* and *E. maxima* and in the commercial rabbit industry to control *Eimeria intestinalis*, *E. flavescens*, *E. magna*, *E. media*, *E. perforans* and *E. stiedai* (Aquilina et al., 2011; Kantor et al., 1970).

1.3.1 Safety and toxicity of robenidine

Robenidine is considered to be a relatively safe drug with no identifiable genotoxicity or mutagenicity. There is also a large gap between doses required to kill coccidian parasites and that which induce reproductive effects in the host (mainly an increase in stillbirth and decreased weight gain of rabbit kits). Several studies into the sub-chronic and chronic effects of the drug have been completed which did not show any adverse effects. However, these studies were lacking in detail and therefore an official 'no observable adverse effect level (NOAEL) could not be identified (Aquilina et al., 2011).

1.3.2 Spectrum of activity of robenidine

As mentioned before, robenidine is effective against *Eimeria* spp. in poultry and rabbits. It has also been tested against a range of other parasites *in vitro*, including *Entamoeba*, *Neospora*, *Cryptosporidium* and *Toxoplasma*, with varying reports of efficacy (Lindsay et al., 1994; Ricketts and Pfefferkorn, 1993). In addition, a recent study found robenidine to be an effective treatment for *Babesia microti* infection in mice (Yao et al., 2015).

Few studies investigating the antibacterial activity of robenidine have been performed, mainly in relation to the potential environmental effect robenidine could have when chicken manure is used as a fertiliser. In one particular study, robenidine, in addition to several breakdown products, was found to effectively prevent growth of unknown soil bacteria with an EC₅₀ as low as 2.4 µM (Hansen et al., 2009). A small study to determine if robenidine would be an effective

control drug for *Clostridium perfringens* in rabbits found that robenidine was able to inhibit growth of several isolates of the bacteria at concentrations of 4 µg/ml. This study also used *S. aureus* and *E. faecalis* as controls which were inhibited by concentrations of 4 and 8 µg/ml of robenidine respectively (Marien et al., 2008).

Preliminary studies into the potential antibacterial activity of robenidine and a single structural analogue named NCL 062 (identical to robenidine except for methyl imine substitutions) was commissioned by Neoculi Pty. Ltd. This study demonstrated that both compounds are narrow spectrum, inhibiting Gram-positive organisms, including *S. aureus*, *E. faecalis* and *S. pneumoniae*. Both compounds were equally effective against methicillin-sensitive (MSSA) and methicillin-resistant strains of *S. aureus* and vancomycin-resistant and -sensitive strains of *E. faecalis* (VSE). Robenidine was most effective against VRE with a reported minimum inhibitory concentration (MIC) range of 2 – 4 µg/ml, MIC₅₀ of 2 µg/ml, MIC₉₀ of 2 µg/ml, and an MIC mode of 2 µg/ml (Neoculi; personal communication). Preliminary activity of robenidine against *S. aureus* was undertaken by The University of Adelaide. An overall MIC₅₀ of 4 µg/ml, MIC₉₀ of 8 µg/ml and an MIC range of 2 – 8 µg/ml were observed. The MBC range, MBC₅₀ and MBC₉₀ were the same as the MIC (i.e.: 2 -8 µg/ml, 4 µg/ml and 8 µg/ml, respectively) (Ogunniyi et al., 2017). Interestingly, it was found that robenidine had lower MIC's against MSSA and community-acquired MRSA (CA-MRSA) compared to hospital-acquired MRSA strains (HA-MRSA)(Ogunniyi et al., 2017). Finally, robenidine has been tested against *S. pneumoniae* with an MIC₅₀, MIC₉₀, MBC₅₀ and MBC₉₀ of 8 µg/ml, and an MIC range and MBC range of 4 -8 µg/ml (Ogunniyi et al., 2017). Due to the similarity of the MIC and MBC concentrations, these data suggest that robenidine and related compounds are bactericidal rather than bacteriostatic in activity (Marr et al., 2006).

1.3.3 Mechanism of action of robenidine

Exploration into the mechanism of action of robenidine against coccidian parasites has been attempted previously in the 1970s. The coccidian parasite has a complex lifecycle consisting of several rounds of merogony which result in formation of merozoites followed by sexual reproduction and release of oocysts from the host. The oocysts sporulate in the environment and go on to infect a new host and the cycle is repeated (McDonald and Shirley, 2009). Through inducing experimental coccidiosis in chickens, it is possible to determine at which stage of the lifecycle an anticoccidial drug will work by delaying drug treatment for defined periods of time. The defined periods of time correspond to the development of different stages of the parasite. Using this approach, it was determined that robenidine inhibits the parasite at the stage directly preceding the formation of first generation merozoites. It was also determined that the primary

action of robenidine is coccidiostatic as short exposure to the drug results in a return of infection. However robenidine is possibly coccidiocidal if treatment is long enough (Ryley and Wilson, 1971).

The precise mechanism of action of robenidine has been investigated in two published studies. Robenidine was found to inhibit ADP stimulated respiration in intact and submitochondrial fractions of rat mitochondria suggesting that robenidine is an inhibitor of oxidative phosphorylation (Wong et al., 1972). However, electron microscopy studies of both *in vivo* and *in vitro* grown parasitic coccidia exposed to robenidine demonstrated that the mitochondria were affected last and the effect was probably due to disintegration of the cell rather than a direct effect of the drug itself (Lee and Millard, 1972). In this second study, the drug was mainly observed to affect the perinuclear space, golgi apparatus and endoplasmic reticulum, resulting in distension occasionally accompanied by visible membrane disintegration. After longer exposure to the drug, lysosomal like bodies were observed in the parasite and the host cell and finally the outer membrane of the cell began to break down. The authors suggest that based on these observations the primary site of action may be the ribosomes, which stimulate the over-production of proteins resulting in self-destruction of the cell (Lee and Millard, 1972). All of these observations could be artifacts of an agent that primarily acts on the cell wall.

Unpublished research initiated by Neoculi Pty. Ltd. has looked into the mechanism of action of robenidine against bacteria. In initial studies the inhibition of macromolecular pathways in *S. aureus* by robenidine was determined. This study identified that all 5 pathways tested (DNA synthesis, RNA synthesis, protein synthesis, lipid synthesis and cell wall synthesis) were equally inhibited (100%). The fact that global inhibition was observed suggests that robenidine has a mechanism of action that targets the cell membrane causing a leakage of ions and metabolites essential to all 5 processes ((Ogunniyi et al., 2017); Figure 1.1).

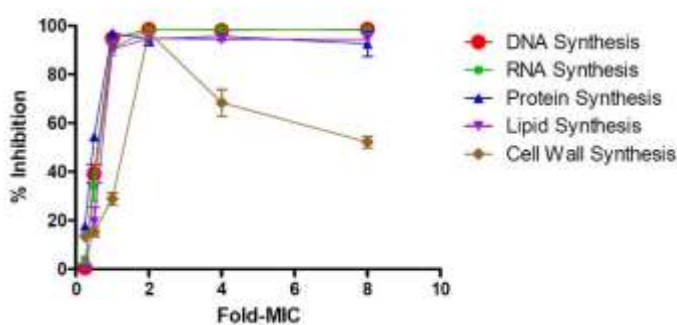


Figure 1.1 Inhibition of macromolecular synthesis by robenidine. *The inhibition of DNA, RNA, protein, lipid and cell wall synthesis by robenidine. Data unpublished, provided by Dr. Stephen Page, Neoculi.*

Following this a second assay was commissioned which measured the ATP leakage for *S. aureus* cells. Leakage of ATP can indicate that the integrity of the cell membrane has been lost (Higgins et al., 2005). It was found that robenidine at concentrations inhibitory to *S. aureus* growth, resulted in a large increase in extracellular ATP. This result in conjunction with the previous assay suggests that robenidine may target the cell membrane in Gram-positive bacteria ((Ogunniyi et al., 2017); Figure 1.2).

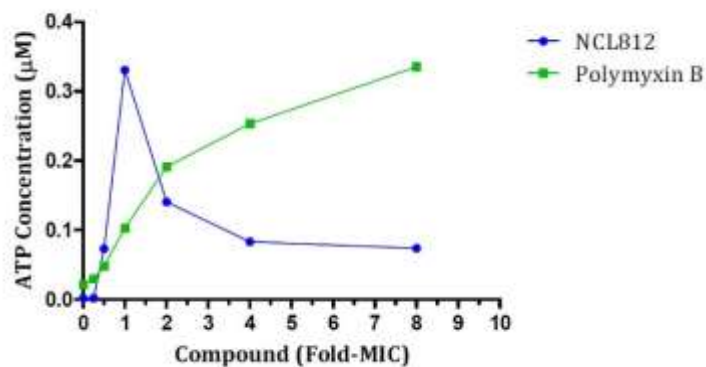


Figure 1.2 The effect of robenidine on ATP release from *S. aureus* ATCC 29213. NCL812 = robenidine. The fall in ATP concentration at higher concentrations of robenidine may be due to precipitation of robenidine causing a reduction in dissolved and therefore biologically available compound. Data provided by Dr. Stephen Page, Neoculi.

In addition to the initial studies performed with *S. aureus*, further studies have been performed with *S. pneumoniae* using transmission electron microscopy (TEM). *S. pneumoniae* cells exposed to robenidine for 6 or 12 hours were examined using TEM. After only six hours of exposure to 16 µg/ml of robenidine an increase in the thickness of the cell membrane and periplasmic space was observed. It has been proposed that the increased thickness of the cell membrane could be due to the accumulation of electron dense material beneath the cell membrane, while the increase in the thickness of the periplasmic space may be due to disruption of the cell membrane, either by depolarisation or the inhibition of ATPase (Ogunniyi et al., 2017). However, the increase in both cases was not extensive and the results are preliminary, suggesting further studies are required.

In an attempt to continue to understand the mechanism of action of robenidine a closely related analogue has also been included in this review. CGP 40215A was a very promising lead candidate in the discovery of new therapeutic agents for African trypanosomiasis but was abandoned due to the inability of the compound to cross the blood-brain barrier and therefore cure late stages of the disease (Brun et al., 2001a). Nevertheless, before the compound was abandoned the mechanism of action was extensively studied. CGP 40215A is considered an

analogue of methylglyoxalbisguanylylhydrazone (MGBG) and therefore a polyamine synthesis inhibitor. It is also a structural analogue of robenidine where the aromatic chloride molecules have been replaced with amidine moieties (Figure 1.3). CGP 40215A has been shown to inhibit the S-adenosylmethionine (AdoMet) decarboxylase enzyme isolated from *Trypanosoma brucei* cells, however this inhibition is much lower than other known decarboxylase inhibitors. In addition, whole cells were exposed to CGP 40215A before the AdoMet decarboxylase activity in cell extracts were measured and it was found that this drug decreased activity of the target enzyme by 68%. Furthermore, the putrescine levels were increased by 20% and the spermidine levels decreased by 36%, a secondary indicator that the AdoMet decarboxylase enzyme was not working optimally in these cells (Bacchi et al., 1996; Brun et al., 2001a). Further research with CGP 40215A to examine the mechanism of action in *Plasmodium falciparum*, as CGP 40215A is a potent inhibitor of *P. falciparum* *in vitro*, found that the drug did not affect cellular polyamine levels and inhibition could not be antagonized by the addition of spermidine or putrescine, unlike other inhibitors of polyamine synthesis (Das Gupta et al., 2005).

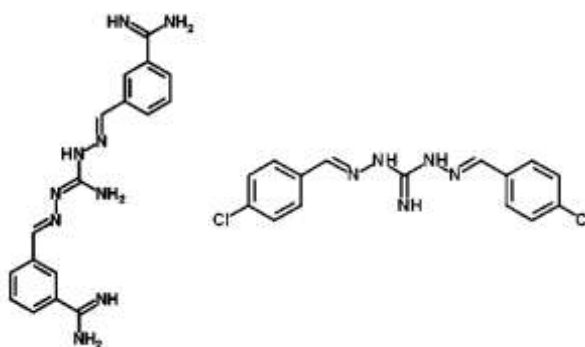


Figure 1.3: Structure of CGP 40215A (left) and robenidine (812) (right).

Additionally, CGP 40215A forms a strong bond with the AT region of DNA, which was unexpected, as the shape of the molecule does not match the curvature of the groove. Based on X-ray crystallography, the linker NH groups, which are conserved in robenidine, form direct hydrogen bonds with the thymine associated oxygen groups in the DNA helix. In addition, the amidine groups directly interact with the DNA. While only one amidine group is able to form direct bonds with the DNA at any time, due to the shape of the molecule, the linker guanine group acts as a hinge, so that the two amidines can switch between direct and indirect DNA interactions (Nguyen et al., 2002).

Given the information available in the literature, it is not possible to make a conclusion about the precise mechanism of action of robenidine. While robenidine was able to inhibit enzymes involved in oxidative phosphorylation in rat mitochondria, robenidine was only observed to

affect the mitochondria of *Eimeria* parasites after long exposure times and this effect is thought to be the result of the loss of cell integrity, not a direct action of robenidine itself (Lee and Millard, 1972; Wong et al., 1972). Although studies with the structural analogue CGP 20415A presented conflicting results in the ability of the drug to inhibit polyamine synthesis in different organisms, it was also found to bind strongly to the AATT region of DNA through the NH moieties in the core of the structure, a structural feature which is also found in robenidine (Bacchi et al., 1996; Das Gupta et al., 2005; Nguyen et al., 2002). Recent data obtained by Neoculi Pty. Ltd. have demonstrated the global inhibition of all macromolecular synthesis pathways in addition to the release of cellular ATP in *S. aureus* after exposure to the drug ((Ogunniyi et al., 2017); Figure 1.2). In addition, preliminary work has shown that robenidine increases the thickness of the periplasmic space and cell membrane of *S. pneumoniae* (Ogunniyi et al., 2017). TEM studies examining the effect of robenidine on the coccidian parasite *Eimeria* noted the distension of several membrane bound organelles in conjunction with membrane degradation (Lee and Millard, 1972). Taking this information into account it is likely that robenidine has a primary target within/of the cell membrane which would result in inhibition of oxidative phosphorylation and effect polyamine synthesis in addition to other essential cell functions. It is also possible that robenidine binds to DNA, as it shares the same linker as CGP 40215A, and this may be a secondary mechanism of action. However, to properly understand the mechanism of action of robenidine, further investigation is required.

1.3.4 The repurposing of robenidine

Robenidine has been used extensively in various animal production industries but has the potential for ‘repurposing’ for the treatment of alternative infectious diseases in animals, and possibly humans. Considering the history of use, safety profile and the preliminary data obtained by Neoculi Pty Ltd. robenidine appears to be an ideal candidate for further investigation as an antibacterial and antiparasitic agent.

1.4 Bacterial infections

Bacterial infections account for a significant proportion of global infections and are the leading cause of hospital acquired infections, with the two most prevalent causes of hospital acquired infections being MRSA and VRE (Fan et al., 2011; Zetola et al., 2005). While multidrug-resistant bacteria were originally only considered a problem in hospitals, serious community associated (CA)-MRSA strains that have a greater array of virulence factors are becoming more common. These strains differ in their degree of multidrug resistance when compared to hospital acquired strains and, unlike the hospital acquired strains, may cause serious disease in otherwise healthy individuals, including necrotising pneumonia (Zetola et al., 2005). Gram-negative

organisms such as *Enterobacteriaceae* spp. including *Escherichia coli*, *Klebsiella*, *Enterobacter* and *Pseudomonas aeruginosa* which are resistant to multiple antimicrobials, including those conferred by extended-spectrum beta-lactamases and carbapenemases, are also causing significant problems worldwide, especially in hospitals (Poole, 2003; Umland et al., 2014).

Although multi-drug resistant (MDR) hospital acquired infections are a significant threat to public health, there are also several pathogens prevalent in the community causing serious issues. For example, up to 30% of *S. pneumoniae* isolates, the leading cause of pneumonia worldwide resulting in ~ 1 million child deaths per year, are MDR (Neu, 1992; O'Brien et al., 2009). The development of MDR tuberculosis and now extensive drug resistant tuberculosis is a major concern for international health (Gandhi et al., 2010). Currently there are organisms that are pan-resistant to all available antimicrobials, making the need for new antimicrobial drugs extremely urgent (Pendleton et al., 2013; Rice, 2008).

1.4.1 Bacterial resistance mechanisms

The two main types of antimicrobial resistance in bacteria are intrinsic resistance, which may be a result of mechanisms that prevent drug access through the outer membrane of Gram-negative organisms, or acquired resistance such as an increase in efflux pumps (Kaye and Kaye, 2000).

1.4.1.1 Intrinsic Resistance

Intrinsic resistance is a form of resistance inherent in a microorganism. A very relevant form of intrinsic resistance in drug discovery is biofilm formation (Kaye and Kaye, 2000). Biofilms are formed on a surface when bacteria encase themselves in a complex matrix (Stewart and Costerton, 2001; Suh et al., 2010). This protective matrix can house thousands of bacterial cells and provide up to a 1000 times more resistance to many antimicrobials than the individual bacterial cells would otherwise have (Suh et al., 2010). Biofilms are able to persist after antimicrobial therapy causing recurrent symptomatic infections (Rendueles et al., 2013). Due to the presence of metabolically inactive persister cells within the biofilm matrix, many of the currently registered antibiotics are ineffective in biofilm eradication. This is due to the fact that many of the currently registered antimicrobials are only effective against metabolically active cells as they target the metabolic synthesis pathways of proteins, nucleic acids and the cell wall (Hurdle et al., 2011).

1.4.1.2 Acquired Resistance

Acquired resistance is a change in the genetic structure of an organism which confers resistance to an antimicrobial to which that organism was once susceptible (Kaye and Kaye, 2000). Genetic resistance can be encoded on chromosomal or plasmid DNA. Plasmid-encoded antimicrobial resistance can be easily transferred from one bacterium to another and can even be passed between species, e.g. from *Enterococcus* spp. to *Staphylococcus* spp. (Tenover, 2006). There are four recognised phenotypic expressions of genetic resistance; the action of efflux pumps, which transport the antimicrobial out of the cell so it cannot affect the target, the production of antimicrobial altering or degrading enzymes, which inactivate the antimicrobial and stop it from working, alterations in the target site such as changing the binding site and acquiring new pathways to bypass the antimicrobial targeted pathways (Neu, 1992).

1.4.2 Antimicrobials that affect bacterial membranes

The majority of current antimicrobial agents target one of five biosynthetic processes (synthesis of RNA, DNA, protein, folic acid or peptidoglycan) that are present in metabolically active bacteria (Hurdle et al., 2011). However, many infections are caused by stationary or quiescent bacteria that are not significantly metabolically active, therefore the traditional antimicrobials prove ineffective in eradicating these infections (Hurdle et al., 2011). Recently it has been noted that molecules that target the membrane of bacteria are able to kill metabolically active as well as metabolically inactive bacteria due to the necessity of the bacterial membrane for cell viability in both states. This discovery has led to the suggestion that bacterial membrane function is an ideal target for treating chronic bacterial infections, such as biofilms, but would also be effective in treating metabolically reproducing cells (Hurdle et al., 2011). In addition, there is experimental evidence that antimicrobials that affect the cell membrane are effective in treating parasitic protists such as *Plasmodium* and *Leishmania* (Torrent et al., 2012). The two main advantages of using cell membrane inhibitors, apart from the fact that they can destroy persistent infections, is the difficulty in developing resistant isolates and a multi-target effect (Hurdle et al., 2011; Ooi et al., 2009). This thesis focusses on the potential of repurposing robenidine as an antimicrobial agent. Based on preliminary data it has been suggested that robenidine potentially affects the cell membrane of target cells (Ogunniyi et al., 2017). Therefore, due to the large number of antibacterials available, only antimicrobials that affect the cell membrane and therefore could provide some insight into the mechanism of action of robenidine have been included in this review. There are currently a number of cell membrane inhibitors on the market including daptomycin, the polymyxins and the gramicidins, all of

which are classified as antimicrobial peptides (Hancock and Sahl, 2006; Straus and Hancock, 2006).

1.4.2.1 Antimicrobial peptides

Antimicrobial peptides are produced by all living organisms from bacteria to humans and form part of the innate immune response. Although there is a large variety of compounds in this group they all consist, at least in some part, of various combinations of amino acids (Epan and Vogel, 1999; Fan et al., 2011). All the antimicrobial peptides currently in clinical use originate from microbial organisms with the majority targeting the bacterial cell membrane, however there are some exceptions such as vancomycin which inhibits cell wall synthesis (Allen and Nicas, 2003; Mangili et al., 2005; Reynolds, 1961). For the purpose of this review, only antimicrobial peptides that target the cell membrane will be mentioned. The three main classes of antimicrobial peptides that contain compounds that target the cytoplasmic membrane are cationic antimicrobial peptides, lipopeptides and glycopeptides (Allen and Nicas, 2003; Hale and Hancock, 2007; Straus and Hancock, 2006).

1.4.2.2 Cationic antimicrobial peptides

Cationic antimicrobial peptides (CAMPs) are positively charged amphiphilic molecules composed of amino acids (usually between 15 – 50) that have shown antimicrobial activity under physiological conditions (Fox, 2013). CAMPs generally have broad spectrum antibacterial activity and most commonly form stabilised β -sheets or α -helices (Deslouches et al., 2005a; Hancock, 1997). Several CAMPs have successfully been taken into pre-clinical and clinical trials, however gramicidins are the only class of CAMPs currently in clinical use. Gramicidins are small linear peptides with the exception of gramicidin S which is a dimer forming a cyclic structure. Gramicidins have toxic side effects, limiting them to topical or local applications only (Deslouches et al., 2005a; Hancock, 1997). Work on other pre-clinical CAMPs indicate that toxicity issues are easily overcome via slight modifications to amino acid composition, which could possibly be applied to the gramicidins to expand their possible clinical uses (Deslouches et al., 2007; Deslouches et al., 2005a).

Currently there are several CAMPs that are in clinical or pre-clinical trials including MX-266, Omiganan, A3-APO, WLBU2 and Ctriporin. Both MX-266 and Omiganan are presently in phase III clinical trials, MX-266 for the treatment of mild to moderate acne and Omiganan for the prevention of catheter associated infections (Deslouches et al., 2005a; Fan et al., 2011; Hancock and Sahl, 2006; Marr et al., 2006; Szabo et al., 2010). A3-APO, WLBU2 and Ctriporin have been shown to be promising candidates in mouse models for the treatment of Gram-negative (A3-APO and WLBU2) or Gram-positive (Ctriporin) infections. Both A3-APO and

WLBU2 have potential use as systemic peptides, over gramicidins, curing mice of septicaemia while ctriporin has potential application as a topical ointment for the treatment of MRSA and other multi-drug resistant Gram-positive infections (Deslouches et al., 2005a; Fan et al., 2011; Hancock and Sahl, 2006; Marr et al., 2006; Szabo et al., 2010)

1.4.2.3 Lipopeptides

The lipopeptides have proven to be the most successful antimicrobial peptides in clinical settings. The majority of lipopeptides are cyclic with a fatty acyl side chain which allows interaction with the cell membrane (Qian et al., 2012). The two most prominent antibacterial lipopeptides are daptomycin and the polymyxins. Both are cyclic lipopeptides, however daptomycin is anionic showing specificity towards Gram-positive organisms while polymyxins are cationic showing specificity towards Gram-negative organisms (Jeu and Fung, 2004; Mogi and Kita, 2009).

1.4.2.4 Glycopeptides

Glycopeptides are peptides that contain carbohydrates and as antimicrobial compounds are generally considered to inhibit peptidoglycan synthesis. There is a small sub-group of this class which has recently been approved for use in the USA and Europe, known as lipoglycopeptides, which have been shown to be effective against cell membranes. Currently available compounds from this class include dalbavancin and telavancin (Bouza et al., 2017; Gudiol et al., 2017). This sub-group contains fatty acyl side chains as well as carbohydrates. (Zhanel et al., 2010; Zhanel et al., 2012).

1.4.2.5 Advantages and disadvantages of using antimicrobial peptides

There are several advantages in the use of peptides as antimicrobial agents. Firstly, it is difficult to select for resistance to antimicrobial peptides in microorganisms, secondly they tend to be bactericidal rather than bacteriostatic, thirdly they have a multi-target effect and finally they are usually effective in the treatment of biofilms (Bahar and Ren, 2013; Overhage et al., 2008).

The main disadvantages of using antimicrobial peptides in medicine is potential toxicity to the host, their sensitivity to proteases and the cost of production (Fox, 2013). The first two issues can be easily overcome by creating small chemical modifications to the peptides which significantly reduce toxicity and decrease sensitivity to proteases as proven by the synthetic peptide WLBU2 (Bahar and Ren, 2013; Deslouches et al., 2007; Deslouches et al., 2005b). The high cost of peptide production is the main hindrance in their clinical use with a single dose costing hundreds of dollars to produce in some cases. There has been research into the potential

of large-scale production of antimicrobial peptides at a reasonable price using bacterial recombinant expression systems (Hancock and Lehrer, 1998).

Another concern raised in the use of antimicrobial peptides is the development of cross-resistance in bacterial populations to the innate immune peptides, particularly when human derived peptides are used. Although this is a possibility, it seems highly unlikely to cause major problems as development of resistance to peptides seems to be rare (Hancock and Sahl, 2006).

1.4.2.6 Other classes of bacterial cell membrane inhibitors

1.4.2.7 Porphyrins

Only one member of this class, XF-73 with a Gram-positive spectrum, has been identified. It has a structure distinct from other antimicrobial classes and it targets the bacterial cell membrane with activity against slow growing organisms observed. After 55 passages at sub-inhibitory levels of XF-73, no resistant organisms were identified (Ooi et al., 2009; Ooi et al., 2010).

1.4.2.8 Quinoline-like molecules

Quinoline molecules are a group of related natural and synthetic compounds which share a bicyclic core structure and commonly have antibacterial activity (Aldred et al., 2014). HT61 was discovered in 2010 after screening a large number of possible antimicrobial agents for activity against 10-day old stationary phase *S. aureus* cells (Hu et al., 2010). HT61 was identified as a quinoline-like molecule which is active against the cell membrane of Gram-positive bacteria, but not Gram-negative bacteria (Hu et al., 2010). HT61 is very effective at killing stationary phase cells when compared with currently available drugs. Additionally, animal trials show that a skin infection of stationary phase *S. aureus* can be completely killed in 2 hours (Hu et al., 2010). Further investigation is needed to determine if there is similar activity towards biofilms as was seen against stationary cells, which have different antimicrobial defence systems.

1.4.2.9 Riminophenazines

Define riminophenazines as a class of compounds where the ‘imino’ part of the molecule has been modified (Reddy et al., 1999). Clofazimine is a synthetic riminophenazine antimicrobial that is known to be effective against mycobacteria including tuberculosis and leprosy. Although the drug was first identified in 1957 it wasn’t until 1998 that its activity against Gram –positive organisms such as *S. aureus* was identified (Oliva et al., 2004; Reddy et al., 1999). Initial studies into the mechanism of action of clofazimine suggested the main target of clofazimine was RNA and DNA. However more recent studies suggest that clofazimine causes non-specific

membrane damage, resulting in inhibition of RNA, DNA and protein synthesis (Oliva et al., 2004).

1.5 Protistan infections

Protists are an extremely diverse group of primarily unicellular eukaryotic organisms encompassing both free-living and parasitic groups. Some of the most devastating human parasitic pathogens belong to this kingdom including *Plasmodium*, *Trypanosoma*, *Trichomonas* and *Giardia*. Encompassed within this kingdom are the flagellates – a group of organisms that move via the use of one or more flagella at some stage within their lifecycle. Several parasitic protists belong to this group and cause widespread human and animal disease. For the purposes of this review, and the thesis in general, three model organisms from this group will be discussed - *Giardia duodenalis*, a diplomonad, *Trypanosoma brucei* and *Leishmania donovani*, both kinetoplasts. *G. duodenalis* is the most common cause of waterborne diarrhoea worldwide, contributing to numerous deaths (Lloyd and Williams, 2014), while *T. brucei* and *L. donovani* contribute to 100 000 deaths per year with over 3 million people at risk (Alvar et al., 2012; Turrens 2004; Stuart et al., 2008).

1.5.1 Kinetoplasts – *Trypanosoma brucei* and *Leishmania donovani*

The kinetoplastid protists that cause leishmaniasis and human African trypanosomiasis (HAT) share similar biochemical features, such as a unique thiol metabolism system, and have a similar structure, characterised by a kinetoplast, which is a discretely structured DNA body located in the mitochondrion. Other shared structural features include a glycosome; specific organelles for glycolysis, a single mitochondrion and a sub-pellicular microtubular corset (Barrett and Croft, 2012; Stuart et al., 2008).

Leishmaniasis, often considered as a disease complex, is caused by several different species of *Leishmania*, including *L. donovani*. There are two major manifestations of the disease, cutaneous leishmaniasis and visceral leishmaniasis (kala azar), with several rarer manifestations including mucocutaneous leishmaniasis and post-kala azar dermal leishmaniasis (Barrett and Croft, 2012; Grevelink and Lerner; Stuart et al., 2008). It is estimated that there are currently 0.2 - 0.5 million cases per year of visceral leishmaniasis predominantly caused by *L. donovani*, which is fatal if left untreated (Alvar et al., 2012; Stuart et al., 2008). While cutaneous leishmaniasis (CL) establishes as an open sore at the location of the vector bite, it will usually heal spontaneously leaving a scar (Barrett and Croft, 2012). Visceral leishmaniasis manifests initially as skin lesions before developing into gross inflammation within the viscera – in particular the liver and spleen (Barrett and Croft, 2012). *L. donovani* is transmitted by an insect

vector, the *Phlebotomus* sandflies. The sandfly ingests cells infected with *Leishmania* amastigotes. The amastigotes transform into promastigotes in the gut of the sandfly, multiply and migrate to the proboscis. Promastigotes are transferred from the sandfly to the victim during a blood meal. The parasites are phagocytized by mononuclear phagocytic cells where they transform into amastigotes and replicate (Figure 1.3).

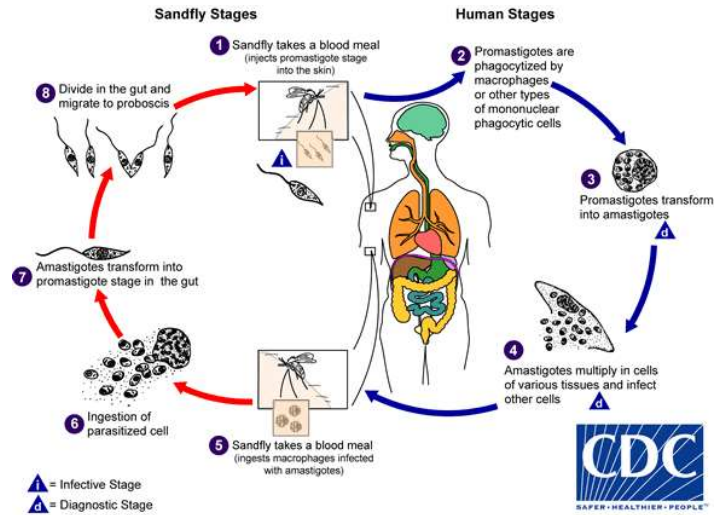


Figure 1.4 Lifecycle of *Leishmania*. Promastigotes are released into the human bloodstream via an infected sandfly as it bites. The promastigotes are phagocytosed and transform into amastigotes. The amastigotes multiply in the cells before moving on to infect naive cells. The parasite is transferred to the sandfly during a blood meal as amastigotes which transform into promastigotes in the sandfly gut. Image in the public domain credited to CDC-DPDx/Alexander J. da Silva, PhD.

Trypanosomiasis, in particular caused by *T. brucei*, is endemic to various regions of the sub-Saharan Africa and commonly known as sleeping sickness as late stages of the disease include altered sleep-wake cycles (Barrett and Croft, 2012; Field et al., 2017). It was estimated in 2006 that ~ 70 000 individuals were infected (Lutje et al., 2013). Infection is transmitted via the bite of an infected Tsetse fly (Figure 1.4).

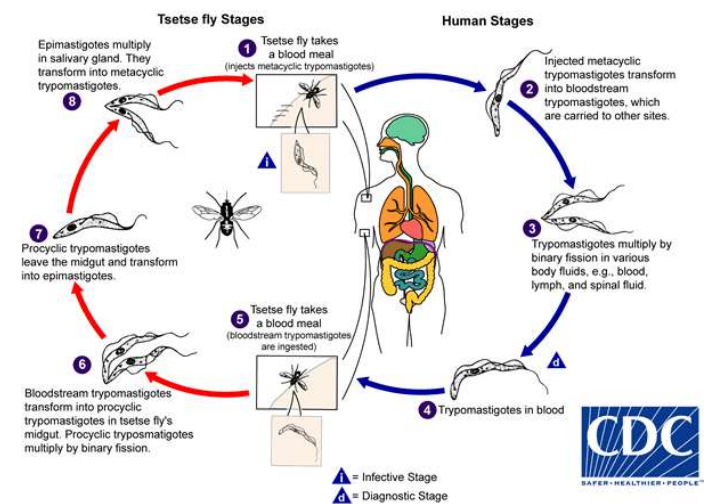


Figure 1.5 Lifecycle of *Trypanosoma* sp. Parasites are injected into the bloodstream via the bite of the tsetse fly. They multiply in various bodily fluids. Parasites are transferred to the Tsetse fly during a blood meal where they multiply in the midgut, transform into epimastigotes and travel to the salivary glands. Image in the public domain credited to CDC-DPDx/Alexander J. da Silva, PhD.

In the first stage of the disease parasites proliferate in the lymphatic system and blood, causing symptoms such as headaches, intermittent fever and lymphadenopathy (Barrett and Croft, 2012; Buscher et al., 2017; Lutje et al., 2013; Stuart et al., 2008). The second stage of the disease is characterised by the invasion by parasites of the central nervous system, including the brain. Symptoms of the second stage of disease are a result of neurological breakdown and include altered sleep-wake cycles, narcolepsy, semi coma, chronic meningoencephalitis and psychiatric disorders including depression. The rate of progression from stage 1 to stage 2 disease depends on the subspecies of trypanosome causing the disease but varies from 2 weeks to 18 months (Barrett and Croft, 2012; Lutje et al., 2013; Stuart et al., 2008). The disease is invariably fatal if left without treatment and is considered one of the hardest diseases to control in sub-Saharan Africa due to difficulty in diagnosis and treatment as well as civil unrest (Buscher et al., 2017; Lutje et al., 2013).

Chagas disease, caused by *T. cruzi*, is also a significant problem. Chronic reactivation and congenital Chagas disease is likely to cause significant problems in the future with an estimated 16 million people already infected (Hemmige et al., 2012).

1.5.2 Current drugs in the treatment of leishmaniasis and trypanosomiasis

Leishmaniasis

There are five available drugs for the treatment of leishmaniasis; pentavalent antimonials, amphotericin B, miltefosine, paromomycin and pentamidine, with varying efficacy against different *Leishmania* sp. (Barrett and Croft, 2012; Croft, 2008; de Menezes et al., 2015).

Pentavalent antimonials have been widely used historically. There is variable effectiveness against different forms of leishmaniasis (35 – 95%) and resistance is common in certain places making the drug obsolete (e.g. >65% in Bihar, India) (Barrett and Croft, 2012; Croft, 2008; de Menezes et al., 2015). Administration can be intravenous, intramuscular or intralymphatic once per day for 20 days (de Menezes et al., 2015). Serious side effects of using antimonials include vomiting, anorexia, myalgia and headaches. In rare cases, antimonials can cause fatal cardiac arrhythmia (de Menezes et al., 2015).

Amphotericin B has become the first line drug in certain states in India where resistance to pentavalent antimonials has restricted their use (Croft, 2008). It is also used to treat specific types of cutaneous leishmaniasis in South America (Barrett and Croft, 2012). Amphotericin B

is delivered intravenously which causes infusion-related reactions such as rigor, fever and chills and the drug itself has been associated with more serious side effects such as myocarditis and nephrotoxicity (de Menezes et al., 2015). Alternative formulations to reduce toxicity have been developed. These formulations do not remove all side effects and are much more expensive but they significantly shorten treatment times, from once per day for 20 days to a single dose (de Menezes et al., 2015).

Pentamidine has an efficacy of treatment from 35 – 96% depending on the *Leishmania* species being targeted (de Menezes et al., 2015) and is generally limited to the treatment of specific types of cutaneous leishmaniasis in South America (Barrett and Croft, 2012). Intramuscular administration over 8 days is required and a high rate of hyperglycemia is reported (de Menezes et al., 2015).

Paromomycin has been used to treat leishmaniasis in various formulations for several decades (Barrett and Croft, 2012). It is delivered either intramuscularly for visceral leishmaniasis or topically to cutaneous forms of the disease daily for 17- 21 days. It is relatively cheap and highly efficacious in India with the major side effects including severe nephrotoxicity, ototoxicity and hepatotoxicity (de Menezes et al., 2015).

Miltefosine is the first oral drug to be developed for the treatment of leishmaniasis (Croft, 2008). It is highly efficacious in both India and Africa requiring daily dosing for 28 days (de Menezes et al., 2015). There has been some variable species dependent effectiveness against CL reported (Barrett and Croft, 2012). Miltefosine is contraindicated for use in pregnant women due to teratogenic effects seen in rodents. Side effects of miltefosine use include vomiting, diarrhea, hepatotoxicity and nephrotoxicity (de Menezes et al., 2015).

Trypanosomiasis

There are five drugs currently used for the treatment of human African trypanosomiasis (HAT), but only four have been approved for clinical use (Barrett and Croft, 2012; Buscher et al., 2017; Fairlamb, 2003; Field et al., 2017). All of these drugs were introduced for use \geq 40 years ago. Currently suramin and pentamidine are recommended for early stage disease while melarsoprol and eflornithine are used in the late stage of disease. Nifurtimox is used on compassionate grounds to treat late stage disease when other drugs fail (Fairlamb, 2003). Unfortunately, all current therapies for HAT are unsatisfactory due to toxicity, poor efficacy, resistance and undesirable administration requirements (Barrett and Croft, 2012; Fairlamb, 2003).

Pentamidine was introduced in 1973 and is the first line treatment for stage 1 infections caused by *T. b. gambiense*. It is only used as a secondary treatment for stage 1 *T. b. rhodesiense*

infections when Suramin is contra-indicated (due to lower reliability) (Fairlamb, 2003). Pentamidine is not used to treat 2nd stage disease as it does not effectively cross the blood-brain barrier. Pentamidine can cause damage to several organs including the pancreas which can lead to diabetes (Fairlamb, 2003). Intramuscular administration is preferred as the drug has poor oral availability and intravenous administration can cause severe hypotensive reactions (Barrett and Croft, 2012; Fairlamb, 2003).

Suramin was introduced in the early 1900s and is the first treatment option for early stage disease caused by *T. b. rhodesiense*. Administration is via slow intravenous injection over a 4-week period. Immediate side effects include nausea, vomiting, collapse and shock while long term toxic side effects can include pyrexia, nephrotoxicity, urticarial neuropathy, severe diarrhea and haemolytic anaemia (Barrett and Croft, 2012; Fairlamb, 2003).

Melarsoprol, an arsenical, was first introduced as a treatment for HAT in 1949. It is used to treat the late stage of disease after parasites have crossed into the CNS (Fairlamb, 2003). It is the only treatment option for stage 2 *T. b. rhodesiense*. Serious reactive encephalopathy afflicts 5-10% of patients, half of which die. Other side effects include pyrexia, headache, pruritus, thrombocytopenia, vomiting, abdominal colic and heart failure (Barrett and Croft, 2012; Fairlamb, 2003). Administration is via intravenous injection over 10 days (Barrett and Croft, 2012). Resistance to melarsoprol is becoming a problem in the field (Barrett and Croft, 2012).

Eflornithine is used as a first line treatment for late stage disease caused by *T. b. gambiense*. It is not very effective in treatment of disease caused by *T. b. rhodesiense* and therefore is not recommended (Barrett and Croft, 2012; Fairlamb, 2003). Administration is time consuming and costly requiring intravenous infusion multiple times per day for up to 14 days (Barrett and Croft, 2012; Fairlamb, 2003). Side effects include fever, headache, hypertension, macular rash, peripheral neuropathy, tremor and gastrointestinal problems e.g. diarrhea (Barrett and Croft, 2012).

Although Nifurtimox is registered for the treatment of Chagas disease, caused by *T. cruzi*, it is only used on compassionate grounds for the treatment of late stage HAT when melarsoprol and eflornithine fail (Fairlamb, 2003). There is also a promising new drug undergoing clinical trials, fexinidazole, which could be approved as early as 2018 (Maxmen, 2017).

1.5.3 Diplomonads - *Giardia duodenalis*

Giardia duodenalis (syn. *G. lamblia*, *G. intestinalis*) is the most common enteric parasitic protist worldwide with estimates of 1 billion infections annually, mostly occurring in children in resource poor communities where infection rates can be as high as 100%. In developed

nations infection is generally estimated at 7% (Fletcher et al., 2012; Halliez and Buret, 2013; Upcroft and Upcroft, 1998; Upcroft and Upcroft, 2001a). Due to the association of infection with undeveloped countries, *Giardia* has been included as part of the WHO neglected diseases initiative (Savioli et al., 2006). Infectious cysts are ingested by the host through contaminated food or water or directly via the faecal oral route with symptoms being noticed several days to weeks after exposure. Symptoms may include diarrhoea, abdominal cramps, flatulence, bloating and weight loss which can last for several weeks if left untreated. Chronic infections, particularly in children, can lead to failure to thrive syndrome which includes growth stunting and decreased intellectual development (Buret, 2008). More recently giardiasis has been recognised as being associated with the development of other diseases including arthritis, post-infectious irritable bowel syndrome and chronic fatigue syndrome (Halliez and Buret, 2013).

There are several classes of anti-giardial agents on the market, including the nitroimidazoles and benzimidazoles. With the emergence of drug resistance, adverse side effects of available drugs and sub-optimal dosing regimens, the utility of the available drugs is limited (Bendesky et al., 2002; Jokipii and Jokipii, 1979; Watkins, 2003; Wright et al., 2003). Due to the limitations of the available drugs and the consequences of infection it is of high priority to develop new drugs for the treatment of giardiasis. The development of new drugs is dependent on robust *in vitro* tests to first identify and characterise potential candidates followed by *in vivo* efficacy, toxicity and PK/PD studies to confirm *in vitro* results. Although there is an unmet need for new anti-giardial agents, there is a lack of standardised systems for the development of potential drug candidates *in vitro* and *in vivo* which, among other things, limits inter-laboratory comparisons (Benere et al., 2007; Gardner and Hill, 2001). In this section of the review the current treatment options, efficacy screens available *in vitro* and *in vivo* to facilitate the standardisation of the evaluation of new anti-giardial agents and allow the potential for inter-laboratory comparisons, as well as promising new anti-giardial compounds are discussed.

The desired profile for new anti-giardial drugs would include the inability for the selected compound to travel across the intestinal barrier and a slow passage through the gastrointestinal tract as *Giardia* trophozoites attach to the epithelial cells but do not invade (Thompson, 2000). In addition, it would be beneficial for the compounds to have high selectivity for *Giardia* over other microorganisms as, with most of the current drugs available, treatment can result in significant disruption to the gastrointestinal microbiota which can cause a cascade effect of further health problems (Adamsson et al., 1999; Jakobsson et al., 2010; Jernberg et al., 2007; Shreiner et al., 2015).

1.5.4 Current drug therapies available for the treatment of *Giardia*

Several antiparasitics have been developed for the treatment of *G. duodenalis* infections, the main classes currently and historically used being acridine derivatives, nitroimidazoles, nitrofurans, benzimidazoles, nitrothiazolyl derivatives and aminoglycosides (Figure 1.5). Each class has advantages and disadvantages to use (Escobedo and Cimerman, 2007; Upcroft et al., 1996).

Acridine derivatives

Quinacrine, an acridine derivative, was the first drug widely used in the treatment of giardiasis before the introduction of metronidazole in the 1960s. The clinical efficacy of quinacrine has been reported as high as 90% when administered over 5-10 days, with the recommended treatment lasting for 5 days (Miyamoto and Eckmann, 2015). Side effects of the drug include nausea and vomiting and the compound is reported to have a bitter taste which contributes to poor compliance amongst patients. More severe side effects have included toxic psychosis and other psychiatric disturbances. Discolouration of the skin and nails has also been reported. In addition, this drug is contra-indicated in patients with glucose-6-phosphate dehydrogenase deficiency due to haemolysis and in pregnancy due to cross-placental transfer and a possible link to spina bifida and renal agenesis in the foetus. There is also a disulfiram like effect (which includes headaches, nausea, vomiting, chest pain, blurred vision and difficulty breathing) when taken in conjunction with alcohol (Escobedo and Cimerman, 2007; Gardner and Hill, 2001; Upcroft et al., 1996). The mechanism of action of this class of anti-giardials is not fully understood, it was originally thought to interfere with DNA synthesis, as this was observed *in vitro*, and it has been understood to inhibit the cytoplasmic NADH oxidase enzyme. However, studies involving the natural fluorescence of the molecule did not locate it to the nucleus of the parasite where DNA is located or in the cytoplasm with the oxidase enzyme, instead it appears to localise at the cell membrane which continues to deteriorate over time after exposure to the drug. (Upcroft et al., 1996; Upcroft and Upcroft, 2001b).

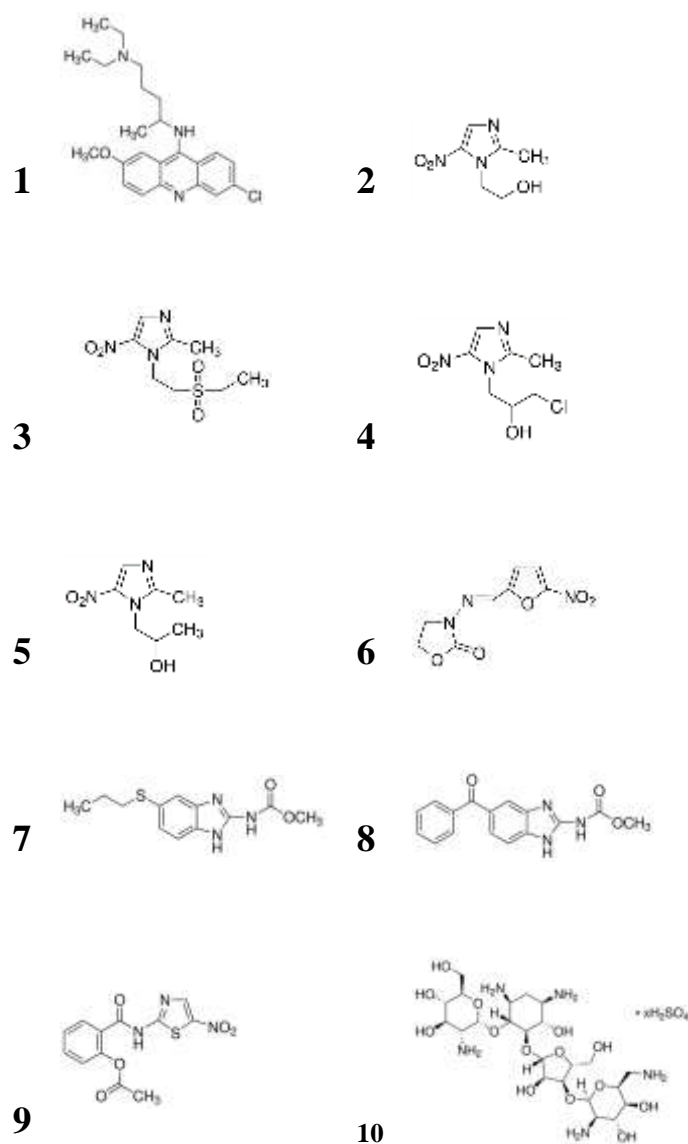


Figure 1.6 Drug structures of currently and historically used anti-giardials. 1 – quinacrine, 2 – metronidazole, 3 – tinidazole, 4 – ornidazole, 5 – secnidazole, 6 – furazolidone, 7 – albendazole, 8 – mebendazole, 9 – nitazoxanide, 10 – paromomycin.

5- nitroimidazoles

Antigiardial activity of the 5-nitroimidazoles was first discovered in the 1950s with the identification of metronidazole, which is the current ‘gold-standard’ treatment for giardiasis, and has been a mainstay in treatment for the last 50 years. Other 5-nitroimidazoles that can be used in therapy include tinidazole, ornidazole and secnidazole but these are not available in all countries. The mean efficacy of metronidazole is around 88% when taken for 5-10 days (Gardner and Hill, 2001). Longer durations of dosing as well as shorter higher doses have been tested but both result in a drop in efficacy, due to poor compliance and side effects in the former case. Mild side effects can include a metallic taste, nausea and headaches, which in addition to long dosing periods, can contribute to poor compliance amongst patients. More significant side effects include central nervous system toxicity, particularly with higher doses. Studies in bacteria and animals suggest that metronidazole is mutagenic and carcinogenic however at therapeutic doses there is no evidence to suggest that metronidazole is a significant risk for the development of cancer in humans (Gardner and Hill, 2001). Studies into the use of metronidazole during all stages of pregnancy do not show any increase in congenital abnormalities in relation to metronidazole use (Koss et al., 2012). Metronidazole is contraindicated with the ingestion of alcohol due to a disulfiram like effect (Escobedo and Cimerman, 2007). Development of resistance to metronidazole has been induced in the laboratory as well as documented in the clinic (Gardner and Hill, 2001; Tejman-Yarden et al., 2013; Upcroft and Upcroft, 2001b; Wright et al., 2003).

The mechanism of action of nitroimidazoles requires activation of the drug by reduction of the nitrogroup via anaerobic metabolic pathways in *Giardia*. *In vitro* this can be done by pyruvate:ferredoxin oxidoreductase (PFOR) or ferredoxin and metronidazole resistant organisms show a down regulation of PFOR and ferredoxin enzymes (Upcroft and Upcroft, 2001b). Once active the drug damages important biomolecules such as lipids, proteins and DNA and is also thought to inhibit oxygen consumption of the parasite by acting as an alternate electron acceptor (Ansell et al., 2016; Escobedo and Cimerman, 2007).

Tinidazole has a similar cure rate to metronidazole however it has one significant advantage – only a single dose is required with a mean efficacy of 92% (Gardner and Hill, 2001). As with metronidazole there are still side effects such as a bitter taste or a rash and tests in bacteria suggest it has a similar mutagenic profile to metronidazole. In addition, as a precaution it is not recommended for use in pregnant patients although studies in pregnant animals did not identify any developmental delays in offspring of exposed mothers (Escobedo and Cimerman, 2007).

Ornidazole is also usually given as a single dose in the treatment of giardiasis and is generally better tolerated than metronidazole and tinidazole however there have been rare reports of the development of hepatitis and cholangitis, which improved after discontinuation of the drug (Escobedo and Cimerman, 2007; Gardner and Hill, 2001).

Nitrofurans derivatives

Furazolidone, the representative anti-giardial from this family, is slightly less effective than quinacrine and metronidazole, with a reported clinical efficacy rate of 80%. The major advantage of furazolidone over the examples from previous classes described is the ease of administration to young children with a liquid formulation available (Gardner and Hill, 2001). Treatment is required over 5 to 10 days and common side effects include diarrhoea, nausea and vomiting which all contribute to patient non-compliance. Furazolidone is contraindicated in glucose-6-phosphate D deficiency (due to haemolysis), in patients already taking monoamine oxidase inhibitors (as furazolidone has a monoamine oxidase inhibitory effect) or breastfeeding mothers and neonates, as infants can develop haemolytic anaemia. In addition, as with acridine derivatives and nitroimidazoles, alcohol should be avoided due to a disulfiram like effect. Although furazolidone is carcinogenic in animals a similar effect has not been observed in humans but this could be due to a lack of surveillance in exposed populations rather than a lack of risk (Gardner and Hill, 2001).

Similarly to nitroimidazoles, nitrofurans derivatives are reduced by the NADH oxidase enzyme to nitro radicals which damage essential cellular components such as DNA (Escobedo and Cimerman, 2007).

Benzimidazoles

The benzimidazoles, including albendazole and mebendazole, are relatively new additions to the anti-giardial arsenal. Although these drugs are more effective than metronidazole and quinacrine *in vitro* this is not translated to clinical efficacy (as the benzimidazoles have clinical efficacy reportedly between 35 and 96% depending on the dosing schedule). Side effects are uncommon but can include abdominal pain, vomiting, nausea and diarrhoea. In addition, benzimidazoles (i.e. albendazole) are not recommended in pregnancy due to a teratogenic effect observed in rats, which is yet to be observed in humans (Escobedo and Cimerman, 2007; Gardner and Hill, 2001). The mechanism of action of albendazole has been extensively studied and it is known to target β -tubulin resulting in impaired glucose uptake and inhibition of cytoskeleton polymerisation in the parasite (Escobedo and Cimerman, 2007).

Nitrothiazolyl derivatives

Nitazoxanide and its metabolite tizoxanide have demonstrated *in vivo* efficacy much greater than metronidazole and even albendazole. In the clinical environment nitazoxanide has relatively good efficacy ranging between 64 and 94% and is recommended once per day for 3 days. The mechanism of action is thought to affect the plasma membrane of the parasite resulting in the formation of large empty vacuoles in the cytoplasm and general cell swelling. The mechanism of action is thought to be reliant on the nitro group, as with the other nitro containing classes of anti-giardials, however the action of this class is not dependant on same reduction pathways as the nitroimidazoles. Therefore, this class of drug is still an effective choice for treating parasites resistant to nitroimidazoles, such as metronidazole. In addition, there are few side effects observed with the most significant being abdominal discomfort. Other side effects are similar to previous drug classes mentioned including diarrhoea, vomiting and nausea. Furthermore, studies in animals have not demonstrated any adverse side effects on fertility or identified any mutagenic effect however, use in pregnancy is not recommended as no human clinical studies have been performed in pregnant patients with this drug (Escobedo and Cimerman, 2007).

Aminoglycosides

Paromomycin is the currently used aminoglycoside in the treatment of giardiasis and has a very broad spectrum ranging from complex parasites such as helminths to single celled prokaryotes. It is considered a much safer drug than others available and is recommended for the treatment of pregnant women however it can accumulate in patients with impaired renal function resulting in renal toxicity. Although side effects are rare they can include nausea and diarrhoea. Clinically paromomycin has shown less efficacy when compared to metronidazole, is required to be taken for 10 days and can disrupt the normal gut microflora (Escobedo and Cimerman, 2007; Gardner and Hill, 2001). This group of anti-giardials is thought to inhibit protein synthesis by binding to giardial ribosomes.

1.5.5 Potential anti-giardial candidates identified in assays to date

Numerous studies in recent years have involved the high throughput screening (HTS) of thousands of drug-like chemicals for activity against *G. duodenalis*. Of these studies many end after *in vitro* testing. In the last five years only a handful of compounds that have been identified as anti-giardial *in vitro* have had *in vivo* activity confirmed, all of which are already approved for use in humans for other diseases. The three drugs presented here, while promising anti-giardial agents, still have several limitations which, ideally, need to be overcome

(Figure 1.6). These limitations include little selectivity for the parasite in question, with activity against other microorganisms and side effects in the human host (Gardner and Hill, 2001).

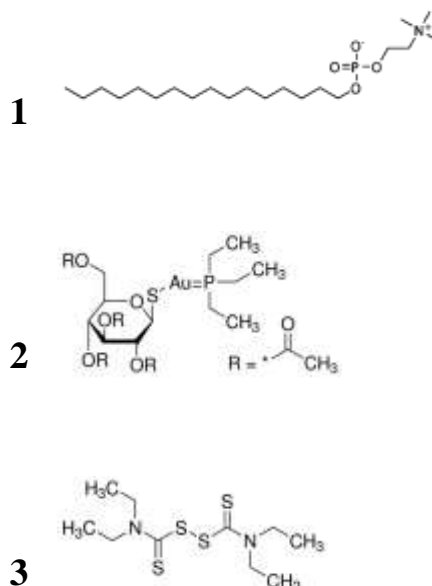


Figure 1.6 Structures of experimental drugs for treatment of giardiasis. 1 – miltefosine, 2 – auranofin, 3- disulfiram.

Miltefosine

Miltefosine is an alkylphosphocholine that is used as a treatment for breast cancer skin metastases and as an oral treatment for leishmaniasis. In addition, it has demonstrated antibacterial, antifungal and anthelmintic activity in addition to anti-giardial activity. Possible side effects can include nausea, diarrhoea and vomiting and there is potential for teratogenicity, which would exclude pregnant women from treatment. *In vitro* it has superior activity to metronidazole with an 100% inhibitory effect at 40 μ M after just 1 hour. In addition, it has been tested in a mouse model with three days of a single oral dose of 20 mg/kg able to cure an infection. As with most anti-giardial drugs the mechanism of action appears to be complex and is not fully understood. Based on electron microscopy studies, miltefosine is thought to interact with the cell membrane causing cell lysis and possibly also disintegrating the microtubules of the parasite, which affects its ability to attach to the host's intestinal surface (Eissa and Amer, 2012). In addition, it is thought that miltefosine causes a buildup of ceramide in the cell by interfering with sphingomyelin biosynthesis resulting in an apoptosis like response (Eissa and Amer, 2012).

Auranofin

A HTS of 910 chemical entities, 603 FDA approved and 143 approved for human use in at least one country, were tested for efficacy against *G. duodenalis in vitro* using an image based assay for detection of trophozoite adherence (Gut et al., 2011). From this screen, ~20 promising anti-giardial agents were discovered and auranofin, currently used in the treatment of rheumatoid arthritis, was considered the most promising candidate to continue with as it has a well-established toxicity profile and is considered safe for use in humans. Auranofin, is composed of a gold molecule with attached thiol and phosphate groups, with the potential to treat a wide range of diseases from cancer to bacterial infections (Roder and Thomson, 2015). It has been shown to be a potent inhibitor of the *Giardia* flavoenzyme thioredoxin oxidoreductase isolated from the parasite and this is assumed to be the mechanism of action by which the drug affects the parasite. In addition, *in vivo* efficacy in two animal models has been demonstrated, mice and gerbils, when treated once/day for 5 days. It is able to kill metronidazole resistant parasites and causes cellular blebbing similar to other thioredoxin oxidoreductase inhibitors (Tejman-Yarden et al., 2013; Watkins, 2003).

Disulfiram

Disulfiram is an FDA approved disulphide drug that has traditionally been used in the treatment of alcoholism as it causes unpleasant side effects, similar to a hangover, upon the consumption of alcohol. Use in the treatment of alcoholism has declined due to poor patient compliance and other possible uses of the drug are being explored, one of which is as an anti-giardial. Disulfiram and its metabolite, which is more potent, thiram are able to inhibit metronidazole resistant *Giardia in vitro*. The *in vivo* activity of both compounds has also been confirmed in an adult mouse model with 5 mg/kg per day for 3 days, significantly reducing the number of intestinal trophozoites. Disulfiram is thought to inhibit *Giardia* trophozoites by inhibiting the carbamate kinase enzyme that catalyses the final step in the arginine dihydrolase pathway, which is essential for energy metabolism and survival of the parasite (this enzyme is not present in higher eukaryotes such as humans) (Galkin et al., 2014).

1.5.6 Approach to anti-giardial screening

With the array of negative side effects, limited availability of drugs in some countries, extended dosing schedules leading to patient non-compliance and the increasing development of resistance, it is important to develop novel therapeutic options. In addition, the new candidate anti-giardial drugs identified in the last five years that have demonstrated *in vivo* efficacy also have limitations in treating *Giardia*. These limitations include a low specificity for *Giardia*, a range of potential side-effects in the host. All of these factors necessitate the development of

novel anti-*Giardia* agents that have a high specificity for *Giardia* over host cells and beneficial microorganisms reducing the potential for negative side-effects very low.

Currently there are a wide variety of *in vitro* assays to assess the anti-*Giardia* activity of various chemicals, which makes comparison between different drugs difficult. In this section of the review the available techniques are highlighted and a potential screening effort for streamlining screening projects is suggested.

1.5.7 Current *in vitro* screening of potential anti-*Giardia* agents

The *in vitro* characterisation of new drugs requires an initial screen to identify any ‘hits’ and ideally this screen would be high through-put, to increase the likelihood of identifying any new anti-*Giardia* agents. This initial screen should be simple, cost effective, reliable, reproducible, accessible and amenable to automation (Benere et al., 2007). Following the initial screen, it is important to confirm any ‘hits’ identified with a secondary screen. Preferably this second screen would target an alternative measurement of anti-*Giardia* activity and as with the first assay, simplicity, cost effectiveness, reliability, reproducibility and accessibility would all be important characteristics of the chosen assay. Although automation of the second assay could be achievable, it is probably not that essential as the number of molecules progressing to this stage would be markedly less than in the original identification assays (Bonilla-Santiago et al., 2008). Several methods for the identification of active drugs have been developed including assays that target inhibition of adherence, cell viability or metabolic activity, each lending itself differently to HTS, however there is currently no standardised method for the identification of potential anti-*Giardia* drug candidates and, as far as is known, a thorough review of the methods available has not been completed. The current assays available can be roughly divided into three categories based on the screening parameter being used i.e. metabolism, trophozoite adherence or proliferation. There are also a few other assays which do not fall into these categories. Various detection methods for these screening parameters have been identified, with their own advantages and disadvantages.

Measurement of cell adherence and proliferation

The adherence of *Giardia* trophozoites to the surface of intestinal epithelial cells is crucial for disease progression and this characteristic of the parasite has been exploited *in vitro* to test the anti-*Giardia* activity of various compounds, since the beginning of assessment of anti-*Giardia* agents. Assays that measure cell proliferation have also been developed and both are included here as many of them use similar detection techniques. Original drug testing assays involved treating the *Giardia* trophozoites with the compound of interest and then counting the number

of remaining cells using a haemocytometer and this method has become the gold standard of anti-giardial testing to which all other methods are compared to (Bell et al., 1991; Busatti and Gomes, 2007; Chen et al., 2011). This method is extremely simple, uses minimal equipment and is universally accessible, however it is time consuming and has a possibility for human bias (Chen et al., 2011). The identification of false positives due to the electrostatic interaction between certain drugs and the culture flask has been reported, but this can be overcome by providing a layer of mammalian cells for the trophozoites to attach to, which adds a level of complexity to the assay and is not commonly used (Favennec et al., 1992). Due to the time consuming nature of cell counting these methods requiring a haemocytometer are not amenable to automation or HTS.

To overcome the time consuming nature of counting cells as described above, several assays have been developed which measure trophozoite proliferation by using a fluorescent stain and computer software to count the number of trophozoites (Bonilla-Santiago et al., 2008; Gut et al., 2011). These assays reduce the time involved and increase the number of potential drug candidates that can be screened. Both of these assays involving a fluorescent stain, either propidium iodide or DAPI, are set-up for automation and use computer software to count the number of cells (Bonilla-Santiago et al., 2008; Gut et al., 2011). Both of the assays include the adherent and non-adherent fractions of the sample, are relatively simple, reliable, have been validated as HTS, are automated (though they can be completed without automation if desired) and are significantly less time consuming than traditional adherence assays (Bonilla-Santiago et al., 2008; Gut et al., 2011). The protocol using a DAPI stain has the advantage over the propidium iodide stain as it does not require any wash steps (Gut et al., 2011). Although these assays have advantages over the traditional adherence assay, they require expensive equipment and produce a large number of electronic files which have to be stored. In addition, they cannot discriminate between live and dead cells (Gut et al., 2011).

Alternative methods to measure cell proliferation have been developed, the earliest of which involved the incorporation of radioactive thymidine. This assay introduced the problem of radioactive waste disposal and was not amenable to HTS (Bell et al., 1991). A more recent assay has been developed that measures cell proliferation of adherent trophozoites using a methylene blue dye (Busatti and Gomes, 2007). After exposure to experimental drugs, the cells are fixed, treated with methylene blue, lysed and the OD recorded (Busatti and Gomes, 2007). This assay is amenable to HTS, does not require any specialist equipment and is cheap, reliable and efficient, although it is not based on cell counting it indirectly measures proliferation of adherent cells.

Measurement of metabolism assays

Probably equal in popularity to adherence and proliferation assays is the measurement of metabolic activity to determine the anti-giardial activity of potential drugs. The metabolic detection assays developed for anti-giardial screening rely on a substrate that is altered by metabolically active cells to give a recordable signal e.g. absorbance. Kang *et al* developed a colourimetric assay using enzymes from the purine salvage pathways. Although this assay is sensitive and simple the required substrates do not seem to be readily available and the assay has not been utilised outside of this group for screening of anti-giardials (Kang *et al.*, 1998; Upcroft and Upcroft, 2001a). Several other colourimetric assays have been developed using substrates that are metabolised to the formazan dye, including MTT and XTT, where XTT has the obvious advantage of being water soluble, while MTT requires extra steps to solubilise the product. In addition, XTT is not considered toxic to the cells and therefore the cells can be reused (Benere *et al.*, 2007; Wright *et al.*, 1992). More recently an assay using resazurin which is reduced to resofurin (both a colourimetric indicator as well as a fluorescent indicator) has been published (Benere *et al.*, 2007). This method has an advantage over all the other metabolic assays previously described as the dye is non-toxic and it is much more sensitive than the MTT and XTT substrates, requiring less dye to measure a result. However, as with other assays relying on the reduction of chemicals to gain a signal, resazurin is readily reduced by the culture media, therefore a wash with PBS is required before addition of the dye (Benere *et al.*, 2007).

Other assays

The only additional assay to be reviewed in this paper is the measurement of ATP which is an important marker of functional integrity of living cells and which quickly decreases during and after cell death. This assay uses a commercially available kit which measures ATP content using luminescence. This assay is highly sensitive, simple and requires no wash steps, however a luminescence reader would be required. In addition, this assay measures both the adherent and non-adherent cells (Kulakova *et al.*, 2014).

1.5.8 Current *in vivo* screening of anti-giardial compounds

After identification of *in vitro* activity and selection of promising candidates it is essential to assess *in vivo* efficacy. Several models of *Giardia* infection have been developed in various animal hosts from ruminants to mice. As an effective model for drug efficacy studies, an infection model needs to be easily accessible by researchers, be reliable and give results that are translational to the final target host (Sande, 1999). Although several large animal models are available in cattle, sheep and dogs they will not be reviewed here as due to the size and cost of the animals they are considered impractical for initial drug screening efficacy assays, as

drugs used in efficacy studies are usually only available in small quantities and initial drug screening costs need to be kept low. In addition, the environment of these animals and housing is not always available and would have many variations/variables between different areas. Instead this review will focus on small animal models. There are two main models that are reportedly used for *Giardia* infection, mice and gerbils (Sande, 1999). While some papers mention a rat model this is not described in detail (Sande, 1999). Gerbils are known to be easily infected with human strains of *Giardia* and have similar symptoms to humans however the availability of gerbils is limited in certain areas due to import/quarantine restrictions (Sande, 1999). The second and more prolifically described model in the literature is a mouse model of infection. Mice have the advantage over gerbils because they are universally available and they have been the mammal of choice in recent anti-giardial discovery projects (Eissa and Amer, 2012; Reynoldson et al., 1991; Tejman-Yarden et al., 2013). In addition, mice are commonly used in research of human diseases and information on drug behaviour in humans can be inferred based on previous experiences in mice. There are a range of mouse models described to varying degrees that have been used in the assessment of *in vivo* anti-giardial activity of several drugs including albendazole, miltefosine and auranofin (Eissa and Amer, 2012; Reynoldson et al., 1991; Tejman-Yarden et al., 2013). It has been shown that the strain, age, immunocompetency and gut microbiota of the mouse and the isolate of *Giardia* being used all play a role in the establishment of a reliable model (Byrd et al., 1994; Hill et al., 1983; Singer and Nash, 2000). It appears that no model has been used routinely however streamlining of the animal model would be much more difficult than *in vitro* studies due to the reasons mentioned above. Several of the models have been developed to study the progression of infection and the effects of infection, not specifically for drug development.

Neonatal models of infection

Models of infection using neonatal mice usually infect the pups by oral gavage with trophozoites or cysts around 6-9 days of age (Hill et al., 1983). It is thought that due to the immature immune system, infection is established in a high number of animals and lasts for a relatively long period before the maturation of the neonatal immune system clears the infection (Hill et al., 1983). Establishment of infection is determined via one of two methods. The first method relies on the shedding of cysts to determine the course of infection and animals are treated shortly after cyst shedding is first identified, while the second method establishes the model, sacrificing pups at various time points to determine when the trophozoites have begun to proliferate in the gut (Reynoldson et al., 1991; Singer and Nash, 2000; Tejman-Yarden et al., 2013). Based on this information the animals in future studies will be treated with a drug a few days after the

infection would have been expected to be established (Reynoldson et al., 1991; Tejman-Yarden et al., 2013).

A description of the first method is given by Reynoldson *et al* using a cat strain to test the efficacy of albendazole while the second method has been described by Tejman-Yarden. Reynoldson used strains from their personal collection while Tejmen-Yarden described a model with 3 different strains, two assemblage A including the widely used WB strain and one assemblage B strain, therefore it appears this model could be used universally with whatever strains are available (Tejman-Yarden et al., 2013).

Although the neonatal pup model is a simple and reliable model which can be established with a range of *Giardia* isolates and mice strains, and has proven useful in the past for the development of various anti-giardial agents, it is possible the translatability of the information from animals to humans would not be a direct scale-up as was demonstrated with albendazole, where a much larger dose was required to clear the infection in mice than is required in humans (Reynoldson et al., 1991).

Weaned mouse models of infection

More recently several weaned models of infection have been developed to further study the pathogenesis of *Giardia* infection in both immunocompromised and immunocompetent mice (Eissa and Amer, 2012; Singer and Nash, 2000). One study has reported infection of Swiss adult mice with uncharacterised cysts from human patients to determine the efficacy of miltefosine (Eissa and Amer, 2012). Other models include malnourishment of mice to induce immunocompromise or the use of genetically immunocompromised or immunolimited strains of mice (Bartelt et al., 2013; Byrd et al., 1994; Kulakova et al., 2014; Singer and Nash, 2000). In addition, models which alter the gut microbiota using antibiotics may be a viable method for establishment of infection but would not be ideal for use in drug discovery as the interaction between different drugs cannot be predicted. In addition, immunocompromised mice require special housing to limit exposure to unwanted pathogens.

It would seem that the suckling mouse model would be the ideal model for initial *in vivo* efficacy trials and could be further validated with an adult model of infection as described by Tejman-Yarden (Tejman-Yarden et al., 2013).

1.5.9 Suggested experimental screening flow for anti-giardial discovery

Based on the methods outlined above, the following model of screening potential anti-giardial compounds which incorporates the need for the initial assay to have (a) the potential for high-throughput screening, (b) require minimal specialised equipment, (c) be sensitive and (d) be

low cost is suggested. In addition, it would be beneficial to have an assay that can be used to both screen the anti-*Giardia* activity of a compound and the potential toxicity of the compound against mammalian cells. Having an assay with a dual purpose simplifies the drug discovery process and ensures that the same parameters of effect are being measured e.g. metabolic activity or ATP content rather than metabolic activity for *Giardia* and ATP content for mammalian cells. This will also ensure comparison between anti-*Giardia* activity and toxicity. With these requirements in mind it is suggested that the initial screen involve a colourimetric assay based on the use of a resazurin dye (Benere et al., 2007). Although this assay does require the media to be removed prior to the addition of the dye (due to the reduction potential of the media), this assay can be used for measuring anti-*Giardia* activity of potential drug candidates as well as potential toxicity towards mammalian cells. As with most of the assays developed the resazurin assay only measures the metabolic activity of the adherent parasites, therefore would not be able to distinguish between metabolic inhibitors and adherence inhibitors unless cells were collected from the supernatant (Benere et al., 2007). Equally it does not distinguish between metabolic inhibitors, drugs that cause cell death and proliferation inhibitors but would be able to pick-up any drugs that affect any of these pathways.

Following initial identification of any compounds with activity against *Giardia* in the resazurin assay, a secondary assay to confirm anti-*Giardia* activity would be ideal. The ideal assay for the secondary screen would target another measure of efficacy and in this case we recommend an adherence assay, as adherence is crucial in disease progression. Traditional adherence assays are time consuming and have a high possibility for error therefore we recommend the methylene blue assay described above as it is simple, easily accessible and a direct measure of adherent trophozoites (Busatti and Gomes, 2007).

Following confirmation of anti-*Giardia* activity, each potential drug candidate should undergo selectivity assays using mammalian cells for potential host toxicity and bacteria for specificity studies towards *Giardia*. It is considered important that the compounds have limited if any activity towards bacteria as these microorganisms comprise the beneficial gut bacteria necessary for normal gastrointestinal function (Adamsson et al., 1999; Jakobsson et al., 2010; Jernberg et al., 2007; Shreiner et al., 2015).

Ideally, a treatment for *Giardia* would remove the parasite without upsetting the gastrointestinal microbiota, allowing the host to make a swift recovery and possibly prevent against future infection. In addition, compounds should be screened against a range of representative strains of *Giardia* including various assemblages. The process of *in vitro* screening would ideally take

the minimum amount of time to ensure maximum efficiency. Validation of *in vivo* efficacy should be of high priority, as it has been well established that *in vitro* efficacy does not always translate to *in vivo* efficacy (Sande, 1999). Following *in vitro* screening, drugs would progress to *in vivo* models using a neonatal mouse model as this is the most cost effective, accessible and reliable model available.

Following verification of *in vivo* efficacy, preliminary toxicology, PKPD and lead optimisation can occur if desired. This will lead to the selection of the most promising candidate to progress to preclinical and clinical trials in the shortest possible time (Figure 1.7).

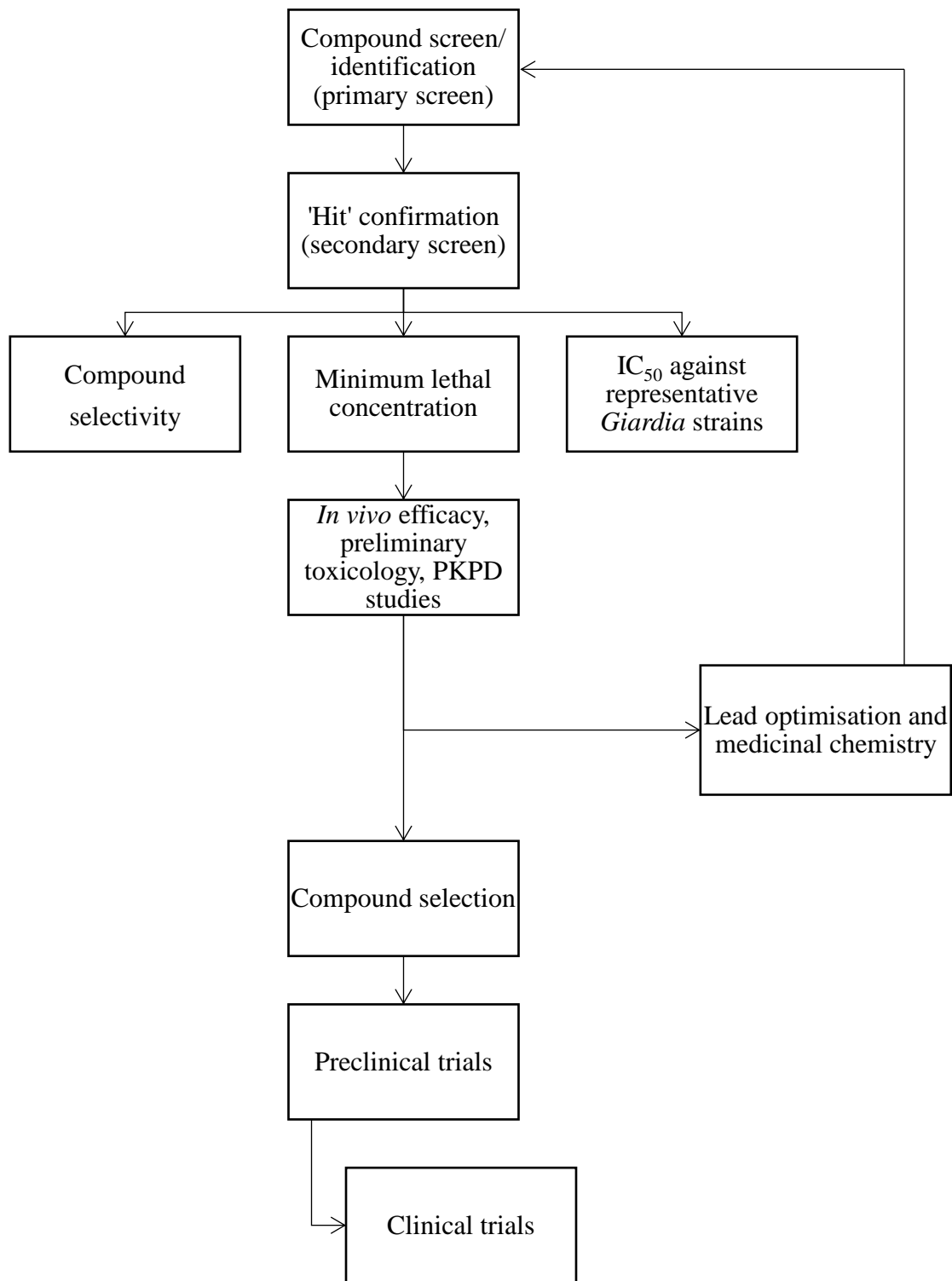


Figure 1.7 Efficacy models for anti-giardial drug discovery

1.6 Aims and outline of thesis

As reviewed above there is a need for the development of novel antimicrobial agents to treat a wide range of infectious diseases. This thesis focussed on the continued development of robenidine and an extensive library of structurally related analogues as potential treatments for bacterial and protistan infections. Initially the spectrum of activity of the library against a range of pathogenic organisms was determined. These organisms included various species of bacteria, the kinetoplasts *T. brucei* and *L. donovani* as well as *G. duodenalis*. Although the initial antibacterial activity of several analogues had already been investigated (as reviewed above) this thesis examined the method of bacterial killing and Gram-negative antimicrobial potential of the lead candidates. In addition, several new analogues were developed during the course of candidature, which require antibacterial testing. The antiprotozoal activity of the structural analogues against *T. brucei*, *L. donovani* and *G. duodenalis* has not been previously described. Based on the information from initial screening results completed in this study and the resources and expertise available, further characterisation of the library against *G. duodenalis* was completed. This included initial screening of a large number of compounds using a resazurin assay followed by mechanism of action studies involving electron microscopy. To determine the *in vivo* efficacy of the library establishing animal models was in both pigs and mice. Although a model was not established in pigs, a model was established in mice using the same strain of *Giardia* utilised in *in vitro* experiments.

Specific aims of the study were to:

1. Determine the *in vitro* efficacy of novel structural analogues against bacteria (both representative Gram-positive and Gram-negative organisms), including time-kill experiments
2. Determine if the target of this library of compounds is present within Gram-negative organisms, such as *E. coli* and *P. aeruginosa*, through the use of membrane permeabilising agents and development of cell-wall deficient cells
3. Determine the *in vitro* efficacy of a sample of structural analogues against the kinetoplasts *T. brucei* and *L. donovani*, including selectivity profiles over host cells
4. Determine the *in vitro* efficacy of a sample of analogues against *G. duodenalis* followed by mechanism of action studies and further *in vitro* characterisation
5. Develop an animal model of giardiasis for *in vivo* characterisation of select analogues

Chapter 2: Robenidine Analogues as Gram-positive Antibacterial Agents

2.1 Statement of Authorship

Title of Paper	Robenidine analogues as Gram-positive antibacterial agents
Publication Status	<input checked="" type="checkbox"/> Published <input type="checkbox"/> Accepted for Publication <input type="checkbox"/> Submitted for Publication <input type="checkbox"/> Unpublished and Unsubmitted work written in manuscript style
Publication Details	Robenidine Analogues as Gram-Positive Antibacterial Agents. Abraham RJ , Stevens AJ, Young KA, Russell C, Qvist A, Khazandi M, Wong HS, Abraham S, Ogunniyi AD, Page SW, O'Handley R, A, Trott DJ. J Med Chem. 2016 Mar 10;59(5):2126-38. doi: 10.1021/acs.jmedchem.5b01797. Epub 2016 Feb 10.

Principal Author

Name of Principal Author (Candidate)	Rebecca Jane Abraham		
Contribution to the Paper	Performed all biological assays except initial analogue screening and biofilm screening assay. Interpreted biological data (except for initial screening). Wrote the manuscript in conjunction with Andrew Stevens (chemist)		
Overall percentage (%)	40% (equal contributing first author)		
Certification:	This paper reports on original research I conducted during the period of my Higher Degree by Research candidature and is not subject to any obligations or contractual agreements with a third party that would constrain its inclusion in this thesis. I am an equal contributing first author of this paper.		
Signature		Date	13 th December 2017

Co-Author Contributions

By signing the Statement of Authorship, each author certifies that:

- i. the candidate's stated contribution to the publication is accurate (as detailed above);
- ii. permission is granted for the candidate to include the publication in the thesis; and
- iii. the sum of all co-author contributions is equal to 100% less the candidate's stated contribution.

Name of Co-Author	Andrew J. Stevens		
Contribution to the Paper	Preparation of chemicals reported in the paper and interpretation of screening results. Preparation of the manuscript. Equal contributing first author.		
Signature		Date	14 th December 2017

Name of Co-Author	Kelly A. Young		
Contribution to the Paper	Preparation of chemicals used in the study		

Signature		Date	3 rd January 2018
-----------	--	------	------------------------------

Name of Co-Author	Cecilia Russell		
Contribution to the Paper	Preparation of chemicals used in the study		
Signature		Date	14 th December 2017
Name of Co-Author	Anastasia Qvist		
Contribution to the Paper	Preparation of chemicals used in the study		
Signature		Date	3 rd January 2017

Name of Co-Author	Manouchehr Khazandi		
Contribution to the Paper	Initial screening of analogues against bacteria		
Signature		Date	13 th December 2017

Name of Co-Author	Hui San Wong		
Contribution to the Paper	Performed biofilm screening assay		
Signature		Date	14 th December 2017
Name of Co-Author	Sam Abraham		
Contribution to the Paper	Performed biofilm screening assay		
Signature		Date	14 th December 2017

Name of Co-Author	Abiodun D Ogunniyi		
Contribution to the Paper	Help with cytotoxicity assays		
Signature		Date	7 th December 2017
Name of Co-Author	Stephen W Page		
Contribution to the Paper	Initial cc the mar k, help in experimental design, data analysis and editing of		
Signature		Date	6 th December 2017

Name of Co-Author	Ryan O'Handley		
Contribution to the Paper	Supervision and help in experimental design		
Signature		Date	8 th December 2017

Name of Co-Author	Adam McCluskey		
Contribution to the Paper	Supervised development of work and data analysis (chemistry) and editing of manuscript. Corresponding author.		
Signature		Date	13 th December 2017

Name of Co-Author	Darren Trott		
Contribution to the Paper	Supervised development of work and data analysis (Biology) and editing of the manuscript. Corresponding author		
Signature		Date	7 th December 2017

2.2 Abstract

Screening confirmed the antibiotic activity of Robenidine, **1** (2,2'-bis[(4-chlorophenyl)methylene]carbonimidic dihydrazide hydrochloride), against both MRSA and VRE with MIC values of 8.1 and 4.7 μM respectively (Figure 2.2). SAR analysis revealed tolerance for 4-Cl isosteres with the 4-F (**8**), 3-F (**9**), 3-CH₃ (**22**), 4-C(CH₃)₃ (**28**) returning moderate (23.7-71 μM) and the 3-Cl (**3**), 4-CH₃ (**21**), 4-CH(CH₃)₂ (**27**) good potency (8.1-13.0 μM). Imine carbon alkylation revealed the presence of a methyl/ethyl binding pocket which also accommodated a CH₂OH moiety (**75**). Analogues **1**, **27** and **69**, had rapid and potent bactericidal activity against 24 clinical MRSA and MSSA isolates, with **69** retaining activity with 2% serum. Analogues **1**, **27** and **69** displayed no dose limiting cytotoxicity at $\geq 2\times$ the MIC or haemolysis at $\geq 8\times$ the MIC. Addition of polymyxin B engendered Gram-negative activity with *E. coli* and *P. aeruginosa* MIC values of 4.2-21.6 μM . Analogues **1** and **75** displayed excellent human and mouse microsomal stability, intrinsic clearance and hepatic extraction ratios with $T_{1/2} > 247$ min, $CL_{\text{int}} < 7$ $\mu\text{L}/\text{min}/\text{mg}$ protein and $EH < 0.22$ in both human and mouse liposomes for **1**, and human liposomes with **75**.

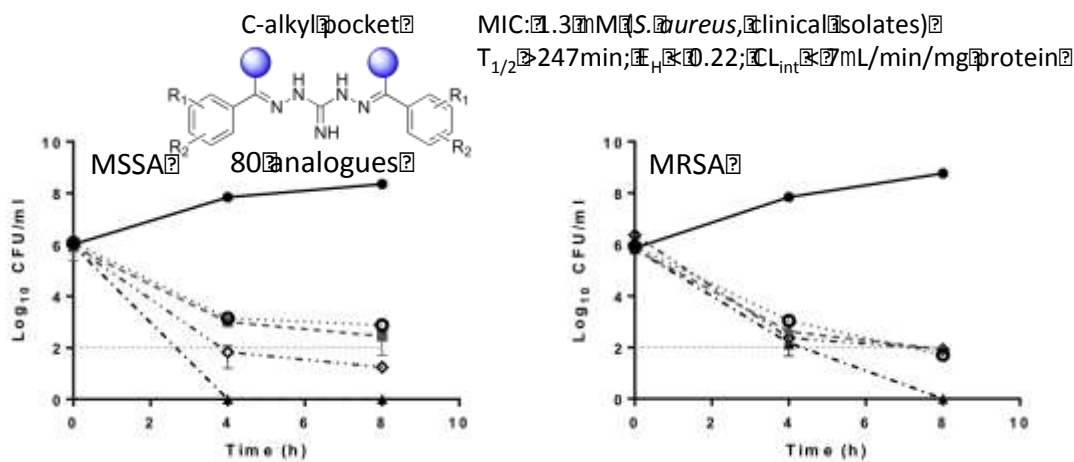


Figure 2.1 Graphical abstract

2.3 Introduction

The management of bacterial infections has become increasingly difficult with the emergence of antimicrobial resistance. In particular the ESKAPE pathogens (*Enterococcus faecium*, *Staphylococcus aureus*, *Klebsiella pneumoniae*, *Acinetobacter baumannii*, *Pseudomonas aeruginosa*, and *Enterobacter* species), are causing significant problems worldwide (Pendleton et al., 2013). Methicillin-resistant *S. aureus* (MRSA) is a major pathogen causing both hospital and community-acquired infections. In addition to methicillin resistance, *S. aureus* isolates resistant to the last line antimicrobials vancomycin, linezolid, daptomycin, anti-MRSA cephalosporins (ceftobiprole and ceftaroline) and mupirocin have been isolated from clinical cases (Antonov et al., 2015; Chan et al., 2015; Endimiani et al., 2011; Hiramatsu, 2001; Marty et al., 2006).

Concurrent with the increasing prevalence of antimicrobial resistance, there has been a large gap in the development of new antimicrobials to treat these pathogens and as time from initial identification to release of a product onto the market can take ten years, alternatives for treatment need to be rapidly identified to alleviate the problem in the short term. One attractive approach is the repurposing of food and drug administration (FDA) approved drugs in clinical use as potential antimicrobials. Another under evaluated area is re-examination of compounds previously developed for use to support animal health for antimicrobial activity as candidates for further structural modification for possible use in human medicine. These approaches offer known safety and development pathways with associated time and cost savings (Chong and Sullivan, 2007).

Within the animal medicine sphere, robenidine (**1**, 2,2'-bis[(4-chlorophenyl)methylene]-carbonimidic dihydrazide hydrochloride; Figure 2.2) is a well-known anti-coccidial agent which has been used worldwide since the early 1970s in the prevention of coccidian infections in commercial poultry and rabbit production (Douglas et al., 1977; Kantor et al., 1970).

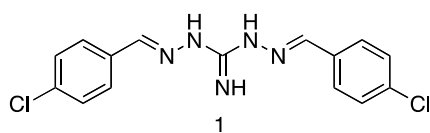


Figure 2.2 Chemical structure of robenidine (1).

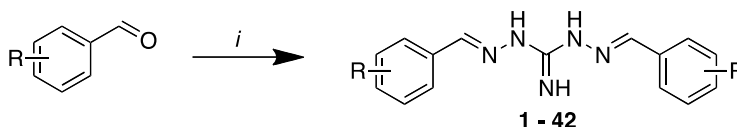
Robenidine **1** belongs to the aminoguanidine compound class, a diverse group of bioactive compounds used in the treatment of a broad range of diseases from bacterial infections through to cancer and diabetes and many are already approved for human use (Saczewski and Balewski,

2009, 2013). Excellent activity against *Babesia microti* infection has been reported in mouse models with 100% inhibition noted at 25 and 50 mg/kg (Yao et al., 2015).

Despite **1** having a long history of use in animals there have been no in-depth evaluations as a potential antibacterial agent, although early work demonstrated robenidine had activity against unidentified Gram-positive soil bacteria (Hansen et al., 2009). Herein we report on the *in vitro* antibacterial activity of **1** and the development of preliminary structure activity relationship (SAR) data around this scaffold. The efficacy of selected analogues against clinical isolates of MRSA is also examined.

2.4 Results and Discussion

Access to a focused library of robenidine analogues was realized by the condensation of selected mono-substituted benzaldehydes with 1,3-diaminoguanidine hydrochloride [14]. Under ethanol reflux conditions low (18%) to excellent (93%) yields of the desired analogues (**1** – **31**) were obtained (Scheme 2.1). The minimum inhibitory concentration (MIC) of these analogues was determined against two strains of MRSA and VRE, and one strain each of *E. coli* and *P. aeruginosa* and the data presented in Table 2.1.



Scheme 2.1 Reagents and conditions: (i) 1,3-diaminoguanidine hydrochloride, EtOH, reflux, 16 h.

Ampicillin was used as an internal control and showed both Gram-negative (*E. coli*, 45.8 μ M; *P. aeruginosa*, 366 μ M) and Gram-positive (MRSA, 183 μ M; VRE 11.5 μ M) activity. However none of the robenidine analogues, **1** – **31**, showed Gram-negative activity (Table 2.1). Robenidine, **1** inhibited the growth of MRSA and VRE with MIC values of 8.1 and 4.7 μ M respectively. Removal of the 4-Cl moiety with the synthesis of **2** resulted in a complete loss of activity. A halogen scan revealed a preference for the 4-Cl moiety, with a two-fold loss in VRE activity with the 3-Cl (**3**) and no activity with 2-Cl (**4**) analogues. Other halogen substituents were poorly tolerated with only 3-Br (**6**), 4-F (**8**) and 3-F (**9**) displaying modest levels of activity (MIC < 75 μ M). The 3-Br (**6**) displayed a near 10-fold VRE vs. MRSA selectivity. Of the additional electron withdrawing groups examined: CN, NO₂ and CF₃, only the 4-CF₃ (**11**) displayed moderate levels of activity with MIC values of 36.5 and 11.4 μ M against MRSA and VRE respectively (Table 2.1 and supplementary data). These data suggest that an electron-withdrawing group is poorly tolerated and that the effect of the 4-Cl moieties in **1** may be steric.

Hydrogen bond donors, e.g. **12-14**, were poorly tolerated with the 4-OH (**12**) analogue ~25-fold less MRSA and ~60-fold less VRE active than **1**. Methylation saw a modest activity improvement, but only with the 3-OMe (**16**). The more electronegative 4-OCF₃ (**18**) retained VRE activity but was two-fold less active against MRSA. The corresponding 4-SCH₃ (**19**) was more active, particularly against VRE with a MIC of 12.7 μM. The 4-SCF₃ (**20**) showed reduced activity, again suggesting a poor tolerance for electronegative substituents (Table 2.1).

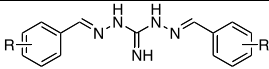
In general, alkyl substituents were well tolerated with the 4-CH₃ (**21**) displaying comparable MRSA (MIC 9.1 μM) activity to **1**. The equivalent 3- and 2-CH₃ (**22** and **23**) were an order of magnitude less active, as were the 4-propyl and butyl analogues (**24** and **25**). The 4-*iso*-propyl (**26**) with MIC values of 9.1 and 13.0 μM against MRSA and VRE respectively, displayed activity comparable with **21** and **1**. However, the *iso*-propyl moiety is known to be metabolized via highly reactive intermediates, which resulted in our examination of replacement with both 4-*tert*-butyl (**27**) and 4-NMe₂ (**28**), but both were less active than **26** (Aprile et al., 2011; Hansen et al., 2009). A 2- or 4- Ph moiety (**29** and **30**) was poorly tolerated, but the 4-ethynyl (**31**) showed moderate (MIC 17.2 μM) and selective activity against VRE. Polar substituents such as 4-CH=CHCOOH, 4-NHCOCH₃ and 3-COOH were inactive (MIC > 128 μg.mL⁻¹; supplementary data).

With an understanding of the SAR of the simple phenyl rings, the effects of multiple moieties were next explored. These analogues were synthesized as described in Scheme 2.1 from the corresponding aldehydes and the outcome of screening is presented in Table 2.2.

The inclusion of two halogens was initially investigated. Interestingly, despite the parent 2-F (**10**) and the 2,5-di-F (**32**) analogues being inactive, combination with 4-Cl (**33**) gave MRSA and VRE activity comparable to **1**. The 3,4-di-F (**34**) saw a reduction in MRSA activity but retention of VRE activity. A 4-Cl moiety in combination with a 2-NH₂ (**38**), 2-NHCH(OH)CH₃ (**39**), and 2-OH (**42**) afforded good to modest MRSA and VRE activity. These data suggest that the 2-F of **33** may be acting as a hydrogen bond isostere. In an attempt to improve aqueous solubility, the 4-Cl was replaced with 4-NMe₂ with 2-OH retention with the synthesis of **43**, but this resulted in a loss of activity. Combining the 2-OH with 3-CH₃ (**41**), both individually active substituents (Table 2.1, **14** and **22**), resulted in no activity, possibly due to the proximity of the substituents interfering with their respective interactions. Of the catechol bearing analogues (**44 – 46**), only modest activity was noted with **44**. The introduction of a third OH moiety (**50 – 52**) saw both the reintroduction of low levels of activity against MRSA and VRE, and with **52** also a low level of activity against *P. aeruginosa* (MIC 322 μM). These catechol analogues were not investigated further, nor were the variations that saw methylation or OH to

Br exchange or introduction of pentafluoro moiety examined as these analogues, **53** – **57**, were inactive across all bacterial strains examined.

Table 2.1 The inhibition of MRSA, VRE, *E. coli* and *P. aeruginosa* growth by 1,3-aminoguanidine Schiff base analogues possessing mono-substituted aromatic rings (1 – 31).

					
		MIC (μM)			
Compound	R	MRSA	VRE	<i>E. coli</i>	<i>P. aeruginosa</i>
Ampicillin	-	183	11.5	45.8	366
1	4-Cl	8.1	4.7	- ^a	-
2	H	-	-	-	-
3	3-Cl	8.1	10.8	-	-
4	2-Cl	-	-	-	-
5	4-Br	-	-	-	-
6	3-Br	-	15.4	-	-
7	2-Br	-	-	-	-
8	4-F	47	23.7	-	-
9	3-F	47	71	-	-
10	2-F	-	-	-	-
11	4-CF ₃	36.5	11.4	-	-
12	4-OH	192	288	-	-
13	3-OH	192	288	-	-
14	2-OH	36.0	240	-	-
15	4-OCH ₃	-	-	-	-
16	3-OCH ₃	88	88	-	-
17	2-OCH ₃	-	358	-	-
18	4-OCF ₃	187	85	-	-
19	4-SCH ₃	61	12.7	-	-
20	4-SCF ₃	96	135	-	-
21	4-CH ₃	9.1	12.1	-	-

22	3-CH ₃	24.4	24.4	-	-
23	2-CH ₃	121	61	-	-
24	4-(CH ₂) ₂ CH ₃	83	73	-	-
25	4-(CH ₂) ₃ CH ₃	232	193	-	-
26	4-CH(CH ₃) ₂	9.1	13.0	-	-
27	4-C(CH ₃) ₃	24.2	29.0	-	-
28	4-N(CH ₃) ₂	30.9	30.9	-	-
29	4-Ph	282	106	-	-
30	2-Ph	-	-	-	-
31	4-CCH	-	17.2	-	-

^a “-” = No inhibitory activity observed at 128 µg.mL⁻¹.

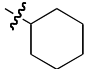
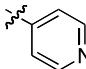
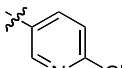
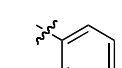
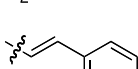
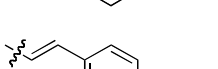
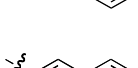
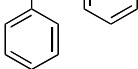
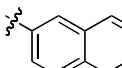
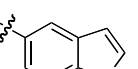
Table 2.2 The inhibition of MRSA, VRE, *E. coli* and *P. aeruginosa* growth by 1,3-diaminoguanidine Schiff base analogues possessing di-, tri- and poly-substituted aromatic rings (32 - 57).

Compound	R	MIC ₅₀ (μM)			
		MRSA	VRE	<i>E. coli</i>	<i>P. aeruginosa</i>
32	2,5-F	- ^a	-	-	-
33	2-F, 4-Cl	6.1	7.4	-	-
34	3,4-F	40.1	10.7	-	-
35	2,4-Cl	-	-	-	-
36	2,6-Cl	-	-	-	-
37	3,5-Cl	-	-	-	-
38	2-NH ₂ , 4-Cl	5.0	6.3	-	-
39	2-NHCH(OH)CH ₃ , 4-Cl	66	98	-	-
40	2-NHCOCH ₃ , 4-Cl	-	-	-	-
41	2-OH, 3-CH ₃	-	-	-	-
42	2-OH, 4-Cl	80	45	-	-
43	2-OH, 4-N(CH ₃) ₂	229	76 ^b	-	-
44	2,3-OH	88	262	-	-
45	2,4-OH	-	-	-	-
46	3,4-OH	-	-	-	-
47	3-OH, 4-OCH ₃	-	-	-	-
48	3-OCH ₃ , 4-OH	244	163	-	-
49	3,4-OCH ₃	-	-	-	-
50	2,3,4-OH	161 ^b	161 ^b	-	-
51	2,4,5-OH	161	322	-	-
52	3,4,5-OH	161	-	-	322
53	3-OCH ₃ , 4,5-OH	-	-	-	-
54	3-NO ₂ , 4-OH	-	-	-	-
55	2,3,4,5,6-F	-	-	-	-
56	2-Br, 4,5-OCH ₃	-	-	-	-
57	3-Br, 4,5-OCH ₃	-	-	-	-

^a “-” = No inhibitory activity observed at 128 μg.mL⁻¹; ^b active against only one of the two strains examined within either MRSA or VRE.

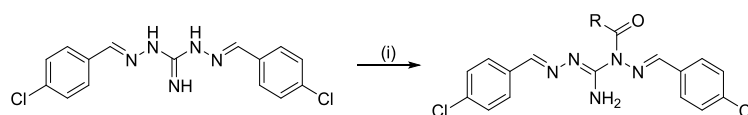
The introduction of phenyl ring isosteres, fused aromatics, heterocyclic and methylene spaced analogues (**58-67**) was accomplished as per Scheme 2.1 (Meanwell, 2011). These analogues were screened for MRSA and VRE activity (Table 2.3). In virtually all instances the phenyl ring isosteric modification resulted in a significant loss of both MRSA and VRE activity relative to **1**. In multiple instances selectivity towards MRSA (**63, 64**) and VRE (**67**) was observed. With the pyridyl analogues only the 4-Cl (**60**) was active, suggesting again a key role for a 4-Cl substituent in this class of compounds. Other fused aromatics, 2-hydroxynaphthyl, 3-quinolinyl, 2-quinoxaliny and chromene analogues were inactive (data not shown).

Table 2.3 Inhibition of MRSA and VRE by 1,3-diaminoguanidine Schiff bases bearing extended linkers, non-aromatic and isosteric phenyl ring replacements (58 – 67).

	R	MIC ₅₀ (μM)	
		MRSA	VRE
58		408	306
59		-	-
60		172	86 ^b
61		-	-
62		-	-
63		309	-
64		61 ^b	-
65		239	159 ^b
66		31.6	42
67		-	33.1 ^b

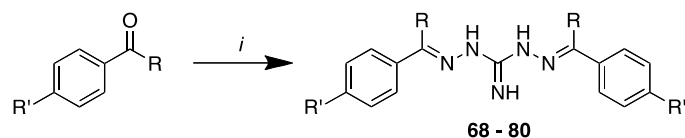
^a “-” = No inhibitory activity observed at 128 μg mL⁻¹; ^b active against only one of the two strains examined within either MRSA or VRE.

Installation of a range of isocyanates and chloroformates to afford the respective carbamate and urea analogues of **1**, only resulted in a complete loss of activity (Scheme 2.2; Supplementary Data).



Scheme 2.2 Reagents and conditions: (i) N-substituted isocyanate or O-substituted chloroformate, *i*-PrNEt₂, CH₃CN, reflux, 2.5 h (for full detail of ‘R’ see supplementary data).

Potential imine carbon based modifications were explored through coupling of phenones with 1,3-diaminoguanidine hydrochloride to afford alkyl substituted analogues (**68-80**) (Scheme 2.3; Table 2.4). While the compounds were evaluated against the Gram-negative pathogens, no activity was observed (data not shown).



Scheme 2.3 Reagents and conditions: (i) 1,3-diaminoguanidine hydrochloride, EtOH, reflux, 16 h.

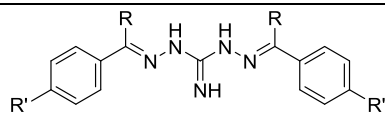
Introduction of a methyl substituent at the imine carbon imparted activity to compounds whose methine counterpart bore no activity, such as **68** and **70** whereas their desmethylated analogues **2** and **5**, respectively were MRSA and VRE inactive (Table 2.1). In a similar manner ‘C-methylation’ of **1** to afford **69** provided a marginal improvement in activity (Table 2.4). However, this ‘C-alkylation’ strategy was not universally applicable, as it appears to be incompatible with the CF₃ substitution of **71**, abolishing MRSA activity with retention of VRE inhibition.

Sequential probing of this space with straight chain aliphatics (**72 - 74**) suggested the presence of a C-methyl/ethyl binding pocket with the C-ethyl (**72**); the largest C-alkyl substituent to retain antibacterial activity. Further probing of this region with hydrogen bond donor/acceptor atoms, bearing either neutral or ionic qualities, showed that the pocket would tolerate a neutral hydrogen bond donor/acceptor (CH₂OH; **75**), however introduction of ionic species in **76** (CH₂NH₂) and **77** (COOH) resulted in abolition of potency (Table 2.4).

Coupling of the favorable aromatic substituents, the 4-methyl (**21**) and 4-*tert*-butyl (**27**), moieties from the parent phenyl analogues with the C-methyl substituents from this series of analogues gave rise to **78** and **79**, which were amongst the most potent analogues developed herein with MIC values in 4.5 – 36.2 μM. Attempts to enhance compound solubility through the introduction of a 4-piperazin-1-yl moiety (**80**) were unsuccessful with a significant loss in potency noted (Table 2.4).

Having established the antibacterial activity of this class of compounds, we examined the activity of **1**, **27** and **69** against twenty clinically obtained isolates of MRSA and four methicillin-sensitive *S. aureus* (MSSA) isolates obtained from the ATCC. All three analogues (**1**, **27** and **69**) were bactericidal against all the *S. aureus* strains tested with MBC:MIC ratios of ≤2 (Table 2.5).

Table 2.4 Inhibition of MRSA and VRE by 1,3-diaminoguanidine Schiff base analogues (68 – 80) bearing imine substitution.



Compound	R	R'	MIC ₅₀ (μM)	
			MRSA	VRE
68	CH ₃	H	18.2	49
69	CH ₃	Cl	7.5	3.8
70	CH ₃	Br	16.4	24.6
71	CH ₃	CF ₃	- ^a	17.2
72	CH ₂ CH ₃	Cl	56	18.7
73	(CH ₂) ₂ CH ₃	Cl	-	-
74	(CH ₂) ₃ CH ₃	Cl	-	-
75	CH ₂ OH	Cl	20.3	15.2
76	CH ₂ NH ₂	H	-	-
77	COOH	H	-	-
78	CH ₃	CH ₃	11.2	8.4
79	CH ₃	C(CH ₃) ₃	4.5	36.2
80	CH ₃	piperazin-1-yl	243	278

^a “-” = inactive at 128 μg.mL⁻¹.

Table 2.5 MIC and MBC concentrations for **1**, **27**, **69** and ampicillin against 20 clinically isolated MRSA and 4 ATCC MSSA bacterial strains.

<i>S. aureus</i> (n = 24)					
	MIC range	2% Serum ^a	50% Serum	MBC range	MIC:MBC
	μM				
1	5.4	43.1	>250	5.4 – 10.8	1 (96%)
27	4.8 – 38.6	38.6	>250	4.8 – 38.6	1 (87.5%)
69	1.3 – 5.0	10.0	>250	2.5 – 5.0	1 (87.5%)
Ampicillin	0.3 – 143	^b	^b	2.0 – 143	-

^a MIC in serum determined using *S. aureus* ATCC 29213 only; ^b ^c = not determined

The lead, **1**, was uniformly active across all clinical isolates with a 5.4 μM MIC value, **27** displayed a broader range of activity from 4.8 – 38.6 μM and **69** from 1.3 – 5.0 μM. A profound and negative impact on the MIC values with a 4-fold decrease with **1** and **27** at 2% and no activity at 50% serum was observed. The effect with **69** was less stark with the MIC values dropping to 10 μM at 2% serum. This suggests a high level of protein binding of these analogues, but does not necessarily render these analogues ineffective *in vivo* (Lee *et al.*, 1991). As anticipated none of these analogues displayed any Gram-negative activity against *E. coli* or *P. aeruginosa* (Table 2.6). However in the presence of polymyxin B nonapeptide (PMBN; 4.1 μM), a peptide which disrupts the outer membrane, **1** and **69** showed at least a 10-fold MIC improvement suggesting that the lack of Gram-negative antibacterial activity for this compound was a consequence of lack of compound penetration of the bacterial outer membrane (Randall *et al.*, 2013). With **1** and **69**, MIC values were comparable with those observed with Clofazimine (Table 2.6) (Vaara, 1992).

Table 2.6 MIC for **1**, **27** **69** and clofazimine against *E. coli* ATCC 25922 and *P. aeruginosa* ATCC 27853.

	<i>E. coli</i> 25922		<i>P. aeruginosa</i> 27853	
	MIC	+PMBN ^b	MIC	+PMBN
μM				
1	>250	21.6	>250	21.6
27	>250	>250	>250	>250
69	>250	10.0	>250	5.0
Clofazimine	>250	4.2-8.4	>250	8.4

^a PMBN – polymyxin B nonapeptide

Time kill curve evaluation of **1**, **27** and **69** at 1, 2, 4 and 8 times their MIC against one susceptible *S. aureus* isolate (ATCC 29213) and one clinical MRSA isolate (USA300) confirmed their bactericidal activity resulting in a ≥ 4 -log reduction in bacterial cell numbers over an 8 hour period across all the analogue doses evaluated (Figure 2.3). After 24 hours some bacteria regrowth was observed with all compounds at all concentrations tested (data not shown).

Of the analogues evaluated, only **1** showed statistically significant activity against *S. aureus* biofilms (based on a one-way ANOVA analysis). Significant biofilm retardation was only noted at concentrations $> 43.2 \mu\text{M}$, and resulted in a ≤ 3 -log reduction in cells irrespective of analogue concentration.

Hemolysis was evident with **1** at $\geq 173 \mu\text{M}$ while no hemolysis was observed with **27** or **69** at concentrations as high as $600 \mu\text{M}$. Low to moderate levels of cytotoxicity against a normal human lung fibroblast cell line (HEL 299) with **1**, **27** and **69** were observed with growth inhibition (GI_{50}) values of 17.7, 28.8 and $6.7 \mu\text{M}$ respectively; and against a human hepatocellular carcinoma cell line (Hep G2) returned GI_{50} values of 25.4, 26.3 and $13.8 \mu\text{M}$ respectively. These values are at least twice the observed MIC_{50} values for these three analogues. It is important to note that an *in vitro* cytotoxicity screening assay does not provide a “go/no-go” step in the drug development process. Indeed, when used in a prospective manner, they have not been highly predictive of *in vivo* toxicity (Halder et al., 2015). A single *in vitro* screening platform is unlikely to provide the data required to evaluate risk and predict human toxicity. In this regard, it is widely accepted that additional models using a tiered toxicity screening approach are required in order to define and predict clinical toxicity. In addition extensive *in vivo* studies have been performed previously with **1** which determined the oral

LD₅₀ to be ~3000 mg/kg in rats and 1500 mg/kg and 2900 mg/kg per day in male and female rabbits respectively (Aquilina et al., 2011). Robenidine, **1** has been used safely since the early 1970's as an oral anti-coccidial agent in poultry and rabbits (Kantor et al., 1970). Furthermore, no adverse effects were reported after dosing mice with 50 mg/kg p.o. of **69** (Sondhi et al., 2009).

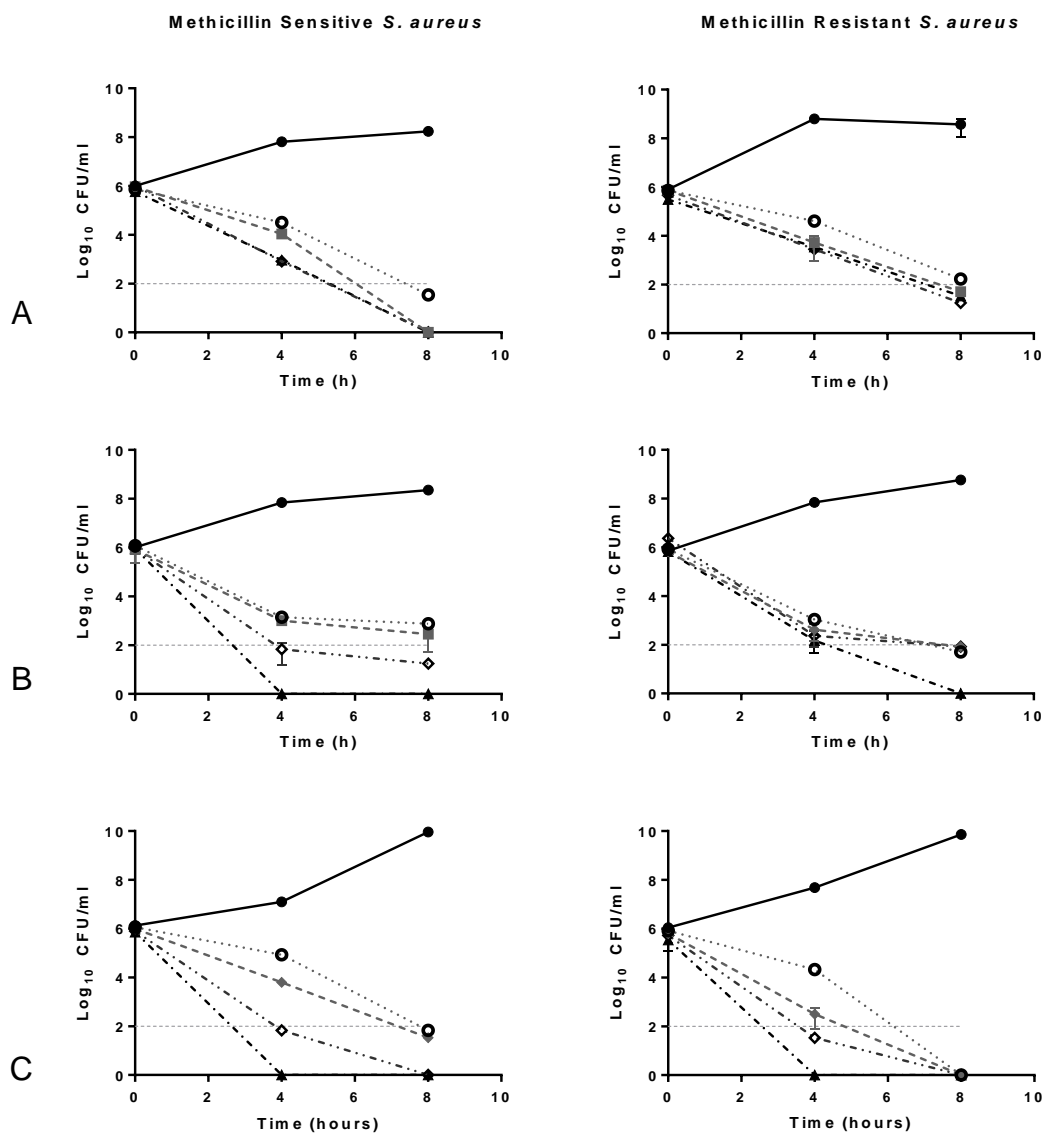


Figure 2.3 Time-kill assay of (A) **1** (robenidine), (B) **27** and (C) **69**; against methicillin-sensitive (left) and methicillin-resistant (right) strains of *S. aureus*. Cultures were inoculated with 10⁶ CFU/mL bacteria and exposed to increasing concentrations of compounds for 8 hours. Samples were taken at 4 and 8 hours to determine viable cell numbers. Key: closed circles (●) – control, open circles (○) - MIC, closed diamonds (◆) – 2x MIC, open diamonds (◇) – 4x MIC, closed triangles (▲) - 8x MIC and grey broken line – detection limit. Error ±SD.

Analogues **1**, **27** and **69** were considered for preliminary *in vivo* stability and degradation studies, however we were concerned that the C-methyl imine moiety might be highly susceptible to oxidation, and as such examined the stability and degradation of the related CH₂OH substituted **75**, which also afforded the possibility of enhanced solubility as a consequence of the additional polar moiety (cf. **69**). We examined the physicochemical and metabolism parameters of **1**, **27** and **75** in human and mouse liposomes and this data is presented in Table 2.7. As anticipated these analogues broadly conformed with Lipinski's rules and presented moderately favorable LogD values at both pH 3.0 and 7.4, although the solubility was modest, but highest with **1** and **75** (Lipinski et al., 1997). Of the three analogues evaluated, **27** displayed the lowest T_{1/2} and correspondingly higher intrinsic elimination and hepatic extraction ratios, CL_{int} and E_H respectively (Table 2.7). Both CL_{int} and E_H with **1** and **75** were considerably more favorable with T_{1/2} > 247 min, CL_{int} < 7 μL/min/mg protein and E_H < 0.22 in both human and mouse liposomes for **1**, and human liposomes with **75**. The metabolic parameters were slightly poorer with **75** in mouse liposomes, but still acceptable at 131 min, 13 μL/min/mg protein and 0.22 for T_{1/2}, CL_{int} and E_H respectively (Obach, 1999; Ring et al., 2011).

Table 2.7 physicochemical and Metabolism Results for **1**, **27**, and **75**.

compound	Physicochemical parameters										Metabolism parameters			
	MW	PSA (Å ²)	FRB	HBA	HBD	Log D		Solubility (μg/mL)		species	T _{1/2}	CL _{int} (μL/min/mg protein)	E _H	
						pK _s	pH 3.0	pH 7.4	pH 2.0					pH 6.5
1	334.20	72.6	4	3	3	5.0: imine 1.2: amine	3.7	4.5	6.3 – 12.5	<1.6	human mouse	>247 ^a >247 ^a	<7 ^b <7 ^b	<0.22 ^c #
27	337.54	72.6	6	3	3	5.1: imine 2.4: amine	4.9	>5.3	<1.6	<1.6	human mouse	20 25	89 70	0.78 0.60
75	394.26	113.1	6	3	3	5.1: imine	3.2	4.0	25-50	<1.6	human mouse	>247 ^a 131	<7 ^b 13	<0.22 0.22

^a<15% compound loss in 60 min. ^bBelow sensitivity limit of 7 μL/min/mg protein based on 0.4 mg/L microsomal protein concentration. ^cBelow sensitivity limit based on 0.4 mg/mL microsomal protein concentration. ^dThe microsomal-predicted hepatic extraction ratios (E_H), obtained based on relative rates of test compound degradation *in vitro*, were used to classify compounds as low (<0.3), intermediate (0.3-0.7), high (0.7-0.95), or very high (>0.95) extraction compounds.

2.5 Conclusions

Our screening confirmed robenidine, **1**; a widely used poultry industry anti-coccidial agent was active against both MRSA and VRE. Removal of the 4-Cl moiety resulted in loss of activity, however a wide array of isosteric and other mono-substituents were moderately (4-F (**8**), 3-F (**9**), 3-CH₃ (**22**), 4-C(CH₃)₃ (**27**)) to well tolerated (3-Cl (**3**), 4-CH₃ (**21**), 4-CH(CH₃)₂ (**26**). Bulky substituents were poorly tolerated. The introduction of di-substituted phenyl moieties was well tolerated with 2-F,4-Cl (**33**) and 2-NH₂,4-Cl (**38**). No noteworthy potency

was observed with only the indole (**66**) and benzothiophene (**67**) showing modest levels of activity. Similarly, no activity was noted with the development of carbamate and urea analogues. Modifications at the imine carbon revealed the presence of a methyl/ethyl binding pocket with good activity with **69-70** and the CH₂OH analogue **75**.

Analogues **1**, **27** and **69**, had rapid and potent bactericidal activity against MRSA *in vitro*. Robenidine **1** displayed promising activity against *S. aureus* biofilms *in vitro*. These promising results were further validated with excellent *in vitro* antibacterial profiles against clinical *S. aureus* (MRSA and MSSA) isolates. Of particular note was the limited effect of 2% serum on the MIC values of **69**, where both **1** and **27** were rendered essentially inactive. Moreover, none of these analogues displayed dose limiting cytotoxicity against the two cell lines examined, returning GI₅₀ values at least two-fold higher than the compound MIC₅₀, no significant hemolysis was observed until compound concentrations reached at least 8-times the MIC value. Efficacy against Gram-negative *E. coli* and *P. aeruginosa* was only observed in the presence of polymixin B, with activities comparable with Clofazimine (Vaara, 1992).

Preliminary evaluation of physicochemical and metabolic parameters in human and mouse liposomes further supports the development of these analogues as potential clinical antibiotic leads with both **1** and **75** displaying excellent stability, intrinsic clearance rates (CL_{int}) and hepatic extraction (E_H) ratios. Both CL_{int} and E_H with **1** and **75** were highly promising for future development with T_{1/2} > 247 min, CL_{int} < 7 μL/min/mg protein and E_H < 0.22 in both human and mouse liposomes for **1**, and human liposomes with **75** (Obach, 1999; Ring et al., 2011).

2.6 Experimental

2.6.1 Chemistry - General Methods

All reactions were performed using standard laboratory equipment and glassware. Solvents and reagents were purchased from Sigma Aldrich, Lancaster International or TCI and used as received. Organic solvents were bulk quality, and were distilled from glass prior to use. Organic solvent extracts were dried with magnesium sulfate (MgSO₄), and dried under reduced pressure with either Büchi or Heidolph rotary evaporators. Melting points were recorded in open capillaries on a Stuart SMP11 Melting Point Apparatus. Temperatures are expressed in degrees Celsius (°C). Where available, literature values are provided and appropriately referenced. Electrospray mass spectra were recorded using 10% DMSO/H₂O or HPLC-grade methanol or acetonitrile as carrier solvents on a Shimadzu LC-MS spectrometer.

Nuclear magnetic resonance (NMR) spectroscopy was performed on a Bruker Avance 300 MHz spectrometer, where proton NMR (¹H-NMR) spectra and carbon NMR (¹³C-NMR) spectra were acquired at 300 and 75 MHz respectively, or a Bruker Avance III 400 MHz spectrometer, where ¹H-NMR and ¹³C-NMR were acquired at 400 and 100 MHz respectively. All spectra

were recorded in deuterated dimethyl sulfoxide (DMSO-*d*₆), obtained from Sigma Aldrich or Cambridge Isotope Laboratories Inc., unless otherwise stated, with the residual solvent peaks used as the internal reference (δ 2.49 (quintet) and δ 39.7 (septet) for ¹H-NMR and ¹³C-NMR respectively). Chemical shifts (δ) were measured in parts per million (ppm) and referenced against the internal reference peaks. Coupling constants (*J*) were measured in Hertz (Hz).

NMR assignments were determined through the interpretation of one- and two-dimensional spectra, specifically gradient heteronuclear single quantum correlation (gHSQC), gradient heteronuclear multiple bond correlation (gHMBC) and distortionless enhancement by polarization transfer quaternary (DEPTQ) spectroscopy. Multiplicities are denoted as singlet (s), broad singlet (br s), doublet (d), doublet of doublets (dd), doublet of doublet of doublets (ddd), triplet (t), triplet of doublets (td), doublet of triplets (dt), quartet (q), quintet (quin) and multiplet (m). Peaks are listed in increasing chemical shift in the following format: chemical shift (integration (¹H), multiplicity (¹H), coupling constant (¹H), ascribed assignment).

2.6.2 Microbiology

Antimicrobial agents

Robenidine (**1**, NCL812) was provided by Neoculi Pty. Ltd. Ampicillin and clofazimine used in this study were sourced from Sigma Aldrich.

Bacterial isolates

A total of 20 MRSA clinical isolates were kindly provided by Associate Professor Geoffrey Coombs (Department of Microbiology, Pathwest Laboratory Medicine WA). MSSA strains ATCC 25923, 6538, 49775 and 29213 were obtained from the American Type Culture Collection together with *E. coli* ATCC 25922 and *P. aeruginosa* ATCC 27853. Isolates used in initial screening assay were sourced as follows: *SCCmec* type IV MRSA, VRE, multidrug-resistant *E. coli* and *P. aeruginosa* clinical isolates were kindly provided by Prof Mary Barton, University of South Australia.

Susceptibility testing

The MIC of all analogues was determined according to CLSI guidelines in cation-adjusted Mueller-Hinton broth (CAMHB) at a total volume of 100 μ L with test concentration increasing 2-fold from 0.25 μ g.mL⁻¹ to 128 μ g.mL⁻¹ (CLSI, 2008). All analogues were dissolved in 100% DMSO to a concentration of 12.8 mg.mL⁻¹ prior to dilution in broth.

The MIC₅₀ and MIC₉₀ for **1**, **27** and **69** was determined using a modified MIC assay based on CLSI guidelines (CLSI, 2008). Luria Bertani (LB) broth was used instead of CAMHB as it has been previously shown that **1** can chelate calcium ions (Rozengart and Saakov, 2002). In

addition, the antimicrobial dilutions of **1**, **27** and **69** were completed in 100% DMSO, with 2 μL added to each well, as the compounds are hydrophobic. The assay was performed in a total volume of 200 μL in 96 well plates. Antimicrobials were tested in final concentrations as follows; **1**: 0.7 – 345.3 μM , **27**: 0.6 – 309.2 μM and **69**: 0.6 – 321 μM . MIC tests involving ampicillin were performed according to CLSI guidelines in CAMHB. Plates were incubated for 20 - 24 hours at 37°C before determination of the MIC. For Gram-negative organisms the MIC was determined as above with and without supplementation of media with polymyxin B nonapeptide (PMBN) (4.1 μM). Clofazimine was used as control in PMBN studies and prepared as the test compounds (Vaara, 1992).

The effect of serum on the MIC of the compounds was also determined. MIC assays were performed as described above, however the media was supplemented with 2, 10 or 50% heat inactivated adult bovine serum.

Minimum bactericidal concentration

The minimum bactericidal concentration (MBC) was determined according to the CLSI guidelines.²⁶ Briefly, the MIC assay was extended and after determination of the MIC 10 μL aliquots were taken from all wells above the MIC and spotted onto sheep blood agar. The plates were incubated for 24 and 48 hours before determination of the MBC as the lowest concentration where 99.9% of the final inoculum is killed.

Time kill assays

Time kill assays were performed in 20 μL samples at 1x, 2x, 4x and 8x the MIC of each compound in glass flasks according to CLSI guidelines with LB broth replacing the CAMHB (NCCLS, 1999). The compounds were serially diluted in 100% DMSO at 100x the final desired concentration and 200 μL of appropriate concentrations added to each flask. Cultures were incubated at 37 °C with samples taken at 0, 4, 8 and 24 hours.

Biofilm Assays

Biofilm activity was determined using the MBEC assay system as previously outlined (Ceri et al., 2001). Briefly, biofilms were allowed to grow for 24 hours on MBEC pegs before exposure to the compounds for a further 24 hours. After exposure the biofilms were dispersed by sonication and the CFU.mL⁻¹ determined via spot plating. Again all compounds were serially diluted in 100% DMSO before addition to treatment wells (as outlined in MIC assays).

Toxicity assays

Haemolysis assay

Sheep erythrocytes were exposed to various concentrations of **1**, **27** and **69** as described previously (Leejae et al., 2013). Briefly, erythrocytes were washed three times in saline, re-suspended to a final concentration of $\sim 10^{10}$ cells.mL⁻¹ and 5 μ L of compound dissolved in DMSO was added. Erythrocytes were incubated at 37 °C for 30 minutes with gentle shaking before being put on ice for 5 minutes and centrifuged to pellet cells. The positive control was erythrocytes exposed to water resulting in 100% lysis. After centrifugation the absorbance of the supernatant was recorded at 550 nm.

Tissue culture cytotoxicity

HEL 299 (ATCC CCL-137) and Hep G2 (ATCC HB-8065) human cell lines were maintained in Dulbecco's Modified Eagle's Medium (DMEM; Gibco Cat No: 12430) supplemented with 10% (vol/vol) foetal bovine serum and 1% PenStrep (100 U/mL Penicillin and 100 μ g/mL Streptomycin) and passaged ~ every 3 days. Assays were performed in duplicate in 96 well plates seeded with $\sim 50\,000$ cells per well. Twenty-four hours after seeding the plates, media was removed, washed once with medium without antibiotics and fresh media was added. Two hours later, **1**, **27** and **69** were diluted in DMSO and added to each well at a concentration of 1% in doubling dilutions starting at the same concentrations used for MIC testing. After 24 hours exposure WST-1 reagent was added to each well at a final concentration of 10%. Absorbance at 450 nm was recorded after 1 hour of incubation with WST-1 reagent. The GI₅₀ values were determined via non-linear regression using GraphPad Prism v6 software.

Synthetic Chemistry (See Appendix 1 for specific synthesis methods.)

Compounds **3**, **4**, **8**, **9-11**, **15-17**, **21-23**, **69**, **71**, **S1**, **S3**, and **S5-S7**, **S36**, **S37** were synthesized by an external contractor, EpiChem Pty Ltd (Melbourne Australia).

General Method A

A suspension of the appropriate aldehyde (2.2 eq.) and *N,N*-diaminoguanidine hydrochloride (1.0 eq.) in EtOH was heated at reflux for 16 h. The mixture was cooled and diluted with Et₂O to effect crystallization. The resulting precipitate was collected and washed with Et₂O to afford the carbonimidic dihydrazide.

General Method B

A suspension of aldehyde (2.2 eq.) and *N,N*-diaminoguanidine hydrochloride (1.0 eq.) in EtOH (5 mL) was subjected to microwave irradiation (150 W) at 100 °C for 10 minutes. Most of the solvent was then removed *in vacuo*, Et₂O (5 mL) was added and the flask was chilled to effect crystallization. The resulting precipitate was collected and washed with Et₂O (5 mL) to afford the carbonimidic dihydrazide.

Chapter 3: Potential of Novel Robenidine Analogues as Antibacterial Agents Targeting Gram-Negative Pathogens

3.1 Statement of Authorship

Title of Paper	Potential of Novel Robenidine Analogues as Antibacterial Agents Targeting Gram-Negative Pathogens
Publication Status	<input type="checkbox"/> Published <input type="checkbox"/> Accepted for Publication <input type="checkbox"/> Submitted for Publication <input checked="" type="checkbox"/> Unpublished and Unsubmitted work written in manuscript style
Publication Details	NA

Principal Author

Name of Principal Author (Candidate)	Rebecca Jane Abraham		
Contribution to the Paper	Design and completion of experimental work, interpretation of results and preparation of the manuscript		
Overall percentage (%)	95		
Certification:	This paper reports on original research I conducted during the period of my Higher Degree by Research candidature and is not subject to any obligations or contractual agreements with a third party that would constrain its inclusion in this thesis. I am the primary author of this paper.		
Signature		Date	13 th December 2017

Co-Author Contributions

By signing the Statement of Authorship, each author certifies that:

- i. the candidate's stated contribution to the publication is accurate (as detailed above);
- ii. permission is granted for the candidate to include the publication in the thesis; and
- iii. the sum of all co-author contributions is equal to 100% less the candidate's stated contribution.

Name of Co-Author			
Contribution to the Paper			
Signature		Date	

Name of Co-Author			
Contribution to the Paper			
Signature		Date	

Please cut and paste additional co-author panels here as required.

3.2 Abstract

Recently 79 structural analogues of robenidine were developed to explore antibacterial structure activity relationships (SAR). Several of these analogues were active against the Gram-positive pathogens *S. aureus* and *E. faecalis*, however no activity against Gram-negative pathogens was observed. Although no inherent Gram-negative activity was observed among the 79 analogues, the MIC decreased 10 fold in the presence of a membrane permeabilising agent. In this study spheroplasts of *E. coli* were developed to better understand the Gram-negative activity of robenidine. In addition, the SAR was further explored with the intention to induce native Gram-negative activity. As expected, studies with spheroplasts confirmed that the target of robenidine is present in Gram-negative organisms and demonstrated a bactericidal mechanism of action. In addition, novel analogues were developed with activity against Gram-negative bacteria, with minimum inhibitory concentrations (MICs) against *E. coli* and *P. aeruginosa* ranging between 16 and 128 µg/ml.

3.3 Article

The development of MDR pathogenic bacteria is an emerging concern for the global healthcare system. In particular, the 'ESKAPE' pathogens (*Enterococcus faecium*, *Staphylococcus aureus*, *Klebsiella pneumoniae*, *Acinetobacter baumannii*, *Pseudomonas aeruginosa* and *Enterobacter* species) cause the majority of nosocomial infections and can readily share resistance genes (Rice, 2008). Of greatest concern are the Gram-negative bacteria resistant to critically important antimicrobials. To further add to the issue, there is limited development of novel antimicrobials to combat MDR Gram-negative bacteria. A recent review of drugs under development for treatment of MDR Gram-negative pathogens by the Infectious Diseases Society of America stated that progress in this area remains alarmingly slow. Of the 7 drugs reported in clinical development none were active against the entire range of Gram-negative bacilli (Boucher et al., 2013; WHO, 2017). In this study, we examined the potential of a new class of antimicrobials, based on the structure of the coccidostat robenidine, to be developed for use as Gram-negative antibacterial agents.

The antibacterial activity of robenidine (2,2' – bis[(4-chlorophenyl) methylene]-carbonimidic dihydrazide hydrochloride) and 79 structural analogues has been recently reported. In the reported study, none of the analogues had intrinsic activity against Gram-negative bacteria. However, a small subset was able to inhibit Gram-negative bacteria in the presence of polymyxin B nonapeptide (PMBN), a membrane permeabilising agent (Abraham et al., 2016).

In this study, the activity of robenidine against Gram-negative bacteria was explored further by producing spheroplasts (cells lacking a cell wall) of *E. coli* to investigate the kill profile of robenidine. In addition, a further 32 novel analogues were screened for antibacterial activity.

Methicillin susceptible *S. aureus* strains ATCC 25923, 6538 and 29213 were obtained from the American type tissue culture collection along with *Escherichia coli* ATCC 25922, *Escherichia coli* ATCC 25923 and *Pseudomonas aeruginosa* ATCC 27853. *E. faecalis*, *Pseudomonas* spp., MRSA 1, MRSA 2, VRE 1 and VRE 2 were obtained from The University of Adelaide School of Animal and Veterinary Science (SAVS) bacterial collection. All robenidine analogues were supplied by Prof. Adam McClusky (University of Newcastle). All other antimicrobials were sourced from Sigma Aldrich.

The induction of *E. coli* (ATCC 25922) spheroplasts was performed with ampicillin. An overnight broth culture was diluted to approximately 1×10^9 cells/ml in Cation-adjusted Mueller-Hinton broth (CAMHB) supplemented with 50 µg/ml ampicillin, 0.4 M sucrose and 8 mM MgSO₄ (Lederberg, 1956; Randall et al., 2013). The culture was incubated for ~ 2hrs, until the majority of cells had become spherical, as observed under phase contrast microscope. The regeneration of spheroplast cells, necessary to determine spheroplast formation efficiency and activity of robenidine, was determined using brain heart infusion agar. Assays to determine the effect of robenidine against *E. coli* spheroplasts were performed in test tubes. An aliquot (3 ml) of spheroplast culture was added to each test tube with 50 µl of robenidine at an appropriate concentration (8, 16, 32, 64 or 128 µg/ml) and gently inverted to mix. DMSO (compound solvent) only was used as a positive control. Spheroplasts were incubated at 37°C for 24 hrs, with samples taken at 0, 2, 4, 6, 8 and 24 hours. At each sampling, the tubes were gently inverted to mix the culture. Samples were serially diluted 1:10 and 10 µl of each dilution spotted onto brain heart infusion agar (in triplicate). Samples were incubated at 37°C for 48 hrs and colonies counted at 24 and 48 hrs post incubation. At 24 hrs post robenidine exposure, a sample was taken from each concentration, stained with Trypan blue and imaged at 100X magnification. Each assay was repeated in duplicate, in duplicate.

Susceptibility testing of the analogues was completed according to Clinical Laboratory Standards Institute (CLSI) guidelines for testing antimicrobial agents (CLSI, 2008). Initially, CAMHB was used but was replaced with Luria Bertanini broth (LBB) due to interactions observed with the test compounds and CAMHB (Rozengart and Saakov, 2002) (Appendix 3). Antimicrobial stocks and bacterial suspensions were prepared according to CLSI guidelines. Modifications were made to the standard protocol due to the insoluble nature of the novel

analogues. All analogues were serially diluted in DMSO at 100 X the final desired concentration and 2 µl of dilution added to individual wells of the assay plate. CAMHB or LBB was added to a final volume of 180 µl and finally 20 µl of diluted bacterial suspension was added to give an assay concentration of $\sim 5 \times 10^5$ cells/ml per well. The assay was incubated for 20-24 hrs at 37°C before interpretation of the results. All assays were repeated in duplicate.

In this study, the potential for robenidine to target Gram-negative bacteria was explored through the development of *E. coli* spheroplasts. Spheroplasts are viable bacterial cells in which the cell wall is almost completely lacking, causing the cells to take on a spherical shape (Poole, 1993). In this case, the cell wall was removed by the addition of sub-inhibitory concentrations of ampicillin. Although the cells are still viable, they are unable to reproduce (Appendix 3). Once the ampicillin has been removed, cells are able to regenerate and continue normal growth. The spheroplast formation frequency in this study was >99% with a regeneration frequency of >70%. Time-kill curve evaluation of robenidine against *E. coli* spheroplasts indicated bactericidal activity of the compound resulting in a > 4 log reduction of cells at the 2 highest concentrations of robenidine after 24 hr exposure (Figure 3.1).

In addition, all concentrations tested resulted in some inhibition of spheroplast regeneration after 24 hrs. These results confirm the previous findings (Abraham et al., 2016) where robenidine and a second structural analogue were able to inhibit bacterial growth in the presence of PMBN, a membrane permeabilizing agent, with a ≥ 10 -fold reduction in minimum inhibitory concentration (MIC). The results in the present study demonstrated that the bactericidal activity of robenidine in Gram-negative organisms is similar to that seen in Gram-positive organisms (Abraham et al., 2016). Furthermore, it is possible to hypothesise from this information that robenidine may have a potential target site that doesn't involve the cell wall as robenidine still had an inhibitory effect despite removal of the cell wall. Cell samples from each concentration were taken at 24 hours for microscopic observation (Figure 3.2). At concentrations of 16 µg/ml, spheroplasts appeared swollen in size compared to untreated cells and were no longer clearly defined. As the concentration of robenidine increased, the cells became increasingly pleomorphic in shape.

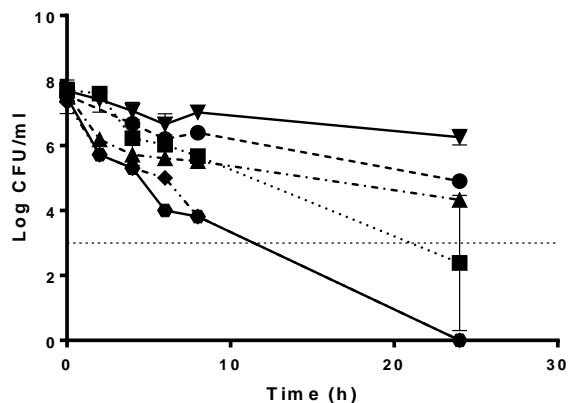


Figure 3.1 The activity of robenidine against *E. coli* spheroplasts. *E. coli* spheroplasts were induced with sub-lethal concentrations of ampicillin before exposure to robenidine at concentrations ranging from 0 – 128 µg/ml. The experiment was repeated in triplicate and a representative result has been portrayed here. Error is \pm SD. Key: triangles 0 µg/ml robenidine; circles 8 µg/ml robenidine; squares 16 µg/ml robenidine; inverted triangles 32 µg/ml robenidine, diamonds 64 µg/ml robenidine and hexagons 128 µg/ml robenidine. Broken line indicates the detection limit. A log₃ reduction in cell number signifies statistical significance as described by CLSI guidelines.

In this study, a novel subset of robenidine analogues were also screened against representative bacterial pathogens (Table 3.1 and 3.2). Of this group of compounds, 18 showed antibacterial activity against at least one Gram-positive pathogen with MICs ranging from 4 – 128 µg/ml further confirming the Gram-positive spectrum of this series of compounds (Abraham et al., 2016). More interestingly, seven of the novel analogues demonstrated inhibitory activity towards Gram-negative pathogens with MICs ranging from 16 – 128 µg/ml. All the Gram-negative active agents were effective in inhibiting the growth of *E. coli* while three were active against both *E. coli* and *P. aeruginosa*. All of the compounds that were active against the Gram-negative organisms were smaller in size (mw <310 g/mol) and had an exposed guanidine terminus. Although the smaller size of the Gram-negative active agents could be important to the Gram-negative activity (presumably through the ability to traverse outer membrane porins), it is also possible that the guanidine terminus, a moiety that induces cell membrane permeability, is a more important attribute assisting in transfer of the compound across the bacterial membrane, as permeabilisation of the Gram-negative outer-membrane has been shown to extend the spectrum of activity of the lead to Gram-negative organisms (Abraham et al., 2016; Pantos et al., 2008).

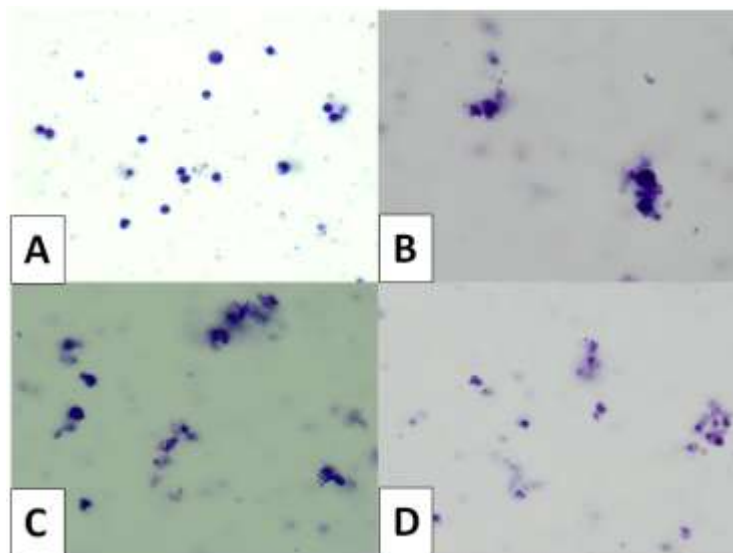
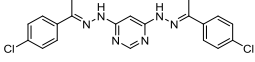
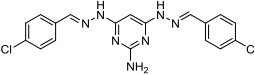
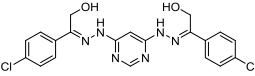
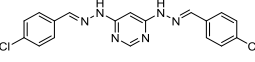
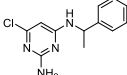
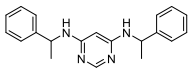
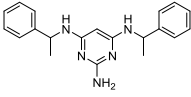
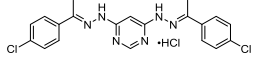
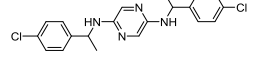
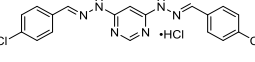
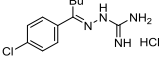
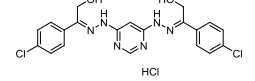
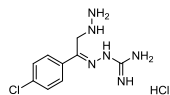


Figure 3.2 Morphological effect of robenidine on *E. coli* spheroplasts after 24-hour exposure. *E. coli* spheroplasts were treated with A: 0 ug/ml, B: 16 ug/ml, C: 32 ug/ml or D 64 ug/ml of robenidine before staining with trypan blue and imaging. As the concentration of robenidine increased the cells became more pleomorphic in shape which corresponded to relative bactericidal activity at the various drug concentrations. Cells imaged at 100 X magnification.

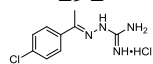
In conclusion we confirmed the target of robenidine is present in Gram-negative bacteria and that the compound has bactericidal activity. In addition, several novel analogues were identified with antibacterial activity, and these were also demonstrated to have activity against Gram-negative pathogens including *P. aeruginosa*. The extension of the spectrum of activity could be in part due to the small molecular weight of the active analogues as well as the guanidine terminus increasing the membrane permeability potential of the analogues. Based on this study, further work investigating the structure activity relationship conferring Gram-negative activity is warranted.

Table 3.1 Selection of analogues chosen to be tested for antibacterial activity against both Gram-positive and Gram-negative bacteria. Analogues were tested according to CLSI guidelines in cation adjusted Mueller Hinton broth. Each analogue was tested in duplicate and ampicillin was used as a control drug.

ID Structure	MIC (μM)			
	<i>S. aureus</i> ^c	<i>E. faecalis</i> ^b	<i>Pseudomonas</i> ^b	<i>E. coli</i> ^a
178 	- ^d	-	-	-
179 	10.0	20.0	-	-
180 	-	143.7	-	-
181 	-	-	-	-
182 	-	-	-	-
183 	-	-	-	-
184 	-	191.4	-	-
185 	-	-	-	-
186 	-	-	-	-
187 	-	-	-	-
188 	83.0	83.0	-	202.9
189 	-	-	-	-
190	173.2	230.9	-	-

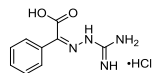


191



- - - -

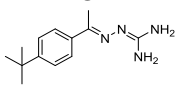
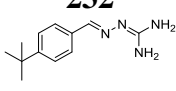
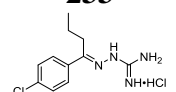
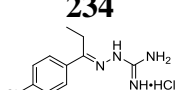
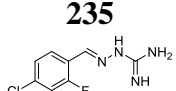
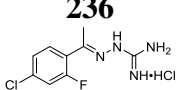
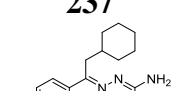
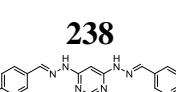
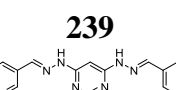
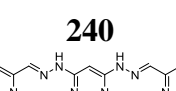
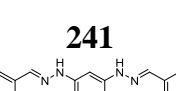
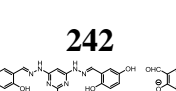
192

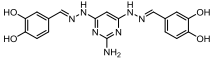
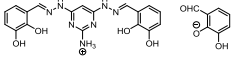
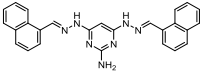
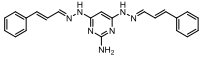
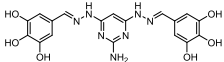


- - - -

^a*E. coli* ATCC 25922, ^bIsolates from The University of Adelaide SAVS collection (*Pseudomonas* #8, *E. faecalis* #32), ^c*S. aureus* ATCC 29213. ^d = inactive at 64 μg/ml.

Table 3.2 Selection of robenidine analogues screened for antibacterial activity. The compounds were screened according to CLSI guidelines with LB broth replacing CAMHB and prior dilution of analogues in DMSO. Assays were repeated in duplicate.

ID Structure	MIC (μM)				
	<i>S. aureus</i> ^a	MRSA ^b	VRE ^b	<i>Pseudomonas</i> ^b	<i>E.coli</i> ^c
231 	137.7	104.7 – 137.7	137.7	275.5	137.7
232 	146.6	73.3 - 146.6	293.2	293.2	293.2
233 	116.3- 232.6	116.3	116.3	465.2	232.6
234 	245.1	245.1	245.1	- ^d	490.1
235 	596.4	596.4	596.4	-	-
236 	60.4	120.7	120.7- 241.4	-	482.8
237 	13.0- 25.9	25.9	25.9	-	51.8
238 	/ ^e	/	/	/	/
239 	96.0	24.0- 96.0	48.0	-	-
240 	-	12.0 – 384.0	96.0 - 384.0	-	-
241 	-	-	192.0	-	-
242 	-	-	-	-	-

243 	-	-	-	-	-
244 	30.0	15.0	15.0	-	-
245 	18.5	18.5	148.3	-	-
246 	20.9	20.9- 41.7	-	-	-
247 	-	299.5	-	-	-

^a *S. aureus* ATCC 29213, ^bIsolates from The University of Adelaide SAVS collection (MRSA 1, MRSA2, VRE 1, VRE 2, *Pseudomonas* #8, *E. faecalis* #32), ^c *E. coli* ATCC 25922, ^d = no inhibition at 128 µg/ml. ^e = no inhibition at 64 µg/ml.

Chapter 4: Anti-trypanosomatid Activity of Novel Robenidine Analogue

4.1 Statement of Authorship

Title of Paper	Anti-trypanosomatid Activity of Novel Robenidine Analogues
Publication Status	<input type="checkbox"/> Published <input type="checkbox"/> Accepted for Publication <input type="checkbox"/> Submitted for Publication <input checked="" type="checkbox"/> Unpublished and Unsubmitted work written in manuscript style
Publication Details	

Principal Author

Name of Principal Author (Candidate)	Rebecca Jane Abraham		
Contribution to the Paper	Completed all experimental work, interpretation of results and preparation of manuscript. The following people were involved in experimental design, sharing of expertise and student training in techniques: Dr Armando Jardim (The University of McGill) and Dr. Norma Batista (The University of McGill)		
Overall percentage (%)	95%		
Certification:	This paper reports on original research I conducted during the period of my Higher Degree by Research candidature and is not subject to any obligations or contractual agreements with a third party that would constrain its inclusion in this thesis. I am the primary author of this paper.		
Signature		Date	13 th December 2017

Co-Author Contributions

By signing the Statement of Authorship, each author certifies that:

- i. the candidate's stated contribution to the publication is accurate (as detailed above);
- ii. permission is granted for the candidate to include the publication in the thesis; and
- iii. the sum of all co-author contributions is equal to 100% less the candidate's stated contribution.

Name of Co-Author			
Contribution to the Paper			
Signature		Date	

Name of Co-Author			
Contribution to the Paper			
Signature		Date	

4.2 Abstract

Trypanosomatids cause significant human morbidity and mortality, with an estimated 1.3 million new cases per year resulting in ~ 30 000 deaths occurring due to *Leishmania* sp. alone. In addition to this, trypanosomatids, such as *Trypanosoma brucei* (endemic to Africa), cause significant morbidity and mortality to humans, as well as significant losses in the livestock industry. Currently the chemotherapy available for these organisms is limited and has unwanted toxic side effects. In this study we investigated the antitrypanosomatid activity of several novel chemical entities, based on the structure of the well characterised coccidiostat robenidine, against promastigote stages of the *L. donovani* and *T. brucei* parasites. The sensitivity of the parasite towards the compounds was measured using the metabolic dye resazurin and toxicity towards mammalian cells, was determined with a WST-1 dye. Several of the drugs were highly effective against both parasites in primary screens. The drugs were not selective for *T. brucei* over mammalian cells. However, several of the compounds had very promising results against *L. donovani* with selectivity indices > 20. Based on the results of this study, several novel chemical entities were identified as potential antileishmanial agents which warrant further investigation.

4.3 Introduction

Trypanosomatids, including *Trypanosoma* spp. and *Leishmania* spp., cause significant morbidity and mortality in tropical regions of the world. These parasites are included as a part of the WHO neglected diseases initiative and, combined, are estimated to infect 20 million people globally with at least a further 300 million at risk (Lopes et al., 2010; Santos et al., 2008). Two of the most devastating disease agents from this family are *Trypanosoma brucei* and *Leishmania donovani*, both of which can result in fatal consequences if not treated (Barrett and Croft, 2012; Lopes et al., 2010; No, 2016).

T. brucei is endemic to Africa and is responsible for the disease commonly known as sleeping sickness, which is 100% fatal if left untreated. In the year 2000, there are an estimated 70 000 new infections with *T. brucei* each year with 60 million people at risk, mostly in rural villages (Burri et al., 2000). However the estimated cases had dropped to less than 15 000 in 2014 (WHO, Global Health Observatory data repository). *T. brucei* is spread via the insect vector, the tsetse fly, and, depending on the subspecies of parasite, can result in an acute disease that lasts for months or a chronic disease that can last for years. The first stage of the disease, where the parasite is found in the lymphatic system and blood stream, includes symptoms such as fever, chills, headache and lymphadenopathy. As the disease progresses, the parasite moves into the central nervous system (CNS) with symptoms including severe headache, psychiatric manifestations and mental deterioration which progresses to seizures, coma and eventually, death (Barrett and Croft, 2012; Buscher et al., 2017; Field et al., 2017; Lopes et al., 2010; Lutje et al., 2013).

L. donovani is more widespread than *T. brucei*, found in Africa, Asia and Europe. As seen with *Trypanosoma* spp., *Leishmania* is also transmitted by an insect vector; the phlebotomine sandfly. Several disease manifestations of *Leishmania* occur, including visceral and various severities of cutaneous leishmaniasis. Visceral leishmaniasis, caused by *L. donovani*, is fatal if left untreated and is characterised by fever, weight loss and swelling of the liver and spleen, while cutaneous leishmaniasis is characterised by severe skin lesions that can leave disfiguring scars (Barrett and Croft, 2012). Unlike *Trypanosoma* spp., *Leishmania* spp. have an intracellular stage in the human host, residing and multiplying in the macrophages eventually leading to macrophage lysis, release of the parasite and progression of the disease (Santos et al., 2008).

Although the disease burden caused by trypanosomatids is high, there is a significant lack of effective and safe treatment options (Field et al., 2017). For the treatment of *T. brucei* pentamidine and suramin are used during the early stages of the disease (before migration to

the CNS) and melarsoprol and eflornithine are used in the late stages of the disease (after CNS migration). While eflornithine seems to be relatively safe it is significantly more expensive than melarsoprol (Brun et al., 2001a; Brun et al., 2001b; Burri et al., 2000; Kennedy, 2013). The other 3 drugs mentioned have severe side effects including nephrotoxicity and renal complications, severe allergic reactions in some individuals and reactive encephalopathy which can result in death in up to 70% of afflicted patients (Burri et al., 2000; Kennedy, 2013; Lopes et al., 2010).

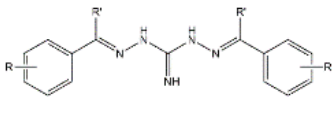
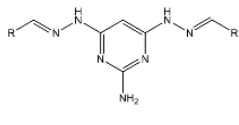
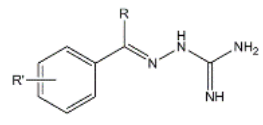
The drugs available for the treatment of leishmaniasis have similar limitations to those used in the treatment of *T. brucei*. Currently pentavalent antimonials are used which are highly toxic. More recently, amphotericin B, paromomycin and miltefosine have been used in treatment in various countries (Richard and Werbovetz, 2010).

In addition to the side effects of the drugs, there have also been reports of treatment failures due to the development of drug resistance within the parasite population (Lira et al., 1999; Matovu et al., 2001).

With the severe side effects and treatment failures, which are increasing as drug resistance increases, it is crucial to continue the discovery and development of novel antitrypanosomatids (Santos et al., 2008). This has proven difficult in the past, with several promising candidates being rejected due to toxic side effects or the inability to treat late stages of disease in animal models (Brun et al., 2001a). With the prohibitive cost and time consuming nature of drug development in mind and the need for new treatments as soon as possible, the repurposing of chemically characterised biologically active compounds has become popular, as it is a relatively cheaper and quicker method of drug development than starting with completely novel chemical entities or plant extracts (Chong and Sullivan, 2007; Field et al., 2017).

We performed a preliminary study into the potential efficacy of robenidine (**812**) and several novel analogues against both *T. brucei* and *L. donovani in vitro*. Robenidine is a coccidostat that has been used in the poultry and commercial rabbit industries since the 1970s to control *Eimeria* (Kantor et al., 1970). Safety and toxicity studies have shown it to have no genotoxic, carcinogenic or reproductive toxicity *in vitro* or in animal models, making it a good choice for other antiparasitic applications. In this study, 19 analogues of **812**, in addition to **812** itself, were tested against the procyclic and promastigote stages of the respective parasites as these stages are easily grown *in vitro* and are a good preliminary indicator for activity against the stages that occur in the human host (Table 4.1).

Table 4.1 Chemical identity of the novel chemical entities tested for inhibitory activity against *Leishmania donovani* and *Trypanosoma brucei*

Scaffold 1			Scaffold 2		Scaffold 3		
							
ID	R	R'	ID	R	ID	R	R'
812	4-Cl	H	195	4-CH ₃ C ₆ H ₄	041	H	4-CF ₃
024	4-CN	H	197	5-OHC ₆ H ₄	042	H	2-CF ₃
026	3-CN	H	201	4-N(CH ₃) ₂ C ₆ H ₄	052	H	3-Cl
028	2-OCH ₃	H	245	C ₁₀ H ₈	191	CH ₃	4-Cl
062	4-Cl	CH ₃	246	C(C ₆ H ₅)	231	CH ₃	4-C(CH ₃) ₃
099	4-C(CH ₃) ₃	H					
113	4-N(CH ₃) ₂	H					
166	4-SCF ₃	H					
171	2-OH, 4-N(CH ₃) ₂	H					
219	4-C(CH ₃) ₃	CH ₃					

4.4 Materials and methods

4.4.1 Antimicrobial agents

Compounds were synthesised at the University of Newcastle and are all considered structural analogues of robenidine. The compounds were all dissolved in DMSO to a final concentration of 10 mM. Pentamidine (Sigma) was used as a positive control and dissolved in DMSO to a final concentration of 10 mM.

4.4.2 *Leishmania donovani* screening

Procyclic promastigotes from exponentially growing cultures maintained in DME-L+ Bob additions in a humidified incubator at 28°C with 5 % CO₂ were used for all assays. To determine the antitrypanosomatidial activity, compounds were diluted in culture media to a final volume of 10 µM in 96 well plates. Promastigotes were diluted to a density of ~8 x 10⁵ cells/ml then added to the assay plate resulting in a final cell density of 4 x 10⁵ cells/ml. Cells were incubated for 96 hrs at 28°C before the addition of resazurin dye (Sigma). Fluorescence was read at excitation 530 nm and Emission 590 nm (Synergy H4 hybrid reader, BioTek). To determine IC₅₀'s, compounds that showed inhibitory activity at 10 µM were further investigated. Compounds were serially diluted in thirds, in a 96 well plate, in cell growth media so that concentrations ranged from 0.005 to 10 µM and promastigotes were added to a final concentration of 1 x 10⁶ cells/ml. Cells were incubated at 27°C for 72 hrs before the addition of resazurin dye (Sigma). Fluorescence was measured as above. Results were analysed using a t-test in Graphpad Prism v7 software.

4.4.3 *Trypanosoma brucei* screening

Procyclic promastigotes from exponentially growing cells maintained in SDM-79 medium in a humidified incubator at 28°C with 5 % CO₂ were used in all assays. Compounds were initially screened at 10 µM for activity, diluted in culture media before the addition of promastigotes (final concentration 4 x 10⁵ cells/ml). Cells were incubated for 48 hrs at 27°C before the addition of resazurin dye. Fluorescence was measured as for *L. donovani* activity assays. Compounds that showed inhibition at 10 µM were further characterised to determine IC₅₀ values. Compounds were serially diluted in thirds in culture media resulting in final concentrations ranging from 0.005 – 10 µM. Promastigotes were added at a final concentration of 4 x 10⁵ cells/ml. Cells were incubated at 27°C for 48 hrs before the addition of resazurin dye. In addition, promastigotes, at a concentration of 8 x 10⁵ cells/ml were exposed to 10 µM of **026** for 1.5 hours before removal of the drug via centrifugation at 5000 rpm for 7 minutes and resuspension of cells in culture media. Following this, cells were incubated for 96 hours at 27°C and observed daily for metabolic activity (resazurin dye) and morphological changes. A DMSO

treated culture was used as a negative control. Results were analysed using a t-test in Graphpad Prism v7 software.

4.4.4 Cell toxicity assays

RAW 264.7 cells, a mouse macrophage line, were grown in RPMI1640 media supplemented with L-glutamine and either 10 % FCS (general maintenance of cell line) or 5 % FCS (cytotoxicity assays) and were routinely subcultured when 80 % confluent, approximately every 3-4 days. To determine *in vitro* cytotoxicity, cells were diluted to a final concentration of 1×10^5 cells/ml and assays were performed in a final volume of 200 μ l in 96 well plate (nunc; Thermo Fisher Scientific). After inoculation of plates, cells were incubated in a humidified incubator for 2 hrs at 37°C with 5% CO₂ before the addition of analogues diluted in DMSO (2 μ l / well) or DMSO only for the growth control. Cells were incubated for a further 24 hrs at 37°C with 5% CO₂. After incubation the metabolic activity of the cells was determined using the WST-1 assay system according to manufacturer's instructions (Roche Australia). Briefly, cells were washed with PBS and incubated with a final concentration of 10 % WST-1 reagent in PBS for 1 hour (humidified 37°C, 5% CO₂). Absorbance was measured at 450 nm (iMark Microplate Reader S/N 12510, Bio-Rad Laboratories). The IC₅₀ was determined via graphpad prism software using the nonlinear regression function with a normalised response. The selectivity index of the compounds was determined by dividing the IC₅₀ of the compound against macrophages by the IC₅₀ against the respective parasite.

4.5 Results

Robenidine and 19 structural analogues were screened for activity against the promastigote stage of *L. donovani* and *T. brucei* at 10 μ M. Of the compounds tested 70% showed a $\geq 90\%$ reduction of metabolic activity in *L. donovani*, while only 10% showed a similar reduction of metabolic activity in *T. brucei* (Figure 4.1). Only one of the analogues (**197**) showed no activity against *L. donovani* at the concentration tested and only minimal activity towards *T. brucei* and is considered the least active of the analogues tested. Analogues **026**, **062** and **246** were very effective against both species of parasites. The majority of compounds showed activity against *L. donovani* with **026**, **028**, **041**, **042**, **062**, **099**, **195**, **201**, **219** and **246** being the most active. The activity of the analogues against *T. brucei* was more varied with **026**, **062**, and **246** having the greatest activity while **041**, **042**, **191** and **231** were the least effective. Further investigation of a selection of compounds that had the greatest activity against the parasites was completed to determine the IC₅₀ values. Against *L. donovani* the IC₅₀ value was determined for **028**, **099**, **166**, **201**, **245**, **246** and **812**. The IC₅₀ range was 0.37 μ M (**028**) to 6.48 μ M (**245** and **246**). The IC₅₀ value was determined against *T. brucei* with the 6 most effective analogues; **024**, **026**, **062**,

171, 195 and **246**. Of these analogues **026, 171** and **195** were the most effective with IC₅₀ values of 1.7, 1.4 and 1.5 μ M respectively. The highest IC₅₀ value determined was 4.2 μ M for **246**.

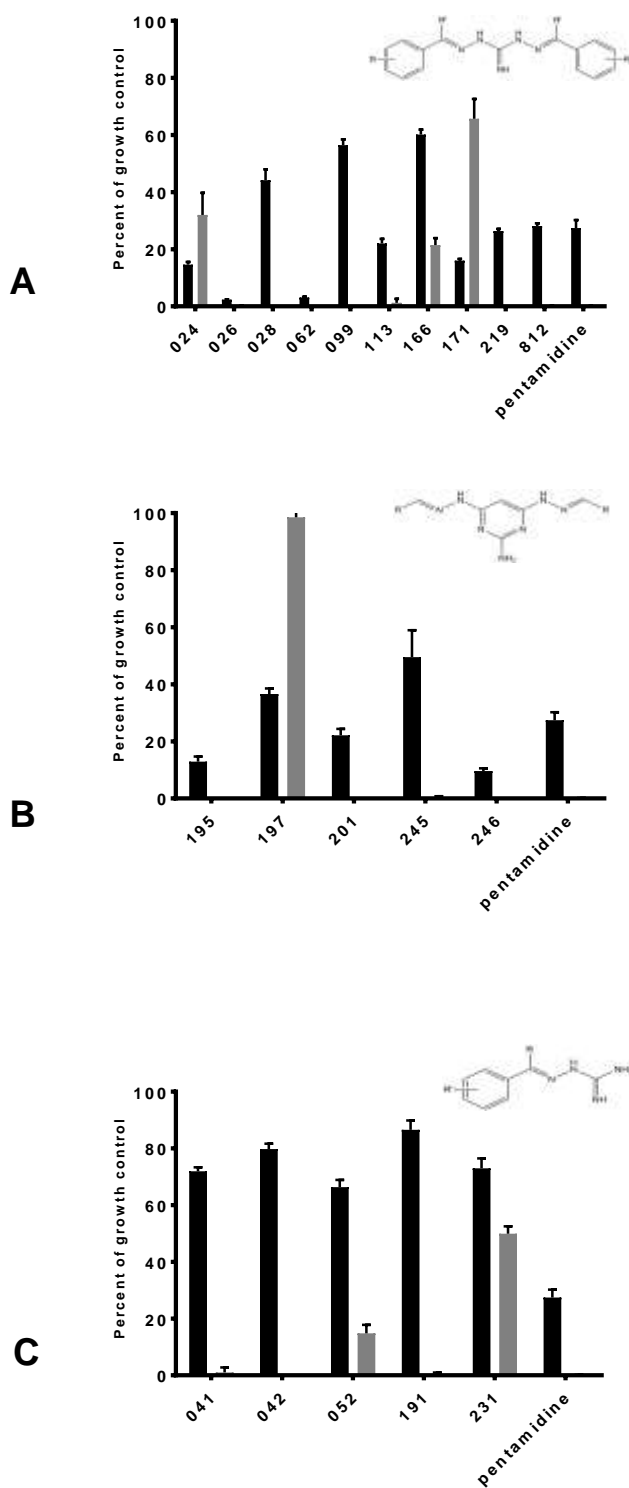


Figure 4.1 Antitrypanosomatid activity of robenidine and 19 structural analogues. The activity of the potential drug candidates was assessed using the promastigote stages of the *Trypanosoma brucei* (black) or *Leishmania donovani* (grey) parasites and measured with a fluorescent dye. The analogues were divided into three groups based on core scaffolds: A - scaffold 1, B - scaffold 2 and C - scaffold 3. Refer to Table 4.1 for detailed structural information. All novel analogues were significantly different than the control, except NCL197 against *Leishmania*, as analysed by a *t*-test. $p < 0.001$.

In vitro toxicity of the most active antiprotozoal analogues investigated in this study was determined using RAW 264.7 cells (Table 4.2). Fifty percent Growth inhibition (GI₅₀) concentrations ranged from 3.7 ± 0.7 μM to 19.3 ± 3.8 μM and were used to calculate the selectivity index (SI) of the analogues for the parasite over mammalian cells.

An assay to determine the ability of *T. brucei* to recover after a short exposure to **026** was performed. After 1.5 hrs of exposure to the **026** compound, promastigotes were pleomorphic in appearance. Metabolic activity of the culture was determined at 48 and 96 hours post exposure and no activity was observed.

Table 4.2 The selectivity of active analogues for trypanosomatid parasites over mammalian cells. Cells were exposed to increasing concentrations of the compounds for select periods of time to determine the GI₅₀ or IC₅₀. The selectivity index (SI) was determined by dividing the GI₅₀ of macrophages by the IC₅₀ of parasites. An SI ≥10 was considered selective for the parasite. Assays were repeated in triplicate. Error ± SD. '-' = not determined. Results in bold highlight selective analogues.

ID	GI ₅₀ Macrophage (μM)	<i>T. brucei</i>		<i>L. donovani</i>	
		IC ₅₀ (μM)	SI	IC ₅₀ (μM)	SI
812	14.8 ± 1.3	-	-	2.9 ± 0.2	5.1
024	12.7 ± 2.8	3.4 ± 0.1	3.8	-	-
026	9.6 ± 1.0	1.7 ± 0.6	5.7	2.5 ± 0.1	3.8
028	8.1 ± 2.8	-	-	0.3 ± 0.1	27.9
062	7.2 ± 1.3	4.0 ± 0.8	1.8	-	-
099	7.7 ± 0.6	-	-	0.4 ± 0.1	20.7
113	12.9 ± 3.5	-	-	0.9 ± 0.1	14
166	9.5 ± 0.1	-	-	3.2 ± 1.0	2.8
171	12.5 ± 3.6	1.4 ± 0.1	9.1	-	-
195	5.8 ± 0.3	1.5 ± 0.8	3.8	-	-
201	12.3 ± 2.1	-	-	2.9 ± 0.2	4.2
219	19.3 ± 3.8	-	-	0.8 ± 0.1	24.1
245	3.7 ± 0.7	-	-	7.2 ± 2.1	0.6
246	13.8 ± 0.1	4.2 ± 0.4	3.3	6.7 ± 3.0	2.1

4.6 Discussion

Nineteen structural analogues of **812**, in addition to **812** were tested for activity against the promastigote stages of representative *Leishmania* and *Trypanosoma* parasites *in vitro*. The *Leishmania* parasite was, overall, more sensitive towards the drug library than the *Trypanosoma* parasite. This could be due to the longer exposure time tested with *L. donovani* (96 hrs) compared to *T. brucei* (48 hrs), which was due to the different growth conditions of each parasite. Nevertheless, several of the agents were effective in inhibiting *T. brucei*, with **026** being the most active. In addition, *T. brucei* parasites were unable to recover from a short

exposure to **026** instead becoming pleomorphic in structure and undetectable using metabolic indicator dye. The drugs tested against the parasites were characterised into 3 structural groups based on the core scaffold of each compound (Table 4.1). Although only a small number of analogues were used in this study, some comparison between structures can be made. **812** was very effective against *L. donovani* (100% inhibition) and inhibited *T. brucei* ~70 % in comparison to non-treated cells. When the aromatic chloride moieties were replaced with cyanide (**024**) activity against *L. donovani* decreased from 100% parasite inhibition to 65% inhibition, while *T. brucei* inhibition increased to > 80%. Similar inhibition to **812** of both parasites was observed when the Cl's were replaced with 4-C(CH₃)₃ (**099**) while activity towards *T. brucei* decreased significantly when the same moieties were replaced with 4-N(CH₃)₂ (**113**). Activity towards both parasites decreased when a 4-SCF₃ (**166**) change was made. Imine substitution of **812** with a methyl group improved activity towards *T. brucei* (**062**). Imine substitution of **099** also improved activity towards *T. brucei* (**219**). Addition of an alcohol group to the aromatic rings (**171**) of **113** resulted in a large decrease in activity against both parasites. The compounds from scaffold 3, non-symmetrical adjuncts of scaffold 1, showed no significant activity towards *T. brucei* under the current assay conditions, but the majority had activity against *L. donovani*. Tri-fluoride groups on the aromatic ring (**041** and **042**) of scaffold 3 in different positions appear to be equally effective in inhibiting *L. donovani* in the screening assay. Removal of one aromatic imine portion of **062** (**191**) resulted in a complete loss of activity towards *T. brucei* suggesting that the symmetry of **062** is related to activity, at least in *T. brucei*. Some analogues belonging to scaffold 2 had relatively good activity towards both parasites. The only exception was **197** which was moderately active towards *T. brucei* but inactive against *L. donovani*. The activity of the analogues towards *T. brucei* does not appear to be selective over activity towards mammalian cells as investigated in this paper, with **171** being the most selective but still with a SI below 10. On the other hand, 4 of the analogues active against *L. donovani* were considered selective for the parasite over mammalian cells. **028** was the most selective with an SI of 27.9. **099** (SI 20.7) was also very selective for *L. donovani* and both **028** and **099** also showed selectivity for *L. donovani* over *T. brucei*.

Despite promising results in promastigote stages of the parasites it is crucial to test these drugs against amastigotes, especially the intracellular amastigotes of *L. donovani*. Although results with promastigotes can be predictive of results with amastigotes, it has been shown that some compounds can be selective for different stages of the parasite (De Muylder et al., 2011; Vermeersch et al., 2009). In addition, potential for the analogues to transfer across the blood brain barrier in treating *T. brucei* is also important as in late stages of the disease, when most

treatment cases present, the parasite has crossed the blood brain barrier, resulting in treatment failure with drugs that are excluded by this barrier (Brun et al., 2001a).

In this study we investigated the potential of several novel analogues of the anti-parasitic drug robenidine to kill the kinetoplast parasites *L. donovani* and *T. brucei*. The activity of the analogues was varied between the parasite species with *L. donovani* being more susceptible than *T. brucei* to the chemical entities investigated.

In this study an $SI \geq 10$ was considered selective for the parasite. Based on this classification none of the active analogues were selective for *T. brucei* over mammalian cells while 4 (**028**, **099**, **113** and **219**) were considered highly selective for *L. donovani* with SI 's ≥ 14 . In addition, these 4 analogues showed less activity towards *T. brucei* in original screening assays suggesting they have a greater selectivity for the *Leishmania* parasite over other parasites and would make good candidates for future experiments, firstly in amastigote stages of the *L. donovani* parasite potentially followed by *in vivo* experiments.

**Chapter 5: Antigiardial Activity and Mechanism of Action of Robenidine
and a Library of Related Novel Aminoguanidines**

5.1 Statement of Authorship

Title of Paper	Antigiardial activity and mechanism of action of robenidine and a library of related novel aminoguanidines
Publication Status	<input type="checkbox"/> Published <input type="checkbox"/> Accepted for Publication <input type="checkbox"/> Submitted for Publication <input checked="" type="checkbox"/> Unpublished and Unsubmitted work written in manuscript style
Publication Details	

Principal Author

Name of Principal Author (Candidate)	Rebecca Jane Abraham		
Contribution to the Paper	Designed and completed all experimental work, interpretation of results and preparation of the manuscript. Assistance in design and technical troubleshooting was provided by Dr. Sam Abraham, Dr. Mark O'Dea and Dr. Stephen Page. Lyn Waterhouse from the CMCA electron microscopy facility (The University of Adelaide) assisted with TEM study design and setting of samples in resin as well as sectioning and use of microscope. Dr. Peta Clode and Lyn Kirilak from the University of Western Australia CMCA assisted with SEM preparation and imaging (training and general sample preparation techniques).		
Overall percentage (%)	90%		
Certification:	This paper reports on original research I conducted during the period of my Higher Degree by Research candidature and is not subject to any obligations or contractual agreements with a third party that would constrain its inclusion in this thesis. I am the primary author of this paper.		
Signature		Date	13 th December 2017

Co-Author Contributions

By signing the Statement of Authorship, each author certifies that:

- i. the candidate's stated contribution to the publication is accurate (as detailed above);
- ii. permission is granted for the candidate to include the publication in the thesis; and
- iii. the sum of all co-author contributions is equal to 100% less the candidate's stated contribution.

Name of Co-Author			
Contribution to the Paper			
Signature		Date	

Name of Co-Author			
Contribution to the Paper			
Signature		Date	

Please cut and paste additional co-author panels here as required.

5.2 Abstract

Giardia duodenalis is a ubiquitous parasitic pathogen that causes significant morbidity and mortality worldwide. Failures in drug therapy are common due to poor patient compliance as a result of the need for repeated administration, off target drug effects and increasing drug resistance in parasite populations. In this study, the efficacy and selectivity of robenidine (**812**) and 119 structural analogues against *Giardia in vitro* was determined. In addition, electron microscopy (SEM and TEM) studies were carried out. A total of forty-six analogues, in addition to robenidine, had anti-giardial activity. After 5 hours, compound exposure IC_{50} 's as low as 0.2 μ M were observed with corresponding MICs of 2.8 μ M. This is in contrast to metronidazole (the standard treatment for giardiasis), which required 24 hrs to exhibit inhibitory activity, with an MIC 3-fold higher and an IC_{50} 19-fold higher than the best analogues in this study. Elimination of activity against bacteria and mammalian cells while maintaining anti-giardial activity was also observed with 14 analogues, a significant advantage over already registered drugs. Electron microscopy studies showed that a *Giardia* selective analogues had a multifaceted effect on *Giardia* trophozoites, which differed from the parent compound. In addition, no *in vivo* toxicity in mice was observed for selected analogues at 100 mg/kg delivered orally once per day for 3 days. In conclusion several new chemical entities were identified that were selective for *Giardia* over other cells. Two analogues in particular met all selection criteria with rapid giardicidal activity and a multifaceted phenotypic response involving cell disfiguration and membrane disintegration.

5.3 Introduction

Giardia duodenalis (syn. *Giardia lamblia*, *Giardia intestinalis*) is a bi-nucleate parasitic protist causing between 200 million and 1 billion human infections annually, making it the most common enteric parasitic pathogen worldwide (Halliez and Buret, 2013; Upcroft and Upcroft, 1998; Upcroft and Upcroft, 2001b). Although infections are common in developed nations they are more prevalent in developing nations. *Giardia* has been recognised by the World Health Organisation as an important pathogen by its addition to the neglected diseases initiative (Savioli et al., 2006). *Giardia* infection is established via ingestion of cysts directly through a faecal-oral route or via contaminated food or water (Savioli et al., 2006; Thompson, 2000). *Giardia* causes a malabsorptive gastrointestinal disease with symptoms including diarrhoea, bloating and abdominal cramping (Buret, 2008). Symptoms may be acute or chronic and re-occurring. Persistent infection, especially in children and immunocompromised hosts, results in long term effects including malnutrition, developmental delay and failure to thrive syndrome (Wright et al., 2003).

Globally there are several classes of anti-giardial drugs used to treat giardiasis. The most common include the nitroimidazoles, nitrothiazole, nitrofurans, acridine, benzimidazole, quinolone and aminoglycoside compound classes (Wright et al., 2003). The most frequently used nitroimidazoles, metronidazole and tinidazole, have a treatment success rate of 80 – 90%; while albendazole, a benzimidazole, has a reported efficacy of 62 – 95% (Wright et al., 2003). Treatment failures with these drugs are commonly reported and many exhibit unwanted side effects including but not limited to genotoxicity, nausea, fatigue and malaise (Wright et al., 2003). Metronidazole, is known to cause vomiting, weakness and headaches and is potentially carcinogenic (Bendesky et al., 2002; Jokipii and Jokipii, 1979). Furthermore, treatment failure due to the development of resistant organisms has been reported for all the commonly used drugs (Bendesky et al., 2002; Jokipii and Jokipii, 1979).

The combination of ineffective treatments resulting from adverse side effects and emerging resistance to all classes of anti-giardial drugs provides an imperative to identify and develop low side effect, low toxicity anti-giardial compounds that ideally are selective for *Giardia* over other microorganisms to minimise dysbiosis and ensure maintenance of optimal gut bacteria (Jernberg et al., 2007). To potentially expedite discovery and reduce development costs, others and we are actively examining the re-purposing of existing clinical and veterinary medicines. One such agent is robenidine, a symmetrical chloroaromatic compound linked via a guanidinal core (Table 5.1). It has been in use in the commercial poultry and rabbit industries as an anticoccidial agent since the early 1970s (Kantor et al., 1970). In this study we evaluated the

antigiardial activity of robenidine and 119 structural analogues and performed preliminary site and mechanism of action studies using electron microscopy.

5.4 Materials and methods

5.4.1 Chemicals

Robenidine used in this study was provided by Neoculi Pty Ltd (Burwood, Vic, Australia). All analogues of robenidine used in the study were previously developed at The University of Newcastle for use in another drug discovery program, grant reference number LP110200770 (Abraham et al., 2016). The remaining drugs used in this study were sourced from Sigma Chemical Company (St Louis, Missouri).

Chemicals used for the culture of *Giardia in vitro* were sourced as follows: glucose and L-cysteine (ACROS organics, Thermo Fisher Scientific, Scoresby, Vic), ammonium iron (III) citrate, ascorbic acid (Sigma-Aldrich, Castle Hill, NSW), potassium dihydrogen orthophosphate (UNIVAR, Ingleburn, NSW), bovine bile (Fluka analytical (BD)), di-potassium hydrogen orthophosphate (Fronine laboratory supplies, Riverstone, NSW).

5.4.2 Cell culture

G. duodenalis (BAH2c2 strain) was cultivated according to the method of Clark and Diamond in Keister's modified TYI-S-33 medium, supplemented with heat inactivated foetal bovine serum (Hyclone™, Thermo Fisher Scientific, Scoresby, Vic) at 37°C in plastic 9 mL screw-capped test tubes (nunc). Subcultures were performed once a confluent monolayer was observed, approximately 2 – 3 times per week (Clark and Diamond, 2002).

CaCo-2 cells, a human cell line derived from a primary colonic tumour, were sourced from Cellbank Australia and were maintained in MEM supplemented with 2 mM glutamine, 1% non-essential amino acids and 10% FCS (Thermo Fisher Scientific). Cells were passaged when confluent, approximately 1-2 times per week.

5.4.3 In vitro drug efficacy assays

Resazurin Reduction Assay

To evaluate the *in vitro* efficacy of the compounds, a resazurin reduction assay was used as previously described (Benere et al., 2007). The compounds were initially screened at 50 and 25 µM and any compound with > 50% inhibitory activity at 25 µM was further tested to identify the IC₅₀ and minimum inhibitory concentration (MIC). For all assays the media of confluent cultures was replaced with fresh media and the cultures were placed on ice for 40 minutes to detach trophozoites. Trophozoites were enumerated using a haemocytometer and 50 000 trophozoites were added to each test well of a 96 well plate. Either single concentrations (final

concentration 25 or 50 μM) for the screening assay or tripling dilutions of the test compounds (highest concentration 25 μM) for IC_{50} and MIC determinations in DMSO were added to wells. The assays were repeated in triplicate with three individual biological replicates per compound. Metronidazole and a DMSO vehicle only used as controls. Plates were incubated under anaerobic conditions (anaerogen sachet, Thermo Fisher Scientific) for 5 or 24 hours at 37°C , following which, the viability of treated cells was determined using the resazurin reduction assay (Benere et al., 2007). The media was removed and replaced with an equal volume of warm PBS. Resazurin (Sigma) was then added at 10% of the total volume of the wells. Plates were further incubated for colour development and absorbance read at 570 nm and 630 nm. Resazurin reduction was then calculated according to the following formula:

$$\frac{((E_{\text{oxi}630} \times A_{570}) - (E_{\text{oxi}570} \times A_{630}))}{((E_{\text{red}570} \times C_{630}) - (E_{\text{red}} \times C_{570}))} \times 100$$

Where: $E_{\text{oxi}630} = 34798$, $E_{\text{oxi}570} = 80586$, A_{570} = absorbance at 570nm, A_{630} = absorbance at 630 nm, $E_{\text{red}570} = 155677$, $E_{\text{red}630} = 5494$, C_{630} = absorbance of negative control well at 630 nm and C_{570} = absorbance of negative control well at 570 nm.

Modified adherence assay

A second screening method, based on counting adherent trophozoites, was developed and used to validate the primary screen with a select number of analogues. The assay was prepared in 24 well plates with plastic coverslips placed in the bottom. Trophozoites were prepared as above by placing on ice and $\sim 5 \times 10^5$ cells/ml were added to each well. Drugs prepared in DMSO were added at the required concentration, with the DMSO concentration never exceeding 1%. Assays were incubated for 5 hrs at 37°C under anaerobic conditions before the media was removed and cells were fixed with glutaraldehyde or methanol. Once the coverslips were dry, cells were stained with a Romanowsky stain variant (Rapid stain), fixed to a glass slide and imaged at 10 X magnification. Images were processed with dotcount v1.2 software (obtained from <http://reuter.mit.edu/>, 2008 – 2012 copyright by Martin Reuter) to count the number of cells present and data analysed using GraphPad Prism version 6.00 for Windows, GraphPad Software, La Jolla California USA, www.graphpad.com paired t-test function. Assays were repeated in duplicate.

5.4.4 Recovery assay

G. duodenalis trophozoites were harvested on ice as outlined above and 5×10^5 cells/ml were added to 1.5 ml centrifuge tubes. Cells were exposed to 5 μM of select analogues, metronidazole or DMSO (1%) only for 5 hrs under anaerobic conditions at 37°C . After exposure cells were collected by placing tubes on ice for 40 minutes followed by centrifugation at 900 X g for 5

minutes. The supernatant was removed and cells were resuspended in 8 ml of fresh media (in 9 ml culture tube). The number of trophozoites were counted using a haemocytometer and cells were incubated for 48 hrs with cell numbers being determined at 24 and 48 hrs. Assays were repeated in duplicate. data was analysed using a t-test.

5.4.5 Antibacterial activity

The antibacterial activity was determined using *S. aureus* ATCC 29213 and *E. coli* ATCC 25922 in Luria Bertanini broth (LBB). Compounds were diluted in DMSO to 100 X the final desired (25 or 50 μ M) concentration and 2 μ l added to 178 μ l of broth. Bacterial cells were suspended in 0.9 % saline to a concentration equivalent to a 0.5 McFarland standard, diluted 1:20 in saline and 20 μ l of diluted suspension added to the assay plate to give a final cell concentration of $\sim 5 \times 10^5$ CFU/ml. Cells were incubated for 18-24 hrs before interpretation of results. Assays were repeated in duplicate.

5.4.6 Mechanism of Action Studies

Transmission Electron Microscopy

To determine any effects robenidine (**812**) has on the ultrastructure of *Giardia* trophozoites and to further elucidate the mechanism of action, transmission electron microscopy was performed. *Giardia* BAH2c2 trophozoites were exposed to 6 μ g/mL robenidine for 30 minutes, 1 or 4 hrs, placed on ice for 40 minutes to detach trophozoites then washed twice with PBS (900 X g, 10 min 4°C) and fixed with a combination of glutaraldehyde and formaldehyde overnight. Cells were washed with PBS + 4% sucrose before fixation with osmium tetroxide for 1 hour. Samples were dehydrated through a graded ethanol series (70 – 100%) followed by suspension in propylene oxide for ten minutes. Samples were centrifuged and suspended in 1:1 mixture of propylene oxide and epoxy resin for an hour before centrifugation. Following overnight suspension in 100% epoxy resin samples were resuspended in fresh resin and polymerized at 70°C for 24 hours. After sectioning samples were stained with uranyl acetate and lead citrate. Sections were imaged with a FEI tecnai G2 Spirit Transmission Electron microscope (CMCA University of Adelaide). Three individual replicates of each treatment were prepared and pooled for TEM processing.

Scanning Electron Microscopy

To determine the effect that robenidine, **139** and **135** has on the cell surface of the *Giardia* trophozoites and potentially elucidate a mechanism of action, scanning electron microscopy was performed as follows. *Giardia* BAH2c2 trophozoites were prepared as for TEM, however

they were exposed to compounds for 2 hours. After fixation with glutaraldehyde cells were attached to plastic coverslips (pre-treated with poly-L-Lysine for 10 minutes) and washed with PBS + 4% sucrose before dehydration through a graded ethanol series (70 – 100%). Following ethanol dehydration coverslips were dried using a critical point drier, coated with platinum and observed using a ZIESS SEM (CMCA University of Western Australia) Two individual replicates were prepared and observed for morphological changes.

5.4.7 Cytotoxicity

CaCo-2 cells, maintained as outlined above, were collected via trypsinisation and enumerated using trypan blue and a haemocytometer. Select analogues were prepared in DMSO so that the final concentration in the assay would be either 25 or 50 μM . 1×10^5 cells/ml were added to each assay with the appropriate drug dilution. Assays were completed in 96 well plates and incubated for 24 hours at 37°C, 5% CO₂ in a humidified incubator. After incubation cells were washed with warm PBS before the addition of 10% resazurin in PBS. Assays were incubated to allow colour development and absorbance read at 630 and 570nm. Activity of the analogues against mammalian cells was calculated according to the formulation stated above. Each compound was tested in triplicate.

5.4.8 *In-vivo* Toxicity of Select Analogues

Suckling mice (Arc:arc(s) – Swiss origin mice) were obtained from the animal resource center at Murdoch (WA) and were 3-4 weeks old at the time of the trial. Each litter had 10 mice and was housed independently. Mice were given 100 mg/kg of robenidine (**812**), **135**, **139** or metronidazole orally once per day in a volume of 0.1 ml for 3 days. Control groups were given an equivalent volume of saline or the formulation used to deliver the compounds. Post exposure mice were sacrificed via cervical dislocation and organs were observed for gross pathological changes. Animal ethics granted through Murdoch University (permit number: R2855/16).

Compound preparation for *in vivo* toxicity

All analogues were provided by Prof. Adam McClusky at The University of Newcastle. Metronidazole was sourced from Sigma Aldrich. All drugs, including metronidazole, were suspended in an aqueous formulation and saline was used as the no treatment control. Drugs were delivered in a final volume of 0.1 ml via oral gavage. Mice were treated with ~100 mg/kg, once a day, p.o. for 3 days.

5.4.9 Statistical analysis

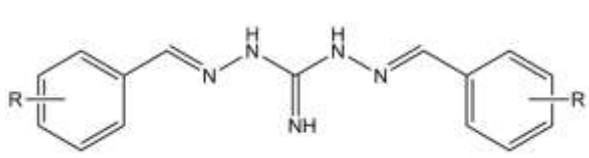
The results for the *in vitro* drug efficacy studies were analysed using GraphPad Prism version 6.00 for Windows, GraphPad Software, La Jolla California USA, www.graphpad.com. For the resazurin reduction assay the mean and standard error of the mean was determined with each assay completed in triplicate. The IC₅₀ was calculated using the log (inhibitor) vs. normalised response – variable slope function in Graphpad Prism. For the adherence assay mean and standard error of the mean were calculated and data analysed using an unpaired t-test, comparing each treated sample to the growth control.

5.5 Results and discussion

5.5.1 Antigiardial activity

This study investigated the potential anti-giardial activity of robenidine and related structural analogues. In total, 119 analogues from the library, were screened which have been divided into 9 groups based on similar core structures, were screened (Tables 5.1 – 5.9). The *in vitro* anti-giardial activity of the parent compound robenidine has previously been demonstrated as described by the patent US4310541A, where robenidine was found to be 4 times more active than metronidazole with an IC₅₀ of 1.5 ppm. In the current study robenidine had relatively good inhibitory activity towards *G. duodenalis* with an IC₅₀ of 0.2 µM and an MIC of 2.8 µM after just 5 hours, while metronidazole, the current gold-standard drug had an IC₅₀ of >25 and MIC of >25 at 5 hours in the same assay (IC₅₀ of 2.8 µM after 24 hrs). Removal of the Cl moiety on the benzene ring (**100**) resulted in a 50% decrease in activity when compared to robenidine while replacement of the Cl with a Br group resulted in only a two-fold decrease in activity (**134**) when compared to robenidine, with an IC₅₀ of 1.7 µM and an MIC of 8.3 µM after 24 hrs (Table 5.1).

Table 5.1 Antigiardial activity of 1,3-Diaminoguanidine Schiff Base analogues with mono-substituted aromatic rings.



ID	R	Inhibition (% growth control)*	<i>Giardia</i>				Toxicity (% growth control)*	Antibacterial
			IC ₅₀		MIC (µM)			
			5 hr	24 hr	5 hr	24 hr		
812	4-Cl	0±0	0.2	0.9	2.8	2.8	40.7±22.6	Y
134	4-Br	0±0	0.5	1.7	8.3	8.3	97.1±1.6	N

109	3-NO ₂	0±0	1.4	17.3	8.3	8.3	85.9±6.7	N
129	2-Br	0±0	3.4	0.8	25	25	79.1±2.3	N
116	2-Ph	0±0	52.8	2.8	>25	>25	75.4±3.4	N
160	4-OCF ₃	0±0	0.3	0.2	8.3	2.8	- ^a	Y
166	4-SCF ₃	3.7±6.4	0.7	0.2	8.3	2.8	-	Y
112	4-Ph	0±0	0.4	0.4	8.3	2.8	-	Y
140	4-SCH ₃	0±0	0.2	0.9	25	8.3	-	Y
136	4- (CH ₂) ₃ CH ₃	0±0	0.3	1.9	25	8.3	-	Y
099	4-C(CH ₃) ₃	0±0	2.9	3.2	25	8.3	-	Y
121	4- (CH ₂) ₂ CH ₃	0±0	5.9	0.8	>25	8.3	-	Y
120	4- CH(CH ₃) ₂	0±0	9.3	1.9	>25	8.3	-	Y
131	3-Br	0±0	1.1	2.9	25	25	-	Y
126	4-CCH	0±0	27.1	1.2	>25	25	-	Y
100	H	55.8±10.6	-	-	-	-	-	N
102	2-NO ₂	82.3±3.2	-	-	-	-	-	N
110	4-NO ₂	86.8±36.7	-	-	-	-	-	N
151	4-OH	172.9±4.9	-	-	-	-	-	Y
098	3-COOH	113.1±10.6	-	-	-	-	-	N
108	3-OH	147.4±25.5	-	-	-	-	-	Y
119	4- NHCOCH ₃	130.6±16.9	-	-	-	-	-	N
107	2-OH	112.8±10.4	-	-	-	-	-	Y
026[^]	3-CN	-	-	-	-	-	-	N
024[^]	4-CN	-	-	-	-	-	-	N
028[^]	2-OCH ₃	-	-	-	-	-	-	Y

^a not progressed due to non-selective activity or unsatisfactory screening results, [^] only screened at 50 μM. * concentration of compound used in this assay is 25 μM.

In addition, this 4-Br substitution eliminated antibacterial activity and reduced the *in vitro* toxicity significantly. While the 4-Br substitution appears to be the most effective for maintenance of anti-*Giardia* activity, 2-Br and 3-Br substitutions (**129**, **131**) also exhibit similar anti-*Giardia* activity with IC₅₀'s of 0.8 and 2.9 μM respectively after 24 hours. However, the MIC for each of these compounds is 3 fold higher than the 4 Br substitution at 25 μM after 24 hours. Like the 4-Br substitution, the 2-Br substitution did not display antibacterial activity. Of the additional electron withdrawing groups investigated in this group (**110**, **109**, **026**, **024** and **102**), only 3-NO₂ substitution retained anti-*Giardia* activity with a MIC of 8.3 μM at 5 hrs. In addition, this analogue (**109**) was selective for *Giardia* trophozoites over both bacterial and mammalian cells. Hydrogen bond donors (**107**, **108** and **151**) were all inactive and methylation (**028**) did not improve activity. 4-OCF₃ and 4-SCH₃ substitutions (**160** and **140**) had similar activity to the parent molecule with IC₅₀'s of 0.2 and 0.9 μM respectively after 24 hours while 4-SCF₃ (**166**) substitution also demonstrated improved activity over the parent molecule (0.2 μM at 24 hrs). All the alkyl substituents tested (**126**, **121**, **120**, **136**, **099**) demonstrated activity no more than two-fold higher than the parent molecule. The propyl group was the most active (**121**) with an IC₅₀ of 0.8 μM after 24 hrs. The alkyl moieties were slower acting than the parent molecule and required a full 24 hrs to reach MICs similar to the parent molecule. Compound **126** was the slowest acting with no activity observed at 5 hrs and a MIC of 25 μM reached only after 24 hrs (compared to 8.3 μM for all other alkyl substituents tested.) Substitution with polar groups at the 3 or 4 position (**119**, **148** and **098**) resulted in a loss of anti-*Giardia* activity. A 2- or 4- phenyl moiety (**112**, **116**) demonstrated good activity with IC₅₀'s at 24 hrs of 2.8 and 0.4 μM, respectively. The 4-Ph substitution resulted in more rapid and complete activity than the 2- Ph substitution, with an IC₅₀ of 0.4 μM reached at 5 hrs and an MIC of 2.8 μM. In contrast, the 2-Ph substitution was unable to completely inhibit the metabolic activity of *Giardia* at the concentration tested and no anti-*Giardia* activity was observed at the 5 hr time point.

More complex substitution of the phenyl rings resulted in few improvements in activity (Table 5.2). No single F substitution of the phenyl ring was investigated in this study (due to availability of compounds from the library) but 2,5 -F and 2,3,4,5,6 -F substitution resulted in no observable anti-*Giardia* activity (**128**, **118**). On the other hand, 3,4 di-substitution with F resulted in good activity (**123**) with an IC₅₀ of 1.2 μM and an MIC of 8.3 μM after 24 hrs. Addition of a 2-NHCOCH₃ (**170**) molecule onto the parent structure did not noticeably change the IC₅₀ at 24 hrs however the MIC at 24 hrs was increased 12 -fold while the toxicity towards CaCo-2 cells was decreased 2-fold. 2-Br (**129**) substitution, described above, gave comparable activity to robenidine and the addition of 4, 5- OCH₃ (**135**) further improved the potency and

speed of action of the molecule while improving the safety profile and retaining specificity towards *Giardia* over bacteria. **135** had a 4-fold improvement in the IC₅₀ and a 12-fold improvement in the MIC and maximum activity was reached much sooner, at 5 hrs instead of 24 hrs when compared to the parent drug. In addition, no significant toxicity was observed in the mammalian cell assay. The remaining analogues in this group all bearing catechol analogues were mostly poorly tolerated. Only the 3-NO₂, 4-OH and the 3-OCH₃, 4-OH analogues (**122** and **117**) demonstrated any inhibitory activity towards *Giardia*. An IC₅₀ was not calculated for **117** as, in the second assay, no dose response was observed. This could possibly be a result of instability of the compound in the solvent or storage conditions used.

The next group of molecules probed for activity were 1,3-diaminoguanidine Schiff base analogues with imine substitutions (Table 5.3). Imine substitution of robenidine with various carbon chains (**153**, **154**, **062** and **156**) resulted in similar IC₅₀'s at 24 hrs compared to the parent drug. The MIC at 24 hrs for the ethyl, propyl and butyl substitutions were increased at least 12 fold. In contrast, the MIC for the methyl substitution improved 3-fold, however the improved MIC was in conjunction with $\geq 40\%$ increase in toxicity toward mammalian cells (**062**). While the methyl and ethyl imine substitutions maintained antibacterial activity the longer propyl and butyl chains eliminated antibacterial activity. Di-halogen substitution, 2-F, 4-Cl, with a methyl imine substituent decreased activity compared to the parent molecule with a 12-fold decline in MIC at 24 hrs (**215**). Methyl imine substitution of **100**, an inactive analogue, imparted moderate anti-giardial activity with an IC₅₀ of 7.6 μM after 24 hrs (**143**). However, imine substitution of COOH or CH₂NClH₃ (**167**, **165**) did not improve activity of **100**. Methyl substitution of **134** did not improve activity while a similar substitution of **099** resulted in a 5-fold improvement in the 24 hr IC₅₀ (**155**, **219**).

The next group of analogues tested focussed on the same core structure as the previous 3 groups but involved substitution with extended linkers and nonaromatic and isosteric phenyl ring replacements, in addition to an imine substitution (**172**) (Table 5.4). All of the analogues tested from this group had a H at the imine position, except **172**, which had a methyl moiety. Furyl substituents (**095**, **144**, **133**, **145**) did not exhibit any anti-giardial activity, in fact a 4-bromofuryl moiety increased the metabolic activity of *Giardia* greater than 5 X the growth control. Similarly, pyridyl substituents (**172**, **149**, **175**) were not inhibitory towards *Giardia*. The substitution of a benzyl group (**096**) resulted in a 60% decrease in metabolic activity at 25 μM and when replaced with an anisyl group, activity improved to 100% inhibition at 25 μM , with an IC₅₀ of 0.3 μM and an MIC of 2.8 μM at 24 hrs (**150**). **138** also had moderately good activity. Of the fused aromatic substituents only **146**, **139**, **132**, **141** and **124** had anti-giardial activity.

Both **139** and **132** were selective for *Giardia* over both mammalian and bacterial cells, however **139** was more lethal toward *Giardia* than **132** with an MIC of 2.8 μM .

A small number of the analogues with asymmetrical substitution of the molecule core were tested but none had anti-*giardial* activity potent enough to pursue in this study (Table 5.5).

A larger number of phenylmethylidene guanidines were probed for activity. Of these, only one (**237**) had anti-*giardial* activity with an IC_{50} of 10.9 μM . All of the remaining analogues tested from this group were considered inactive (<50% inhibitory activity at 25 μM) for this study, suggesting that larger molecules are required to instigate anti-*giardial* activity; or perhaps symmetry in the molecule is important (Table 5.6).

A selection of 1,4-bis-pyrimidine analogues from the library with various aromatic ring and imine substitutions were tested (Table 5.7). Several of these analogues have similar aromatic and imine substitutions as those from the first 3 structural groups and the majority of these displayed similar activity profiles, suggesting the substituents are the instigators of activity rather than the core structure. There were several analogues that either gained or lost activity compared to the corresponding Schiff base, which may be due to a loss of flexibility within the molecule.

Single Cl substitution on the aromatic ring of the bis-pyrimidine core, as seen with the parent molecule robenidine, had a large loss in activity when compared to robenidine with < 50% reduction in metabolic activity for **187**. However, replacement of the Cl for a F or Br group restored activity similar to that seen with robenidine, as did a 3,4-F substitution. Methyl imine substitution with a 4-Cl moiety on the aromatic ring (**204**) afforded activity, however this was many fold higher than the corresponding Schiff base, **062**, and a further decrease in activity was seen when the NH_2 was removed from the central pyrimidine ring (**185**). As seen in previous structural classes, substitution with catechol moieties, whether mono-, di- or tri-, did not provide anti-*giardial* activity. 4- CH_3 substitution (**195**) did not result in activity, while the slightly larger 4- $\text{C}(\text{CH}_3)_3$ alkyl group (**198**) significantly improved the IC_{50} when compared to robenidine but resulted in an unfavourable MIC. A 4- OCH_3 (**230**) substitution also resulted in similar activity to the parent compound. While H-replacement of all aromatic or imine substituents with structure 1 (**100**) resulted in a loss of activity, the same substitution with structure 5 had anti-*giardial* activity, although slightly higher than robenidine (**199**). Further imine substitution, either with O or CH_3 , significantly decreased anti-*giardial* activity (Table 5.7).

Substitution of the bis-pyrimidine structure with extended linkers, non-aromatic or isosteric ring replacements resulted in two analogues with IC_{50} 's equal to or better than robenidine (**245**,

246) (Table 5.8). Although **096** has the same extended aromatic linker as **246**, the anti-*Giardia* activity of **096** was limited. The remaining analogues in this group were not pursued further as the inhibition of *Giardia* at the screening concentration of 25 μ M was not considered high enough.

The final structural group investigated in this study had a triazine core (Table 5.9). Phenyl substitution with a 4-Cl in combination with an imine methyl group (as seen in **062** and **204**) (**208**) resulted in a loss of activity, which is in contrast to the corresponding analogues **062** and **204**, both of which had similar substitutions but different core structures and the best anti-*Giardia* activity observed, however unselective. As seen with other analogues previously, catechol substitution of the aromatic rings resulted in no anti-*Giardia* activity (**211**, **207**). While substitution with 4-Br was the only change to show activity from the limited molecules of this group that were investigated.

After initial screening was completed and IC_{50} determined for active analogues select results of the screening assay were validated with a secondary activity assay looking at cell adherence. In this assay **812**, **099** and **062** were chosen as representative compounds due to good anti-*Giardia* activity and availability of large enough quantities of compound. Adherence assays supported the original resazurin assay with a significant reduction in adherent trophozoites after treatment with all three drugs (Figure 5.1).

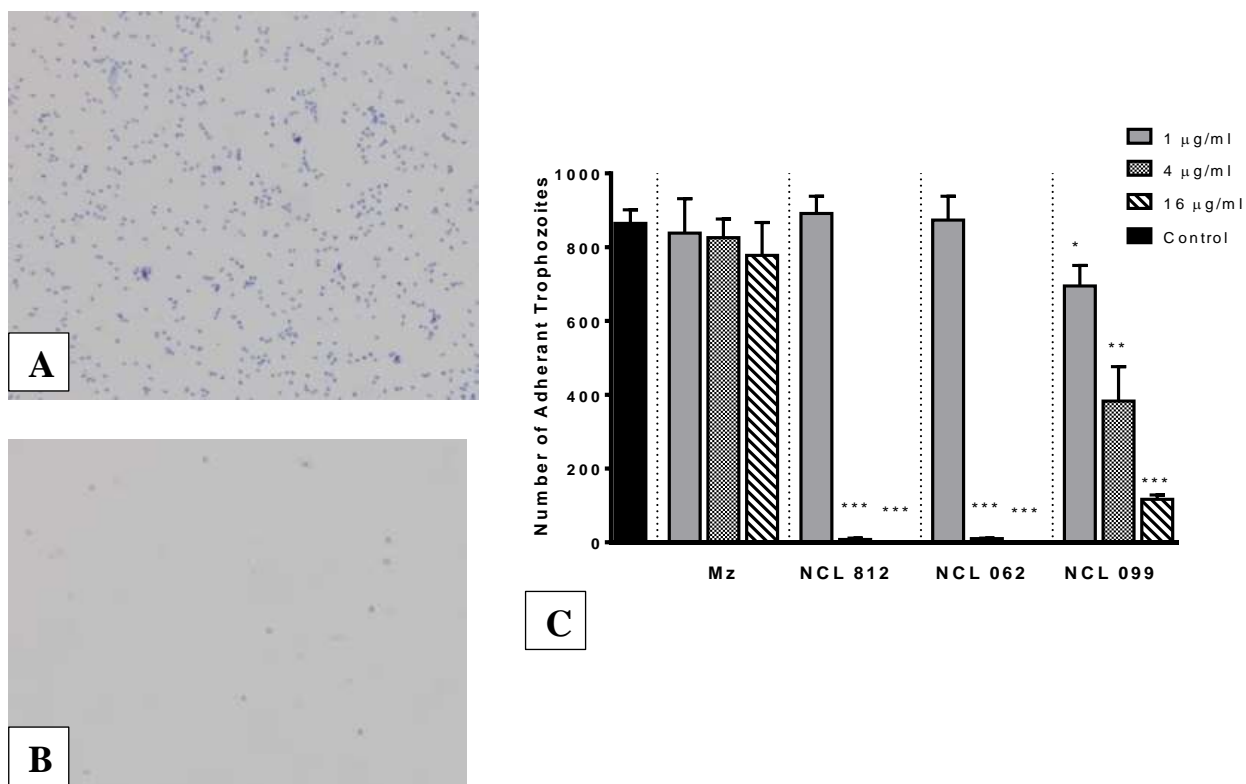
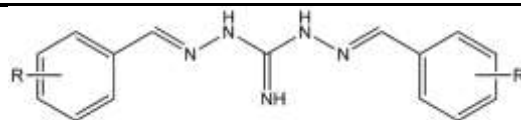


Figure 5.1 Inhibition of adherence of *Giardia duodenalis* by robenidine (**812**) and two structural analogues, **062** and **099**. Cells were exposed to the compounds for 5 hours before staining. Stained cells were imaged at 10 X magnification and counted using DotCount™ software. Each assay was completed in triplicate. **A** – Adherence of control cells (each blue dot represents 1 cell), **B**- adherence of cells exposed to robenidine (3 µg/ml) for 5 hours, **C** – graph of number of adherent trophozoites after exposure to each compound for 5 hours. Data expressed as mean number of trophozoites ± SEM. * *p*-value 0.0448, ** *p*-value 0.0030, *** *p*-value <0.0001.

Table 5.2 Antigiardial activity of 1,3-Diaminoguanidine Schiff base analogues with di-, tri- and polysubstituted aromatic rings

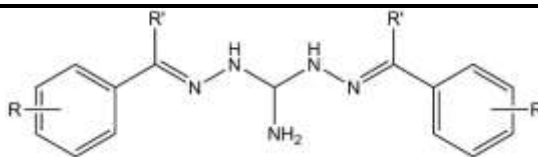


ID	R	Inhibition (% growth control)*	<i>Giardia</i>				Toxicity (% growth control)*	Antibacterial
			IC ₅₀		MIC (μM)			
			5 hr	24 hr	5 hr	24 hr		
135	2-Br, 4,5- OCH ₃ ,	0±0	0.1	0.2	2.8	2.8	94.7±3.9	N
170	2- NHCOC H ₃ , 4-Cl	10.3±11.8	8.3	0.8	>25	25	83.1±4.4	N
123	3,4-F	0±0	0.7	1.2	25	8.3	- ^a	Y
117	3-OCH ₃ , 4-OH	0±0	>25	>25	>25	>25	-	Y
171	2-OH, 4- N(CH ₃) ₂	86.4±18.7	4.8	2.5	>50	50	-	Y
122	3-NO ₂ , 4-OH	27.5±35.9	-	-	-	-	-	N
128	2,3,4,5,6 -F	72.0±8.3	-	-	-	-	-	N
152	2-OH, 3- CH ₃	110.7±5.3	-	-	-	-	-	N
118	2, 5-F	99.8±14.9	-	-	-	-	-	N
111	3,4-OH	109.2±4.4	-	-	-	-	-	Y

103	2,4-OH	129.9±22. 8	-	-	-	-	-	N
101	2,3-OH	107.7±9.8	-	-	-	-	-	Y
097	3,4,5-OH	180.7±32. 3	-	-	-	-	-	Y
104	2,4,5-OH	100.6±12. 9	-	-	-	-	-	Y
106	3-OCH ₃ , 4,5-OH	93.3±18.1	-	-	-	-	-	N
105	2,3,4-OH	108.6±8.2	-	-	-	-	-	Y

^a not progressed due to non-selective activity or unsatisfactory screening results at 25 μM. * concentration of compound used in this assay is 25 μM.

Table 5.3 Antigiardial activity of 1,3-Diaminoguanidine Schiff base analogues with imine substitutions


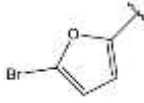
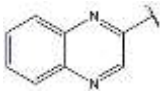
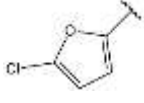
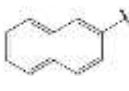
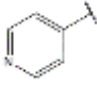
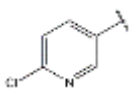
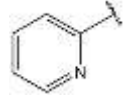
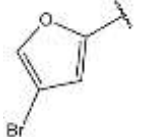


ID	R	R'	Inhibition (% growth control)*	<i>Giardia</i>				Toxicity (% growth control)*	Antibacterial
				IC ₅₀		MIC (μM)			
				5 hr	24 hr	5 hr	24 hr		
154	4-Cl	(CH ₂) ₃ CH ₃	39.3±2.9	3.8	1.4	50	50	90.7±7.0	N
156	4-Cl	(CH ₂) ₂ CH ₃	0±0	1.8	0.5	>25	25	79.1±5.5	N
062	4-Cl	CH ₃	0±0	0.2	0.4	2.8	0.9	0±0	Y
219	4- C(C H ₃) ₃	CH ₃	0±0	0.2	0.6	2.8	2.8	- ^a	Y
155	4-Br	CH ₃	0±0	0.2	0.2	8.3	8.3	-	Y
153	4-Cl	CH ₂ CH 3	0±0	4.5	2.2	>25	25	-	Y
215	2-F, 4-Cl	CH ₃	0±0	0.4	4.3	>25	25	-	Y
167	H	COOH	107.0±7.6	-	-	-	-	-	N
165	H	CH ₂ NC H ₃	181.9±70. 3	-	-	-	-	-	N

^a not progressed due to non-selective activity or unsatisfactory screening results at 25 μM. * concentration of compound used in this assay is 25 μM.

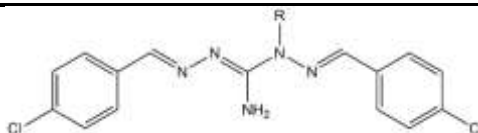
Table 5.4 Antigiardial activity of 1,3-Diaminoguanidine Schiff Base analogues with extended linkers and nonaromatic and isosteric phenyl ring replacements

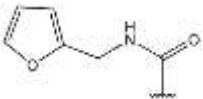
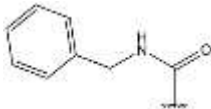
ID	R	R'	Inhibition (% growth control)*	<i>Giardia</i>				Toxicity (% growth control)*	Antibacte- -rial
				IC ₅₀		MIC (μ M)			
				5 hr	24 hr	5 hr	24 hr		
139		H	0 \pm 0	0.1	0.4	$\frac{>2}{5}$	2.8	87.4 \pm 3.7	N
132		H	0 \pm 0	0.7	1.6	$\frac{>5}{0}$	25	97.1 \pm 0.7	N
124		H	19.4 \pm 30.1	-	1.2	$\frac{>2}{5}$	$\frac{>2}{5}$	90.1 \pm 3.8	N
150		H	0 \pm 0	0.3	0.3	2.8	2.8	- ^a	Y
146		H	0 \pm 0	1.6	1.4	25	8.3	-	Y
141		H	0 \pm 0	0.3	1.5	25	8.3	-	Y
138		H	0 \pm 0	0.4	3.7	$\frac{>2}{5}$	25	-	Y
096		H	60.4 \pm 25.8	-	-	-	-	-	N

095		H	96.3±6.6	-	-	-	-	-	N
144		H	96.9±41.8	-	-	-	-	-	N
147		H	83.4±40.1	-	-	-	-	-	N
145		H	104.7±27.4	-	-	-	-	-	N
093		H	109.6±30.0	-	-	-	-	-	Y
149		H	171.3±120.3	-	-	-	-	-	N
175		H	93.1±9.7	-	-	-	-	-	Y
172		CH ₃	214.4±68.8	-	-	-	-	-	Y
133		H	566.9±62.8	-	-	-	-	-	N

^a not progressed due to non-selective activity or unsatisfactory screening results at 25 μM. * concentration of compound used in this assay is 25 μM.

Table 5.5 Antigiardial activity of 1,3-Diaminoguanidine Schiff Base analogues with non-symmetrical substitution of the guanidine linker



ID	R	Inhibition (% growth control)*	<i>Giardia</i>		Toxicity (% growth control)*	Antibacterial
			IC ₅₀	MIC (μ M)		
226	CONHCH ₂ CH ₃	96.0 \pm 2.7	- ^a	-	-	N
224	COOCH ₂ CH ₃	72.5 \pm 8.3	-	-	-	N
229		57.5 \pm 2.0	-	-	-	N
227		100.6 \pm 0.8	-	-	-	N
225	COOCH ₂ CH(CH ₃) ₂	87.1 \pm 2.6	-	-	-	N

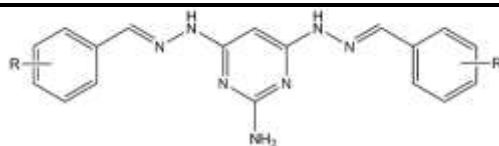
^a not progressed due to non-selective activity or unsatisfactory screening results at 25 μ M. * concentration of compound used in this assay is 25 μ M.

Table 5.6 Antigiardial activity of substituted phenylmethylidene guanidines.

ID	R	R'	Inhibition (% growth control)*	Giardia				Toxicity (% growth control)*	Antibacterial
				IC ₅₀		MIC (μM)			
				5 hr	24 hr	5 hr	24 hr		
237	2-OH, 4-Cl	CH ₂ C ₆ H ₁₁ (ring)	0±0	0	10.9	>25	25	- ^a	Y
235	2-F, 4-Cl	H	89.2±13.3	-	-	-	-	-	Y
236	2-F, 4-Cl	CH ₃	89.2±34.1	-	-	-	-	-	Y
232	4-C(CH ₃) ₃	H	83.6±5.7	-	-	-	-	-	Y
192	H	COOH	74.8±9.7	-	-	-	-	-	N
233	4-Cl	(CH ₂) ₂ CH ₃	85.4±2.8	-	-	-	-	-	Y
234	4-Cl	CH ₂ CH ₃	90.5±4.7	-	-	-	-	-	Y
042 [^]	2-CF ₃	H	-	-	-	-	-	-	N
041 [^]	4-CF ₃	H	-	-	-	-	-	-	Y
052 [^]	3-Cl	H	-	-	-	-	-	-	Y
191 [^]	4-Cl	CH ₃	-	-	-	-	-	-	N
231 [^]	4-C(CH ₃) ₃	CH ₃	-	-	-	-	-	-	Y

^a not progressed due to non-selective activity or unsatisfactory screening results at 25 μM, [^] only screened at 50 μM. * concentration of compound used in this assay is 25 μM.

Table 5.7 Antigiardial activity of 1,4-bis pyrimidine analogues with mono-, di-, tri- and poly-substituted aromatic rings, imine substitution.



ID	R	R'	Inhibition (% growth control)*	<i>Giardia</i>				Toxicity (% growth control)*	Antiba cterial
				IC ₅₀		MIC (μM)			
				5 hr	24 hr	5 hr	24 hr		
230	4-OCH ₃	H	0±0	0.5	1.4	25	8.3	-	N
198	4- C(CH ₃) ₃	H	0±0	2.5	0.04	25	25	-	N
222	3,4-F	H	0±0	0.5	0.7	25	2.8	-	N
193	4-Br	H	0±0	4.0	1.2	25	2.8	-	Y
220	4-F	H	0±0	0.6	0.7	25	8.3	-	Y
199	H	H	0±0	0.9	7.3	25	25	-	Y
204	4-Cl	CH ₃	0±0	2.4	3.2	>25	25	-	Y
197	3-OH	H	-	-	-	-	-	-	Y

195 [^]	4-CH ₃	H	-	-	-	-	-	-	Y
196	4-OH	H	73.7±26.0	-	-	-	-	-	Y
223	4-NHCOC H ₃	H	65.7±4.5	-	-	-	-	-	N
194	H	O	69.5±20.1	-	-	-	-	-	N
184	H	CH ₃	88.8±6.8	-	-	-	-	-	Y
242	2,5-OH	H	106.6±5.3	-	-	-	-	-	N
244	2,3-OH	H	117.2±34.4	-	-	-	-	-	Y
243	3,4-OH	H	81.1±3.3	-	-	-	-	-	N
247	3,4,5-OH	H	102.2±15.3	-	-	-	-	-	N
189	4-Cl	CH ₂ OH	68.0±16.0	-	-	-	-	-	N
185	4-Cl	CH ₃	30.1±11.1	-	-	-	-	-	N
187	4-Cl	H	57.1±1.5	-	-	-	-	-	N

^a not progressed due to non-selective activity or unsatisfactory screening results at 25 μM, [^] only screened at 50 μM. * concentration of compound used in this assay is 25 μM.

Table 5.8 Antigiardial activity of 1,4-bis pyrimidine analogues with extended linkers and nonaromatic and isosteric phenyl ring replacements

		<i>Giardia</i>						
ID	R	Inhibition (% growth control)*	IC ₅₀		MIC (μM)		Toxicity (% growth control)*	Antibact erial
			5 hr	24 hr	5 hr	24 hr		
245		0±0	5.5	0.7	25	2.8	- ^a	Y
246		0±0	7.7	0.04	>25	25	-	Y
203		45.0±18.2	-	-	-	-	-	Y
239		78.3±13.1	-	-	-	-	-	Y
238		99.6±9.3	-	-	-	-	-	N
241		76.9±1.9	-	-	-	-	-	Y

^a not progressed due to non-selective activity or unsatisfactory screening results at 25 μM. * concentration of compound used in this assay is 25 μM.

Table 5.9 Anti-giardial activity of robenidine analogues with a triazine core

<i>Giardia</i>									
ID	R	R'	Inhibition (% growth control)*	IC ₅₀		MIC (μ M)		Toxicity (% growth control)*	Antibacterial
				5 hr	24 hr	5 hr	24 hr		
212	4-Br	H	0 \pm 0	0.3	2.7	25	25	-	Y
208	4-Cl	CH ₃	54.7 \pm 38.6	-	-	-	-	-	N
211	4-OH	H	65.2 \pm 14.9	-	-	-	-	-	N
214	H	H	77.2 \pm 4.0	-	-	-	-	-	N
207	2-OH	H	77.8 \pm 5.0	-	-	-	-	-	Y

^a not progressed due to non-selective activity or unsatisfactory screening results at 25 μ M. * concentration of compound used in this assay is 25 μ M.

5.5.2 Recovery assay

To determine the long-term effect on *Giardia* of short term exposure to robenidine and 13 novel analogues, cells were exposed to the analogues for 5 hours before drug withdrawal. Of the 14 compounds tested 4, including robenidine, resulted in the inability of *Giardia* to recover 48 hrs post compound removal (Figure 5.2). The remaining 10 compounds had growth patterns similar to the no-treatment control. Metronidazole exposed cells were also able to recover after 5 hrs exposure. The ability of **139**, **135** and **109** to prevent the growth of *Giardia* cells after short exposure times is an advantage over compounds that require longer exposure periods to have a long lasting effect. Another advantage of these compounds, over the lead robenidine and commercially available drugs, is the selectivity for *Giardia* over bacterial and mammalian cells. In addition, **139** and **135** both had improved efficacy against *Giardia* when compared to robenidine, at least halving the IC₅₀. Based on the aforementioned *in vitro* results, **135** and **139** were selected for further study, with robenidine included as the original lead candidate.

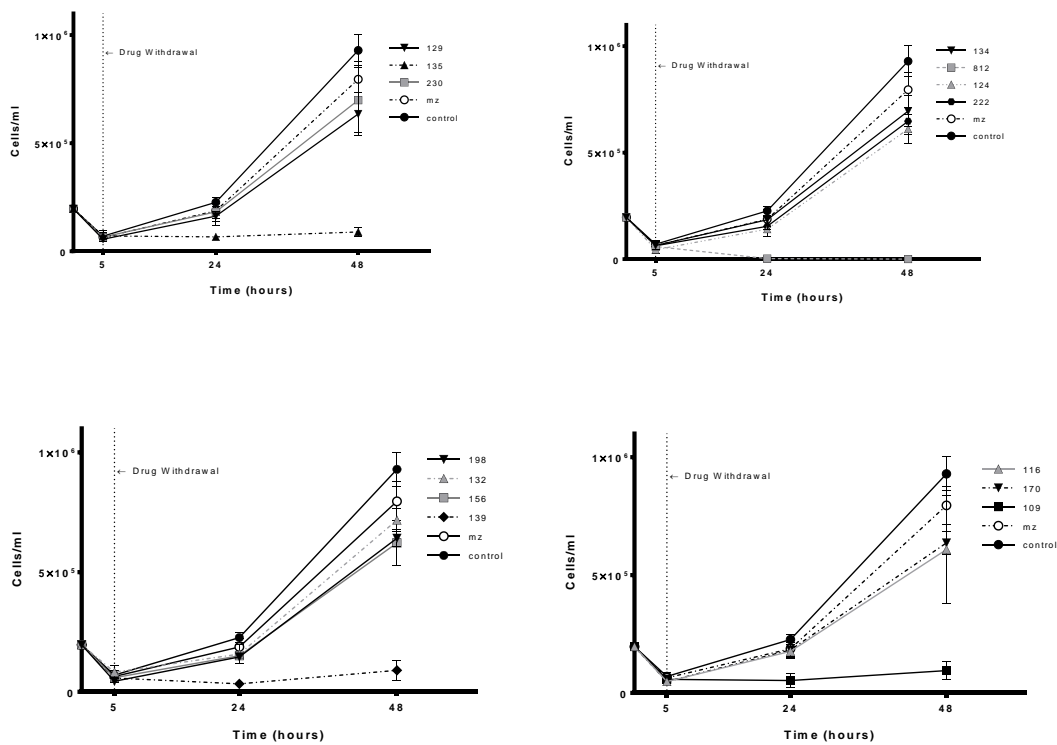


Figure 5.2: Recovery assay of *Giardia duodenalis* exposed to robenidine and selected robenidine analogues. *Giardia* trophozoites were exposed to the analogues for 5 hours before centrifugation to remove the compounds. Cell numbers were determined at 24 and 48 hrs post exposure. Error \pm SD. Metronidazole (Mz) and growth control included on all figures as a comparison. 812, 135, 139, 198, 109, 124 were all significantly different than the growth control at 24 and 48 hrs according to a *t*-test, $p < 0.001$.

5.5.3 Mechanism of action

Despite robenidine being used for the past 40 years the mechanism of action is not known. Previous studies of the mechanism of action of robenidine have been inconclusive with some suggesting that ATPase is the primary target while others have identified no obvious morphological effect in *E. tenella* on mitochondria or the nucleus, with chiefly the golgi body and endoplasmic reticulum being affected (Lee and Millard, 1972; Wong et al., 1972). In the same study, swelling of the perinuclear space was noted by the authors who suggested this could be due to the overproduction of proteins potentially indicating an increase in metabolism causing the cells to self-destruct (Lee and Millard, 1972). In this study, we performed electron microscopy studies to try to elucidate a possible mechanism of action of robenidine and the two most promising analogues **135** and **139**.

Electron microscopy showed gross morphological changes in the trophozoites after 1 hour of exposure to robenidine (Figure 5.3). TEM studies revealed that the treated trophozoites developed extreme membrane blebbing, most significantly affecting the adhesive disc, scattered with electron dense material. In addition, unusual vacuolar membranous structures appeared within the cytoplasm. Several trophozoites also exhibited rupturing of the dorsal cytoplasmic membrane and all observed trophozoites had various degrees of disintegration of the cytoplasmic space. SEM studies also showed extreme membrane blebbing, as seen in TEM, after 2 hour of exposure. Furthermore, these images showed that there was severe damage to the cell wall of the engorged adhesive disk with distinct lesions observed on the surface. Based on the electron microscopy results of this study it appears that robenidine exposure results in a general swelling of the cells leading to rupture of the cell membrane and ultimately cell death (Figure 5.3-5.4).

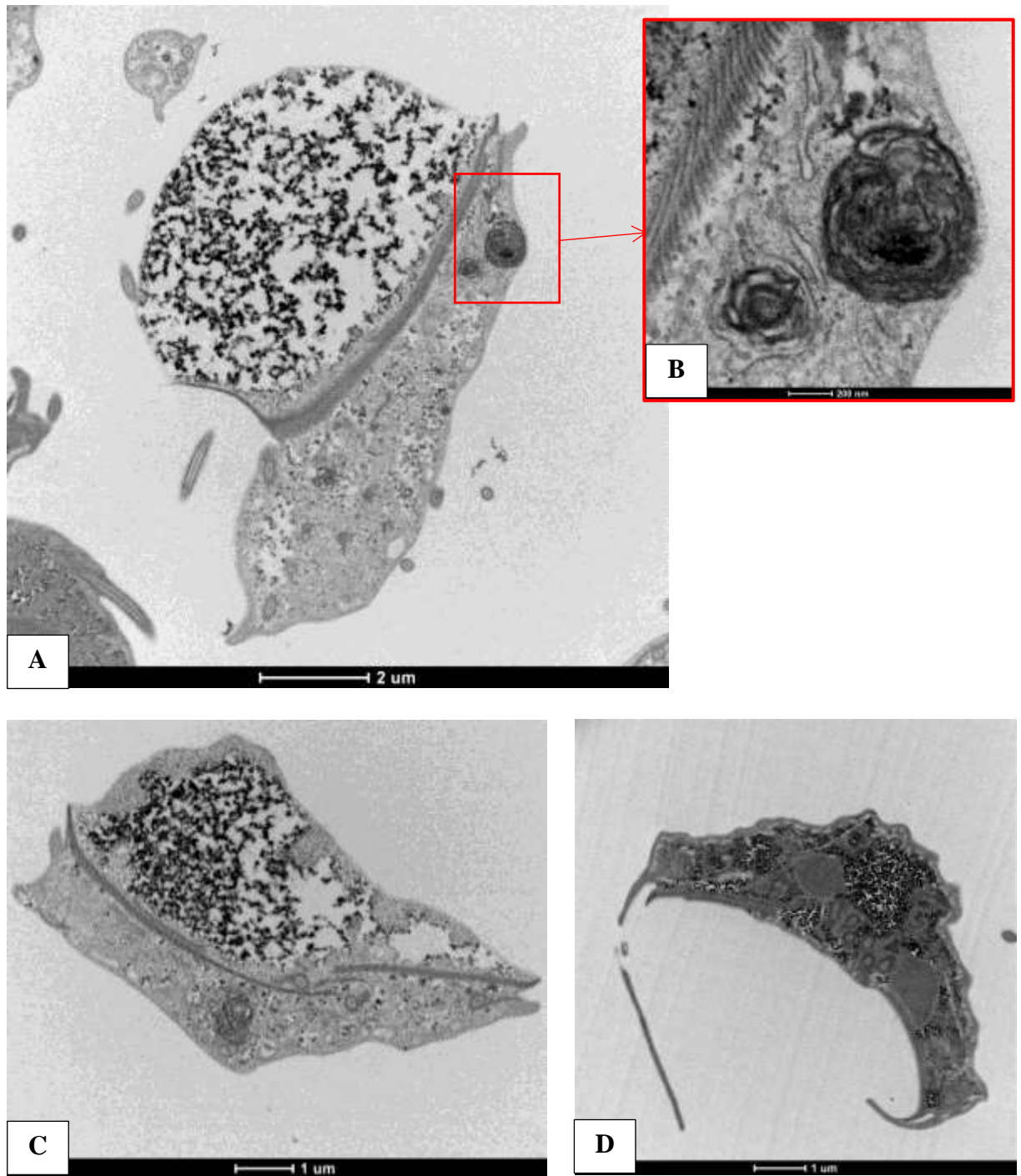


Figure 5.3 Transmission electron microscopy of *Giardia duodenalis* trophozoites exposed to 6 ug/ml robenidine for 1 hour. *Image A - demonstrating extreme membrane blebbing at the adhesive disk and development of membranous structures within the cytoplasm, Image B – magnification of the membranous structures observed in Image A, Image C – membrane blebbing and development of membranous structures within the cytoplasmic space., Image D – unexposed Giardia duodenalis trophozoite*

SEM studies with cells exposed to **135** and **139** at 3 X the MIC for two hours also demonstrated significant morphological changes. While **135** and **139** are structurally related to robenidine the terminal moieties are quite distinct. While there were similarities between all three compounds in destruction of the adhesive disc (Figure 5.4-5.7), the membrane disintegration caused by robenidine was not as distinct with **135** and **139**. In addition to membrane degradation both **135** and **139** caused severe cell swelling, with cells taking on a spherical conformation, a feature which was not observed after exposure to robenidine (Figure 5.6 -5.7). After exposure the **135** aggregates of trophozoites were observed suggesting that **135** may have an additional mechanism of action (Figure 5.6).



Figure 5.4 Scanning electron microscopy of *Giardia duodenalis* *TOP*: unexposed trophozoites, *BOTTOM*: exposed to metronidazole (3 X IC_{50}) for 2 hours, both dorsal and ventral views.

It is possible that robenidine causes the plasma membrane of the protist to become destabilized, altering membrane properties leading to cell swelling and modifications of the cytoplasmic space. Another possible theory is that robenidine has a similar mechanism of action as the thiazolides which demonstrate a disintegration of the cytoplasmic space as observed by TEM and development of membrane ruptures on the adhesive disc resulting in a loss of osmotic

potential (Muller et al., 2006). In addition, research into the mechanism of action of CGP 40215A, effectively a structural analogue of robenidine where the chlorides have been substituted with amine groups, identified a strong bond with the AT region of DNA (Nguyen et al., 2002). The strong bond was facilitated by the guanidine backbone which is conserved in robenidine and both **135** and **139**, potentially providing another alternative mechanism of action for this series of compounds. The binding of robenidine analogues with appropriate structural, spatial and hydrogen bond characteristics to the AT region of DNA could result in a cascade of events resulting in a disruption of normal cellular process and eventually, cell death. Although **135** and **139** also damage the cell membrane this damage is not to the extent of that induced by robenidine in the same period of time, therefore, it appears to be a secondary mechanism of action. The most distinct difference observed in **139** treated cells compared to non-treated cells, and also present in the populations of **135** treated cells, was extensive cell swelling resulting in a loss of distinctive cell features. Finally, **135** appeared to cause conglomeration of trophozoites, an attribute not observed with **812** or **139**.



Figure 5.5 Scanning electron microscopy of *Giardia duodenalis* exposed to robenidine (**812**) ($3 \times IC_{50}$) for 2 hours. *Images demonstrate the severe degradation of the adhesive disk. Other areas of the cell surface also appear to be damaged.*

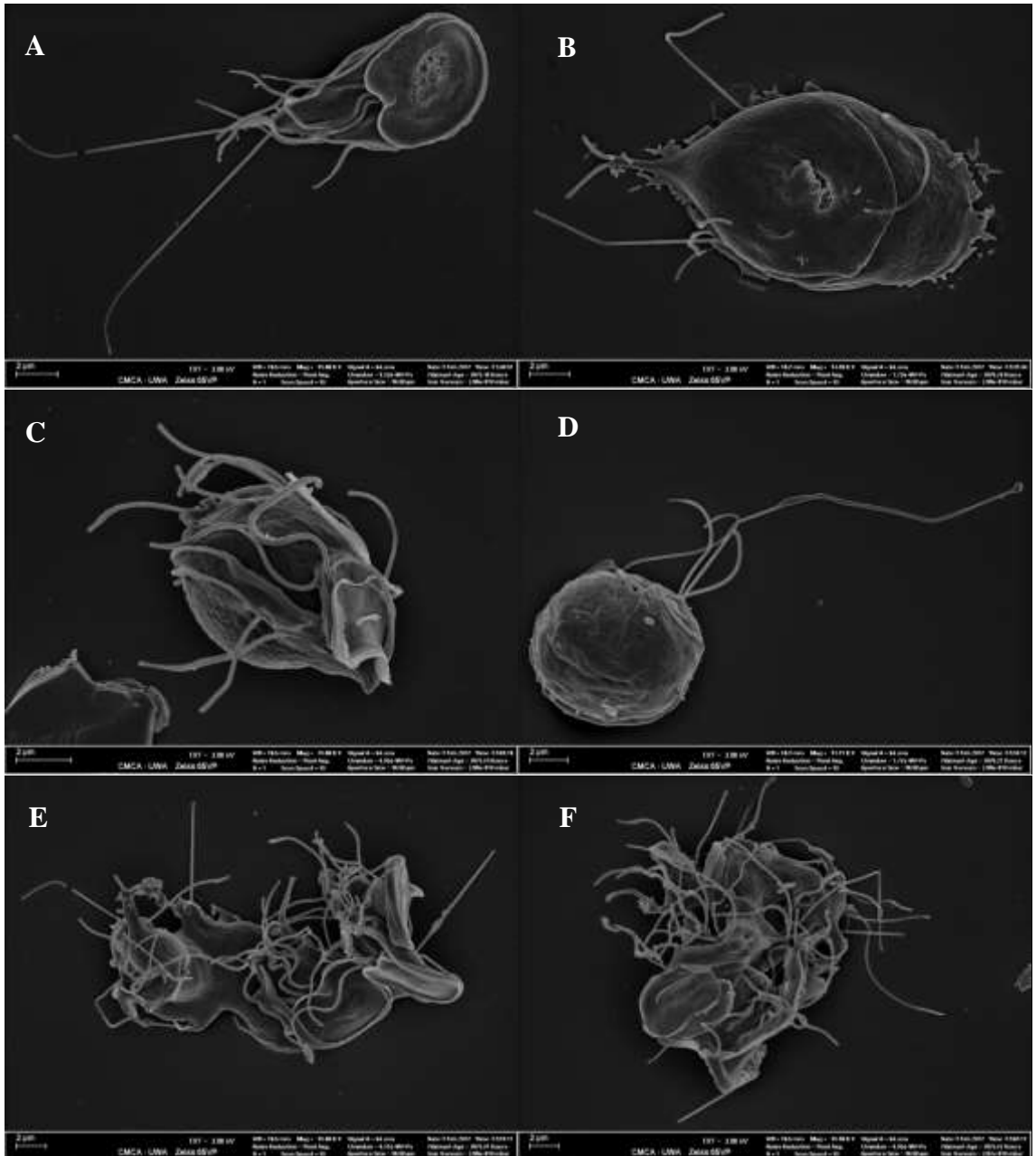


Figure 5.6 Scanning electron microscopy images of *Giardia duodenalis* exposed to **135** ($3 \times IC_{50}$) for 2 hours. Image A-B showing membrane damage to the ventral and dorsal sides, C-D showing cell swelling and E-F demonstrating aggregation of trophozoites.

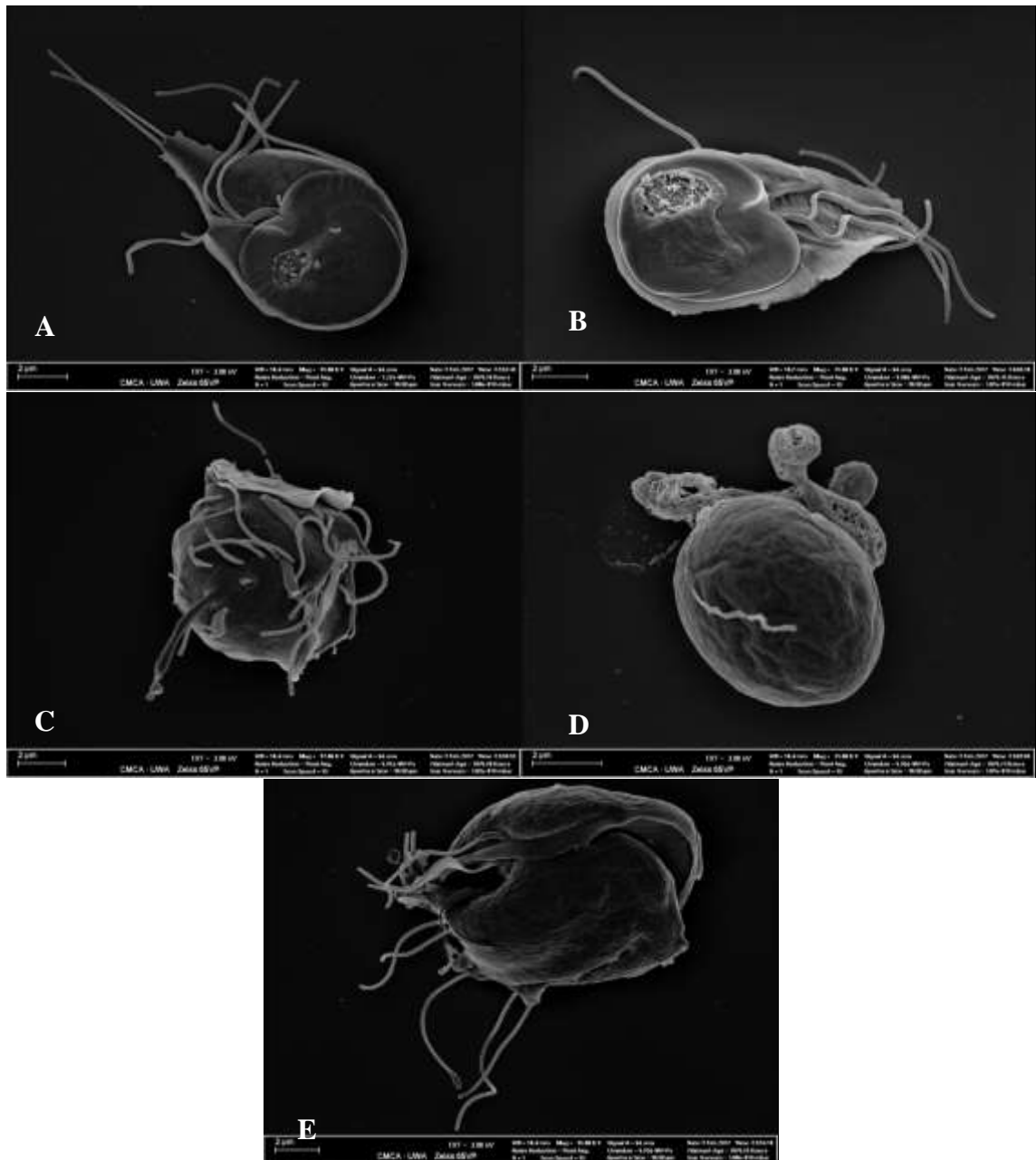


Figure 5.7 Scanning electron microscopy of *Giardia duodenalis* after exposure to **139** ($3 \times IC_{50}$) for 2 hours. Image A-B demonstrating membrane damage to adhesive disc, C-E demonstrating severe cell swelling.

5.5.4 *In vivo* toxicity of select analogues

Of the 13 most promising analogues (those with irreversible anti-giardial activity, no antibacterial activity or mammalian cell toxicity) 2 were chosen for preliminary *in vivo* toxicity testing, based on *in vitro* toxicity, MIC, recovery assays, and structural diversity of the analogues, namely **135** and **139**. Metronidazole and **812** were also included. Neonatal mice were treated orally for 3 days with 100 mg/kg of the compounds or saline or formulation only and no behavioural signs of toxicity were observed.

5.6 Conclusion

In this study we demonstrate that robenidine and several analogues at the concentrations tested have potent rapid activity against *G. duodenalis in vitro* with no observed *in vivo* toxicity. In conclusion the analogues investigated in this study show excellent potential as future anti-giardial agents as they are potent, relatively quick acting and have the potential to concentrate at the target site due to aqueous insolubility. This study also moved a step closer to determining the mechanism of action of robenidine and two promising analogues, demonstrating that severe cell damage is acquired after only 1 – 2 hours of drug exposure. However, further study is required to elucidate the exact mechanism of action. In addition, both **135** and **139** displayed no toxic effects in neonatal mice following oral administration of doses of 100 mg/kg over 3 days as observed under the current study conditions.

Chapter 6: Development of Animal Models of Giardiasis

Chapter 6.1: Cross-Species Transmission of *Giardia duodenalis* in Livestock

Introduction:

Background: Current models of human giardiasis infection usually involve the use of rodents, either gerbils or more commonly mice. While these models have their advantages including small size and animal availability, there are several disadvantages of using rodent models in the evaluation of drugs for human disease. Infection and disease progression is highly dependent on mouse strain and trophozoite infection number as well as mouse age (Byrd 1994). Other models using neonatal mice are limited by the development of the mouse immune system, which clears the infection.

Although infection models in mice are improving significantly, accurately portraying symptoms seen in human disease, it has been reported that mice can behave very differently to humans when treated with experimental compounds. While a compound may be effective in a mouse model it could still be ineffective in human trials. It has been reported that pig models are much more likely to be predictive of therapeutic outcome in humans than rodent models. In addition, pigs are much more similar to humans in relation to the immune system (>80% analysed features similar, <10% in mice), anatomy including the gastrointestinal tract, genetics and physiology than mice are to humans (Kararli, 1995; Meurens et al., 2012; Miller and E., 1987; Zhang et al., 2013).

A giardiasis model in pigs would have several advantages over mice due to the similarities mentioned above (Meurens et al., 2012; Zhang et al., 2013). Pigs are becoming a favoured large animal model for many areas of medical research including toxicology as it is believed that pigs will respond to novel agents in a way that is more predictive of human reactions than rodents (Kararli, 1995).

Therefore, in this study we attempted to establish an infection model in post-weaned piglets in an effort to mimic human giardiasis infection and provide a model for the development of human anti-giardial agents.

Pigs have been reported to be infected with assemblage A (a strain infectious to humans) and assemblage E (a livestock specific strain, though recent reports have documented infection in humans with this assemblage) based on PCR analysis of faeces (Armson et al., 2009). In addition, a heavy infection in pigs caused by an assemblage E isolate was confirmed by the isolation of trophozoites from the GIT (Koudela et al., 1991). As an initial step in the establishment of a pig giardiasis model for the development of anti-giardial agents, cysts isolated

from infected calves (chosen because they will provide the number of cysts needed and should contain cysts of assemblages infectious to pigs) were used to infect pigs, in the hope that a reliable model of giardiasis could be established in swine.

6.1.1 Statement of Authorship

Title of Paper	Cross-Species Transmission of <i>Giardia duodenalis</i> in Livestock
Publication Status	<input type="checkbox"/> Published <input type="checkbox"/> Accepted for Publication <input type="checkbox"/> Submitted for Publication <input checked="" type="checkbox"/> Unpublished and Unsubmitted work written in manuscript style
Publication Details	Submitted to Veterinary Parasitology

Principal Author

Name of Principal Author (Candidate)	Rebecca Jane Abraham		
Contribution to the Paper	Experimental design, completion of labwork except what is mentioned below. Primary care of animals in the study and sample collection. Interpretation of data. Preparation of manuscript. Acting as corresponding author on submitted manuscript		
Overall percentage (%)	90		
Certification:	This paper reports on original research I conducted during the period of my Higher Degree by Research candidature and is not subject to any obligations or contractual agreements with a third party that would constrain its inclusion in this thesis. I am the primary author of this paper.		
Signature		Date	13 th December 2017

Co-Author Contributions

By signing the Statement of Authorship, each author certifies that:

- i. the candidate's stated contribution to the publication is accurate (as detailed above);
- ii. permission is granted for the candidate to include the publication in the thesis; and
- iii. the sum of all co-author contributions is equal to 100% less the candidate's stated contribution.

6.1.2 Abstract:

Giardia duodenalis is a ubiquitous enteric parasite that infects a wide range of mammals including humans. Molecular characterisation of *G. duodenalis* has identified eight Assemblages (A-H) with different host specificities, livestock are predominantly infected with assemblage E. An understanding of the transmission dynamics of assemblage E between different livestock hosts is lacking, but is important to better understand the spread of infection on farms. In the present study, we attempted to infect pigs with a calf derived Assemblage E isolate of *G. duodenalis*. No infection was observed in the pigs and further research is required to determine the degree of host-specificity within livestock species.

Keywords: *Giardia* transmission livestock

6.1.3 Article:

Giardia duodenalis (syn. *intestinalis*, *lamblia*) is a ubiquitous enteric parasitic protist that can infect a broad range of mammalian hosts. The parasite is capable of causing significant pathological changes to the intestine, resulting in a malabsorption syndrome (Buret, 2007), but clinical signs can range from asymptomatic infections to short term bouts of severe diarrhoea to chronic infections that can cause malnutrition and developmental delays (Berkman et al., 2002; Homan and Mank, 2001; Lengerich et al., 1994). Recent research has linked *Giardia* infection in humans with the development of secondary diseases such as irritable bowel syndrome and chronic fatigue (Hanevik et al., 2014; Wensaas et al., 2012) and in production animals, infections in livestock may adversely affect weight gain resulting in production losses (Olson et al., 1995).

Despite the impact *G. duodenalis* has on human and animal hosts, cross-species transmission of *G. duodenalis* remains poorly understood. There is extensive debate into the potential host specificity of various *G. duodenalis* isolates and the likelihood of transmission of *G. duodenalis* between various host species. In particular, the zoonotic potential of *G. duodenalis* has resulted in several studies evaluating the cross-species infectivity, but few studies have directly demonstrated transmission of *Giardia* from an animal source to humans. *Giardia* derived from gerbils was found to infect a human volunteer (Majewska, 1994), however the genotypic characterisation of the isolate was lacking. The majority of cross-transmission studies have investigated the zooanthroponotic potential of human derived isolates of *G. duodenalis* to infect various animal hosts. The results of these studies were mixed, with some isolates able to cause infection between hosts, while others could not cause infection between hosts. These studies, while shedding considerable light on cross-species transmission of *G. duodenalis*, lacked

molecular characterisation of the isolates used (Erlandsen et al., 1988; Gasser et al., 1987; Hewlett et al., 1982; Majewska, 1994; Visvesvara et al., 1988).

With the development of molecular tools, recent research has focused on the molecular characterisation of a large number of *G. duodenalis* isolates derived from different hosts in the hope of better understanding the epidemiology of this parasite. These studies have been completed in various parts of the world with a range of hosts. To date, within the species *G. duodenalis*, there are eight distinct assemblages designated A-H (Ryan and Caccio, 2013). The host range of these assemblages has been examined based on characterisation of *G. duodenalis* isolated from the faeces of different hosts and this has led to the proposal of *G. duodenalis* as a species complex, with each assemblage representing a distinct species, due to the genetic variation observed between assemblages (Monis et al., 2003). It is currently accepted that Assemblages A and B are the main assemblages to commonly cause infection in humans, but these Assemblages have also been detected in the faeces of other mammals, including dogs and cattle. Assemblages C and D are generally limited to dogs but assemblage C has been reported in the faeces of humans in China and Slovakia and assemblage D in German travelers (Broglia et al., 2013; Liu et al., 2014; Strkolcova et al., 2015). Until recently, assemblage E was considered to only infect hoofed livestock, however recent studies have identified assemblage E in the faeces of humans in Egypt, Brazil and Australia (Abdel-Moein and Saeed, 2016; Fantinatti et al., 2016; Foronda et al., 2008; Helmy et al., 2014; Scalia et al., 2016; Zahedi et al., 2017). In one study, assemblage E was detected in the faeces of 62.5% (25/40) of children living in agricultural areas in Egypt (Abdel-Moein and Saeed, 2016). More recently, in Australia, assemblage E was detected in 6.8% (6/88) of *Giardia*-positive faecal samples from Queensland (Zahedi et al., 2017). Similarly, Assemblage F, although mainly found in cats, has been reported in the faeces of humans in Ethiopia (Gelanew et al., 2007). Assemblages G and H have only been reported in rats and marine mammals respectively to date. While molecular genetic typing of *Giardia* cysts or DNA excreted in the faeces can classify isolates into the appropriate assemblage and provide information on the potential host range, the cross-species transmission of different isolates cannot be definitively determined using these methods. In addition, the majority of research into *G. duodenalis* has focussed on humans, however *G. duodenalis* is also known to have a negative impact on production animal health. Previous studies in ruminant models have shown that infection with *G. duodenalis* causes changes in the intestinal microvilli of the host resulting in decreased nutrient absorption (O'Handley et al., 2000) potentially leading to decreased weight gain and subsequent production loss (Olson et al., 1995). Despite the potential impact giardiasis has on production animals, the cross-species

transmission of *G. duodenalis* between livestock species is not well understood. While it is known that hoofed livestock are predominantly infected with assemblage E isolates, they can also be infected with assemblage A and assemblage B isolates.

In this study, we attempted to establish a *Giardia* infection in pigs using cysts obtained from a dairy calf in order to better understand the pathogenesis of the infection in pigs and the response of the infection to chemotherapy. Here, we report the results of the infection trial in order to provide important information on the cross-species transmission of *Giardia*.

For this study, 24 weaned piglets (large white x landrace), ~8 weeks old, weighing between 9 - 17 kg, were obtained from a commercial piggery in South Australia. The piglets were confirmed negative for *Giardia* cyst excretion via zinc sulphate faecal floatation on two separate occasions prior to transfer to the trial facility, once at pre-weaning and once at ~6 weeks old. Upon arrival (Day 1) pigs were weighed and randomly assigned to 4 groups. The piglets were housed in groups of six in adjacent concrete floored pens using a deep litter system (straw), and contact between groups was limited. Once allocated to groups, they were infected orally with $\sim 6 \times 10^4$ *G. duodenalis* cysts obtained from a naturally infected calf. During the study, pigs were fed a standard non-medicated pelleted piglet food (Lienert Advantage 500, Lienert Australia) ad lib until day 7 when they were fed a follow on post-weaning pellet (Lienert Advantage 300, Lienert Australia) until the end of the trial. Pigs were monitored daily for clinical signs of infection including diarrhoea, lethargy and inappetence. On days 4, 7, 11, 15, 23, 25 and 30, faecal samples (1g per animal) were obtained from piglets via rectal stimulation and examined for the presence of *Giardia* cysts. On day 18, a randomly selected pig was sacrificed to determine trophozoite numbers in the small intestine. On day 36 all pigs with a positive faecal cyst count were sacrificed and $\sim 1\text{cm}^2$ sections of the ileum, jejunum and duodenum were collected and parasite numbers enumerated. This study was approved by the University of Adelaide Animal Ethics Committee, permit number S-2014-064

To prepare the *Giardia* inoculum, a fresh (<5 days) faecal sample from an infected calf with a high cyst count was suspended in water and filtered through surgical gauze. The liquid was then layered over sucrose (specific gravity 1.15) in 50 ml centrifuge tubes and centrifuged at 900g for 10 minutes. The top layer and the gradient were transferred to a clean tube and centrifuged at 900 g for 10 minutes. The supernatant was discarded and the pellet resuspended in water. The number of cysts in 10 μl of water was enumerated and the volume adjusted to give a cyst density of 6×10^4 cysts/ml. Cysts were kept at 4°C until infection of pigs (< 2weeks). The viability of the cysts was tested following previously described methods (Bingham and Meyer,

1979). Purified cysts were suspended in HCl pH 2 (in a ratio of 1:10), washed and suspended in TYI-S-33 medium and observed for excystation.

A previously described method was used to determine faecal *Giardia* cyst number (O'Handley et al., 2000). Approximately 1 g of faeces was suspended in 7 ml of water then filtered through a gauze swab. The filtrate was layered over 5 ml of sucrose (specific density 1.15) in a 15 ml centrifuge tube. The samples were centrifuged at 800 x g for 5 minutes. The top layer of liquid, including the gradient was placed into a clean centrifuge tube and centrifuged again at 800 x g for 5 minutes. The supernatant was discarded and the pellet resuspended in 1 ml of water. 10 µl was air-dried on a Poly-L lysine treated slide (Emgrid Australia), then 20 µl of anti-*Giardia* specific fluorescent antibody (Sapphire Biosciences) was layered over the top of the dried sample and incubated for 30 minutes before mounting a coverslip over the sample and counting the number of cysts under a fluorescent microscope.

To identify trophozoites in the gastrointestinal tract (GIT) of trial animals, sections of the ileum, duodenum and jejunum were removed, cut to approximately 1cm lengths, then incised longitudinally into the lumen and placed into sterile cold PBS. The tissue was rocked for 30 minutes at room temperature to detach trophozoites. Samples of supernatant (20 µl) were placed onto a glass slide and covered with a coverslip then viewed microscopically for trophozoites.

For PCR analysis, cysts from the inoculum and positive pig faecal samples were purified as above then purified cysts were freeze-thawed 5 times before DNA was extracted using a Power Soil DNA Kit (MoBio, Carlsbad, California). Extraction blanks (no faecal sample) were used in each extraction group. Purified DNA was stored at -20°C prior to PCR.

Nested PCR amplification of the triose phosphate isomerase (*tpi*) gene using assemblage A, B and E specific primers was performed as previously described (Geurden et al., 2008; Levecke et al., 2009; Sulaiman et al., 2003). The glutamate dehydrogenase (*gdh*) gene was amplified with a nested PCR using GDHeF and GDH2 primers in the primary reaction and the GDHiF and GDH4 primers in the secondary reaction following the PCR reaction protocol of Caccio *et al* (2008) with the annealing temperature changed to 55°C and 52°C for the primary and secondary reactions respectively (Caccio et al., 2008; Read et al., 2004). The amplified DNA from the secondary *tpi* PCR products were separated by gel electrophoresis and purified for sequencing using an in house filter tip method (Yang et al., 2013). Purified PCR products were sequenced independently using an ABI Prism™ Dye Terminator Cycle Sequencing kit (Applied Biosystems, Foster City, California) according to the manufacturer's instructions at 64°C, 62°C and 67°C annealing temperature for assemblages A, B and E *tpi* PCR products,

respectively (Geurden et al., 2008; Levecke et al., 2009; Read et al., 2004). Amplified DNA from the secondary *gdh* PCR were then directly Sanger sequenced by the Australian Genome Research Facility.

All random samples taken from the original herd before transfer of the trial piglets to the research facility were negative for *Giardia* cysts via sucrose floatation or immunofluorescent detection. Samples collected on days 4, 7, 11 and 15 were all negative for *Giardia* cysts based on immunofluorescent detection. The pre-patent period of giardiasis varies depending on species and source of infection. Previously it has been reported that the pre-patent period can be up to 23 days in beavers given human derived cysts however a prepatent period in pigs could not be identified (Erlandsen et al., 1988). As no cysts were detected during the first 15 days, a random pig was chosen on day 18 to determine if there were any trophozoites present within the GIT. All sections collected (duodenum, ileum and jejunum) were negative for trophozoites, indicating that no infection had established to date. In order to take into account a longer prepatent period, faecal collection was continued for a further 15 days. One faecal sample collected on day 23 was positive for *Giardia* cysts with a faecal count of ~ 1000 cysts/gram of faeces. A faecal sample from the same piglet, as well as a piglet in the same pen and one in a separate pen, were positive for *Giardia* cysts on day 25 with cyst counts of between 60 and 300 cysts/gram of faeces. On day 30, only 1 animal remained positive with *Giardia* cysts (~66 cysts per gram of faeces), all other animals were negative. On day 36, all three pigs that had previously shown a positive faecal cyst count were euthanized and samples were taken from the ileum, duodenum and jejunum. A single trophozoite was identified in the mid-jejunum of one pig with a positive faecal cyst count. Both of the other animals and all other intestinal sections were negative for trophozoites. The faecal material of the euthanized pigs was also negative for cysts.

DNA sequences from the inoculum used to infect the pigs and the positive samples collected were compared. Collection of the trophozoite DNA was also attempted but this was unsuccessful. The initial inoculum and DNA from cysts excreted in a single sample from one of the pigs were typed as assemblage E at both the *tpi* and *gdh* loci. The *tpi* locus was highly conserved between both samples however there were 4 single nucleotide polymorphisms (SNPs) in the *gdh* region between the calf sample used as the inoculum and the pig sample. Each sample aligned 100% with previously described samples in Genbank over a 585 bp segment. The calf sequence from this study had 100% similarity to another calf sample obtained from the same region (Roseworthy, South Australia), while the pig *gdh* sequence had 100% similarity to a pig derived isolate, P-15 which is in axenic culture but was originally initiated

via trophozoites collected from the intestine of infected pigs in Europe (Genbank accession numbers: **AY178740** and **AY178741**). The significance of this finding is yet to be determined as further study would be required to determine if the mutational changes represent natural genetic variation or a shift towards host adaptation in a different livestock species.

Although a small number of pigs (12%) were excreting *Giardia* cysts in their faeces, the number of cysts/gram of faeces was very low and the time until cysts were observed in the faeces was prolonged. Both of these factors indicate the possibility that the pigs re-ingested the original inoculum, which could have passed through the pigs following the initial challenge. Nevertheless, only a single trophozoite was observed in a single section of small intestine from one of the four pigs sacrificed. Thus, based on the results of this study, these pigs were not a suitable host for *Giardia* obtained from a calf. The results demonstrate a low potential for cross-species establishment of infection with the isolate used.

Previous molecular studies in Australia and overseas have detected *G. duodenalis* in pigs at a frequency between 0.1 and 41 %. One such study in Australia identified post-weaned piglets had the highest prevalence of *G. duodenalis* (32 %), with the majority of isolates belonging to assemblage E and the remaining isolates belonging to assemblage A (Armson et al., 2009). In addition, another study in Europe confirmed giardiasis in post-weaned pigs (8 weeks) by isolation of trophozoites from the GIT (Koudela et al., 1991). Further study in Europe demonstrated the cross-species transmission of a pig derived *G. duodenalis* isolate to goat kids suggesting low host specificity of the isolate used, however the neonatal goat kids were fed with cow's milk, removing the GIT protective effect of the parent milk and the isolate used to infect the kids was not characterised (Koudela and Vitovec, 1998). Despite reports of *G. duodenalis* infection occurring naturally in pigs, in the present study, post-weaned piglets were unable to be unequivocally experimentally infected, which could be due to the possible host specificity of the inoculum. However, it is possible that if younger piglets were used (e.g. preweaned) or the pigs were immunocompromised, an infection may have established with the isolate used.

This study demonstrates that using an assemblage E isolate of *G. duodenalis* from cattle we were unable to establish a reliable infection in pigs. Further work is warranted to understand the cross-species transmission of *G. duodenalis* assemblages and the role it plays in livestock health and production.

Acknowledgements:

The Authors would like to acknowledge advice and support in pig husbandry provided by Lauren Staveley and Dr. Willian van Wettere.

6.2 *Giardia duodenalis* Mouse Model for the Development of Novel Antigiardial Agents

6.2.1 Statement of Authorship

Title of Paper	<i>Giardia duodenalis</i> Mouse Model for the Development of Novel Antigiardial Agents
Publication Status	<input type="checkbox"/> Published <input checked="" type="checkbox"/> Accepted for Publication <input type="checkbox"/> Submitted for Publication <input type="checkbox"/> Unpublished and Unsubmitted work written in manuscript style
Publication Details	

Principal Author

Name of Principal Author (Candidate)	Rebecca Jane Abraham		
Contribution to the Paper	Design and completion of experimental work (except where mentioned below) and interpretation of data. Preparation of manuscript. Acting as corresponding author on the manuscript		
Overall percentage (%)	60%		
Certification:	This paper reports on original research I conducted during the period of my Higher Degree by Research candidature and is not subject to any obligations or contractual agreements with a third party that would constrain its inclusion in this thesis. I am the primary author of this paper.		
Signature		Date	13 th December 2017

Co-Author Contributions

By signing the Statement of Authorship, each author certifies that:

- i. the candidate's stated contribution to the publication is accurate (as detailed above);
- ii. permission is granted for the candidate to include the publication in the thesis; and
- iii. the sum of all co-author contributions is equal to 100% less the candidate's stated contribution.

Name of Co-Author	Mark O'Dea		
Contribution to the Paper	Experimental design. Delivery of substances to animals (gavage) and sample collection. Assistance in PCR. Manuscript editing and preparation		
Signature		Date	6 th December 2017

Name of Co-Author	Bertha Rusdi		
-------------------	--------------	--	--

Contribution to the Paper	Assistance in care of animals and sample collection. Performed qPCR and assisted with fluorescent microscopy of samples.		
Signature		Date	8 th December 2017

Name of Co-Author	Stephen Page		
Contribution to the Paper	Experimental design and manuscript editing		
Signature	-	Date	6 th December 2017

Name of Co-Author	Ryan O'Handley		
Contribution to the Paper	Expertise in animal model development, editing of manuscript		
Signature		Date	8 th December 2017

Name of Co-Author	Sam Abraham		
Contribution to the Paper	Experimental design and interpretation of results. Study supervision and manuscript editing.		
Signature		Date	14 th December 2017

6.2.2 Abstract:

In this study we describe a neonatal mouse model of *Giardia* infection for the development of novel anti-giardial compounds. Using this model, mice were consistently infected with the Assemblage A BAH2c2 strain which had been maintained in axenic culture, with 10⁵ trophozoites per animal recovered. This model proved to be robust, consistent and ideal for preliminary drug efficacy trials and further drug development.

6.2.3 Article

Giardia duodenalis (aka. *G. lamblia*) is one of the most common enteric pathogens worldwide and is especially prominent in children in developing nations, often resulting in chronic infections with long lasting side effects such as malnourishment, developmental delays and general failure to thrive (Berkman et al., 2002; Homan and Mank, 2001; Lengerich et al., 1994). In addition, a correlation between giardiasis and the development of other diseases such as irritable bowel syndrome has also been established (Hanevik et al., 2014). Although there are current treatments available for giardiasis, treatment failures occur often, due in part to poor adherence to dosing schedules, unpleasant side effects and the development of drug resistance in the parasite (Jokipii and Jokipii, 1979; Wright et al., 2003). An important step in the development of novel chemotherapeutics for the treatment of giardiasis is preliminary evaluation of potential anti-giardials in animal models, as *in vitro* efficacy does not always translate to *in vivo* efficacy (Sande and Zak, 1999).

Attempts to develop mouse models of giardiasis have been undertaken in both adult and neonatal mice. In immunocompetent adult mice only one characterised human derived isolate (GS(M)/H7 – assemblage B) was able to cause infection over several weeks. However, development of infection is highly dependent on mouse strain and intestinal microflora (Byrd et al., 1994; Singer and Nash, 2000). Other models using cysts of uncharacterised human derived strains (e.g. H3 – assemblage B) have been shown to cause longer infections. However, these models are not ideal for drug development as the strains cannot be characterised *in vitro*, they require the animals be maintained on an antibiotic cocktail (which could interfere with the activity of novel compounds) (Bartelt et al., 2013; Singer and Nash, 2000). In addition, not all isolates can cause successful infections in mice, identified by the shedding of cysts and presence of trophozoites in the intestine upon necropsy. The neonatal mouse model, on the other hand, is ideal for early anti-giardial compound testing as pre-weaned pups have been shown to be susceptible to a wide variety of *Giardia* strains including those available in axenic culture allowing comparison between different strains and *in vitro* and *in vivo* results (Lemee et al., 2000; Reynoldson et al., 1991).

In this study we describe modifications of the suckling mouse model of *Giardia* infection first described in 1983 and used in preliminary testing of albendazole efficacy in the 1990's (Hill et al., 1983; Reynoldson et al., 1991). The *Giardia* strain used, BAH2c2, was isolated from an Australian human patient, maintained in axenic culture (TYI-S-33 media, passaged 2-3 times per week) and has not previously been reported to infect mice (Wielinga et al., 2011). The additional modifications made to this model include highly sensitive techniques for detection and monitoring of infection including fluorescent antibody staining and qPCR. These modifications make the identification of infection more accurate and reliable.

All work was performed with the approval of Murdoch University Animal Ethics Committee (Permit #R2855/16) Animals used were arc:arc (S) Swiss origin mice sourced from the Animal Resource Centre, Murdoch, Perth, Western Australia. Suckling mice were obtained when 6 days old (7-13 mice per group, number of mice in initial trial determined using a power calculation with a confidence of 95%, and an estimated 30% of animals becoming infected) and were acclimatised for 2-3 days in the PC2 facility. Mice were housed in plastic cages with wire lids with food and water supplied *ad lib*. Housing and nesting material were also provided. All mice were inoculated when nine days old via oral gavage using a flexible gavage needle (Walker Scientific, Joondalup DC WA Australia 6919). In the initial establishment model mice were inoculated with either 1×10^4 or 1×10^5 *Giardia duodenalis* trophozoites of the P1c10 strain (a clone of the Portland 1 strain, previously shown to cause infection in neonatal mice) or the BAH2c2 strain (a clone isolated from a human from Woodanilling, south-western Australia (Meloni et al., 1990; Wielinga et al., 2011) in a volume of 100 μ L of 0.9% saline. In all subsequent trials animals were inoculated with 1×10^5 trophozoites of the BAH2c2 strain in a volume of 100 μ L of 0.9% saline. Faecal samples were collected by removing groups to a separate cage without bedding. Due to the small volume of faeces produced by neonatal mice, faecal samples were pooled by group in order to obtain sufficient sample for testing. Faeces were examined for cysts via sucrose gradient centrifugation and observed via optical microscopy, immunofluorescent microscopy as described previously and qPCR (O'Handley et al., 2000). Briefly, cysts were concentrated by sucrose gradient centrifugation (prepared in-house, specific gravity 1.13, centrifugation: 900 X g, 5 minutes) and samples taken for each cyst detection method. For immunofluorescent detection, 20 μ l of concentrated cysts were placed onto a glass slide (Polysciences, Inc., Warrington, PA United States 18976) and air dried. An aliquot of *Giardia* specific fluorescein-labelled antibody (Giardi-a-Glo, Sapphire Bioscience, Redfern NSW Australia 2016, 20 μ l) was placed over the top of the sample and incubated at 37°C in a humidified box for 30 minutes. Excess antibody was removed by gentle

washing with phosphate buffered saline (PBS) and a coverslip was mounted onto a slide using aquapolymount (Thermo Fisher Scientific, Scoresby VIC Australia 3179). Samples were viewed with an Olympus BX41 microscope and the number of *Giardia* cysts/mg faeces calculated. The qPCR for the detection of giardial glutamate dehydrogenase (*gdh*) DNA in faeces was based on the method of Yang *et al* 2014. The protocol used the primers *gdhF1* 5' GGGCAAGTCCGACAACGA 3', the reverse primer *gdhR1* 5' GCACATCTCCTCCAGGAAGTAGAC 3', developed by Yang *et al.*, and the probe modified to include FAM as the reporter dye 5'-(6FAM)-TCATGCGCTTCTGCCAG BHQ2 3' (Yang *et al.*, 2014). Concentrated cyst material from the sucrose clarification was freeze-thawed five times using liquid nitrogen, before total DNA was extracted using a Purelink Genomic DNA extraction kit (Invitrogen, Thermo Fisher Scientific, Scoresby VIC Australia 3179). Reactions were performed using TaqPath qPCR mastermix (Thermo Fisher Scientific, Scoresby VIC Australia 3179) on a Quantstudio6 platform. At the end of the trial period, mice were euthanized via cervical dislocation and the entire small intestine was removed, incised longitudinally and placed in ice-cold PBS. Samples were chilled for at least 30 minutes before enumeration of trophozoites using a haemocytometer.

The BAH2c2 strain with an inoculum of 1×10^5 cells/mouse was found to be the most promising in establishing infection in pups with 100% of animals infected in the first experiment and observation of cysts 13 days post-inoculation. The smaller inoculum of 1×10^4 cells only caused infection in 22% (2/9) of animals and no cysts were observed in the faeces. The P1c10 strain infected 8% (1/13) of mice at the highest inoculum used but failed to infect any mice at the lower inoculum and no faecal cysts were observed in either group 15 d p.i. (Figure 6.2.1).

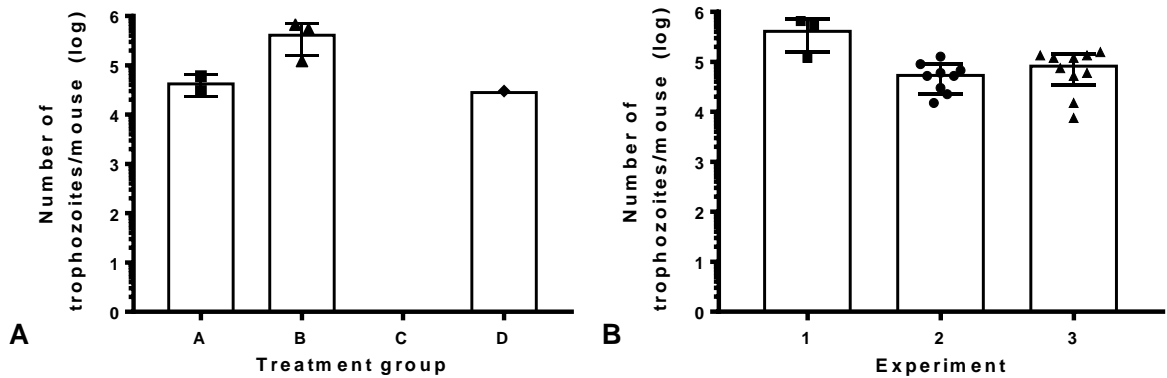


Figure 6.2.1 Experimental infection of neonatal mice with *Giardia duodenalis*. **1A: Establishment of infection** with various strains and inoculum densities of *G. duodenalis*. Neonatal mice were infected at 9 days old with either the P1c10 or BAH2c2 strain of *G. duodenalis*. 15 days p.i. trophozoites were collected from the small intestine and enumerated. A – inoculum BAH2c2, 1×10^4 cells/mouse, 22% of mice infected; B – BAH2c2, 1×10^5 cells/mouse, 100% of mice infected (only subset had trophozoites counted); C – P1c10, 1×10^4 cells/mouse, 0% of mice infected and D – P1c10, 1×10^5 cells/mouse, 8% of mice infected. **1B: Reproducibility of infection** of neonatal mice with the BAH2c2 strain of *G. duodenalis*. Mice were inoculated at ~9 days old with 1×10^5 trophozoites/mouse of the BAH2c2 strain. Once cyst shedding had been observed, trophozoites were harvested from the small intestine and enumerated. Infection was established in 100% of animals based on the presence or absence of trophozoites in the small intestine. Error \pm SD. Individual points represent single animals.

Based on the initial experiment the BAH2c2 strain at the inoculum of 1×10^5 cells/mouse was chosen for future experiments. To ensure reproducibility between litters, infection with the BAH2c2 strain was repeated on two separate occasions. In both cases an infection was established in 100% of the exposed mice with faecal cysts observed 7-8 days post inoculum. Across all three replicates of the trial, a similar number of trophozoites was observed in intestinal samples (Figure 6.2.1).

Three cyst detection methods were evaluated with immunofluorescence microscopy being the most sensitive, detecting the presence of cyst material in the faeces a day earlier than qPCR and traditional microscopy, and is easily used to quantify the number of cysts in a sample when the initial faecal weight of the sample is known. qPCR was the second most effective detection method giving a positive or negative answer while traditional microscopy was least effective (Table 6.2.1). In addition, qPCR and immunofluorescence do not require the specialist training and experience that is required for light microscopy. However, qPCR should be used in conjunction with microscopy detection, rather than as a stand-alone detection method, to ensure infection has been established, as the presence of *gdh* DNA does not necessarily indicate the

presence of viable cysts. Concentration of the cysts via sucrose gradient centrifugation was an important addition to the model in detection of faecal cysts.

Days post inoculation	Light microscopy	qPCR (+/-)	Immunofluorescent microscopy
	(+/-)		(cysts/mg faeces)
7	-	+	Positive but not quantified
8	+	+	97
9	-	+	60
10	+	+	59
11	NT	+	139

Table 6.2.1 Comparison of three methods to detect *Giardia* infection in mice via faeces. Faecal samples from individual animals were pooled and subjected to sucrose gradient centrifugation techniques to concentrate cysts before preparation for microscopy or qPCR. Representative data from pooled samples collected in one experiment with 7 mice per group are shown (the final trial). NT – not tested.

In this study we demonstrate that the neonatal suckling model is useful in the pre-clinical development of anti-giardial agents as it is reproducible, predictable and easy to perform. It has demonstrated an improvement on previous models by utilising immunofluorescence to increase specificity and ease of cyst identification and qPCR for rapid identification of infection and confirmation of immunofluorescence results. This model has been developed specifically for anti-giardial drug screening and development.

Chapter 7: General Discussion and Conclusions

7.1 Introduction

The discovery and development of antimicrobials was one of the biggest advancements in medical history, providing an effective defence against the devastating consequences of infectious diseases. Although antimicrobials have played an important role in the advancement of medical, and veterinary, practise, infectious diseases still remain one of the leading causes of morbidity and mortality worldwide, in part due to infectious disease for which there are limited or no effective antimicrobials, including those included in the neglected diseases initiative.

Antimicrobial resistance is also becoming a problem, with an increase in the detection, development and dissemination of antimicrobial resistance among populations of infectious disease causing organisms, reducing current treatment options. Simultaneously, a decrease in the investment into research and development is occurring, as investment returns are not as lucrative in comparison to pharmaceuticals for alternative applications (Cohen, 2000; French, 2010; Norrby et al., 2005; Spellberg et al., 2004; Ventola, 2015).

The development of novel antimicrobial agents is time consuming and costly, with one study suggesting 8-15 years from identification of novel agents to market entry, requiring > \$2 billion (Gwynn et al., 2010; Tufts, 2014). With the current arsenal of antimicrobials rapidly becoming obsolete, other alternatives for traditional antimicrobial development are being sort, including the repurposing and redevelopment of currently know compounds (Oprea et al., 2011).

In this thesis, the repurposing of robenidine (an anticoccidial agent used in the poultry industry) was explored. This included the examination of a library of chemical analogues of robenidine, in addition to robenidine itself, for inhibitory activity against pathogenic bacterial species as well as the neglected protistann diseases, *Leishmania donovani*, *Trypanosoma brucei* and *Giardia duodenalis* (syn. *Giardia lamblia*, *Giardia intestinalis*).

7.2 General aims and chapter summaries

This thesis explored the potential repurposing of robenidine and the antimicrobial efficacy of a library of robenidine analogues. It was found that robenidine and several analogues had antibacterial activity (chapter 2) that was targeted towards Gram-positive organisms. It was then identified, through the use of membrane permeabilising agents and the production of spheroplasts, that the target of the Gram-positive active analogues was present in Gram-negative organisms (chapter 2 and 3). Furthermore, intrinsic activity towards Gram-negative bacteria was also identified with a small subset of analogues (chapter 3).

The potential for the use of robenidine and related analogues for the treatment of parasitic infections (other than coccidian infections) was also investigated. Subsets of the analogue library were screened for activity against *Trypanosome brucei*, *Leishmania donovani* (chapter 4) and *Giardia duodenalis* (chapter 5).

Several analogues were found to have potent activity against *T. brucei*. However, this activity was unselective, with toxicity to mammalian cells observed at similar concentrations (chapter 4). Four (out of 19) analogues had potent and selective activity for *L. donovani* over mammalian cells with selectivity indices as high as 27 (chapter 4). Forty-six analogues were active against *Giardia* with greater than 50% inhibitory activity at 25 μ M (chapter 5). Importantly 13 of these analogues were selective for *Giardia* over bacterial cells, limiting the potential for off target effects to beneficial microorganisms. Furthermore, 12 also had excellent *in vitro* toxicity profiles with little to no *in vitro* mammalian cell toxicity (chapter 5).

In this thesis, analogues were identified with potent activity against each organism screened. With the exception of some anti-giardial analogues, this activity was generally unselective, either exhibiting mammalian cell toxicity or also affecting other microbial cell types. As mentioned previously, there were several analogues identified that had selective anti-giardial activity, not affecting bacterial organisms or mammalian cells, therefore, the remainder of this thesis focussed on the continued exploration of anti-giardial activity. *In vitro* analysis of 119 analogues available from the robenidine library, identified 13 with potent anti-giardial activity that lacked antibacterial activity and mammalian cell toxicity (chapter 5). The long-term effect on *Giardia* of exposure to these analogues was determined (chapter 5). Three *Giardia* specific analogues were found to inhibit recovery of *Giardia* after only 5 hr exposure times. The effect of two of these lethal analogues, along with the lead compound, robenidine, was explored using electron microscopy to understand the site and mechanism of action (chapter 5). Scanning electron microscopy (SEM) demonstrated significant morphological changes to trophozoites including cell swelling and disruption of the cell membrane (chapter 5). SEM also highlighted the rapid action of these analogues with significant cell changes seen after only 2 hrs of exposure to these analogues. The *in vivo* toxicity of two of the most promising analogues, in addition to robenidine, was determined in suckling mice (chapter 5). Three week old mice were exposed orally to 100 mg/kg of each analogue, administered once per day for three days, with no behavioural or gross pathological signs of toxicity observed (chapter 5).

The promising *in vitro* efficacy and selectivity in addition to no observable *in vivo* toxicity led to the development of an animal model of giardiasis for *in vivo* efficacy testing (chapter 6).

Initially, pigs were chosen as an appropriate model animal due to similarities in gut structure and function to humans (chapter 6.1). However, a satisfactory infection was unable to be established and the model was developed in the mice (chapter 6.2). As a part of this thesis a reliable suckling mouse model of giardiasis was successfully established using a human isolate of *Giardia* (chapter 6.2) which will be useful for future *in vivo* evaluation of the *Giardia* selective analogues identified in this thesis.

7.3 Major findings, implications and future work arising from this thesis

1. Antibacterial activity of robenidine and several analogues.

The level of resistance to antimicrobials within the bacterial population is critical, with extremely limited treatment options for some infections and in some cases 50% risk of mortality due to a lack of effective treatments (Doi et al., 2017). The increasing inefficiency of antibacterials has far reaching implications for human health. Without reliable means to treat infections, the current advances of modern medicine, routinely performed, such as chemotherapy, transplantation and other complex surgeries, will carry greater risk due to the inevitability of untreatable bacterial complications (Brown and Wright, 2016; Doi et al., 2017).

Due to the urgent need for new antibacterial agents, this thesis identified the antibacterial potential of robenidine and 111 structural analogues for the first time. All of the analogues with efficacy in this study were intrinsically active against the Gram-positive organisms *S. aureus* and *Enterococcus* sp. including MRSA and VRE, with MICs and MBCs as low as 2 µg/ml. Time-kill profiles demonstrated a bactericidal mechanism of action. This study included analysis of preliminary structure activity relationship data which facilitated a better understanding of chemical moieties enlisting antibacterial activity (chapter 2). In addition, it was shown that the target for several of the compounds was present in the Gram-negative pathogens *E. coli* and *P. aeruginosa*, when the outer membrane of the bacterium was compromised either partially using PMBN or almost entirely using sub-inhibitory concentrations of ampicillin (chapter 2 and 3). Further manipulation of the chemical structure led to the development of analogues with intrinsic Gram-negative activity (chapter 3).

Given the safety profile of robenidine (EFSA, 2004), the active analogues, identified here for the first time, have the potential to be developed as either narrow spectrum (those limited to Gram-positive activity) or broad spectrum (those with Gram-positive and Gram-negative activity) antibacterial agents. Future work in this area would involve toxicity and *in vivo*

evaluation of the most promising agents using animal models. It is suggested that the analogues with Gram-negative efficacy be the focus of future development as there is a dire need for new Gram-negative active agents, with limited options and upcoming potential drugs being identified and pursued (Boucher et al., 2013; Rice, 2008; WHO, 2017).

There is also potential for the continued chemical development of the Gram-negative active analogues to improve efficacy and druggability and evaluate *in vivo* efficacy.

2. **Antitrypanosomal activity of robenidine and select analogues.**

Trypanosoma brucei is a flagellated extracellular parasitic protist that is endemic to Africa, transmitted by the Tsetse fly and infectious to humans and animals. There is currently a lack of safe and efficacious drugs to cure the disease, and with millions of people at risk of contracting the fatal (if left untreated) disease, there is a need to develop new treatments (Steverding et al., 2016). Although there is a need for the development of new agents, only a handful of papers describing potential new agents have been published in recent years (Buscher et al., 2017). As a part of this thesis, 19 analogues in addition to robenidine from the available library were tested for *in vitro* efficacy against the amastigote stage of the parasite. For the first time, 16 analogues of robenidine were found to have inhibitory properties against *T. brucei* at μM concentrations. Unfortunately, the inhibition was not selective for *T. brucei* with $\text{SI} < 10$. However, there was evidence of a ‘non-flat’ SAR with variations in efficacy of different analogues and corresponding mammalian cell toxicity, providing a starting point for the chemical development of more specific *T. brucei* analogues and the potential for development of a new class of antitrypanosomal drugs.

3. **Antileishmanial activity of robenidine and select analogues.**

Leishmania donovani is one of the main causes of leishmaniasis, a disease that varies in clinical presentation from self-curing cutaneous leishmaniasis, which can leave devastating disfigurement, to potentially lethal visceral leishmaniasis (Tegazzini et al., 2017). There are limited treatment options available for *L. donovani*, which all have significant drawbacks. The most recently developed antileishmanial treatment is miltefosine, which has a huge advantage over other available drugs as it is delivered orally. However, treatment with miltefosine requires almost 1 month of repeated administration, making patient compliance difficult. Furthermore, it has been associated with teratogenicity (Tegazzini et al., 2017). In addition, as is common with infectious diseases, development of resistance to antileishmanials has been reported and for some

drugs is widespread. With the limited compounds available, it is important to develop new agents as highlighted by the inclusion of *L. donovani* in the drugs for neglected diseases initiative. With this in mind, a small subset of robenidine analogues (n=19) were screened for antileishmanial activity *in vitro*. For the first time, as a part of this thesis, antileishmanial inhibitory activity of this library was identified. Four out of the twenty compounds screened had potent selective inhibitory activity towards *L. donovani* with IC₅₀'s as low as 0.3 µM and SI's ≥ 20.

4. The anti-giardial potential of novel analogues of robenidine.

G. duodenalis is a ubiquitous intestinal parasite that can cause long-lasting adverse consequences including failure to thrive syndrome in children and has also been linked to chronic diseases such as irritable bowel syndrome (Buret, 2008; Halliez and Buret, 2013). There are limited treatment options available which are continuing to decrease as drug resistance increases (Upcroft and Upcroft, 2001b; Wright et al., 2003).

In vitro efficacy: In this study it was demonstrated that several structural analogues (n=46), in addition to robenidine itself, had anti-giardial activity *in vitro*. Furthermore 13 of the novel analogues demonstrated distinct advantages over robenidine including better *in vitro* safety profiles and selectivity for *Giardia* over bacteria (suggesting that the potential effect on gut microbiota would be limited). Three selective analogues were identified as being particularly promising, as trophozoites were unable to recover *in vitro* after short exposure times (5 hr).

In vivo toxicity. The top two analogues (**135**, **139**), in addition to robenidine, were administered to pre-weaned mice orally, 100 mg/kg, once per day for 3 days as a preliminary investigation of toxicity. No behavioural or gross pathological signs of toxicity were observed.

Mechanism of action. The mechanism of action of robenidine against its original target, coccidia, is poorly understood, and the site and mechanism of action of these compounds against other parasites is not known (Lee and Millard, 1972; Wong et al., 1972). As a part of this study, electron microscopy was used as an initial step to elucidate the mechanism of action of robenidine and the two most promising analogues against *Giardia*. Significant cell damage was observed using both SEM and TEM (robenidine)

or SEM (alternative analogues) after 2 hrs of compound exposure. Damage under the influence of all three compounds included disintegration of the adhesive disk, which is essential for disease progression as it is essential for attachment of *Giardia* trophozoites to the epithelial cells of the host. In addition, the novel analogues (**139**, **135**) also caused cell swelling to the point that distinctive cell features, such as the adhesive disc and flagella, become unrecognisable. After treatment with **135**, aggregations of cells, often with an unidentifiable number of cells, were observed. These studies highlight the structural and morphological changes induced by very short (≤ 2 hr) exposure to robenidine, **139** and **135**. This study also highlights the similarities in effect between the analogues, such as membrane poration, particularly around the adhesive disc, as well as the differences in effect. Robenidine appears to have a much more pronounced effect on the adhesive disc than **135** and **139**. In addition to the development of membrane pores, **135** and **139** cause extreme cellular swelling, which was not observed with robenidine in these studies. This could be directly related to the selectivity of **135** and **139**, as, in contrast to robenidine, they were selectively observed to inhibit *Giardia* trophozoites *in vitro*, with no antibacterial activity.

5. Establishment of an animal model of giardiasis.

In this thesis, potent (nM) selective anti-giardial compounds that had irreversible effects on trophozoites were identified. Although promising *in vitro* efficacy was observed it is always necessary to determine *in vivo* efficacy as not all effects are translated in an animal host. In order to test *in vivo* efficacy, a reliable model of infection is required. Initially in this thesis a pig model of giardiasis was attempted, however, this was unsuccessful (see point 6 below). Therefore, mice were chosen as an alternative animal host. There have been several published reports of *Giardia* infection models in mice established with cysts or trophozoites using both characterised and uncharacterised isolates (Byrd et al., 1994; Eissa and Amer, 2012; Singer and Nash, 2000). A reliable neonatal mouse model was successfully established using the same *Giardia* isolate used for *in vitro* efficacy studies. This model incorporated the use of qPCR and fluorescent microscopy for quick and reliable intra-study detection of infection.

6. Cross-species transmission of *Giardia duodenalis*.

In an attempt to develop a model of giardiasis for the continued development of the compounds identified in this thesis, pigs were chosen due to the close similarity of their

gastrointestinal tract to that of humans and reports of compounds being metabolised in a way that closely mirrors the experience in humans. There have been no previous reports of a pig model of giardiasis although *Giardia* has been reported to infect pigs (Armson et al., 2009; Koudela et al., 1991). However, under the experimental conditions in this study, a reliable model was not established.

While disappointing from the point of view of drug discovery, it provided valuable information about the cross-species transmission of *Giardia* in livestock and was one of the first studies of its kind in this regard (livestock to livestock transmission).

7.4 Implications of the findings of this thesis

The findings of this thesis are significant in the development of novel therapeutic options for the treatment of infectious diseases. A range of important single-celled pathogens were surveyed as potential targets for this novel compound library providing important preliminary SAR data and potential for future development of the compounds as antimicrobial agents for various pathogens. The majority of this thesis focussed on the characterisation and development of these analogues as anti-giardial agents. Of the 119 analogues available for anti-giardial screening two were identified as highly promising, being selective for *Giardia* over other microorganisms (e.g. beneficial gut microflora) and having an improved safety profile over the parent drug robenidine. In addition, these two analogues appear to have a multifaceted mechanism of action, potentially targeting several essential cell features and processes. The implications for this work are potentially far reaching but in particular advancement of human and animal health through the control of infectious diseases.

7.5 Future work arising from this thesis

Questions arising from this thesis that could direct future work:

1. Further investigation into structural modifications of the lead Gram-negative active agents to improve Gram-negative activity of the compound library
2. *In vivo* confirmation of antibacterial activity of active analogues against target pathogens in an animal host e.g. bacterial blood stream infections in animals
3. Further *in vitro* and *in vivo* efficacy of antileishmanial compounds to evaluate the treatment potential of these analogues, including potential screening of the remaining analogues in the library to identify additional hits and understand the SAR allowing targeted compound design in the future

4. Commencement of animal trials to determine the *in vivo* efficacy of potent and selective analogues that inhibit *Giardia*.

7.6 Conclusions

In conclusion, this thesis identified the antibacterial and antiprotozoal activity of a novel library of chemicals based on the structure of robenidine, a known anticoccidial agent. Members of the library were found to be active against both Gram-positive and Gram-negative bacteria, including methicillin resistant *S. aureus*, vancomycin resistance *E. faecalis*, *E. coli* and *P. aeruginosa*, as well as Protist pathogens, including *G. duodenalis*, *T. brucei* and *L. donovani*. In addition, the mechanism of action of a selection of analogues against *Giardia* was probed using electron microscopy. Electron microscopy demonstrated significant structural damage to giardial trophozoites. Furthermore, chemically diverse analogues appeared to have diverse mechanisms of action causing cell swelling and aggregation of trophozoites. Finally, an improved murine model of giardiasis was developed based on previously published neonatal models using a characterised human strain of *G. duodenalis*, opening the way for future *in vivo* characterisation of the anti-giardial activity of promising compounds identified in this thesis.

Appendices

**Appendix 1: Materials and Methods for chemical synthesis of compounds
described in Chapter 2**

2,2'-Bis[(4-chlorophenyl)methylene]carbonimidic dihydrazide hydrochloride (1) NCL812

Synthesized by according to General Method A from 4-chlorobenzaldehyde to afford the title compound as a white solid. Supplied by Neoculi Pty Ltd.

¹H NMR (DMSO-*d*₆) δ 12.04 (br. s, 2H), 8.48 (br. s, 1H), 8.37 (br. s, 2H), 7.97 (d, *J* = 8.6 Hz, 4H), 7.57 (d, *J* = 8.6 Hz, 4H).

2,2'-Bis(phenylmethylene)carbonimidic dihydrazide hydrochloride (2)

Synthesized according to General Method B from benzaldehyde to afford the title compound as a white solid (88%).

M.P. 234–237°C. ¹H NMR (DMSO-*d*₆) δ 12.39 (br. s, 2H), 8.55 (s, 2H), 8.46 (s, 2H), 8.01 – 7.88 (m, 4H), 7.55 – 7.41 (m, 6H). ¹³C NMR (DMSO-*d*₆) δ 152.9, 148.9, 133.3, 130.8, 128.8, 127.9. HRMS: *m/z* (calcd for C₁₅H₁₅N₅, 265.1327; found 265.1246).

2,2'-Bis[(3-chlorophenyl)methylene]carbonimidic dihydrazide hydrochloride (3)

Synthesized according to General Method A from 3-chlorobenzaldehyde to afford the title compound as a white solid.

¹H NMR (DMSO-*d*₆) δ 12.17 (br. s, 2H), 8.61 (br. s, 2H), 8.38 (br. s, 2H), 8.16 (s, 2H), 7.83 (d, *J* = 7.0 Hz, 2H), 7.56 – 7.50 (m, 4H).

2,2'-Bis[(2-chlorophenyl)methylene]carbonimidic dihydrazide hydrochloride (4)

Synthesized according to General Method A from 2-chlorobenzaldehyde to afford the title compound as a white solid.

¹H NMR (DMSO-*d*₆) δ 12.37 (br. s, 2H), 8.83 (br. s, 2H), 8.63 (br. s, 2H), 8.44 – 8.39 (m, 2H), 7.60 – 7.55 (m, 2H), 7.55 – 7.44 (m, 4H).

2,2'-Bis[(4-bromophenyl)methylene]carbonimidic dihydrazide hydrochloride (5)

Synthesized according to General Method B from 4-bromobenzaldehyde to afford the title compound as a white solid (89%).

M.P. 224–226°C. ¹H NMR (DMSO-*d*₆) δ 12.42 (br. s, 2H), 8.60 (s, 2H), 8.42 (s, 2H), 7.91 (d, *J* = 8.5 Hz, 4H), 7.69 (d, *J* = 8.5 Hz, 4H). ¹³C NMR (DMSO-*d*₆) δ 152.9, 147.7, 132.6, 131.7, 129.7, 124.2. HRMS: *m/z* (calcd for C₁₅H₁₃Br₂N₅, 422.9517; found 422.9320).

2,2'-Bis[(3-bromophenyl)methylene]carbonimidic dihydrazide hydrochloride (6)

Synthesized according to General Method B from 3-bromobenzaldehyde to afford the title compound as a white solid (44%).

M.P. 248–251°C. ¹H NMR (DMSO-*d*₆) δ 12.45 (br. s, 2H), 8.68 (s, 2H), 8.41 (s, 2H), 8.29 (s, 2H), 7.87 (d, *J* = 7.8 Hz, 2H), 7.70 – 7.63 (m, 2H), 7.44 (t, *J* = 7.9 Hz, 2H). ¹³C NMR (DMSO-*d*₆) δ 153.0, 147.4, 135.7, 133.3, 130.9, 129.5, 127.6, 122.3. HRMS: *m/z* (calcd for C₁₅H₁₃Br₂N₅, 422.9517; found 422.9413).

2,2'-Bis[(2-bromophenyl)methylene]carbonimidic dihydrazide hydrochloride (7)

Synthesized according to General Method B from 2-bromobenzaldehyde to afford the title compound as a white solid (72%).

M.P. 267–270°C. ¹H NMR (DMSO-*d*₆) δ 8.84 (s, 2H), 8.69 (s, 2H), 8.41 (dd, *J* = 7.8, 1.7 Hz, 2H), 7.70 (dd, *J* = 8.0, 1.0 Hz, 2H), 7.48 (t, *J* = 7.3 Hz, 2H), 7.44 – 7.37 (m, 2H). ¹³C NMR (DMSO-*d*₆) δ 152.8, 147.3, 133.1, 132.4, 132.1, 128.5, 127.9, 123.9. HRMS: *m/z* (calcd for C₁₅H₁₃Br₂N₅, 422.9517; found 422.9355).

2,2'-Bis[(4-fluorophenyl)methylene]carbonimidic dihydrazide hydrochloride (8)

Synthesized by according to General Method A from 4-fluorobenzaldehyde to afford the title compound as a white solid.

¹H NMR (DMSO-*d*₆) δ 12.11 (br. s, 1H), 8.52 (br. s, 2H), 8.40 (br. s, 2H), 8.05 – 7.96 (m, 4H), 7.39 – 7.30 (m, 4H).

2,2'-Bis[(3-fluorophenyl)methylene]carbonimidic dihydrazide hydrochloride (9)

Synthesized according to General Method A from 3-fluorobenzaldehyde to afford the title compound as a white solid.

¹H NMR (DMSO-*d*₆) δ 12.08 (br. s, 2H), 8.38 (br. s, 2H), 7.97 – 7.94 (m, 2H), 7.69 – 7.67 (m, 2H), 7.56 – 7.53 (m, 2H), 7.35 – 7.31 (m, 2H).

2,2'-Bis[(2-fluorophenyl)methylene]carbonimidic dihydrazide hydrochloride (10)

Synthesized according to General Method A from 2-fluorobenzaldehyde to afford the title compound as a white solid.

¹H NMR (4DMSO-*d*₆) δ 12.18 (br. s, 2H), 8.65 (br. s, 2H), 8.58 (br. s, 2H), 8.34 (t, *J* = 7.6 Hz, 2H), 7.58 – 7.53 (m, 2H), 7.34 (t, *J* = 8.2 Hz 4H).

2,2'-Bis[[4-(trifluoromethyl)phenyl]methylene]carbonimidic dihydrazide hydrochloride (11)

Synthesized according to General Method A from 4-trifluoromethylbenzaldehyde to afford the title compound as a white solid.

^1H NMR (DMSO- d_6) δ 12.32 (br. s, 2H), 8.69 (br. s, 2H), 8.49 (br. s, 2H), 8.18 (d, $J = 7.8$ Hz, 4H), 7.86 (d, $J = 8.2$ Hz, 4H).

2,2'-Bis[(4-hydroxyphenyl)methylene]carbonimidic dihydrazide hydrochloride (12)

Synthesized according to General Method B from 4-hydroxybenzaldehyde to afford the title compound as a yellow solid (18%).

M.P. 246–248°C. ^1H NMR (DMSO- d_6) δ 11.92 (br. s, 2H), 10.13 (br. s, 2H), 8.28 (s, 4H), 7.75 (d, $J = 8.5$ Hz, 4H), 6.86 (d, $J = 8.5$ Hz, 4H). ^{13}C NMR (DMSO- d_6) δ 160.1, 152.4, 148.8, 129.6, 124.3, 115.6. LRMS: m/z (calcd for $\text{C}_{15}\text{H}_{15}\text{N}_5\text{O}_2$, 297.12; found 297.90).

2,2'-Bis[(3-hydroxyphenyl)methylene]carbonimidic dihydrazide hydrochloride (13)

Synthesized according to General Method B from 3-hydroxybenzaldehyde to afford the title compound as a pale yellow solid (61%).

M.P. 121–123°C. ^1H NMR (DMSO- d_6) δ 8.00 (s, 2H), 7.26 – 7.08 (m, 6H), 6.98 – 6.43 (m, 4H). ^{13}C NMR (DMSO- d_6 , DEPT) δ 157.6, 143.8, 136.8, 129.5, 118.0, 116.1, 113.0. HRMS: m/z (calcd for $\text{C}_{15}\text{H}_{15}\text{N}_5\text{O}_2$, 297.1226; found 297.1114).

2,2'-Bis[(2-hydroxyphenyl)methylene]carbonimidic dihydrazide hydrochloride (14)

Synthesized according to General Method B from 2-hydroxybenzaldehyde as a white solid (95%).

M.P. 263–266°C. ^1H NMR (DMSO- d_6) δ 12.19 (s, 2H), 10.25 (s, 2H), 8.70 (s, 2H), 8.34 (s, 2H), 8.06 (d, $J = 7.8$ Hz, 2H), 7.35 – 7.23 (m, 2H), 7.00 (d, $J = 8.2$ Hz, 2H), 6.87 (t, $J = 7.5$ Hz, 2H). ^{13}C NMR (DMSO- d_6) δ 156.9, 152.5, 145.4, 132.0, 126.9, 119.5, 119.1, 116.3. HRMS: m/z (calcd for $\text{C}_{15}\text{H}_{15}\text{N}_5\text{O}_2$, 297.1226; found 297.1125).

2,2'-Bis[(4-methoxyphenyl)methylene]carbonimidic dihydrazide hydrochloride (15)

Synthesized according to General Method B from 4-methoxybenzaldehyde to afford the title compound.

^1H NMR (DMSO- d_6) δ 11.78 (br. s, 2H), 8.31 (br. s, 3H), 7.87 (d, $J = 8.6$ Hz, 4H), 7.04 (d, $J = 8.6$ Hz, 4H), 3.83 (s, 6H).

2,2'-Bis[(3-methoxyphenyl)methylene]carbonimidic dihydrazide hydrochloride (16)

Synthesized according to General Method A from 3-methoxybenzaldehyde to afford the title compound as a white solid.

^1H NMR (DMSO- d_6) δ 11.99 (br. s, 2H), 8.48 (br. s, 2H), 8.36 (br. s, 2H), 7.56 (s, 2H), 7.46 – 7.38 (m, 4H), 7.08 – 7.05 (m, 2H), 3.84 (s, 6H).

2,2'-Bis[(2-methoxyphenyl)methylene]carbonimidic dihydrazide hydrochloride (17)

Synthesized according to General Method A from 2-methoxybenzaldehyde to afford the title compound as a white solid.

^1H NMR (400 MHz, DMSO- d_6) δ 12.00 (br. s, 2H), 8.74 (br. s, 2H), 8.38 (br. s, 2H), 8.22 (d, $J = 6.7$ Hz, 2H), 7.50 – 7.45 (m, 2H), 7.14 (d, $J = 8.2$ Hz, 2H), 7.05 (t, $J = 7.6$ Hz, 2H), 3.88 (s, 6H).

2,2'-Bis[[4-(trifluoromethoxy)phenyl]methylene]carbonimidic dihydrazide hydrochloride (18)

Synthesized according to General Method B from 4-trifluoromethoxybenzaldehyde to afford the title compound as a white solid (69%).

M.P. 258–261°C. ^1H NMR (DMSO- d_6) δ 12.49 (br. s, 2H), 8.65 (s, 2H), 8.49 (s, 2H), 8.10 (d, $J = 8.6$ Hz, 4H), 7.47 (d, $J = 8.3$ Hz, 4H). ^{13}C NMR (DMSO- d_6) δ 153.0, 149.8 (d, $J = 1.6$ Hz), 147.4, 132.6, 129.9, 121.2, 120.0 (q, $J = 256.9$ Hz). LRMS: m/z (calcd for $\text{C}_{17}\text{H}_{13}\text{F}_6\text{N}_5\text{O}_2$, 433.10; found 433.80).

2,2'-Bis[[4-(methylsulfonyl)phenyl]methylene]carbonimidic dihydrazide hydrochloride (19)

Synthesized according to General Method B from 4-thiomethylbenzaldehyde to afford the title compound as an off-white solid (73%).

M.P. 242–245°C. ^1H NMR (DMSO- d_6) δ 12.17 (br. s, 2H), 8.46 (s, 2H), 8.37 (s, 2H), 7.86 (d, $J = 8.2$ Hz, 4H), 7.34 (d, $J = 8.2$ Hz, 4H), 2.53 (s, 6H). ^{13}C NMR (DMSO- d_6 , DEPT) δ 152.7, 148.4, 142.0, 129.7, 128.2, 125.4, 14.2. LRMS: m/z (calcd for $\text{C}_{17}\text{H}_{19}\text{N}_5\text{S}_2$, 357.11; found 357.95).

2,2'-Bis[[4-(trifluoromethylsulfonyl)phenyl]methylene]carbonimidic dihydrazide hydrochloride (20)

Synthesized according to General Method B from 4-thiotrifluoromethylbenzaldehyde to afford the title compound as a white solid (48%).

M.P. 195°C (Decomp.). ^1H NMR (DMSO- d_6) δ 12.68 (s, 1H), 8.73 (s, $J = 48.7$ Hz, 1H), 8.53 (s, 1H), 8.11 (d, $J = 8.2$ Hz, 2H), 7.79 (d, $J = 8.1$ Hz, 2H). ^{13}C NMR (DMSO- d_6) δ

153.06, 147.43, 136.20, 136.16, 129.52 (q, $J = 308.0$ Hz), 129.05, 125.20 – 125.01 (Unresolved quartet). LRMS: m/z (calcd for $C_{17}H_{13}F_6N_5S_2$, 465.05; found 465.60).

2,2'-Bis[(4-methylphenyl)methylene]carbonimidic dihydrazide hydrochloride (21)

Synthesized according to General Method A from 4-methylbenzaldehyde to afford the title compound as a white solid.

1H NMR (DMSO- d_6) δ 11.92 (br. s, 2H), 8.41 (br. s, 2H), 8.36 (br. s, 2H), 7.82 (d, $J = 8.2$ Hz, 4H), 7.30 (d, $J = 7.8$ Hz, 4H), 2.37 (s, 6H).

2,2'-Bis[(3-methylphenyl)methylene]carbonimidic dihydrazide hydrochloride (22)

Synthesized according to General Method A from 3-methylbenzaldehyde to afford the title compound as a white solid.

1H NMR (DMSO- d_6) δ 11.96 (br. s, 2H), 8.44 (br. s, 2H), 8.37 (br. s, 2H), 7.76 (s, 2H), 7.71 (d, $J = 7.8$ Hz, 2H), 7.38 (t, $J = 7.8$ Hz, 2H), 7.31 (d, $J = 7.8$ Hz, 2H), 2.38 (s, 6H).

2,2'-bis[(2-methylphenyl)methylene]carbonimidic dihydrazide hydrochloride (23)

Synthesized according to General Method B from 2-methylbenzaldehyde to afford the title compound as a white solid.

1H NMR (DMSO- d_6) δ 11.99 (br. s, 2H), 8.73 (br. s, 2H), 8.41 (br. s, 2H), 8.19 (d, $J = 7.8$ Hz, 2H), 7.39 (t, $J = 8.0$ Hz, 2H), 7.30 (t, $J = 7.8$ Hz, 4H), 2.46 (s, 6H).

2,2'-Bis[(4-propylphenyl)methylene]carbonimidic dihydrazide hydrochloride (24)

Synthesized according to General Method B from 4-propylbenzaldehyde to afford the title compound as a white solid (77%).

M.P. 218–222°C. 1H NMR (DMSO- d_6) δ 8.60 – 8.30 (m, 4H), 7.84 (d, $J = 8.1$ Hz, 4H), 7.28 (d, $J = 8.1$ Hz, 4H), 2.59 (t, $J = 7.5$ Hz, 4H), 1.64 – 1.54 (m, 4H), 0.88 (t, $J = 7.3$ Hz, 6H). ^{13}C NMR (DMSO- d_6) δ 152.8, 148.8, 145.3, 130.9, 128.7, 127.9, 37.2, 23.9, 13.6. HRMS: m/z (calcd for $C_{21}H_{27}N_5$, 349.2266; found 349.2112).

2,2'-Bis[(4-butylphenyl)methylene]carbonimidic dihydrazide hydrochloride (25)

Synthesized according to General Method B from 4-butylbenzaldehyde to afford the title compound as a pale yellow solid (80%).

M.P. 216–220°C. 1H NMR (DMSO- d_6) δ 12.21 (br. s, 2H), 8.44 (s, 2H), 8.39 (s, 2H), 7.83 (d, $J = 8.2$ Hz, 4H), 7.30 (d, $J = 8.2$ Hz, 4H), 2.63 (t, $J = 7.7$ Hz, 4H), 1.61 – 1.52 (m, 4H), 1.36 – 1.26 (m, 4H), 0.90 (t, $J = 7.3$ Hz, 6H). ^{13}C NMR (DMSO- d_6) δ 152.7, 148.8, 145.5,

130.9, 128.7, 127.9, 34.8, 32.9, 21.7, 13.8. HRMS: m/z (calcd for $C_{23}H_{31}N_5$, 377.2579; found 377.2336).

2,2'-Bis{[4-(1-methylethyl)phenyl]methylene}carbonimidic dihydrazide hydrochloride (26)

Synthesized according to General Method B from 4-isopropylbenzaldehyde to afford the title compound as a white solid (28%).

M.P. 193–196°C. 1H NMR (DMSO- d_6) δ 8.62 – 8.29 (m, 4H), 7.85 (d, $J = 8.2$ Hz, 4H), 7.33 (d, $J = 8.2$ Hz, 4H), 2.98 – 2.87 (m, 2H), 1.21 (d, $J = 6.9$ Hz, 12H). ^{13}C NMR (DMSO- d_6) δ 152.7, 151.4, 148.8, 131.0, 128.0, 126.7, 33.4, 23.6. HRMS: m/z (calcd for $C_{21}H_{27}N_5$, 349.2266; found 349.2112).

2,2'-Bis{[4-(1,1-dimethylethyl)phenyl]methylene}carbonimidic dihydrazide hydrochloride (27)

Synthesized according to General Method B from 4-*tert*-butylbenzaldehyde to afford the title compound as a white solid (50%).

M.P. 150–155°C. 1H NMR (DMSO- d_6) δ 8.56 – 8.32 (m, 4H), 7.85 (d, $J = 8.3$ Hz, 4H), 7.49 (d, $J = 8.3$ Hz, 4H), 1.31 (s, 18H). ^{13}C NMR (DMSO- d_6) δ 153.7, 152.7, 148.8, 130.7, 127.8, 125.6, 34.7, 31.0. HRMS: m/z (calcd for $C_{23}H_{31}N_5$, 377.2579; found 377.2454).

2,2'-Bis{4-(dimethylamino)phenyl}methylene}carbonimidic dihydrazide hydrochloride (28)

Synthesized according to General Method B from 4-(dimethylamino)benzaldehyde to afford the title compound as an orange solid (80%).

M.P. 161–164°C. 1H NMR (DMSO- d_6) δ 11.92 (br. s, 2H), 8.24 (s, 2H), 8.16 (s, 2H), 7.71 (d, $J = 8.9$ Hz, 4H), 6.74 (d, $J = 8.9$ Hz, 4H), 2.98 (s, 12H). ^{13}C NMR (DMSO- d_6) δ 152.1, 151.8, 149.0, 129.2, 120.5, 111.5, 39.7. HRMS: m/z (calcd for $C_{19}H_{25}N_7$, 351.2171; found 351.1966).

2,2'-Bis([1,1'-biphenyl]-4-ylmethylene)carbonimidic dihydrazide hydrochloride (29)

Synthesized according to General Method B from 4-phenylbenzaldehyde to afford the title compound as a yellow solid (81%).

M.P. 264–266°C. 1H NMR (DMSO- d_6) δ 12.48 (br. s, 2H), 8.62 (s, 2H), 8.51 (s, 2H), 8.04 (d, $J = 7.5$ Hz, 4H), 7.85 – 7.69 (m, 8H), 7.54 – 7.36 (m, 6H). ^{13}C NMR (DMSO- d_6) δ 152.8, 148.4, 142.2, 139.3, 132.5, 129.1, 128.5, 128.0, 127.0, 126.8. HRMS: m/z (calcd for $C_{27}H_{23}N_5$, 417.1953; found 417.1831).

2,2'-Bis([1,1'-biphenyl]-2-ylmethylene)carbonimidic dihydrazide hydrochloride (30)

Synthesized according to General Method B from biphenyl-2-carboxaldehyde to afford the title compound as a yellow solid (89%).

M.P. 129–133°C. ¹H NMR (DMSO-*d*₆) δ 12.27 (br. s, 2H), 8.49 (s, 2H), 8.44 – 8.27 (m, 4H), 7.57 – 7.44 (m, 10H), 7.41 – 7.33 (m, 6H). ¹³C NMR (DMSO-*d*₆) δ 152.6, 147.2, 142.4, 138.8, 130.6, 130.4, 129.7, 128.7, 127.8, 127.6, 126.8. HRMS: *m/z* (calcd for C₂₇H₂₃N₅, 417.1953; found 417.1709).

2,2'-Bis[(3-ethynylphenyl)methylene]carbonimidic dihydrazide hydrochloride (31)

Synthesized according to General Method B from 4-ethynylbenzaldehyde to afford the title compound as a yellow solid (93%).

M.P. 220°C (Decomp.). ¹H NMR (DMSO-*d*₆) δ 12.27 (br. s, 2H), 8.58 (s, 2H), 8.42 (s, 2H), 7.96 (d, *J* = 8.3 Hz, 4H), 7.58 (d, *J* = 8.2 Hz, 4H), 4.39 (s, 2H). ¹³C NMR (DMSO-*d*₆) δ 152.9, 148.0, 133.7, 132.0, 128.0, 123.7, 83.2, 83.0. LRMS: *m/z* (calcd for C₁₉H₁₅N₅, 313.13; found 313.80).

2,2'-Bis[(2,5-difluorophenyl)methylene]carbonimidic dihydrazide hydrochloride (32)

Synthesized according to General Method B from 2,5-difluorophenylbenzaldehyde to afford the title compound as a white solid (34%).

¹H NMR (DMSO-*d*₆) δ 12.83 (br s, 2H), 8.76 (s, 2H), 8.69 (s, 2H), 8.31 – 8.21 (m, 2H), 7.45 – 7.31 (m, 4H). ¹³C NMR (DMSO-*d*₆) δ 158.5 (dd, *J* = 240.2, 1.2 Hz), 157.2 (dd, *J* = 247.2, 1.4 Hz), 152.8, 140.7, 122.5 (dd, *J* = 12.2, 8.9 Hz), 119.4 (dd, *J* = 25.1, 9.0 Hz), 117.8 (dd, *J* = 24.0, 8.8 Hz), 113.0 (dd, *J* = 25.9, 2.3 Hz). HRMS: *m/z* (calcd for C₁₅H₁₁F₄N₅, 337.0951; found 338.0877).

N',2-Bis((E)-4-chloro-2-fluorobenzylidene)hydrazine-1-carboximidhydrazide hydrochloride (33)

Synthesized according to General Method A from 4-chloro-2-fluorobenzaldehyde to afford the title compound as a white solid (39%).

¹H NMR (DMSO-*d*₆) δ 12.43 (s, 1H), 8.38 (t, *J* = 8.3 Hz, 1H), 7.61 (dd, *J* = 10.5, 1.9 Hz, 1H), 7.45 (dd, *J* = 8.6, 1.6 Hz, 1H). ¹³C NMR (DMSO-*d*₆) δ 160.7 (d, *J* = 254.5 Hz), 152.8*, 140.8*, 136.3 (d, *J* = 10.8 Hz), 128.5, 125.3, 120.2 (d, *J* = 10.0 Hz), 116.7 (d, *J* = 24.7 Hz).

*Poor resolution failed to resolve doublets.

2,2'-Bis[(3,4-difluorophenyl)methylene]carbonimidic dihydrazide hydrochloride (34)

Synthesized according to General Method B from 3,4-difluorobenzaldehyde to afford the title compound as a white solid (76%).

¹H NMR (DMSO-*d*₆) δ 8.68 (s, 2H), 8.43 (s, 2H), 8.28 – 8.16 (m, 2H), 7.77 – 7.64 (m, 2H), 7.58 – 7.46 (m, 2H). ¹³C NMR (DMSO-*d*₆) δ 153.0, 150.8 (dd, *J* = 250.6, 13.0 Hz), 149.9 (dd, *J* = 245.9, 13.2 Hz), 146.6, 131.2 (dd, *J* = 6.4, 3.4 Hz), 126.0 (dd, *J* = 6.4, 2.8 Hz), 117.8 (d, *J* = 17.7 Hz), 115.7 (d, *J* = 18.5 Hz). HRMS: *m/z* (calcd for C₁₅H₁₁F₄N₅, 337.0951; found 338.0943).

2,2'-Bis[(2,4-dichlorophenyl)methylene]carbonimidic dihydrazide hydrochloride (35)

Synthesized according to General Method B from 2,4-dichlorobenzaldehyde to afford the title compound as a white solid (47%).

¹H NMR (DMSO-*d*₆) δ 12.84 (br s, 2H), 8.84 (s, 2H), 8.74 (s, 2H), 8.46 (d, *J* = 8.6 Hz, 2H), 7.71 (d, *J* = 1.6 Hz, 2H), 7.54 (dd, *J* = 8.6, 1.2 Hz, 2H). ¹³C NMR (DMSO-*d*₆) δ 152.7, 144.0, 135.9, 134.3, 129.7, 129.3, 129.3, 127.8. HRMS: *m/z* (calcd for C₁₅H₁₁Cl₄N₅, 402.9739; found 403.9786).

2,2'-Bis[(2,6-dichlorophenyl)methylene]carbonimidic dihydrazide hydrochloride (36)

Synthesized according to General Method B from 2,6-dichlorobenzaldehyde to afford the title compound as a white solid (63%).

¹H NMR (DMSO-*d*₆) δ 12.94 (br s, 2H), 8.68 (s, 2H), 8.33 (s, 2H), 7.60 (d, *J* = 7.9 Hz, 4H)*, 7.49 (dd, *J* = 8.7, 7.4 Hz, 2H)*. ¹³C NMR (DMSO-*d*₆) δ 153.0, 145.1, 134.1, 131.9, 129.9, 129.0. HRMS: *m/z* (calcd for C₁₅H₁₁Cl₄N₅, 402.9739; found 403.9765). *Poorly resolved ¹H-NMR spectrum.

2,2'-Bis[(3,5-dichlorophenyl)methylene]carbonimidic dihydrazide hydrochloride (37)

Synthesized according to General Method B from 3,5-dichlorobenzaldehyde to afford the title compound as a white solid (84%).

¹H NMR (DMSO-*d*₆) δ 12.67 (br s, 2H), 8.81 (s, 2H), 8.40 (s, 2H), 8.06 (d, *J* = 1.8 Hz, 4H), 7.68 (t, *J* = 1.8 Hz, 2H). ¹³C NMR (DMSO-*d*₆) δ 153.1, 146.1, 136.9, 134.6, 129.7, 126.2.

2,2'-Bis[(2-amino-4-chlorophenyl)methylene]carbonimidic dihydrazide hydrochloride (38)

Synthesized according to General Method B from 2-amino-4-chlorobenzaldehyde to afford the title compound as a pale yellow solid (13%).

¹H NMR (DMSO-*d*₆) δ 11.71 (br s, 2H), 8.40 (s, 2H), 8.37 (s, 2H), 7.29 (d, *J* = 8.4 Hz, 2H), 6.87 (d, *J* = 2.0 Hz, 2H), 6.73 (br s, 4H), 6.59 (dd, *J* = 8.3, 2.0 Hz, 2H). ¹³C NMR (DMSO-*d*₆) δ 152.1, 151.5, 148.9, 136.0, 134.7, 115.1, 114.5, 112.8.

2,2'-Bis[2-(1-hydroxyethylamino)-4-chlorophenyl]methylene}carbonimidic dihydrazide hydrochloride (39)

Synthesized according to General Method A from 4-chloro-2-[(1-hydroxyethyl)amino]benzaldehyde to afford the title compound as a yellow solid (17%).

¹H NMR (DMSO-*d*₆) δ 11.86 (s, 1H), 8.41 (s, 2H), 7.36 (d, *J* = 6.8 Hz, 2H), 6.75 (s, 1H), 6.66 (d, *J* = 7.9 Hz, 1H), 3.44 (d, *J* = 6.9 Hz, 1H)*, 1.24 (t, *J* = 5.3 Hz, 3H), 1.07 (dt, *J* = 13.8, 6.8 Hz, 1H). *Signal eclipsed by water. ¹³C NMR (DMSO-*d*₆) δ 152.0, 148.1, 136.9, 135.1, 114.7, 113.5, 109.7, 64.9, 56.0, 13.9.

2,2'-bis[(2-acetamido-4-chlorophenyl)methylene]carbonimidic dihydrazide (40)

Synthesized according to General Method A from *N*-(5-chloro-2-formylphenyl)acetamide to afford the title compound as an off-white crystalline solid (18%).

M.P. 259°C (Decomp.). ¹H NMR (DMSO-*d*₆) δ 12.29 (s, 1H), 10.29 (s, 1H), 8.55 (s, 1H), 8.45 (s, 1H), 8.13 (d, *J* = 8.5 Hz, 1H), 7.71 (s, 1H), 7.35 (dd, *J* = 8.5, 1.8 Hz, 1H), 2.12 (s, 3H). ¹³C NMR (DMSO-*d*₆) δ 169.2, 152.8, 146.4, 138.4, 135.0, 129.7, 125.0, 124.7, 124.3, 23.6. LRMS: *m/z* (calcd for C₁₉H₁₉Cl₂N₇O₂, 447.10; found 447.80).

2,2'-Bis[(2-hydroxy-3-methylphenyl)methylene]carbonimidic dihydrazide hydrochloride (41)

Synthesized according to General Method B from 2-hydroxy-3-methylbenzaldehyde to afford the title compound as a pale yellow solid (93%).

M.P. 260°C (Decomp.). ¹H NMR (DMSO-*d*₆) δ 12.08 (br s, 2H), 9.35 (s, 2H), 8.66 (s, 2H), 8.48 (s, 2H), 7.67 (d, *J* = 7.2 Hz, 2H), 7.25 (d, *J* = 7.2 Hz, 2H), 6.88 (t, *J* = 7.6 Hz, 2H), 2.23 (s, 6H). ¹³C NMR (DMSO-*d*₆) δ 154.6, 152.1, 149.0, 133.4, 127.0, 125.7, 119.7, 119.1, 16.1. LRMS: *m/z* (calcd for C₁₇H₁₉N₅O₂, 325.15; found 325.85).

2,2'-Bis(4-chloro-2-hydroxyphenyl)methylene}carbonimidic dihydrazide hydrochloride (42)

Synthesized according to General Method A from 4-chlorosalicylaldehyde to afford the title compound as a grey solid (22%).

¹H NMR (DMSO-*d*₆) δ 12.02 (s, 1H), 10.81 (s, 1H), 8.63 (s, 1H), 8.38 (s, 1H), 8.12 (d, *J* = 8.3 Hz, 1H), 7.13 – 6.84 (m, 2H). ¹³C NMR (DMSO) δ 157.5, 128.3, 119.5, 119.0, 115.9.

2,2'-Bis[[4-(dimethylamino)-2-hydroxyphenyl]methylene]carbonimidic dihydrazide (43)

Synthesized according to General Method A from 4-(dimethylamino)salicylic acid to afford the title compound as a brown solid (62%).

M.P. 254°C (Decomp.). ¹H NMR (DMSO-*d*₆) δ 11.63 (s, 1H), 9.84 (s, 1H), 8.46 (s, 1H), 8.02 (s, 1H), 7.74 (d, *J* = 8.8 Hz, 1H), 6.30 (d, *J* = 7.4 Hz*, 1H), 6.17 (s, 1H), 2.94 (s, 6H). ¹³C NMR (DMSO-*d*₆) δ 158.0, 153.1, 151.4, 146.4, 128.4, 107.5, 104.4, 97.7, 39.7*. *Signal eclipsed by the DMSO. LRMS: *m/z* (calcd for C₁₉H₂₅N₇O₂, 383.21; found 383.70). *Poorly resolved doublet gives reduced coupling constant.

2,2'-Bis[(2,3-dihydroxyphenyl)methylene]carbonimidic dihydrazide hydrochloride (44)

Synthesized according to General Method B from 2,3-dihydroxybenzaldehyde to afford the title compound as a yellow solid (75%).

M.P. 217°C (Decomp.). ¹H NMR (DMSO-*d*₆) δ 12.06 (br s, 2H), 9.71 (br s, 2H), 9.21 (br s, 2H), 8.70 (s, 2H), 8.30 (s, 2H), 7.50 (d, *J* = 7.9 Hz, 2H), 6.90 (d, *J* = 7.7 Hz, 2H), 6.70 (t, *J* = 7.7 Hz, 2H). ¹³C NMR (DMSO-*d*₆) δ 152.4, 146.0, 145.8, 145.7, 120.3, 119.2, 117.5, 117.2. HRMS: *m/z* (calcd for C₁₅H₁₅N₅O₄, 329.1124; found 330.1100).

2,2'-Bis[(2,4-dihydroxyphenyl)methylene]carbonimidic dihydrazide hydrochloride (45)

Synthesized according to General Method B from 2,4-dihydroxybenzaldehyde to afford the title compound as a pale yellow solid (73%).

M.P. 234°C (Decomp.). ¹H NMR (DMSO-*d*₆) δ 11.81 (br s, 2H), 10.32 – 9.85 (m, 4H), 8.52 (s, 2H), 8.12 (s, 2H), 7.85 (d, *J* = 8.4 Hz, 2H), 6.43 (s, 2H), 6.33 (d, *J* = 8.5 Hz, 2H). ¹³C NMR (DMSO-*d*₆) δ 161.4, 158.5, 152.0, 145.7, 128.4, 111.2, 108.0, 102.4. HRMS: *m/z* (calcd for C₁₅H₁₅N₅O₄, 329.1124; found 330.1116).

2,2'-Bis[(3,4-dihydroxyphenyl)methylene]carbonimidic dihydrazide hydrochloride (46)

Synthesized according to General Method A from 3,4-dihydroxybenzaldehyde to afford the title compound as a pale yellow solid (21%).

M.P. 250°C (Decomp.). ¹H NMR (DMSO-*d*₆) δ 11.80 (br s, 2H), 10.30 – 9.80 (m, 4H), 8.52 (s, 2H), 8.12 (s, 2H), 7.84 (d, *J* = 8.6 Hz, 2H), 6.42 (d, *J* = 1.8 Hz, 2H), 6.33 (d, *J* = 8.6 Hz, 2H). ¹³C NMR (DMSO-*d*₆) δ 161.4, 158.5, 152.0, 145.7, 128.4, 111.2, 108.0, 102.4. HRMS: *m/z* (calcd for C₁₅H₁₅N₅O₄, 329.1124; found 330.1133).

2,2'-Bis[(3-hydroxy-4-methoxyphenyl)methylene]carbonimidic dihydrazide hydrochloride (47)

Synthesized according to General Method B from 3-hydroxy-4-methoxybenzaldehyde to afford the title compound as a yellow solid (61%).

M.P. 158-161°C. ¹H NMR (DMSO-*d*₆) δ 9.21 (br s, 2H), 8.42 – 8.17 (m, 4H), 7.43 (d, *J* = 1.9 Hz, 2H), 7.25 (dd, *J* = 8.4, 1.9 Hz, 2H), 6.99 (d, *J* = 8.4 Hz, 2H), 3.83 (s, 6H). ¹³C NMR (DMSO-*d*₆) δ 152.5, 150.3, 148.9, 146.7, 126.2, 120.9, 113.8, 111.7, 55.7. HRMS: *m/z* (calcd for C₁₇H₁₉N₅O₄, 357.1437; found 358.1371).

2,2'-Bis[(4-hydroxy-3-methoxyphenyl)methylene]carbonimidic dihydrazide hydrochloride (**48**)

Synthesized according to General Method B from 4-hydroxy-3-methoxybenzaldehyde to afford the title compound as a yellow solid (69%).

M.P. 200-203°C. ¹H NMR (DMSO-*d*₆) δ 9.77 (br s, 2H), 8.36 (s, 2H), 8.29 (s, 2H), 7.58 (d, *J* = 1.5 Hz, 2H), 7.23 (dd, *J* = 8.1, 1.2 Hz, 2H), 6.87 (d, *J* = 8.1 Hz, 2H), 3.86 (s, 6H). ¹³C NMR (DMSO-*d*₆) δ 152.4, 149.7, 149.0, 148.1, 124.7, 122.9, 115.4, 110.4, 55.9. HRMS: *m/z* (calcd for C₁₇H₁₉N₅O₄, 357.1437; found 358.1447).

2,2'-Bis[(3,4-dimethoxyphenyl)methylene]carbonimidic dihydrazide hydrochloride (**49**)

Synthesized according to General Method B from 3,4-dimethoxybenzaldehyde to afford the title compound as a pale yellow solid (100%).

M.P. 218-220°C. ¹H NMR (DMSO-*d*₆) δ 12.09 (br s, 2H), 8.44 (s, 2H), 8.34 (s, 2H), 7.63 (d, *J* = 1.4 Hz, 2H), 7.33 (dd, *J* = 8.3, 1.6 Hz, 2H), 7.03 (d, *J* = 8.4 Hz, 2H), 3.86 (s, 6H), 3.81 (s, 6H). ¹³C NMR (DMSO-*d*₆) δ 152.5, 151.4, 149.2, 148.9, 126.0, 122.9, 111.4, 109.5, 55.9, 55.7. HRMS: *m/z* (calcd for C₁₉H₂₃N₅O₄, 385.1750; found 386.1739).

2,2'-Bis[(2,3,4-trihydroxyphenyl)methylene]carbonimidic dihydrazide hydrochloride (**50**)

Synthesized according to General Method B from 2,3,4-trihydroxybenzaldehyde to afford the title compound as a white solid (84%).

M.P. 225°C (Decomp.). ¹H NMR (DMSO-*d*₆) δ 11.75 (br s, 2H), 9.71 (br s, 2H), 9.15 (br s, 2H), 8.86 – 8.40 (m, 4H), 8.13 (s, 2H), 7.33 (d, *J* = 8.6 Hz, 2H), 6.42 (d, *J* = 8.6 Hz, 2H). ¹³C NMR (DMSO-*d*₆) δ 151.9, 149.1, 147.0, 146.8, 132.9, 118.1, 112.1, 108.1. HRMS: *m/z* (calcd for C₁₅H₁₅N₅O₆, 361.1022; found 362.0995).

2,2'-Bis[(2,4,5-trihydroxyphenyl)methylene]carbonimidic dihydrazide hydrochloride (**51**)

Synthesized according to General Method B from 2,3,5-trihydroxybenzaldehyde to afford the title compound as an orange solid (82%).

M.P. 260°C (Decomp.). ¹H NMR (DMSO-*d*₆) δ 11.72 (br s, 2H), 9.78 (br s, 2H), 9.45 (s, 2H), 8.48 (s, 2H), 8.34 (br s, 2H), 8.04 (s, 2H), 7.33 (s, 2H), 6.44 (s, 2H). ¹³C NMR (DMSO-*d*₆) δ 152.0, 151.4, 150.2, 146.1, 138.9, 112.9, 110.2, 103.4. HRMS: *m/z* (calcd for C₁₅H₁₅N₅O₆, 361.1022; found 362.1043).

2,2'-Bis[(3,4,5-trihydroxyphenyl)methylene]carbonimidic dihydrazide hydrochloride (52)

Synthesized according to General Method B from 3,4,5-trihydroxybenzaldehyde to afford the title compound as a pale brown solid (77%).

M.P. 226°C (Decomp.). ¹H NMR (DMSO-*d*₆) δ 9.06 (br s, 6H), 8.25 – 8.01 (m, 4H), 6.83 (s, 4H). ¹³C NMR (DMSO-*d*₆) δ 152.2, 149.7, 146.2, 136.5, 123.7, 107.4. HRMS: *m/z* (calcd for C₁₅H₁₅N₅O₆, 361.1022; found 362.1044).

2,2'-Bis[(4,5-dihydroxy-3-methoxyphenyl)methylene]carbonimidic dihydrazide hydrochloride (53)

Synthesized according to General Method B from 4,5-dihydroxy-3-methoxybenzaldehyde to afford the title compound as a pale brown solid (88%).

M.P. 144°C (Decomp.). ¹H NMR (DMSO-*d*₆) δ 9.12 (br s, 4H), 8.29 (s, 2H), 8.20 (s, 2H), 7.10 (s, 2H), 6.93 (s, 2H), 3.84 (s, 6H). ¹³C NMR (DMSO-*d*₆) δ 152.4, 149.5, 148.8, 145.8, 137.5, 123.7, 110.1, 103.1, 56.3. HRMS: *m/z* (calcd for C₁₇H₁₉N₅O₆, 389.1335; found 390.1275).

2,2'-Bis[(4-hydroxy-3-nitrophenyl)methylene]carbonimidic dihydrazide hydrochloride (54)

Synthesized according to General Method B from 4-hydroxy-3-nitrobenzaldehyde to afford the title compound as a white solid (80%).

M.P. 269°C (Decomp.). ¹H NMR (DMSO-*d*₆) δ 8.56 (s, 2H), 8.42 (d, *J* = 2.0 Hz, 2H), 8.38 (s, 2H), 8.09 (dd, *J* = 8.7, 2.0 Hz, 2H), 7.29 (d, *J* = 8.7 Hz, 2H). ¹³C NMR (DMSO-*d*₆) δ 153.6, 152.8, 146.9, 137.6, 133.7, 124.7, 124.4, 119.3. HRMS: *m/z* (calcd for C₁₅H₁₃N₇O₆, 388.0917; found 387.0927).

2,2'-Bis[(2,3,4,5,6-pentafluorophenyl)methylene]carbonimidic dihydrazide hydrochloride (55)

Synthesized according to General Method B from 2,3,4,5,6-pentafluorobenzaldehyde to afford the title compound as a white solid (60%).

M.P. 234-236°C. ¹H NMR (DMSO-*d*₆) δ 8.64 (s, 2H), 8.36 (s, 2H). ¹³C NMR (DMSO-*d*₆) δ 152.8, 146.0 (m), 143.4 (m), 142.7 (m), 140.1 (m), 138.6 (m), 138.1, 136.1 (m), 108.9 (td, J = 12.6, 3.8 Hz). HRMS: *m/z* (calcd for C₁₅H₅F₁₀N₅, 445.0358; found 446.0306).

2,2'-Bis[(2-bromo-4,5-dimethoxyphenyl)methylene]carbonimidic dihydrazide hydrochloride (**56**)

Synthesized according to General Method B from 2-bromo-4,5-dimethoxybenzaldehyde to afford the title compound as a white solid (80%).

M.P. 233-235°C. ¹H NMR (DMSO-*d*₆) δ 12.24 (br s, 2H), 8.66 (s, 2H), 8.49 (br s, 2H), 7.79 (s, 2H), 7.24 (s, 2H), 3.88 (s, 6H), 3.85 (s, 6H). ¹³C NMR (DMSO-*d*₆) δ 152.4, 152.0, 148.7, 147.7, 124.0, 116.1, 115.5, 110.1, 56.3, 56.2. HRMS: *m/z* (calcd for C₁₉H₂₁Br₂N₅O₄, 542.9940; found 543.9882).

2,2'-Bis[(3-bromo-4,5-dimethoxyphenyl)methylene]carbonimidic dihydrazide hydrochloride (**57**)

Synthesized according to General Method B from 3-bromo-4,5-dimethoxybenzaldehyde to afford the title compound as a white solid (45%).

M.P. 223-224°C. ¹H NMR (DMSO-*d*₆) δ 8.66 (s, 2H), 8.37 (s, 2H), 7.79 (d, *J* = 1.6 Hz, 2H), 7.68 – 7.62 (m, 2H), 3.92 (s, 6H), 3.78 (s, 6H). ¹³C NMR (DMSO-*d*₆) δ 153.6, 152.8, 147.5, 147.2, 130.7, 123.8, 117.1, 111.8, 60.3, 56.5. HRMS: *m/z* (calcd for C₁₉H₂₁Br₂N₅O₄, 542.9940; found 543.9850).

2,2'-Bis(cyclohexylmethylene)carbonimidic dihydrazide (**58**)

Synthesized according to General Method B from cyclohexane carboxaldehyde to afford the title compound as an orange oil (36%).

¹H NMR (CDCl₃) δ 7.16 (d, *J* = 4.7 Hz, 2H), 6.10 (br. s, 3H), 2.27 – 2.14 (m, 2H), 1.84 – 1.61 (m, 10H), 1.37 – 1.13 (m, 10H). ¹³C NMR (CDCl₃) δ 157.2, 152.7 (br. s), 40.9, 30.6, 26.1, 25.7. HRMS: *m/z* (calcd for C₁₅H₂₇N₅, 277.2266; found 277.2169).

2,2'-Bis(4-pyridinylmethylene)Carbonimidic dihydrazide hydrochloride (**59**)

Synthesized according to General Method B from 4-pyridinecarboxaldehyde to afford the title compound as a yellow solid (74%).

M.P. 231–234°C. ¹H NMR (DMSO-*d*₆) δ 8.75 (d, *J* = 6.1 Hz, 4H), 8.68 (s, 2H), 8.47 (s, 2H), 8.07 (d, *J* = 6.1 Hz, 4H). ¹³C NMR (DMSO-*d*₆) δ 154.4, 148.0, 145.3, 143.0, 122.1. LRMS: *m/z* (calcd for C₁₃H₁₃N₇, 267.12; found 267.90).

2,2'-Bis(4-chloropyridin-3-ylmethylene)Carbonimidic dihydrazide hydrochloride (60)

Synthesized according to General Method B from 4-chloro-3-pyridine carboxaldehyde to afford the title compound as a yellow solid (84%).

M.P. 269–272°C. ¹H NMR (DMSO-*d*₆) δ 12.63 (br. s, 2H), 8.90 (d, *J* = 2.1 Hz, 2H), 8.74 (s, 2H), 8.56 – 8.42 (m, 4H), 7.66 (d, *J* = 8.4 Hz, 2H). ¹³C NMR (DMSO-*d*₆) δ 153.0, 151.7, 149.6, 145.0, 137.8, 128.9, 124.5. LRMS: *m/z* (calcd for C₁₃H₁₁Cl₂N₇, 335.05; found 335.60).

2,2'-Bis(2-aminopyridin-3-ylmethylene)Carbonimidic dihydrazide hydrochloride (61)

Synthesized according to General Method B from 2-amino-3-pyridine carboxaldehyde to afford the title compound as a yellow solid (49%).

M.P. 227–229°C. ¹H NMR (DMSO-*d*₆) δ 11.94 (br. s, 2H), 8.44 (s, 2H), 8.36 (s, 2H), 8.07 (dd, *J* = 4.8, 1.7 Hz, 2H), 7.72 (dd, *J* = 7.6, 1.4 Hz, 2H), 7.19 (s, 4H), 6.67 (dd, *J* = 7.5, 4.9 Hz, 2H). ¹³C NMR (DMSO-*d*₆) δ 156.1, 152.2, 150.4, 149.5, 141.2, 112.0, 110.1. LRMS: *m/z* (calcd for C₁₃H₁₅N₉, 297.15; found 297.70).

2,2'-Bis(3-phenyl-2-propenylidene)carbonimidic dihydrazide hydrochloride (62)

Synthesized according to General Method B from trans-cinnamaldehyde to afford the title compound as a yellow solid (63%).

M.P. 176–178°C. ¹H NMR (DMSO) δ 12.38 (s, 1H), 8.25 (d, *J* = 10.2 Hz, 2H), 7.59 (d, *J* = 7.3 Hz, 2H), 7.39 (m, 3H), 7.20 (d, *J* = 16.1 Hz, 1H), 6.94 (dd, *J* = 16.1, 9.3 Hz, 1H). ¹³C NMR (DMSO-*d*₆) δ 152.3, 150.8, 141.0, 135.5, 129.4, 129.0, 127.2, 124.1. HRMS: *m/z* (calcd for C₁₉H₁₉N₅, 317.1640; found 318.1629).

2,2'-Bis[3-(4-methoxyphenyl)-2-propenylidene]carbonimidic dihydrazide hydrochloride (63)

Synthesized according to General Method B from 4-methoxycinnamaldehyde to afford the title compound as a yellow solid (51%).

M.P. 204–206°C. ¹H NMR (DMSO-*d*₆) δ 12.10 (br s, 2H), 8.23 – 8.07 (m, 4H), 7.55 (d, *J* = 8.7 Hz, 4H), 7.13 (d, *J* = 16.0 Hz, 2H), 6.99 (d, *J* = 8.7 Hz, 4H), 6.81 (dd, *J* = 16.0, 9.4 Hz, 2H), 3.79 (s, 6H). ¹³C NMR (DMSO-*d*₆) δ 160.3, 152.1, 151.2, 140.8, 128.8, 128.2, 121.7, 114.5, 55.3. LRMS: *m/z* (calcd for C₂₁H₂₃N₅O₂, 377.19; found 377.80).

2,2'-Bis(2,3-diphenyl-2-propenylidene)carbonimidic dihydrazide hydrochloride (64)

Synthesized according to General Method A from 2,3-diphenylacrolein to afford the title compound as a yellow solid (46%).

M.P. 137-140°C. ¹H NMR (DMSO-*d*₆) δ 12.12 (br s, 2H), 8.21 (s, 2H), 7.97 (s, 2H), 7.54 – 7.47 (m, 6H), 7.42 – 7.36 (m, 6H), 7.31 – 7.21 (m, 8H), 6.84 (d, *J* = 9.8 Hz, 2H). ¹³C NMR (DMSO-*d*₆) δ 152.0, 150.4, 148.5*, 140.2, 137.6, 130.0, 129.0, 128.7, 128.7, 128.5, 127.4, 123.0. *Confirmed via HSQC analysis. LRMS: *m/z* (calcd for C₃₁H₂₇N₅, 469.23; found 469.85).

2,2'-Bis(2-naphthalenylmethylene)carbonimidic dihydrazide hydrochloride (65)

Synthesized according to General Method A from 2-naphthaldehyde to afford the title compound as a white solid (79%).

M.P. 183-185°C. ¹H NMR (DMSO-*d*₆) δ 8.64 (s, 4H), 8.35 – 8.24 (m, 4H), 8.06 – 7.93 (m, 6H), 7.64 – 7.54 (m, 4H). ¹³C NMR (DMSO-*d*₆) δ 152.9, 148.9, 134.1, 132.8, 131.2, 129.9, 128.5, 128.4, 127.9, 127.6, 126.9, 123.3. HRMS: *m/z* (calcd for C₂₃H₁₉N₅, 365.1640; found 366.1740).

2,2'-Bis(1H-indol-5-ylmethylene)carbonimidic dihydrazide hydrochloride (66)

Synthesized according to General Method B from indole-5-carboxaldehyde to afford the title compound as a pink-brown solid (64%).

M.P. 269°C (Decomp.). ¹H NMR (DMSO-*d*₆) δ 11.97 (br s, 2H), 11.45 (s, 2H), 8.47 (s, 2H), 8.30 (s, 2H), 8.02 (s, 2H), 7.80 (dd, *J* = 8.6, 0.9 Hz, 2H), 7.48 (d, *J* = 8.5 Hz, 2H), 7.45 – 7.40 (m, 2H), 6.53 (s, 2H). ¹³C NMR (DMSO-*d*₆) δ 152.4, 150.6, 137.4, 127.6, 126.7, 124.5, 121.8, 120.3, 111.9, 102.0. LRMS: *m/z* (calcd for C₁₉H₁₇N₇, 343.15; found 343.80).

*2,2'-Bis[(5-chlorobenzo[*b*]thien-3-yl)methylene]carbonimidic dihydrazide hydrochloride (67)*

Synthesized according to General Method B from 5-chloro-1-benzothiophene-3-carbaldehyde to afford the title compound as a pale yellow solid (90%).

M.P. 285-287°C. ¹H NMR (DMSO-*d*₆) δ 8.66 (s, 2H), 8.60 (d, *J* = 1.9 Hz, 2H), 8.52 (br s, 2H), 8.49 (s, 2H), 8.09 (d, *J* = 8.6 Hz, 2H), 7.50 (dd, *J* = 8.6, 2.0 Hz, 2H). ¹³C NMR (DMSO-*d*₆) δ 152.9, 145.4, 138.9, 136.9, 136.5, 131.1, 129.5, 126.0, 125.0, 124.2. LRMS: *m/z* (calcd for C₁₉H₁₃Cl₂N₅S₂, 445.00; found 445.75).

2,2'-Bis[1-phenylethylidene]carbonimidic dihydrazide hydrochloride (68)

Synthesized according to General Method B from acetophenone to afford the title compound as a white solid (60%).

M.P. 253-254°C. ¹H NMR (DMSO-*d*₆) δ 11.91 (br s, 2H), 8.66 (br s, 2H), 8.10 – 8.00 (m, 4H), 7.51 – 7.41 (m, 6H), 2.45 (s, 6H). ¹³C NMR (DMSO-*d*₆) δ 154.2, 153.3, 136.7, 129.9, 128.3, 127.0, 15.0. LRMS: *m/z* (calcd for C₁₇H₁₉N₅, 293.16; found 294.00).

2,2'-Bis[1-(4-chlorophenyl)ethylidene]carbonimidic dihydrazide hydrochloride (69)

Synthesized according to General Method A from 4-chlorobenzaldehyde to afford the title compound.

¹H NMR (DMSO-*d*₆) δ 11.68 (br. s, 2H), 8.78 (br. s, 1H), 8.10 (d, *J* = 8.6 Hz, 4H), 7.52 (d, *J* = 8.6 Hz, 4H), 2.43 (s, 6H).

2,2'-Bis[1-(4-bromophenyl)ethylidene]carbonimidic dihydrazide hydrochloride (70)

Synthesized according to General Method B from 4-bromobenzaldehyde to afford the title compound as a white solid (94%).

M.P. 299°C (Decomp.). ¹H NMR (DMSO-*d*₆) δ 11.63 (s, 2H), 8.76 (s, 2H), 8.01 (d, *J* = 8.6 Hz, 4H), 7.65 (d, *J* = 8.6 Hz, 4H), 2.41 (s, 6H). ¹³C NMR (DMSO-*d*₆) δ 154.1, 152.4, 135.9, 131.3, 129.1, 123.6, 14.7. LRMS: *m/z* (calcd for C₁₇H₁₇Br₂N₅, 450.98; found 449.70).

2,2'-Bis[1-[4-(trifluoromethyl)phenyl]ethylidene]carbonimidic dihydrazide hydrochloride (71)

Synthesized according to General Method A from 4-trifluoromethylbenzaldehyde to afford the title compound.

¹H NMR (DMSO-*d*₆) δ 11.71 (br. s, 2H), 8.91 (br. s, 1H), 8.28 (d, *J* = 7.8 Hz, 4H), 7.82 (d, *J* = 8.2 Hz, 4H), 2.49 (br. s, 6H).

2,2'-Bis[1-(4-chlorophenyl)propylidene]carbonimidic dihydrazide hydrochloride (72)

Synthesized according to General Method B from 4-chloropropiophenone to afford the title compound as a white solid (47%).

M.P. 246-247°C. ¹H NMR (DMSO-*d*₆) δ 11.68 (s, 2H), 8.78 (s, 2H), 8.09 (d, *J* = 8.4 Hz, 4H), 7.52 (d, *J* = 8.6 Hz, 4H), 2.92 (q, *J* = 7.5 Hz, 4H), 1.12 (t, *J* = 7.4 Hz, 6H). ¹³C NMR (DMSO-*d*₆) δ 156.6, 154.2, 134.7, 134.2, 128.9, 128.5, 20.4, 10.9. LRMS: *m/z* (calcd for C₁₉H₂₁Cl₂N₅, 389.12; found 389.90).

2,2'-Bis[1-(4-chlorophenyl)butylidene]carbonimidic dihydrazide hydrochloride (73)

Synthesized according to General Method B from 4-chlorobutyrophenone to afford the title compound as a white solid (26%).

M.P. 246-247°C. ¹H NMR (DMSO-*d*₆) δ 12.18 (s, 2H), 8.71 (s, 2H), 8.08 (d, *J* = 8.0 Hz, 4H), 7.50 (d, *J* = 8.3 Hz, 4H), 3.01 – 2.87 (m, 4H), 1.58 – 1.46 (m, 4H), 1.01 (t, *J* = 7.1 Hz, 6H). ¹³C NMR (DMSO-*d*₆) δ 155.5, 154.2, 134.6, 128.9, 128.4, 28.7, 19.5, 13.6. LRMS: *m/z* (calcd for C₂₁H₂₅Cl₂N₅, 417.15; found 417.80).

2,2'-Bis[1-(4-chlorophenyl)pentylidene]carbonimidic dihydrazide hydrochloride (74)

Synthesized according to General Method B from 1-(4-chlorophenyl)pentan-1-one to afford the title compound as a pale yellow solid (53%).

M.P. 140-142°C. ¹H NMR (DMSO-*d*₆) δ 12.09 (s, 2H), 8.69 (s, 2H), 8.07 (d, *J* = 8.6 Hz, 4H), 7.50 (d, *J* = 8.6 Hz, 4H), 3.01 – 2.88 (m, 4H), 1.49 – 1.39 (m, 8H), 0.88 (t, *J* = 6.6 Hz, 6H). ¹³C NMR (DMSO-*d*₆) δ 155.8, 154.4, 134.7, 129.0, 128.5, 28.3, 27.0, 22.0, 13.9. LRMS: *m/z* (calcd for C₂₃H₂₉Cl₂N₅, 445.18; found 445.80).

2,2'-Bis[1-(4-chlorophenyl)-2-hydroxyethylidene]carbonimidic dihydrazide (75)

Synthesized according to General Method A from 1-(4-chlorophenyl)-2-hydroxyethanone to afford the title compound as a yellow solid (6%).

¹H NMR (DMSO) δ 8.67 (s, 2H), 7.97 (s, 4H), 7.50 (d, *J* = 8.6 Hz, 4H), 4.81 (s, 4H). LRMS: *m/z* (calcd for C₁₇H₁₇Cl₂N₅O₂, 393.08; found 393.60).

2,2'-bis(1-phenyl-2-aminoethylidene)carbonimidic dihydrazide trihydrochloride (76)

Synthesized according to General Method B from 2-aminoacetophenone hydrochloride to afford the title compound as a white solid (8%).

M.P. 250°C (Decomp.). ¹H NMR (DMSO-*d*₆) δ 10.87 (br s, 1H), 9.52 (br s, 1H), 8.76 (br s, 3H), 7.61-7.44 (m, 8H), 7.39 (br s, 3H), 7.26 (br s, 3H), 4.06 (br s, 2H). ¹³C NMR (DMSO-*d*₆) δ 154.4, 150.8, 130.9, 130.2, 129.6, 127.6, 43.0. LRMS: *m/z* (calcd for C₁₇H₂₃N₇, 324.25; found 323.75).

2,2'-Bis(phenylcarboxymethylene)carbonimidic dihydrazide hydrochloride (77)

Synthesized according to General Method B from phenylglyoxylic acid to afford the title compound as an off-white crystalline solid (13%).

M.P. 306°C (Decomp.). ¹H NMR (DMSO-*d*₆) δ 14.09 (s, 1H), 8.12 (d, *J* = 6.9 Hz, 2H), 7.97 (dd, *J* = 6.4, 3.0 Hz, 2H), 7.56 (ddd, *J* = 8.2, 6.7, 2.9 Hz, 7H). ¹³C NMR (DMSO-*d*₆) δ

159.4, 151.3, 149.5, 143.0, 132.0, 131.9, 131.2, 130.2, 129.4, 128.4, 128.3, 128.2. LRMS: m/z (calcd for $C_{17}H_{15}N_5O_4$, 353.11; found 351.75).

N',2-Bis((E)-1-(p-tolyl)ethylidene)hydrazine-1-carboximidhydrazide hydrochloride (78)

Synthesized according to General Method A from 1-(*p*-tolyl)ethan-1-one to afford the title compound as an off-white crystalline solid (71%).

M.P. 288°C (Decomp.). 1H NMR (DMSO- d_6) δ 11.66 (s, 1H), 8.61 (s, 1H), 7.94 (d, J = 8.2 Hz, 2H), 7.25 (d, J = 8.1 Hz, 2H), 2.41 (s, 3H), 2.35 (s, 3H). ^{13}C NMR (DMSO- d_6) δ 154.0, 153.3, 139.7, 133.9, 129.0, 127.0, 20.9, 14.9.

*2,2'-Bis[1-[4-(*t*-butyl)phenyl]ethylidene]carbonimidic dihydrazide hydrochloride (79)*

Synthesized according to General Method A from 4'-(*t*-butyl)acetophenone to afford the title compound as a yellow crystalline solid.

M.P. 310°C (Decomp.). 1H NMR (DMSO- d_6) δ 11.74 (s, 1H), 8.60 (s, 1H), 7.95 (d, J = 8.6 Hz, 2H), 7.45 (d, J = 8.6 Hz, 2H), 2.42 (s, 3H), 1.31 (s, 9H). ^{13}C NMR (DMSO- d_6) δ 154.1, 153.3, 152.6, 134.0, 126.8, 125.0, 34.5, 30.9, 14.9.

2,2'-Bis[1-(4-piperazinylphenyl)ethylidene]carbonimidic dihydrazide hydrochloride (80)

Synthesized according to General Method A from 1-(4-(piperazin-1-yl)phenyl)ethan-1-one to afford the title compound as a mustard-yellow solid (1%).

1H NMR (400 MHz, DMSO- d_6) δ 7.73 (d, J = 8.8 Hz, 2H), 6.92 (d, J = 8.9 Hz, 2H), 3.22 – 3.13 (m, 4H), 2.99 – 2.86 (m, 4H), 2.24 (s, 3H). ^{13}C NMR (101 MHz, DMSO- d_6) δ 156.9, 151.1, 147.7, 129.5, 126.8, 114.7, 47.9, 44.8, 13.3.

Appendix 2: Analysis of Appropriate Broth for Bacterial Assays with Robenidine Analogues

Materials and methods:

Chemicals and bacterial strains are sourced as sited in chapter 2.

Optimisation of future susceptibility testing for robenidine analogues

MIC assays were originally performed following strict CLSI guidelines, however results were not reproducible and growth was seen above the MIC (Figure A2.1) therefore several modifications to the assays were tested to identify the optimum conditions required for repeatability and reproducibility of the antibacterial activity of the robenidine analogues. Antimicrobials and bacterial suspensions were prepared according to CLSI guidelines.

Optimisation in broth

Either CAMH broth or LB broth was used (BD Scientific). Due to the insoluble nature of the robenidine analogues, they were diluted at 100 X higher than the final required concentration and 2 µl added to appropriate wells of the assay plate. Broth was added to a final volume of 180 µl and 20 µl of bacterial suspension diluted to give a final concentration of $\sim 5 \times 10^5$ cells/ml. The assay was incubated for 20-24 hrs at 37°C before interpretation of the results.

Optimisation in agar

Either CAMH agar or LB agar (0.7% agar) was prepared and kept warm. The drugs were prepared as for optimisation of broth assays and 2 µl spotted into appropriate wells. The bacterial suspension was prepared according to CLSI guidelines and diluted in agar to yield a final concentration of $\sim 5 \times 10^5$ cells/ml. While still warm 198 µl of agar containing bacteria was added to each well and allowed to set. Assays were incubated at 37°C for 20-24 hours before interpretation of results.

Results:

During routine assays with the parent analogue, robenidine, several inconsistencies were noticed including consistent growth above the concentration identified as the MIC and failure of the assay to identify an MIC for robenidine on multiple occasions. To identify the problem with the assay an analysis involving several different batches of the compound and different assay broths was performed. Due to the insoluble nature of the compound, all assays involved serial dilution of the compounds in DMSO before addition of the required amount directly to the assay and dilution in the growth media. Seven separate batches were tested consisting of 3

commercial and 4 synthesised by the chemists at Newcastle University. Four of the seven batches had been stored at 4°C while the rest were stored at room temperature. There was no significant difference found in the results between different batches of robenidine under the conditions tested (data not shown). Both CAMH broth and agar (CLSI recommended media) and LB broth and agar were tested for reproducibility of results and clarity of the MIC with robenidine. LB broth, agar and CAMH agar all gave reproducible results, between 1-8 µg/ml, with no growth observed above the MIC. CAMH broth, as observed in the past, resulted in inconsistent, if any reportable MIC with values ranging from 0.25 - >128 µg/ml (Figure A2.1). This phenomenon was even observed within the duplicates of a single assay. Optical density of the bacterial growth at different concentrations of robenidine in various assay conditions demonstrates the high error observed in CAMH broth compared to the agar methods and LB broth. This assay was performed in duplicate by three independent researchers and despite the large variance in inoculum (between 1.5 and 5.9 CFU/ml) the results did not appear to be dependent on inoculum density.

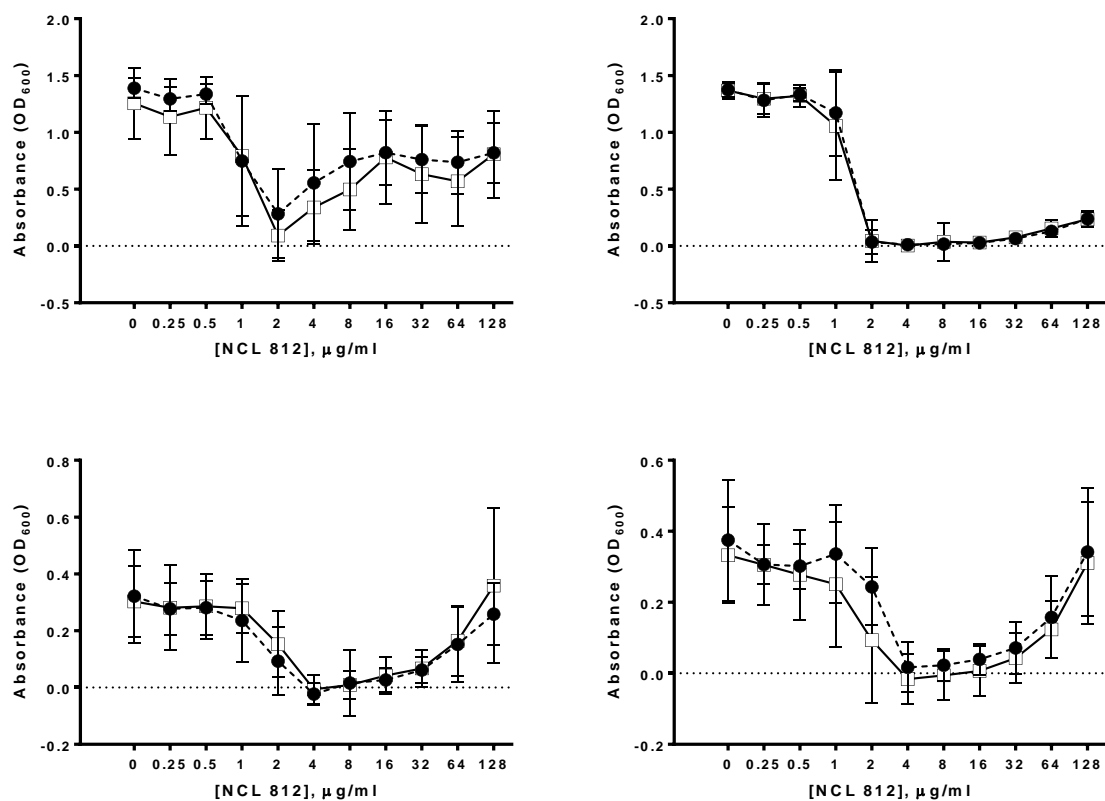


Figure A2.1 Optimisation of the minimum inhibitory concentration assay for the testing of robenidine and associated analogues. Robenidine (812) was tested in various cation adjusted Mueller Hinton broth and agar and Luria Bertaini broth and agar to identify the most reproducible assay system. Robenidine was serially diluted in DMSO and added directly to the test. The increase in absorbance in the agar assays is due to the turbidity of the robenidine compound in the agar. Clockwise from top left: cation adjusted Mueller Hinton broth, Luria Bertanini broth, cation adjusted Mueller Hinton agar and Luria Bertanini agar. Key: black circles – *S. aureus* ATCC 29213, white squares – *S. aureus* ATCC 6538, broken line – detection limit. Error \pm SD.

Appendix 3: Development of Spheroplasts and Regeneration Efficiency Experiments.

Materials and methods:

Bacterial strains and chemicals were sourced as outlined in chapter 3

Ampicillin induced spheroplasts

An overnight broth culture was diluted to approximately 1×10^9 cells/ml in CAMH broth supplemented with 50 $\mu\text{g/ml}$ ampicillin, 0.4 M sucrose and 8 mM MgSO_4 . The culture was incubated for ~ 2 hrs, until the majority of cells had become spherical, as observed under phase contrast microscope.

Lysozyme induced spheroplasts

A 1:100 dilution of an overnight broth culture was performed in CAMH broth. The inoculated broth was grown until an OD_{600} of 0.4 was reached. The bacteria were harvested via centrifugation (4000 rpm, 3 min), washed with an equal volume of Tris(HCl) pH 8 and suspended to a final concentration of $\sim 5 \times 10^8$ cells/ml in Tris buffer (pH8) supplemented with 0.5 M sucrose. Lysozyme was added to a final concentration of 20, 60, 100 or 500 $\mu\text{g/ml}$, for Gram-negative and Gram-positive organisms respectively, while continually stirring. For Gram-negative organisms the culture was incubated at room temperature for a maximum of 10 minutes before the addition of EDTA to a final concentration of 10 mM. Gram-positive organisms were incubated with lysozyme for upto 3 hrs, no EDTA was added. Spheroplast formation was determined by osmotic sensitivity and microscopy.

Lysozyme and ampicillin induced spheroplasts

A 1:4 dilution of overnight culture was prepared in CAMH broth supplemented with 0.4 M sucrose and 50 $\mu\text{g/ml}$ ampicillin. The culture was incubated at 37°C for 1 hr before the addition of 100 $\mu\text{g/ml}$ lysozyme. Changes in morphology were observed under the microscope using trypan blue dye.

Ampicillin and penicillin induced spheroplasts

Cultures were diluted as above in CAMH broth supplemented with 0.4 M sucrose, 8 mM MgSO_4 and 1 mg/ml penicillin, 1 mg/ml ampicillin or both ampicillin and penicillin (1 mg/ml). Cultures were incubated for 24 hours with samples taken periodically to assess morphology and the development of spheroplasts using phase contrast microscopy or trypan blue staining.

Identification of the optimum regeneration media of E. coli spheroplasts

E. coli spheroplasts were induced using the ampicillin method described above. Briefly, two colonies of an overnight culture of the required bacterial strain (*E. coli* ATCC 25922) were used to inoculate ~20 ml of CAMH broth which was further incubated for 18 hours at 37°C. A 1:3 dilution of the overnight culture into fresh CAMH broth (total 20 ml volume) supplemented with 50 mg/ml ampicillin, 0.4 M Sucrose and 8 mM MgSO₄ was performed and this culture was monitored for the formation of spheroplasts using a phase contrast microscope. The number of cells before induction of spheroplasts, after induction of spheroplasts and after exposure of spheroplasts to water was determined on the following agar combinations: brain heart infusion soft agar with sucrose (agar 0.8%, sucrose 0.4 M), brain heart infusion agar with sucrose (agar 1.5%, sucrose 0.4M), brain heart infusion agar (agar 1.5%), sheep blood agar, plate count agar with sucrose (sucrose 0.4 M) or plate count agar. Samples were incubated overnight at 37°C before calculation of spheroplast formation frequency and spheroplast regeneration frequency.

Results:

Several spheroplast induction procedures were performed to identify the most reliable method for the development of spheroplasts. Numerous different species of bacteria were also investigated in the hope that the compounds could be tested against a range of target organisms.

Four methods of spheroplast induction were tested involving ampicillin, penicillin and lysozyme. The lysozyme method was found to be the most impractical with the ability to induce spheroplasts in *E.coli* but these died rapidly. The ampicillin method resulted in the consistent induction of spheroplasts in *E. coli*, the organism with highest priority for this assay as it is considered a representative organism for Gram-negative bacteria. These spheroplasts were induced after 2 hours and were viable for at least 7 days in media supplemented with 0.4 M sucrose, 8 mM MgSO₄ and 50 µg/ml ampicillin (Table A3.1). The development of *S. aureus* spheroplasts was much harder to determine, due to the native spherical shape of the organism, but could be identified by an increase in size, loss of a purple gram-stain and extreme sensitivity to osmotic changes. Based on these 3 identifying features of Gram-positive spheroplasts, ampicillin at 50 µg/ml was able to induce a spheroplast state in *S. aureus*. Of the other organisms tested, spheroplast induction could only be observed in *Lactobacillus reuterii* and *Bacillus coagulans* on one occasion, however this was not repeatable and the number of spheroplasts formed in the cultures was very small. A combination of ampicillin and lysozyme to induce spheroplasts was attempted in *S. aureus*, *Lactobacillus acidophilus*, *L. reuterii* and

B. coagulans and was unsuccessful in all situations. Similarly, an attempt to induce spheroplasts in *L. acidophilus*, *L. reuterii* and *B. coagulans* with a combination of penicillin and ampicillin failed.

The optimum regeneration media for *E. coli* spheroplasts was found to be brain heart infusion agar, followed by sheep blood agar. Plate count agar with sucrose was the least effective for regeneration of spheroplasts (Table A3.2). The temperature at which spheroplasts were incubated did not appear to have an effect on the lifetime of the cells (Figure A3.1).

Table A3.1 The induction of spheroplast transformation in various species of bacteria. *Four treatments were tested to induce spheroplast formation in both Gram-positive and Gram-negative bacteria. “-“ = not tested*

Bacterial Species	Treatment Used to Induce Spheroplast Transformation			
	Ampicillin	Lysozyme	Ampicillin-lysozyme	Ampicillin-penicillin
<i>E. coli</i> ATCC 25922	Yes viable for ≥ 7 days	Yes but died rapidly	-	-
<i>S. aureus</i> ATCC 25923	Yes	Possibly – cells died rapidly	No	-
<i>Bacillus cereus</i>	No	-	-	-
<i>Bacillus subtilis</i>	No	-	-	-
<i>Lactobacillus acidophilus</i>	No	-	No	No
<i>Lactobacillus reuterii</i>	Small number but not repeatable	-	No	No
<i>Bacillus coagulans</i>	Yes – after 3 days – not repeatable	-	No	No

Table A3.2 The regeneration of *E. coli* spheroplasts on various solid media. Agar of various constitutions and concentrations were used to identify the optimum media for the regeneration of *E. coli* spheroplasts. Cultures of *E. coli* were exposed to sub-lethal concentrations of ampicillin to induce the formation of spheroplasts before overnight incubation on agar. The CFU/ml before spheroplast generation and after water treatment (a sample of spheroplasts were diluted 1:10, to destroy any spheroplasts, in water before overnight incubation at 37°C) were determined on plate count agar. Error \pm SD. Soft agar had an agar concentration of 0.8%. Sucrose was added at a concentration of 0.4 M.

Agar composition	Number of cells before spheroplast generation (CFU/ml) (Z)	Number of cells after spheroplast generation (CFU/ml) (X)	Number of cells after exposure to water (CFU/ml) (Y)	Number of spheroplasts (CFU/ml) (X – Y)	Spheroplast formation frequency (X – Y/X)%	Regeneration frequency ((X – Y)/Z)%
Soft Brain heart infusion agar with sucrose	3.03 x10 ⁷	3.03 x 10 ⁶	1.00 x 10 ⁴	3.02 x 10 ⁶	99.67	9.97
Brain heart infusion agar with sucrose	3.03 x10 ⁷	1.13 x 10 ⁷	1.00 x 10 ⁴	1.13 x 10 ⁷	99.91	37.11
Brain heart infusion agar	3.03 x10 ⁷	2.17 x 10 ⁷	1.00 x 10 ⁴	2.16 x 10 ⁷	99.95	71.34
Sheep blood agar	3.03 x10 ⁷	1.94 x 10 ⁷	1.00 x 10 ⁴	1.94 x 10 ⁷	99.95	63.87
Plate count agar with sucrose	3.03 x10 ⁷	6.67 x 10 ⁵	1.00 x 10 ⁴	6.57 x 10 ⁵	98.50	2.16
Plate count agar	3.03 x10 ⁷	4.00 x 10 ⁵	1.00 x 10 ⁴	3.90 x 10 ⁵	97.50	1.29

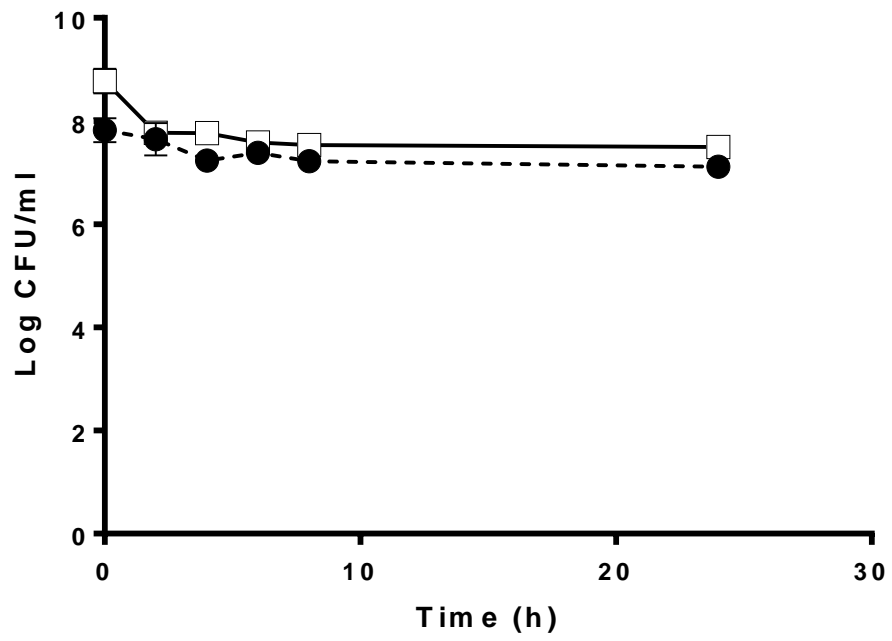


Figure A3.1 Ideal temperature to incubate *E. coli* spheroplasts. Spheroplasts were induced using sub-lethal concentrations of ampicillin and incubated at 27°C (squares) or 37°C (circles) for 24 hours. The experiment was repeated in triplicate and error is \pm SD.

References

- Abdel-Moein, K.A., Saeed, H., 2016. The zoonotic potential of *Giardia intestinalis* assemblage E in rural settings. *Parasitol Res* 115, 3197-3202.
- Abraham, R.J., Stevens, A.J., Young, K.A., Russell, C., Qvist, A., Khazandi, M., Wong, H.S., Abraham, S., Ogunniyi, A.D., Page, S.W., O'Handley, R., McCluskey, A., Trott, D.J., 2016. Robenidine analogues as Gram-Positive antibacterial agents. *J Med Chem* 59, 2126-2138.
- Adamsson, I., Nord, C.E., Lundquist, P., Sjöstedt, S., Edlund, C., 1999. Comparative effects of omeprazole, amoxicillin plus metronidazole versus omeprazole, clarithromycin plus metronidazole on the oral, gastric and intestinal microflora in *Helicobacter pylori*-infected patients. *J Antimicrob Chemoth* 44, 629-640.
- Aldred, Katie J., Robert J. Kerns, and Neil Osheroff. Mechanism of auinolone action and resistance. *Biochemistry* 53.10 (2014): 1565–1574.
- Allen, N.E., Nicas, T.I., 2003. Mechanism of action of oritavancin and related glycopeptide antibiotics. *FEMS Microbiol Rev* 26, 511-532.
- Ansell, B.R., McConville, M.J., Baker, L., Korhonen, P.K., Emery, S.J., Svärd, S.G., Gasser, R.B., Jex, A.R., 2016. Divergent transcriptional responses to physiological and xenobiotic stress in *Giardia duodenalis*. *Antimicrob Agents Chemother* 60, 6034-6045.
- Antonov, N.K., Garzon, M.C., Morel, K.D., Whittier, S., Planet, P.J., Lauren, C.T., 2015. High prevalence of mupirocin resistance in *Staphylococcus aureus* isolates from a pediatric population. *Antimicrob Agents Chemother* 59, 3350-3356.
- Aprile, S., Del Grosso, E., Grosa, G., 2011. In vitro metabolism study of 2-isopropyl-9H-thioxanthen-9-one (2-ITX) in rat and human: evidence for the formation of an epoxide metabolite. *Xenobiotica; the fate of foreign compounds in biological systems* 41, 212-225.
- Aquilina, G., Bories, G., Chesson, A., Cocconcelli, P.S., Knecht, J., Dierick, N.A., Gralak, M.A., Gropp, J., Halle, I., Kroker, R., Leng, L., Haldorsen, A.L., Mantovani, A., Mezes, M., Renshaw, D., Saarela, M., 2011. Scientific Opinion on safety and efficacy of Cycostat® 66G (robenidine hydrochloride) for rabbits for breeding and fattening. *EFSA Journal* 9.
- Armson, A., Yang, R., Thompson, J., Johnson, J., Reid, S., Ryan, U.M., 2009. *Giardia* genotypes in pigs in Western Australia: prevalence and association with diarrhea. *Exp parasitol* 121, 381-383.
- Alvar J, Velez ID, Bern C, et al. Leishmaniasis worldwide and global estimates of its incidence. *PLoS One* 2012
- Bacchi, C.J., Brun, R., Croft, S.L., Alicea, K., Buhler, Y., 1996. In vivo trypanocidal activities of new S-adenosylmethionine decarboxylase inhibitors. *Antimicrob Agents Chemother* 40, 1448-1453.
- Bahar, A.A., Ren, D., 2013. Antimicrobial peptides. *Pharmaceuticals* 6, 1543-1575.
- Barrett, M.P., Croft, S.L., 2012. Management of trypanosomiasis and leishmaniasis. *British medical bulletin* 104, 175-196.
- Bartelt, L.A., Roche, J., Kolling, G., Bolick, D., Noronha, F., Naylor, C., Hoffman, P., Warren, C., Singer, S., Guerrant, R., 2013. Persistent *G. lamblia* impairs growth in a murine malnutrition model. *J Clin Investig* 123, 2672-2684.
- Bell, C.A., Cory, M., Fairley, T.A., Hall, J.E., Tidwell, R.R., 1991. Structure-activity relationships of pentamidine analogs against *Giardia lamblia* and correlation of anti-giardial activity with DNA-binding affinity. *Antimicrob Agents Chemother* 35, 1099-1107.
- Bendesky, A., Menendez, D., Ostrosky-Wegman, P., 2002. Is metronidazole carcinogenic? *Mutat Res* 511, 133-144.

- Benere, E., da Luz, R.A., Vermeersch, M., Cos, P., Maes, L., 2007. A new quantitative in vitro microculture method for *Giardia duodenalis* trophozoites. *J Microbiol Methods* 71, 101-106.
- Berkman, D.S., Lescano, A.G., Gilman, R.H., Lopez, S.L., Black, M.M., 2002. Effects of stunting, diarrhoeal disease, and parasitic infection during infancy on cognition in late childhood: a follow-up study. *Lancet* 359, 564-571.
- Bingham, A.K., Meyer, E.A., 1979. *Giardia* excystation can be induced in vitro in acidic solutions. *Nature* 277, 301-302.
- Bonilla-Santiago, R., Wu, Z., Zhang, L., Widmer, G., 2008. Identification of growth inhibiting compounds in a *Giardia lamblia* high-throughput screen. *Mol Biochem Parasitol* 162, 149-154.
- Boucher, H.W., Talbot, G.H., Benjamin, D.K., Bradley, J., Guidos, R.J., Jones, R.N., Murray, B.E., Bonomo, R.A., Gilbert, D., Amer, I.D.S., 2013. 10 x '20 Progress-Development of new drugs active against Gram-Negative *Bacilli*: an update from the Infectious Diseases Society of America. *Clin Infect Dis* 56, 1685-1694.
- Bouza, E., Valerio, M., Soriano, A., Morata, L., Carus, E.G., Rodrigues, C.R., Hidalgo-Tenorio, M.C., Plata, A., Munoz, P., 2017. Dalbavancin in the treatment of different gram-positive infections: a real-life experience. *Int J Antimicrob Agents*. Agents In Press.
- Brogia, A., Weitzel, T., Harms, G., Caccio, S.M., Nockler, K., 2013. Molecular typing of *Giardia duodenalis* isolates from German travellers. *Parasitol Res* 112, 3449-3456.
- Brown, E.D., Wright, G.D., 2016. Antibacterial drug discovery in the resistance era. *Nature* 529, 336.
- Brun, R., Burri, C., Gichuki, C.W., 2001a. The story of CGP 40 215: studies on its efficacy and pharmacokinetics in African green monkey infected with *Trypanosoma brucei* rhodesiense. *Trop Med Int Health* 6, 362-368.
- Brun, R., Schumacher, R., Schmid, C., Kunz, C., Burri, C., 2001b. The phenomenon of treatment failures in Human African Trypanosomiasis. *Trop Med Int Health* 6, 906-914.
- Buret, A.G., 2007. Mechanisms of epithelial dysfunction in giardiasis. *Gut* 56, 316-317.
- Buret, A.G., 2008. Pathophysiology of enteric infections with *Giardia duodenalis*. *Parasite* 15, 261-265.
- Burri, C., Nkunku, S., Merolle, A., Smith, T., Blum, J., Brun, R., 2000. Efficacy of new, concise schedule for melarsoprol in treatment of sleeping sickness caused by *Trypanosoma brucei* gambiense: a randomised trial. *Lancet* 355, 1419-1425.
- Busatti, H.G., Gomes, M.A., 2007. A simple colourimetric method to determine anti-giardial activity of drugs. *Parasitol Res*. 101, 819-821.
- Buscher, P., Cecchi, G., Jamonneau, V., Priotto, G., 2017. Human African trypanosomiasis. *Lancet* 390, 2397-2409.
- Byrd, L.G., Conrad, J.T., Nash, T.E., 1994. *Giardia lamblia* infections in adult mice. *Infection and immunity* 62, 3583-3585.
- Caccio, S.M., Beck, R., Lalle, M., Marinculic, A., Pozio, E., 2008. Multilocus genotyping of *Giardia duodenalis* reveals striking differences between assemblages A and B. *Int J Parasitol* 38, 1523-1531.
- Ceri, H., Olson, M., Morck, D., Storey, D., Read, R., Buret, A., Olson, B., 2001. The MBEC Assay System: multiple equivalent biofilms for antibiotic and biocide susceptibility testing. *Methods in enzymology* 337, 377-385.
- Chan, L.C., Basuino, L., Diep, B., Hamilton, S., Chatterjee, S.S., Chambers, H.F., 2015. Ceftobiprole- and ceftaroline-resistant methicillin-resistant *Staphylococcus aureus*. *Antimicrob Agents Chemother* 59, 2960-2963.
- Chen, C.Z., Kulakova, L., Southall, N., Marugan, J.J., Galkin, A., Austin, C.P., Herzberg, O., Zheng, W., 2011. High-throughput *Giardia lamblia* viability assay using

- bioluminescent ATP content measurements. *Antimicrob Agents Chemother* 55, 667-675.
- Chong, C.R., Sullivan, D.J., Jr., 2007. New uses for old drugs. *Nature* 448, 645-646.
- Clark, C.G., Diamond, L.S., 2002. Methods for cultivation of luminal parasitic protists of clinical importance. *Clin Microbiol Rev.* 15, 329-341.
- CLSI 2008. Performance standards for antimicrobial disk and dilution susceptibility tests for bacteria isolated from animals; approved standard, 3rd edition, pp. 1-116.
- Cohen, M.L., 2000. Changing patterns of infectious disease. *Nature* 406, 762-767.
- Croft, S.L., 2008. Kinetoplastida: new therapeutic strategies. *Parasite* 15, 522-527.
- Das Gupta, R., Krause-Ihle, T., Bergmann, B., Muller, I.B., Khomutov, A.R., Muller, S., Walter, R.D., Luersen, K., 2005. 3-Aminoxy-1-aminopropane and derivatives have an antiproliferative effect on cultured *Plasmodium falciparum* by decreasing intracellular polyamine concentrations. *Antimicrob Agents Chemother* 49, 2857-2864.
- de Menezes, J.P.B., Guedes, C.E.S., Petersen, A.L.d.O.A., Fraga, D.B.M., Veras, P.S.T., 2015. Advances in development of new treatment for leishmaniasis. *BioMed Research International* 2015.
- De Muylder, G., Ang, K.K., Chen, S., Arkin, M.R., Engel, J.C., McKerrow, J.H., 2011. A screen against *Leishmania* intracellular amastigotes: comparison to a promastigote screen and identification of a host cell-specific hit. *PLoS neglected tropical diseases* 5, e1253.
- Debouck, C., Goodfellow, P.N., 1999. DNA microarrays in drug discovery and development. *Nature Genetics* 21, 48-50.
- Deslouches, B., Gonzalez, I.A., DeAlmeida, D., Islam, K., Steele, C., Montelaro, R.C., Mietzner, T.A., 2007. De novo-derived cationic antimicrobial peptide activity in a murine model of *Pseudomonas aeruginosa* bacteraemia. *J Antimicrob Chemoth* 60, 669-672.
- Deslouches, B., Islam, K., Craigo, J.K., Paranjape, S.M., Montelaro, R.C., Mietzner, T.A., 2005a. Activity of the de novo engineered antimicrobial peptide WLBU2 against *Pseudomonas aeruginosa* in human serum and whole blood: Implications for systemic applications. *Antimicrob Agents Chemo.* 49, 3208-3216.
- Deslouches, B., Phadke, S.M., Lazarevic, V., Cascio, M., Islam, K., Montelaro, R.C., Mietzner, T.A., 2005b. *De nova* generation of cationic antimicrobial peptides: Influence of length and tryptophan substitution on antimicrobial activity. *Antimicrob Agents Chemo.* 49, 316-322.
- Doi, Y., Bonomo, R.A., Hooper, D.C., Kaye, K.S., Johnson, J.R., Clancy, C.J., Thaden, J.T., Stryjewski, M.E., van Duin, D., 2017. Gram-Negative bacterial infections: research priorities, accomplishments, and future directions of the antibacterial resistance Leadership Group. *Clin Infect Dis* 64, S30-S35.
- Douglas, A.W., Fisher, M.H., Fishinger, J.J., Gund, P., Harris, E.E., Olson, G., Patchett, A.A., Ruyle, W.V., 1977. Anticoccidial 1-substituted 4(1H)-pyridinone hydrazones. *J Med Chem* 20, 939-943.
- EFSA, 2004. EFSA panel on additives and products or substances used in animal feed: opinion of the scientific panel on additives and products or substances in animal feed on a request from commission on the re-evaluation of coccidiostat cycostat 66G in accordance with council directive 70/542/EEC. *EFSA Journal* 69, 1 - 40.
- Eissa, M.M., Amer, E.I., 2012. *Giardia lamblia*: A new target for miltefosine. *Int J Parasitol* 42, 443-452.
- Endimiani, A., Blackford, M., Dasenbrook, E.C., Reed, M.D., Bajaksouszian, S., Hujer, A.M., Rudin, S.D., Hujer, K.M., Perreten, V., Rice, L.B., Jacobs, M.R., Konstan, M.W., Bonomo, R.A., 2011. Emergence of linezolid-resistant *Staphylococcus aureus* after prolonged treatment of cystic fibrosis patients in Cleveland, Ohio. *Antimicrob Agents Chemother* 55, 1684-1692.

- Epanand, R.M., Vogel, H.J., 1999. Diversity of antimicrobial peptides and their mechanisms of action. *Bba-Biomembranes* 1462, 11-28.
- Erlandsen, S.L., Sherlock, L.A., Januschka, M., Schupp, D.G., Schaefer, F.W., 3rd, Jakubowski, W., Bemrick, W.J., 1988. Cross-species transmission of *Giardia* spp.: inoculation of beavers and muskrats with cysts of human, beaver, mouse, and muskrat origin. *Appl Environ Microbiol* 54, 2777-2785.
- Escobedo, A.A., Cimerman, S., 2007. Giardiasis: a pharmacotherapy review. *Expert Opin Pharmacother* 8, 1885-1902.
- Fairlamb, A.H., 2003. Chemotherapy of human African trypanosomiasis: current and future prospects. *Trends in parasitology* 19, 488-494.
- Fan, Z., Cao, L., He, Y., Hu, J., Di, Z., Wu, Y., Li, W., Cao, Z., 2011. Ctriporin, a new anti-methicillin-resistant *Staphylococcus aureus* peptide from the venom of the scorpion *Chaerilus tricostatus*. *Antimicrob Agents Chemother* 55, 5220-5229.
- Fantinatti, M., Bello, A.R., Fernandes, O., Da-Cruz, A.M., 2016. Identification of *Giardia lamblia* assemblage E in humans points to a new anthrozoonotic cycle. *J Infect Dis* 214, 1256-1259.
- Fauci, A.S., 2005. Emerging and reemerging infectious diseases: The perpetual challenge. *Acad Med* 80, 1079-1085.
- Favennec, L., Chochillon, C., Magne, D., Meillet, D., Raichvarg, D., Savel, J., Gobert, J.G., 1992. A new screening assay for anti-giardial compounds: effects of various drugs on the adherence of *Giardia duodenalis* to Caco2 cells. *Parasitol Res* 78, 80-81.
- Field, M.C., Horn, D., Fairlamb, A.H., Ferguson, M.A.J., Gray, D.W., Read, K.D., De Rycker, M., Torrie, L.S., Wyatt, P.G., Wyllie, S., Gilbert, I.H., 2017. Anti-trypanosomatid drug discovery: an ongoing challenge and a continuing need. *Nat Rev Microbiol* 15, 447.
- Fletcher, S.M., Stark, D., Harkness, J., Ellis, J., 2012. Enteric protozoa in the developed world: a public health perspective. *Clin Microbiol Rev* 25, 420-449.
- Foronda, P., Bargues, M.D., Abreu-Acosta, N., Periago, M.V., Valero, M.A., Valladares, B., Mas-Coma, S., 2008. Identification of genotypes of *Giardia intestinalis* of human isolates in Egypt. *Parasitol Res* 103, 1177-1181.
- Fox, J.L. 2013. Antimicrobial peptides stage a comeback. *Nature Res.*
- French, G., 2010. The continuing crisis in antibiotic resistance. *Int J Antimicrob Ag* 36, S3-S7.
- Galkin, A., Kulakova, L., Lim, K., Chen, C.Z., Zheng, W., Turko, I.V., Herzberg, O., 2014. Structural basis for inactivation of *Giardia lamblia* carbamate kinase by disulfiram. *J Biol Chem* 289, 10502-10509.
- Gandhi, N.R., Nunn, P., Dheda, K., Schaaf, H.S., Zignol, M., van Soolingen, D., Jensen, P., Bayona, J., 2010. Multidrug-resistant and extensively drug-resistant tuberculosis: a threat to global control of tuberculosis. *Lancet* 375, 1830-1843.
- Gardner, T.B., Hill, D.R., 2001. Treatment of giardiasis. *Clinical microbiology reviews* 14, 114-128.
- Gasser, R.B., Eckert, J., Rohrer, L., 1987. Infectivity of Swiss *Giardia* isolates to jirds and mice, and in vitro cultivation of trophozoites originating from sheep. *Parasitol Res* 74, 103-111.
- Gelanew, T., Lalle, M., Hailu, A., Pozio, E., Caccio, S.M., 2007. Molecular characterization of human isolates of *Giardia duodenalis* from Ethiopia. *Acta Tropica* 102, 92-99.
- Geurden, T., Geldhof, P., Levecke, B., Martens, C., Berkvens, D., Casaert, S., Vercruyse, J., Claerebout, E., 2008. Mixed *Giardia duodenalis* assemblage A and E infections in calves. *Int J Parasitol* 38, 259-264.
- Grevelink, S.A., Lerner, E.A., Leishmaniasis. *Journal of the American Academy of Dermatology* 34, 257-272.
- Gudiol, C., Cuervo, G., Shaw, E., Pujol, M., Carratala, J., 2017. Pharmacotherapeutic options for treating *Staphylococcus aureus* bacteremia. *Expert Opin Pharmacother*, 1-17.

- Gut, J., Ang, K.K., Legac, J., Arkin, M.R., Rosenthal, P.J., McKerrow, J.H., 2011. An image-based assay for high throughput screening of *Giardia lamblia*. *J Microbiol Methods* 84, 398-405.
- Gwynn, M.N., Portnoy, A., Rittenhouse, S.F., Payne, D.J., 2010. Challenges of antibacterial discovery revisited. *Annals of the New York Academy of Sciences* 1213, 5-19.
- Halder, S., Yadav, K.K., Sarkar, R., Mukherjee, S., Saha, P., Haldar, S., Karmakar, S., Sen, T., 2015. Alteration of Zeta potential and membrane permeability in bacteria: a study with cationic agents. *SpringerPlus* 4, 672.
- Hale, J.D.F., Hancock, R.E.W., 2007. Alternative mechanisms of action of cationic antimicrobial peptides on bacteria. *Expert review of anti-infective therapy* 5, 951-959.
- Halliez, M.C., Buret, A.G., 2013. Extra-intestinal and long term consequences of *Giardia duodenalis* infections. *World journal of gastroenterology* 19, 8974-8985.
- Hancock, R.E.W., 1997. Antibacterial peptides and the outer membranes of gram-negative bacilli. *J Med Microbiol* 46, 1-3.
- Hancock, R.E.W., Lehrer, R., 1998. Cationic peptides: a new source of antibiotics. *Trends in Biotechnology* 16, 82-88.
- Hancock, R.E.W., Sahl, H.G., 2006. Antimicrobial and host-defense peptides as new anti-infective therapeutic strategies. *Nat Biotechnol* 24, 1551-1557.
- Hanevik, K., Wensaas, K.A., Rortveit, G., Eide, G.E., Morch, K., Langeland, N., 2014. Irritable bowel syndrome and chronic fatigue 6 years after giardia infection: a controlled prospective cohort study. *Clin Infect Dis* 59, 1394-1400.
- Hansen, M., Krogh, K.A., Brandt, A., Christensen, J.H., Halling-Sorensen, B., 2009. Fate and antibacterial potency of anticoccidial drugs and their main abiotic degradation products. *Environ Pollut* 157, 474-480.
- Hemmige, Vagish, Herbert Tanowitz, and Aisha Sethi. “*Trypanosoma cruzi* infection: a review with emphasis on cutaneous manifestations.” *Int J Dermatol* 51.5 (2012): 501–508. *PMC*. Web. 20 June 2018.
- Helmy, Y.A., Klotz, C., Wilking, H., Krucken, J., Nockler, K., Von Samson-Himmelstjerna, G., Zessin, K.H., Aebischer, T., 2014. Epidemiology of *Giardia duodenalis* infection in ruminant livestock and children in the Ismailia province of Egypt: insights by genetic characterization. *Parasit vectors* 7, 321.
- Hewlett, E.L., Andrews, J.S., Jr., Ruffier, J., Schaefer, F.W., 3rd, 1982. Experimental infection of mongrel dogs with *Giardia lamblia* cysts and cultured trophozoites. *J Infect Dis* 145, 89-93.
- Higgins, D.L., Chang, R., Debabov, D.V., Leung, J., Wu, T., Krause, K.M., Sandvik, E., Hubbard, J.M., Kaniga, K., Schmidt, D.E., Jr., Gao, Q., Cass, R.T., Karr, D.E., Benton, B.M., Humphrey, P.P., 2005. Telavancin, a multifunctional lipoglycopeptide, disrupts both cell wall synthesis and cell membrane integrity in methicillin-resistant *Staphylococcus aureus*. *Antimicrob Agents Chemother* 49, 1127-1134.
- Hill, D.R., Guerrant, R.L., Pearson, R.D., Hewlett, E.L., 1983. *Giardia lamblia* infection of suckling mice. *J Infect Dis* 147, 217-221.
- Hiramatsu, K., 2001. Vancomycin-resistant *Staphylococcus aureus*: a new model of antibiotic resistance. *Lancet Infect Dis* 1, 147-155.
- Homan, W.L., Mank, T.G., 2001. Human giardiasis: genotype linked differences in clinical symptomatology. *Int J Parasitol* 31, 822-826.
- Hu, Y.M., Shamaei-Tousi, A., Liu, Y.J., Coates, A., 2010. A New Approach for the Discovery of Antibiotics by Targeting Non-Multiplying Bacteria: A Novel Topical Antibiotic for Staphylococcal Infections. *PloS One* 5.
- Hurdle, J.G., O'Neill, A.J., Chopra, I., Lee, R.E., 2011. Targeting bacterial membrane function: an underexploited mechanism for treating persistent infections. *Nat Rev Microbiol* 9, 62-75.

- Jakobsson, H.E., Jernberg, C., Andersson, A.F., Sjölund-Karlsson, M., Jansson, J.K., Engstrand, L., 2010. Short-term antibiotic treatment has differing long-term impacts on the human throat and gut microbiome. *Plos One* 5, e9836.
- Jernberg, C., Lofmark, S., Edlund, C., Jansson, J.K., 2007. Long-term ecological impacts of antibiotic administration on the human intestinal microbiota. *ISME J* 1, 56-66.
- Jeu, L.A., Fung, H.B., 2004. Daptomycin: A cyclic lipopeptide antimicrobial agent. *Clin Ther* 26, 1728-1757.
- Jokipii, L., Jokipii, A.M., 1979. Single-dose metronidazole and tinidazole as therapy for giardiasis: success rates, side effects, and drug absorption and elimination. *J Infect Dis* 140, 984-988.
- Kang, E.W., Clinch, K., Furneaux, R.H., Harvey, J.E., Schofield, P.J., Gero, A.M., 1998. A novel and simple colorimetric method for screening *Giardia intestinalis* and anti-giardial activity in vitro. *Parasitol* 117 (Pt 3), 229-234.
- Kantor, S., Kennett, R.L., Jr., Waletzky, E., Tomcufcik, A.S., 1970. 1,3-Bis(p-chlorobenzylideneamino)guanidine hydrochloride (robenzidene): new poultry anticoccidial agent. *Science* 168, 373-374.
- Kararli, T.T., 1995. Comparison of the gastrointestinal anatomy, physiology, and biochemistry of humans and commonly used laboratory animals. *Biopharmaceutics & drug disposition* 16, 351-380.
- Kaye, K.S., Kaye, D., 2000. Multidrug-resistant Pathogens: Mechanisms of Resistance and Epidemiology. *Current infectious disease reports* 2, 391-398.
- Kennedy, P.G., 2013. Clinical features, diagnosis, and treatment of human African trypanosomiasis (sleeping sickness). *The Lancet. Neurology* 12, 186-194.
- Koss, C.A., Baras, D.C., Lane, S.D., Aubry, R., Marcus, M., Markowitz, L.E., Koumans, E.H., 2012. Investigation of metronidazole use during pregnancy and adverse birth outcomes. *Antimicrob Agents Ch, AAC*. 06477-06411.
- Koudela, B., Nohynkova, E., Vitovec, J., Pakandl, M., Kulda, J., 1991. *Giardia* infection in pigs: detection and in vitro isolation of trophozoites of the *Giardia intestinalis* group. *Parasitol* 102 Pt 2, 163-166.
- Koudela, B., Vitovec, J., 1998. Experimental giardiasis in goat kids. *Vet Parasitol* 74, 9-18.
- Kulakova, L., Galkin, A., Chen, C.Z., Southall, N., Marugan, J.J., Zheng, W., Herzberg, O., 2014. Discovery of novel anti-giardiasis drug candidates. *Antimicrob Agents Chemother* 58, 7303-7311.
- Lederberg, J., 1956. Bacterial protoplasts induced by penicillin. *PNAS* 42, 574-577.
- Lee, B.L., Sachdeva, M., Chambers, H.F., 1991. Effect of protein binding of daptomycin on MIC and antibacterial activity. *Antimicrob Agents Chemother* 35, 2505-2508.
- Lee, D.L., Millard, B.J., 1972. Fine-Structural Changes in *Eimeria-Tenella*, from Infections in Chick-Embryos and Chickens, after Exposure to Anticoccidial Drug Robenidene. *Parasitol* 65, 309-&.
- Leejae, S., Taylor, P.W., Voravuthikunchai, S.P., 2013. Antibacterial mechanisms of rhodomycrtone against important hospital-acquired antibiotic-resistant pathogenic bacteria. *J Med Microbiol* 62, 78-85.
- Lemee, V., Zaharia, I., Nevez, G., Rabodonirina, M., Bresseur, P., Ballet, J.J., Favennec, L., 2000. Metronidazole and albendazole susceptibility of 11 clinical isolates of *Giardia duodenalis* from France. *The Journal of antimicrobial chemotherapy* 46, 819-821.
- Lengerich, E.J., Addiss, D.G., Juranek, D.D., 1994. Severe giardiasis in the United States. *Clin Infect Dis* 18, 760-763.
- Levecke, B., Geldhof, P., Claerebout, E., Dorny, P., Vercammen, F., Caccio, S.M., Vercruyse, J., Geurden, T., 2009. Molecular characterisation of *Giardia duodenalis* in captive non-human primates reveals mixed assemblage A and B infections and novel polymorphisms. *Int J Parasitol* 39, 1595-1601.

- Lindsay, D.S., Rippey, N.S., Cole, R.A., Parsons, L.C., Dubey, J.P., Tidwell, R.R., Blagburn, B.L., 1994. Examination of the activities of 43 chemotherapeutic agents against *Neospora caninum* tachyzoites in cultured cells. *Am J Vet Res* 55, 976-981.
- Lipinski, C.A., Lombardo, F., Dominy, B.W., Feeney, P.J., 1997. Experimental and computational approaches to estimate solubility and permeability in drug discovery and development settings. *Adv Drug Deliver Rev* 23, 3-25.
- Lira, R., Sundar, S., Makharia, A., Kenney, R., Gam, A., Saraiva, E., Sacks, D., 1999. Evidence that the high incidence of treatment failures in Indian kala-azar is due to the emergence of antimony-resistant strains of *Leishmania donovani*. *J Infect Dis* 180, 564-567.
- Liu, H., Shen, Y., Yin, J., Yuan, Z., Jiang, Y., Xu, Y., Pan, W., Hu, Y., Cao, J., 2014. Prevalence and genetic characterization of *Cryptosporidium*, *Enterocytozoon*, *Giardia* and *Cyclospora* in diarrheal outpatients in China. *BMC Inf Dis* 14, 25.
- Lloyd, D., Williams, C.F., 2014. Comparative biochemistry of *Giardia*, *Hexamita* and *Spironucleus*: enigmatic diplomonads. *Mol Biochem Parasit* 197, 43-49.
- Lopes, A.H., Souto-Padron, T., Dias, F.A., Gomes, M.T., Rodrigues, G.C., Zimmermann, L.T., Alves e Silva, T.L., Vermelho, A.B., 2010. Trypanosomatids: odd organisms, devastating diseases. *Open Parasitol J* 4, 30 - 59.
- Lutje, V., Seixas, J., Kennedy, A., 2013. Chemotherapy for second-stage human African trypanosomiasis. The Cochrane database of systematic reviews, CD006201.
- Majewska, A.C., 1994. Successful experimental infections of a human volunteer and Mongolian gerbils with *Giardia* of animal origin. *Trans R Soc Trop Med Hyg* 88, 360-362.
- Mangili, A., Bica, I., Snyderman, D.R., Hamer, D.H., 2005. Daptomycin-resistant, methicillin-resistant *Staphylococcus aureus* bacteremia. *Clin Infect Dis* 40, 1058-1060.
- Marien, M., Vancraeynest, D., De Gussem, M., Baele, M., Haesebrouck, F., 2008. *In vitro* activity of robenidine hydrochloride on rabbit *Clostridium perfringens* isolates. *Pathology and Hygiene*, 1005 - 1007.
- Marr, A.K., Gooderham, W.J., Hancock, R.E.W., 2006. Antibacterial peptides for therapeutic use: obstacles and realistic outlook. *Curr Opin Pharmacol* 6, 468-472.
- Marty, F.M., Yeh, W.W., Wennersten, C.B., Venkataraman, L., Albano, E., Alyea, E.P., Gold, H.S., Baden, L.R., Pillai, S.K., 2006. Emergence of a clinical daptomycin-resistant *Staphylococcus aureus* isolate during treatment of methicillin-resistant *Staphylococcus aureus* bacteremia and osteomyelitis. *J Clin Microbiol* 44, 595-597.
- Matovu, E., Seebeck, T., Enyaru, J.C.K., Kaminsky, R., 2001. Drug resistance in *Trypanosoma brucei* spp., the causative agents of sleeping sickness in man and nagana in cattle. *Microbes Infect* 3, 763-770.
- Maxmen, A., 2017. Pill treats sleeping sickness. *Nature* 550, 441.
- McDonald, V., Shirley, M.W., 2009. Past and future: vaccination against *Eimeria*. *Parasitol* 136, 1477-1489.
- Meanwell, N.A., 2011. Synopsis of some recent tactical application of bioisosteres in drug design. *J Med Chem* 54, 2529-2591.
- Meloni, B.P., Thompson, R.C.A., Reynoldson, J.A., Seville, P., 1990. Albendazole - a More Effective Antigiardial Agent *In vitro* Than Metronidazole or Tinidazole. *Trans R Soc Trop Med Hyg* 84, 375-379.
- Meurens, F., Summerfield, A., Nauwynck, H., Saif, L., Gerdt, V., 2012. The pig: a model for human infectious diseases. *Trends Microbiol* 20, 50-57.
- Miller, E.R., E., U.D., 1987. The pig as a model for human nutrition. *Ann. Rev. Nutr.*, 361-382.
- Mills, S.D., 2003. The role of genomics in antimicrobial discovery. *J Antimicrob Chemoth* 51, 749-752.
- Miyamoto, Y., Eckmann, L., 2015. Drug development against the major diarrhea-causing parasites of the small intestine, *Cryptosporidium* and *Giardia*. *Front Microbiol* 6, 1208.

- Mogi, T., Kita, K., 2009. Gramicidin S and polymyxins: the revival of cationic cyclic peptide antibiotics. *Cell Mol Life Sci* 66, 3821-3826.
- Monis, P.T., Andrews, R.H., Mayrhofer, G., Ey, P.L., 2003. Genetic diversity within the morphological species *Giardia intestinalis* and its relationship to host origin. *Infection, genetics and evolution : Infect Genet Evol* Title 3, 29-38.
- Muller, J., Ruhle, G., Muller, N., Rossignol, J.F., Hemphill, A., 2006. *In vitro* effects of thiazolides on *Giardia lamblia* WB clone C6 cultured axenically and in coculture with Caco2 cells. *Antimicrob Agents Chemother* 50, 162-170.
- NCCLS 1999. Methods for determining bactericidal activity of antimicrobial agents; approved guidelines. In NCCLS document M26-A, pp. 1 - 50.
- Neu, H.C., 1992. The Crisis in Antibiotic-Resistance. *Science* 257, 1064-1073.
- Nguyen, B., Lee, M.P.H., Hamelberg, D., Joubert, A., Bailly, C., Brun, R., Neidle, S., Wilson, W.D., 2002. Strong binding in the DNA minor groove by an aromatic diamidine with a shape that does not match the curvature of the groove. *J Am Chem Soc* 124, 13680-13681.
- No, J.H., 2016. Visceral leishmaniasis: Revisiting current treatments and approaches for future discoveries. *Acta Tropica* 155, 113-123.
- Norrby, S.R., Nord, C.E., Finch, R., 2005. Lack of development of new antimicrobial drugs: a potential serious threat to public health. *Lancet Infect Dis* 5, 115-119.
- O'Brien, K.L., Wolfson, L.J., Watt, J.P., Henkle, E., Deloria-Knoll, M., McCall, N., Lee, E., Mulholland, K., Levine, O.S., Cherian, T., 2009. Burden of disease caused by *Streptococcus pneumoniae* in children younger than 5 years: global estimates. *Lancet* 374, 893-902.
- O'Handley, R.M., Olson, M.E., Fraser, D., Adams, P., Thompson, R.C., 2000. Prevalence and genotypic characterisation of *Giardia* in dairy calves from Western Australia and Western Canada. *Vet Parasitol* 90, 193-200.
- Obach, R.S., 1999. Prediction of human clearance of twenty-nine drugs from hepatic microsomal intrinsic clearance data: An examination of *In vitro* half-life approach and nonspecific binding to microsomes. *Drug Metab Dispos* 27, 1350-1359.
- Ogunniyi, A.D., Khazandi, M., Stevens, A.J., Sims, S.K., Page, S.W., Garg, S., Venter, H., Powell, A., White, K., Petrovski, K.R., Laven-Law, G., Totoli, E.G., Salgado, H.R., Pi, H., Coombs, G.W., Shinabarger, D.L., Turnidge, J.D., Paton, J.C., McCluskey, A., Trott, D.J., 2017. Evaluation of robenidine analog NCL195 as a novel broad-spectrum antibacterial agent. *PloS One* 12, e0183457.
- Oliva, B., O'Neill, A.J., Miller, K., Stubbings, W., Chopra, I., 2004. Anti-staphylococcal activity and mode of action of clofazimine. *J Antimicrob Chemoth* 53, 435-440.
- Olson, M.E., McAllister, T.A., Deselliers, L., Morck, D.W., Cheng, K.J., Buret, A.G., Ceri, H., 1995. Effects of giardiasis on production in a domestic ruminant (lamb) model. *Am J Vet Res* 56, 1470-1474.
- Ooi, N., Miller, K., Hobbs, J., Rhys-Williams, W., Love, W., Chopra, I., 2009. XF-73, a novel antistaphylococcal membrane-active agent with rapid bactericidal activity. *J Antimicrob Chemoth* 64, 735-740.
- Ooi, N., Miller, K., Randall, C., Rhys-Williams, W., Love, W., Chopra, I., 2010. XF-70 and XF-73, novel antibacterial agents active against slow-growing and non-dividing cultures of *Staphylococcus aureus* including biofilms. *J Antimicrob Chemoth* 65, 72-78.
- Oprea, T.I., Bauman, J.E., Bologna, C.G., Buranda, T., Chigaev, A., Edwards, B.S., Jarvik, J.W., Gresham, H.D., Haynes, M.K., Hjelle, B., Hromas, R., Hudson, L., Mackenzie, D.A., Muller, C.Y., Reed, J.C., Simons, P.C., Smagley, Y., Strouse, J., Surviladze, Z., Thompson, T., Ursu, O., Waller, A., Wandinger-Ness, A., Winter, S.S., Wu, Y., Young,

- S.M., Larson, R.S., Willman, C., Sklar, L.A., 2011. Drug Repurposing from an Academic Perspective. *Drug Discov Today Ther Strateg* 8, 61-69.
- Overhage, J., Campisano, A., Bains, M., Torfs, E.C., Rehm, B.H., Hancock, R.E., 2008. Human host defense peptide LL-37 prevents bacterial biofilm formation. *Infect Immun* 76, 4176-4182.
- Pantos, A., Tsogas, I., Paleos, C.A., 2008. Guanidinium group: A versatile moiety inducing transport and multicompartmentalization in complementary membranes. *Biomembranes* 1778, 811-823.
- Pendleton, J.N., Gorman, S.P., Gilmore, B.F., 2013. Clinical relevance of the ESKAPE pathogens. *Expert Rev Anti Infect Ther* 11, 297-308.
- Poole, K., 2003. Overcoming multidrug resistance in gram-negative bacteria. *Curr Opin Investig Drugs* 4, 128 - 139.
- Poole, R.K., 1993. The Isolation of Membranes from Bacteria, In: Graham, J.M., Higgins, J.A. (Eds.) *Methods in Molecular Biology*. Humana Press Inc., Totowa, NJ.
- Qian, C.D., Wu, X.C., Teng, Y., Zhao, W.P., Li, O., Fang, S.G., Huang, Z.H., Gao, H.C., 2012. Battacin (Octapeptin B5), a New Cyclic Lipopeptide Antibiotic from *Paenibacillus tianmuensis* Active against Multidrug-Resistant Gram-Negative Bacteria. *Antimicrob Agents Ch* 56, 1458-1465.
- Randall, C.P., Mariner, K.R., Chopra, I., O'Neill, A.J., 2013. The target of daptomycin is absent from *Escherichia coli* and other gram-negative pathogens. *Antimicrob Agents Chemother* 57, 637-639.
- Read, C.M., Monis, P.T., Thompson, R.C., 2004. Discrimination of all genotypes of *Giardia duodenalis* at the glutamate dehydrogenase locus using PCR-RFLP. *Infection, genetics and evolution : Infect Genet Evol* 4, 125-130.
- Reddy, V.M., O'Sullivan, J.F., Gangadharam, P.R.J., 1999. Antimycobacterial activities of riminophenazines. *J Antimicrob Chemoth* 43, 615-623.
- Rendueles, O., Kaplan, J.B., Ghigo, J.M., 2013. Antibiofilm polysaccharides. *Environ Microbiol* 15, 334-346.
- Reynolds, P.E., 1961. Studies on the mode of action of vancomycin. *Biochem Biophys Acta* 52, 403-405.
- Reynoldson, J.A., Thompson, R.C., Meloni, B.P., 1991. In vivo efficacy of albendazole against *Giardia duodenalis* in mice. *Parasitol Res* 77, 325-328.
- Rice, L.B., 2008. Federal funding for the study of antimicrobial resistance in nosocomial pathogens: No ESKAPE. *J Infect Dis* 197, 1079-1081.
- Richard, J.V., Werbovetz, K.A., 2010. New antileishmanial candidates and lead compounds. *Curr Opin Chem Biol* 14, 447-455.
- Ricketts, A.P., Pfefferkorn, E.R., 1993. *Toxoplasma gondii*: susceptibility and development of resistance to anticoccidial drugs in vitro. *Antimicrob Agents Chemother* 37, 2358-2363.
- Ring, B.J., Chien, J.Y., Adkison, K.K., Jones, H.M., Rowland, M., Do Jones, R., Yates, J.W.T., Ku, M.S., Gibson, C.R., He, H.D., Vuppugalla, R., Marathe, P., Fischer, V., Dutta, S., Sinha, V.K., Bjornsson, T., Lave, T., Poulin, P., 2011. PhRMA CPCDC Initiative on Predictive Models of Human Pharmacokinetics, Part 3: Comparative Assessment of Prediction Methods of Human Clearance. *J Pharm Sci-U.S.* 100, 4090-4110.
- Roder, C., Thomson, M.J., 2015. Auranofin: repurposing an old drug for a golden new age. *Drugs in R&D* 15, 13-20.
- Rozengart, E.V., Saakov, V.S., 2002. The chelating ability of the anticoccidial drug 1,3-bis(p-chlorobenzilideneamino) guanidine: the complexes with Ca²⁺ and La³⁺. *Dokl. Biochem. Biophys.* 385, 219-223.
- Ryan, U., Caccio, S.M., 2013. Zoonotic potential of *Giardia*. *Int J Parasitol* 43, 943-956.
- Ryley, J.F., Wilson, R.G., 1971. Studies on Mode of Action of Coccidiostat Robenidene. *Z Parasitenk* 37, 85-&.

- Saczewski, F., Balewski, L., 2009. Biological activities of guanidine compounds. *Expert Opin Ther Pat* 19, 1417-1448.
- Saczewski, F., Balewski, L., 2013. Biological activities of guanidine compounds, 2008 - 2012 update. *Expert Opin Ther Pat* 23, 965-995.
- Sande, M.A., 1999. Handbook of animal models of infection: experimental models in antimicrobial chemotherapy. Academic Press.
- Sande, M.A., Zak, O., 1999. Handbook of Animal Models of Infection: Experimental Models in Antimicrobial Chemotherapy. Elsevier Science.
- Santos, D.O., Coutinho, C.E.R., Madeira, M.F., Bottino, C.G., Vieira, R.T., Nascimento, S.B., Bernardino, A., Bourguignon, S.C., Corte-Real, S., Pinho, R.T., Rodrigues, C.R., Castro, H.C., 2008. Leishmaniasis treatment - a challenge that remains: a review. *Parasitol Res* 103, 1-10.
- Savioli, L., Smith, H., Thompson, A., 2006. *Giardia* and *Cryptosporidium* join the 'Neglected Diseases Initiative'. *Trends Parasitol* 22, 203-208.
- Scalia, L.A., Fava, N.M., Soares, R.M., Limongi, J.E., da Cunha, M.J., Pena, I.F., Kalapothakis, E., Cury, M.C., 2016. Multilocus genotyping of *Giardia duodenalis* in Brazilian children. *Trans R Soc Trop Med Hyg* 110, 343-349.
- Shreiner, A.B., Kao, J.Y., Young, V.B., 2015. The gut microbiome in health and in disease. *Curr Opin Gastroenterol* 31, 69-75.
- Singer, S.M., Nash, T.E., 2000. The role of normal flora in *Giardia lamblia* infections in mice. *J Infect Dis* 181, 1510-1512.
- Sondhi, S.M., Dinodia, M., Jain, S., Kumar, A., 2009. Synthesis of biologically active novel bis Schiff bases, bis hydrazone and bis guanidine derivatives. *Indian J Chem B* 48, 1128-1136.
- Spellberg, B., 2008. Dr. William H. Stewart: Mistaken or maligned? *Clin Infect Dis* 47, 294-294.
- Spellberg, B., Powers, J.H., Brass, E.P., Miller, L.G., Edwards, J.J.E., 2004. Trends in antimicrobial drug development: implications for the future. *Clin Infect Dis* 38, 1279-1286.
- Steverding, D., Antoszczak, M., Huczynski, A., 2016. *In vitro* activity of salinomycin and monensin derivatives against *Trypanosoma brucei*. *Parasit Vectors* 9, 409.
- Stewart, P.S., Costerton, J.W., 2001. Antibiotic resistance of bacteria in biofilms. *Lancet* 358, 135-138.
- Straus, S.K., Hancock, R.E., 2006. Mode of action of the new antibiotic for Gram-positive pathogens daptomycin: comparison with cationic antimicrobial peptides and lipopeptides. *Acta Biochim Biophys* 1758, 1215-1223.
- Strkolcova, G., Madar, M., Hinney, B., Goldova, M., Mojziso, J., Halanova, M., 2015. Dog's genotype of *Giardia duodenalis* in human: first evidence in Europe. *Acta parasitol* 60, 796-799.
- Stuart, K., Brun, R., Croft, S., Fairlamb, A., Gürtler, R.E., McKerrow, J., Reed, S., Tarleton, R., 2008. Kinetoplastids: related protozoan pathogens, different diseases. *J Clin Invest* 118, 1301-1310.
- Suh, J.D., Ramakrishnan, V., Palmer, J.N., 2010. Biofilms. *Otolaryng Clin N Am* 43, 521-+.
- Sulaiman, I.M., Fayer, R., Bern, C., Gilman, R.H., Trout, J.M., Schantz, P.M., Das, P., Lal, A.A., Xiao, L., 2003. Triosephosphate isomerase gene characterization and potential zoonotic transmission of *Giardia duodenalis*. *Emerg Infect Dis* 9, 1444-1452.
- Szabo, D., Ostorhazi, E., Binas, A., Rozgonyi, F., Kocsis, B., Cassone, M., Wade, J.D., Nolte, O., Otvos, L., 2010. The designer proline-rich antibacterial peptide A3-APO is effective against systemic *Escherichia coli* infections in different mouse models. *Int J Antimicrob Ag* 35, 357-361.

- Tegazzini, D., Cantizani, J., Pena, I., Martin, J., Coteron, J.M., 2017. Unravelling the rate of action of hits in the *Leishmania donovani* box using standard drugs amphotericin B and miltefosine. PLoS Negl Trop Dis 11, e0005629.
- Tejman-Yarden, N., Eckmann, L., 2011. New approaches to the treatment of giardiasis. Curr Opin Infect Dis 24, 451-456.
- Tejman-Yarden, N., Miyamoto, Y., Leitsch, D., Santini, J., Debnath, A., Gut, J., McKerrow, J.H., Reed, S.L., Eckmann, L., 2013. A reprofiled drug, auranofin, is effective against metronidazole-resistant *Giardia lamblia*. Antimicrob Agents Chemother 57, 2029-2035.
- Tenover, F.C., 2006. Mechanisms of antimicrobial resistance in bacteria. Am J Med 119, S3-S10.
- Thompson, R.C.A., 2000. Giardiasis as a re-emerging infectious disease and its zoonotic potential. Int J Parasitol 30, 1259-1267.
- Torrent, M., Pulido, D., Rivas, L., Andreu, D., 2012. Antimicrobial Peptide Action on Parasites. Curr Drug Targets 13, 1138-1147.
- Tufts, C.f.t.s.o.D.D. 2014. How the Tufts Center for the Study of Drug Development Pegged the Cost of a new Drug at \$2.6 Billion.
- Turrens, J.F., 2004. Oxidative stress and antioxidant defenses: a target for the treatment of diseases caused by parasitic protozoa. Mol Aspects Med 25, 211-220.
- Umland, T.C., Schultz, L.W., Russo, T.A., 2014. Re-evaluating the approach to drug target discovery in multidrug-resistant Gram-negative bacilli. Future microbiol 9, 1113-1116.
- Upcroft, J., Campbell, R., Upcroft, P., 1996. Quinacrine-resistant *Giardia duodenalis*. Parasitol 112, 309-313.
- Upcroft, J., Upcroft, P., 1998. My favorite cell: *Giardia*. BioEssays. Bioessays 20, 256-263.
- Upcroft, J.A., Upcroft, P., 2001a. Drug susceptibility testing of anaerobic protozoa. Antimicrob Agents Chemother 45, 1810-1814.
- Upcroft, P., Upcroft, J.A., 2001b. Drug targets and mechanisms of resistance in the anaerobic protozoa. Clin Microbiol Rev 14, 150-164.
- Vaara, M., 1992. Agents that increase the permeability of the outer membrane. Microbiol Rev 56, 395-411.
- Venkata M. Reddy, John F. O' Sullivan, Pattisapu R. J. Gangadharam; Antimycobacterial activities of riminophenazines , J Antimicrob Chem, 1999,
- Ventola, C.L., 2015. The Antibiotic Resistance Crisis: Part 1: Causes and Threats. Pharmacy and Therapeutics 40, 277-283.
- Vermeersch, M., da Luz, R.I., Tote, K., Timmermans, J.P., Cos, P., Maes, L., 2009. In vitro susceptibilities of *Leishmania donovani* promastigote and amastigote stages to antileishmanial reference drugs: practical relevance of stage-specific differences. Antimicrob Agents Chemother 53, 3855-3859.
- Visvesvara, G.S., Dickerson, J.W., Healy, G.R., 1988. Variable infectivity of human-derived *Giardia lamblia* cysts for Mongolian gerbils (*Meriones unguiculatus*). J Clin Microbiol 26, 837-841.
- Watkins, B.M., 2003. Drugs for the control of parasitic diseases: current status and development. Trends Parasitol 19, 477-478.
- Wensaas, K.A., Langeland, N., Hanevik, K., Morch, K., Eide, G.E., Rortveit, G., 2012. Irritable bowel syndrome and chronic fatigue 3 years after acute giardiasis: historic cohort study. Gut 61, 214-219.
- WHO, 2017. Antibacterial agents in clinical development: an analysis of the antibacterial clinical development pipeline, including tuberculosis. Geneva, WHO.
- Wielinga, C., Ryan, U., Andrew Thompson, R.C., Monis, P., 2011. Multi-locus analysis of *Giardia duodenalis* intra-Assemblage B substitution patterns in cloned culture isolates

- suggests sub-Assemblage B analyses will require multi-locus genotyping with conserved and variable genes. *Int J Parasitol* 41, 495-503.
- Wong, D.T., Horng, J.S., Wilkinson, J.R., 1972. Robenzidene, an inhibitor of oxidative phosphorylation. *Biochem Biophys Res Commun* 46, 621-627.
- Wright, C.W., Melwani, S.I., Phillipson, J.D., Warhurst, D.C., 1992. Determination of anti-giardial activity in vitro by means of soluble formazan production. *Trans R Trop Med Hyg* 86, 517-519.
- Wright, J.M., Dunn, L.A., Upcroft, P., Upcroft, J.A., 2003. Efficacy of anti-giardial drugs. *Expert Opin Drug Saf* 2, 529-541.
- Yang, R., Jacobson, C., Gardner, G., Carmichael, I., Campbell, A.J., Ryan, U., 2014. Development of a quantitative PCR (qPCR) for *Giardia* and analysis of the prevalence, cyst shedding and genotypes of *Giardia* present in sheep across four states in Australia. *Exp Parasitol* 137, 46-52.
- Yang, R., Murphy, C., Song, Y., Ng-Hublin, J., Estcourt, A., Hijjawi, N., Chalmers, R., Hadfield, S., Bath, A., Gordon, C., Ryan, U., 2013. Specific and quantitative detection and identification of *Cryptosporidium hominis* and *C. parvum* in clinical and environmental samples. *EXP Parasitol* 135, 142-147.
- Yao, J.M., Zhang, H.B., Liu, C.S., Tao, Y., Yin, M., 2015. Inhibitory effects of 19 antiprotozoal drugs and antibiotics on *Babesia microti* infection in BALB/c mice. *J Infect Dev Countr* 9, 1004-1010.
- Zahedi, A., Field, D., Ryan, U., 2017. Molecular typing of *Giardia duodenalis* in humans in Queensland - first report of assemblage E. *Parasitol In Press*.
- Zetola, N., Francis, J.S., Nuernberger, E.L., Bishai, W.R., 2005. Community-acquired methicillin-resistant *Staphylococcus aureus*: an emerging threat. *Lancet Infect Dis* 5, 275-286.
- Zhanel, G.G., Calic, D., Schweizer, F., Zelenitsky, S., Adam, H., Lagace-Wiens, P.R.S., Rubinstein, E., Gin, A.S., Hoban, D.J., Karlowsky, J.A., 2010. New Lipoglycopeptides A Comparative Review of Dalbavancin, Oritavancin and Telavancin. *Drugs* 70, 859-886.
- Zhanel, G.G., Schweizer, F., Karlowsky, J.A., 2012. Oritavancin: Mechanism of Action. *Clin Infect Dis* 54, S214-S219.
- Zhang, Q., Widmer, G., Tzipori, S., 2013. A pig model of the human gastrointestinal tract. *Gut microbes* 4, 193-200.